Proceedings

The 6th ACA

Asia Color Association
Conference : Color & Culture

02-03 NOVEMBER 2021

YOGYAKARTA
INDONESIA

ACA
CONFERENCE
2021

6th Asia Color Association Conference 2021

Proceeding

"Color and Culture"
2-3 November 2021 Yogyakarta, Indonesia

Department of Agro-industrial Technology
Universitas Gadjah Mada

PROCEEDING OF THE 6th ASIA COLOR ASSOCIATION CONFERENCE
COLOR AND CULTURE

Department of Agro-industrial Technology and The Graduate School, Universitas Gadjah Mada

Organizing Committee
General chair   : Adi Djoko Guritno
Co-chair   : Wahyu Supartono
Financial   : Novita Erma Kristanti (coordinator)
                   Shafira Wuryandani
Program   : Anggoro Cahyo Sukartiko (coordinator)
                   Nugroho Dwi Cahyaningtyas
                   Yustinus Nurgiatmoko
Secretary   : Nafis Khuriyati (coordinator)
                   Prasetya Kurniawan
                   Rendayu Jonda Neisyafitri
                   Rosa Amalia
Publication   : Darmawan Ari N (coordinator)
                   Annisa Dwi Astari
Facility   : Moh. Wahyudin (coordinator)

International Advisory Boards
                   Mitsuo Ikeda, Rajamangala University of Technology Thanyaburi, Thailand
                   Adi Djoko Guritno, Universitas Gadjah Mada, Indonesia
                   Tien-Rein Lee, Huafan University, Taiwan
                   Haisong Xu, Zhejiang University, China
                   Chanprapha Phuangsuwan, Rajamangala Univ of Technology Thanyaburi, Thailand
                   Mikiko Kawasumi, Meijo University, Japan
                   Naoyuki Osaka, Kyoto University, Japan
                   Miyoshi Ayama, Utsunomiya University, Japan
                   Hirohisa Yaguchi, Chiba University, Japan
                   Miho Saito, Waseda University, Japan
                   Takahiko Horiuchi, Chiba University, Japan
                   Toshio Fukuda, Meijo University, Japan

Reviewer
                   Wahyu Supartono, Universitas Gadjah Mada, Indonesia
                   Naoyuki Osaka, Kyoto University, Japan
                   Hirohisa Yaguchi, Chiba University, Japan
                   Miho Saito, Waseda University, Japan
                   Miyoshi Ayama, Utsunomiya University, Japan
                   Nafis Khuriyati, Universitas Gadjah Mada, Indonesia
                   Anggoro Cahyo Sukartiko, Universitas Gadjah Mada, Indonesia

Editor-in-Chief: Dr. Adi Djoko Guritno

MESSAGE FROM CONFERENCE CHAIR

Greetings to all of us, may all be healthy and happy.

Praise and gratitude we pray to the presence of Allah SWT who has provided convenience and smoothness in the implementation of the Asia Color Association (ACA) Conference 2021 in Indonesia which will be held at Uiversitas Gadjah Mada whose implementation is managed by the Department of Agroindustrial Technology, Faculty of Agricultural Technology and Faculty of Postgraduate. The ACA 2021 conference uses the theme "Color and Culture" which represents the very broad role of color and its important application in relation to culture wherever it is located. Color is very important as a symbol that is understood by everyone but also has a psychological, religious, cultural effect that is naturally felt by everyone without realizing it.

The ACA 2021 conference involved 16 participating universities from Japan, Taiwan, Thailand, China, India and the host Indonesia. It is very interesting to observe the development of research that continues to develop regarding this color because in almost all human activities it is always related to color, both in the context of health, culture, perception and social values that are different in each country. Color is not only important to be managed and designed for the benefit of human beings but the color of nature which is a gift from God always surrounds our lives so beautifully and this encourages continuous research and understanding of the phenomenon.

The holding of the 2021 ACA Conference feels special because it will be held online due to the unfinished COVID- 19 pandemic situation and due to health and safety considerations, it was decided to hold it in a virtual conference. But I hope that even though this conference is held virtually, it will not reduce its meaning, benefits and excitement for all of us who attend the conference.

On this auspicious occasion, I would also like to thank the executive committee of the Asia Color Association, reviewers, International Advisory Board and scientific committees that I cannot mention one by one, all of whom have played a major role in assisting the screening of the paper. Processing and providing constructive suggestions so that the ACA Conference 2021 can be held, starting from publishing abstract books, organizing conferences and publishing proceedings after the conference. In my welcome I would like to thank the committee members who have worked so hard for this conference, I am always proud of all of you. Thanks again for all of your hard work.

I also thank the Rector of Universitas Gadjah Mada, the Dean and Head of the Study Program from the Faculty of Agricultural Technology and the Faculty of Postgraduates who have been willing to support and host the 2021 ACA Conference. And of course, also thank those who are very valuable and I am always proud of colleagues and all conference participants who have jointly made this event a success.

Finally, I hope that this proceeding will be useful to support the smooth implementation of this conference. I really hope that the network within the Asia Color Association will continue to be well established so that we can all benefit from this conference.

Thank you very much

Conference General Chair ACA 2021

Dr. Adi Djoko Guritno,
Department of Agroindustrial Technology
Universitas Gadjah Mada

KEYNOTE SPEAKERS

Prof. Mitsuo Ikeda

Rajamangala University of Technology
Thanyaburi

INVITED SPEAKERS

Prof. Edia Rahayuningsih

Department of Chemical Engineering-
Universitas GadjahMada
Director of Gama Indigo

AssocProf.PichayadaKatemake

Chulalongkorn University-President ofColor Society
Thailand

Dr. Rr.ParamithaDyah Fitriasari

Performing Arts and Visual Arts Studies School of
Postgraduate
Universitas GadjahMada

Gregorius Stanley

Konica MinoltaIndonesia

Table of Contents

A STUDY ON THE COLOUR OF MASKS FOR FRONTLINE RETAIL STAFFS

Hsien-Hsiang Meng[1*], Ray-Chin Wu[2] and Li-Chieh Chen[3]

[1] *The Graduate Institute of Design Science, PhD student, Tatung University, Taipei, Taiwan, R.O.C.*
[2]*Department of Media Design, Faculty of Design, Tatung University, Taipei, Taiwan, R.O.C.*
[3]*Department of Industrial Design, Faculty of Design, Tatung University, Taipei, Taiwan, R.O.C.*

*Corresponding author: Hsien-Hsiang Meng, mengruny@gmail.com

ABSTRACT

With the outbreak of COVID-19, wearing a mask is one of the most important ways to prevent from this pandemic disease. In Year 2020, indoor workers were requested to wear masks in some countries, but no regulation for colour and material. Since the mask covers half of the frontline staff's facial expression, the appearance of mask may influence customers' judgement on the frontline retail staffs, or probably affect the decision of approaching them or not. Therefore, the objective of this study is to investigate the effect of mask colour on the attributes of frontline staffs' image. By market survey, seven kinds of single colour masks issued by the Department of Health in Taiwan and available to all citizen were collected as the sample for this study. Based on literature review and Delphi Method, twelves adjectives suitable for frontline staffs' image were selected by ten field experts in two rounds. The researchers then categorized twelves adjectives into four major attributes and developed a questionnaire for mask survey. Forty university students participated in the survey. They were asked to pick up the top three masks that were close to the image of each adjective, from the seven single colour masks. Based on data analysis and Chi-Square Test, the most popular mask colours for each of the four attributes were identified. Light pink(ltRP) is close to Friendliness. Light pink(ltRP) and white are close to Expertise. Light purple(ltP) and light pink(ltRP) are close to Aesthetics. White and light pink(ltRP) are close to Self-confidence. The hue-angle of these welcome masks are located from 270º to 360º. This result can be provided to managers and frontline staffs for retail practice and management.

INTRODUCTION

When COVID-19 broke out in 2019, WHO asked for facial mask wearing as one of the safety precautions. Initially, masks with any kind of materials, styles and colours were in need urgently. Now masks with plenty of colours, patterns and materials are available, and the frontline staffs have many different choices of colourful masks on their face. In order to manage consistency in frontline staffs, some department stores and restaurants in Taiwan asked them to wear only "light single colour" or "specific colour" masks. If any disobey, the staff would be fined as penalty. Since a mask covers the expression of the mouse area, the appearance of mask may influence customers' judgement to approach frontline staffs or not. Therefore, the objective of this study is to investigate the effect of mask colour on the attributes for frontline staffs' image and to find out the suitable mask colours for employees in the retail service. In compliance with government regulations and to meet customer preferences, the results of this study will serve as management references to retails staffs and managers.

LITERATURE REVIEW

Impact of Mask Wearing

As COVID-19 outbreak, researches showed that face masks can reduce the total number of infections and deaths, and can delay the peak time of the epidemic [1]. U.S. CDC even advised the general public to wear cloth masks when going outdoors [2]. Wearing mask not only increases the vigilance against the epidemic, but also changes the appearance of frontline workers, thus increasing the difficulty of non-verbal human communication [3] and affecting consumer judgment and satisfaction. Since mask wearing is a daily routine for retail business, masks seem like uniform. Some literature about uniform studies focused on customers' perceptions as image recognition, service quality, and professionalism [4]. However these studies were limited to body uniform. Face masks were not mentioned.

Colour Emotion

Appropriate colour image of uniforms could have a significant and positive correlation with the professionalism, perceived image and popularity of the company [5][6]. Besides, research from Nakajima showed that the perception of facial expressions was influenced by facial colour [7]. Benitez-Quiroz found that visible facial colors allow observers to successfully transmit and visually interpret emotion even in the absence of facial muscle activation [8]. Furthermore, Jonauskaite found that lighter colours were matched to joy and relaxation (positive moods) than fear and sadness (negative moods) [9]. Takahashi and Kawabata found facial expressions are accompanied by facial colour [10]. Facial expressions should relate more closely to facial colour than emotional words. Pinkish colours and orange were given as responses for joy or the emotions relevant to blushes [10].

Although masks cover facial expressions, could have the potential to deliver images by their colours. Facial masks are like makeup, using colours to convey emotions. Based on these scholars' research on face colour emotions, what colour masks can increase customers' preference will be the focus of this study.

METHOD

Masks Sampling and Colour Measuring

In this study, available masks provided by the Department of Health (DOH) Taiwan were collected as samples, due to government's certification with sufficient quantity and budget for all citizens. The quantity of colour sample masks for experiments were determined when the DOH colour masks survey reached 'theoretical saturation' [11]. Finally, seven single-coloured sample masks were selected through theoretical saturation survey, including white (W), light pink (ltRP), light purple (ltP), light yellow (ltY), light blue (ltB), light orange (ltYR), and light green (ltG) shown in Figure 1.

Figure 1. Seven Single Coloured Sample Masks

As the sample masks determined, the NCS Colour PIN instrument was used to measure and obtain CIELAB coordinates. Each sample mask was measured at three different points (left, center, and right), then the average value was calculated.

Colour Image Adjectives selected by Delphi Method

To explore the image of the frontline retail staffs, Shigenobu Kobayashi Colour Image Scale was adopted in this study. Through Delphi method, suitable adjectives were selected from 180 key words in Shigenobu Kobayashi Colour Image Scale. The Delphi method is a forecasting process framework based on the results of multiple rounds of questionnaires sent to a panel of experts. This process combines the benefits of expert analysis with elements of the wisdom of crowds. Ten retail experts were invited into this panel. The final adjectives were organized and categorized into major attributes as the base elements for questionnaire development.

Questionnaire Investigation with Qualified Participants

Forty University students with retail shopping experience were invited as participants for questionnaire survey. They ranked top three colour masks for each question relevant to the colour image adjective. For each question, Chi-square test with 0.05 significance level was used to determine whether there were significant differences among colour masks. The most popular colour masks were then identified based on the highest frequency of ranked first in each question.

RESULTS

The colours of seven sample masks were measured with colour reader (ColourPin II). The results of CIELAB (D65, 2°) coordinates and corresponding chroma C^*_{ab}, hue-angle values h_{ab} were shown in Table 1. According to Table 1, these sample masks were all in high lightness and with low to medium chroma values. Their distributions in the CIE a*-b* coordinates were shown in Figure 2.

Table 1. Color Measurement for Seven Sample Masks

Masks Colors	L	a*	b*	C^*_{ab}	h_{ab}
White	92.89	1.01	-0.78	1.28	322
ltPR	81.14	21.86	-5.32	22.50	346
ltP	74.18	15.87	-18.22	24.16	311
ltY	91.65	-7.70	25.46	26.60	107
ltB	85.07	-5.92	-11.10	12.58	242
ltYR	86.18	10.01	12.50	16.01	51
ltG	88.82	-17.31	11.00	20.51	148
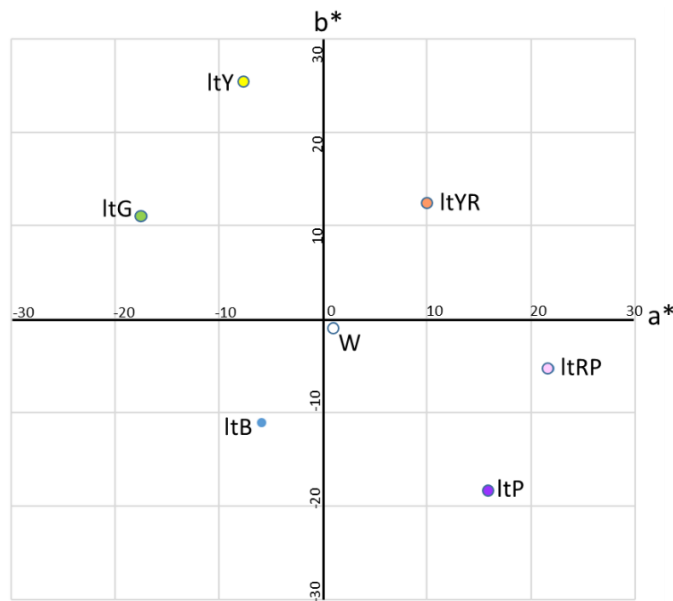
Figure 2. CIE a*-b* of Seven Sample Masks

Through the Delphi Method, 10 retail experts were invited to select the adjectives to fit frontline retail staffs image in two rounds. These adjectives included elegant, stylish, chic, friendly, tender, amiable, intellectual, distinguished, cultivated, mature, steady and tasteful. The twelve adjectives were then categorized into four major attributes (Aesthetics, Friendliness, Expertise and Self-confidence) and developed into a questionnaire with 12-questions. The detailed contents of the questionnaire were shown in Table 2.

Table 2. Questionnaire

Attributes	Item	Adjectives Items Description
Aesthetics	A1	This mask makes salesperson "Bright Complex".
	A2	This mask makes salesperson "Elegant & Fashionable".
	A3	This mask makes salesperson "Chic & Styling".
Friendliness	B1	This mask makes salesperson "Smiling".
	B2	This mask makes salesperson "Friendly".
	B3	This mask makes salesperson "Amiable and No Stress".
Expertise	C1	This mask makes salesperson "Well-Trained".
	C2	This mask makes salesperson "Capable".
	C3	This mask makes me believing salesperson's "Recommendation & Suggestion".
Self confidence	D1	This mask makes salesperson eyes" Steady & Serious".
	D2	This mask makes salesperson "Generous".
	D3	This mask makes salesperson "Trustworthy".

Forty students (25 females, 14 males, and 1 unspecified) participated in the survey, with 62.5% females and 35.0% males. For age, 87.5% participants were under 25 years old. For education, 85% were undergraduate students and 15% were graduate students. The results were shown in Table 3.

Table 3. Respondent Characteristics

Parameter	Level	Frequency [n(%)]
Gender	Male	14(35.0)
	Female	25(62.5)
	Unspecified	1(2.5)
Age(years)	15-19	5(12.5)
	20-24	30(75.0)
	25-29	3(7.5)
	30-34	1(2.5)
	35-39	0
	40-44	0
	45-49	1(2.5)
Education	Undergraduate	34(85.0)
	Graduate	6(15.0)

The results for the frequency of ranked first from the questionnaire were shown in Table 4. According to Chi-square test, there were significant differences in frequency among sample masks for all 12 questions ($p < 0.05$). In Table 4, the frequency of ranked first mask was highlighted with yellow background for each questionnaire item.

For each attribute, light purple (ltP) and light pink (ltRP) were close to Aesthetics, light pink (ltRP) was close to Friendliness. Light pink (ltRP) and white were close to Expertise. White and light pink (ltRP) were close to Self-confidence. The three popular colour masks in Figure 2 were all located in the fourth quadrant in CIE a*-b*coordinate.

Table 4. Frequency of Ranked First for Seven Sample Masks

Attributes	Item	W	ltRP	ltP	ltY	ltB	ltYR	ltG	p Value
Aesthetics	A1	6	12	8	5	1	2	6	0.0270
	A2	5	10	14	4	2	2	3	0.0012
	A3	5	5	12	8	1	6	3	0.0400
Friendliness	B1	7	22	2	7	0	1	1	0.0000
	B2	8	14	4	2	3	2	7	0.0029
	B3	11	13	3	2	2	1	8	0.0003
Expertise	C1	11	5	8	0	1	4	11	0.0019
	C2	8	15	9	0	3	1	4	0.0001
	C3	8	11	9	4	1	2	5	0.0236
Self Confidence	D1	14	5	7	4	3	4	2	0.0088
	D2	8	12	9	4	3	1	3	0.0105
	D3	13	13	2	5	2	2	3	0.0001

CONCLUSION

Based on the result of questionnaire survey, three colour masks, i.e. light pink (ltRP), White (W) and light purple (ltP), were mostly close to four attributes compared to other mask samples. Retail managers can take this result as a reference for mask choosing in the future. Since four attributes yield different results, retail managers can select suitable coloured masks that fit the characteristics of brand attributes, or emphasize and highlight a certain attribute, so that consumers can feel the frontline staff image created by the colours of masks.

RECOMMENDATIONS FOR FURTHER RESEARCH

In Kodzoman's study, it was noted that the color, style, and texture of individual aesthetics expression were related to gender, ethnicity, race, class, nationality, religion, sex, and age [12]. Since this study was conducted with limited variables, it could be extended to incorporate other variables. Furthermore, other mask design parameters, such as surface materials, shape and form styles, and multi-colour patterns could be studies in the future.

REFERENCES

1. Worby, C. J., & Chang, H. H. (2020). Face mask use in the general population and optimal resource allocation during the COVID-19 pandemic. *medRxiv: the preprint server for health sciences*, 2020.04.04.20052696.
2. Tirupathi, R., Bharathidasan, K., Palabindala, V., Salim, S. A., & Al-Tawfiq, J. A. (2020). Comprehensive review of mask utility and challenges during the COVID-19 pandemic. *Le infezioni in medicina*, 28(suppl 1), 57–63.
3. Schlögl, M., & A Jones, C. (2020). Maintaining Our Humanity through the Mask: Mindful Communication During COVID-19. *Journal of the American Geriatrics Society.* 68(5), E12–E13.
4. Shao, C.Y., Baker, J., & Wagner, J. (2004). The effects of appropriateness of service contact personnel dress on customer expectations of service quality and purchase intention: The moderating influences of involvement and gender. *Journal of Business Research*, 57, 1164-1176.
5. Evelina Lidya Wati, Angeline Mia, Mariani, Vini (2015). Uniforms and Perception of Professionalism. *Advanced Science Letters*. Volume 21, Number 4, April 2015, pp. 723-726(4).
6. PARK, H., & PARK, S. (2019). The Effect of Emotional Image on Customer Attitude. *The Journal of Asian Finance*, Economics and Business. 6(3), 259–268.
7. Nakajima, K., Minami, T., & Nakauchi, S. (2017). Interaction between facial expression and color. *Scientific reports,* 7, 41019. **https://doi.org/10.1038/srep41019**
8. Benitez-Quiroz, C. F., Srinivasan, R., & Martinez, A. M. (2018). Facial color is an efficient mechanism to visually transmit emotion. *Proceedings of the National Academy of Sciences of the United States of America*, 115(14), 3581–3586.
9. Jonauskaite, D., Althaus, B., Dael, N., Dan-Glauser, E., & Mohr, C. (2019). What color do you feel? Color choices are driven by mood. *Color Research and Application*, 44, 272-284.
10. Takahashi, F., & Kawabata, Y. (2018). The association between colors and emotions for emotional words and facial expressions. *Color Research & Application*, 43(2), 247–257. **https://doi.org/10.1002/col.22186**
11. Glaser, B., & Strauss, A. (1967). *The Discovery of Grounded Theory: Strategies for Qualitative Research*. New York: Aldine De Gruyter.
12. Kodzoman, Duje. (2019). The Psychology of Clothing: Meaning of Colors, Body Image and Gender Expression in Fashion. *Textile & Leather Review*. 2. 10.31881/TLR.2019.22.

VISUAL OBJECT IDENTIFICATION BY COLORS VS. BY SHAPES – DOES GENDER DIFFERENCE REALLY EXIST?

Akira Asano[1]*, Rina Matsushita[1], and Chie Muraki Asano[2]

[1]Faculty of Informatics, Kansai University, Japan.
[2] Sapporo Campus, Hokkaido University of Education, Japan.

*Corresponding author: Akira Asano, a.asano@kansai-u.ac.jp

Keywords: visual perception, shape and color, gender difference

ABSTRACT

It has been said, especially in Japan, that there is a gender difference in the style of visual object identification. It is suggested that men tend to identify objects based more on shapes than on colors and women vice versa. This research investigates whether it is true through experiments of identifying one of two objects whose colors are interchanged. For example, illustrations of "an orange in red color" and "an apple in orange color" were shown to respondents, and they were requested to select "the illustration you think to be closer to an apple." The respondents are also asked their age and their preferences of colors appearing in the pairs, for example, which of red or orange is preferred. In the experimental results, there is almost no difference between the responses of males and those of females or between the responses of the younger group and those of the older group. It indicates that the style of visual object identification does not depend on gender or age.

INTRODUCTION

It is said that there is a gender difference in the style of visual object identification, especially in Japan, as a kind of popular interest. According to the popular view, men tend to identify objects based more on shapes than on colors and women vice versa.

The view is supported by a paper [1] stating that women are biologically more sensitive to colors than men. The research investigated the difference of color sensitivities between men and women through biological experiments avoiding cultural biases, and it found a small but significant difference. Our previous research [2] also noted that women are more sensitive and precise in preferences of colors and colors of products, according to a survey in Japan. The research investigated gender differences in coincidences of preferences in colors and choices in colors of consumer electronics products. The results showed that women have more tendency that the coincidence is higher for handheld devices, such as smartphones, than for non-portable ones, such as refrigerators in the kitchen.

This research investigates whether the gender difference in the style of visual object identification is true or not through experiments of identifying one of two objects whose colors are interchanged. For example, illustrations of "an orange in red color" and "an apple in orange color" were shown to respondents, and they were requested to select "the illustration you think to be closer to an apple." The pair of "cloverleaf in pink" and "cherry blossom in green" and two pairs of anime characters famous in Japan were also employed in the experiments. The respondents are also asked their age and their preferences of colors appearing in the pairs, for example, which of red or orange is preferred.

According to the experimental results, we found almost no difference between the responses of males and those of females or between the responses of the younger group and those of the older group. It indicates that the style of visual object identification, that by color or that by shape, does not depend on gender or age.

EXPERIMENTS

The experiment examines whether two items in a category are distinguished by color or by shape to present two items whose colors are interchanged and ask which is comparatively properly identified.

The respondents answered their age and gender and selected their preferred color or item from each of the following pairs: red/orange (color), pink/green, red/blue, red/green, and orange (fruit)/apple. Then the respondents were shown the following four pairs of illustrations:

(1) "An orange in red color" and "an apple in orange color," as shown in Fig. 1.
(2) "A set of clover leaves in pink color" and "a piece of cherry blossoms in green color," as shown in Fig. 2.
(3) The *Mario Bros.*, a famous video game, characters [3], "Mario with the green cap (originally red)" and "Luigi with the red cap (originally green).
(4) The *Sesame Street*, a famous TV series, characters [4], "Elmo in blue (originally in red)" and "Cookie Monster in red (originally in blue)."

(Illustrations of (3) and (4) are not shown here to avoid copyright problems.)

The respondents answered which is identified apple/ cherry blossom / Elmo / Mario in each pair. The number of the respondents was 123, including 45 males and 78 females. Their age ranged from 10s to 60s, and almost half of the respondents were younger than 30, and the others were older.
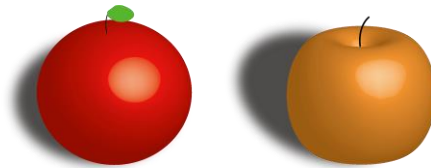
Figure 1. Orange in red (left) and apple in orange (right)

Figure 2. Clover in pink (left) and cherry blossom in green (right)

RESULTS

Tables 1-3 show the results of the experiments of showing the illustrations of "orange in red color" and "apple in orange color" to the respondents and asked, "Which is identified as an apple?" Each of the ratios indicates that in the row. Tables 1, 2, and 3 present the results by gender, by color preference, and by item preference, respectively.

Table 1. Which is identified as an apple? (by gender)

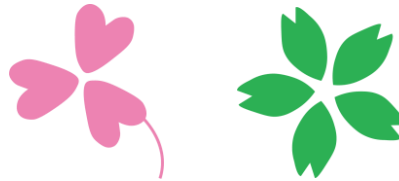| gender	age	orange in red color	apple in orange color	total
men	< 30	9 (90.0%)	1 (10.0%)	10
	>= 30	18 (51.4%)	17 (48.6%)	35
	total	27 (60.0%)	18 (40.0%)	45
women	< 30	46 (86.8%)	7 (13.2%)	53
	>= 30	18 (72.0%)	7 (28.0%)	25
	total	64 (82.1%)	14 (17.9%)	78
total	< 30	55 (87.3%)	38 (12.7%)	63
	>= 30	36 (60.0%)	24 (40.0%)	60
	total	91 (74.0%)	32 (26.0%)	123

Table 2. Which is identified as an apple? (by color preference)

preference	age	orange in red color	apple in orange color	total
red	< 30	27 (84.4%)	5 (15.6%)	32
	>= 30	17 (60.7%)	11 (39.3%)	28
	total	44 (73.3%)	16 (26.7%)	60
orange	< 30	28 (90.3%)	3 (9.7%)	31
	>= 30	19 (59.4%)	13 (40.6%)	32
	total	47 (74.6%)	16 (25.4%)	63
total	< 30	55 (87.3%)	8 (12.7%)	63
	>= 30	36 (60.0%)	24 (40.0%)	60
	total	91 (74.0%)	32 (26.0%)	123

Table 3. Which is identified as an apple? (by item preference)

preference	age	orange in red color	apple in orange color	total
apple	< 30	24 (82.8%)	5 (17.2%)	29
	>= 30	12 (54.5%)	10 (45.5%)	22
	total	36 (70.6%)	15 (29.4%)	51
orange	< 30	29 (90.6%)	3 (9.4%)	32
	>= 30	14 (70.0%)	6 (30.0%)	20
	total	43 (82.7%)	9 (17.3%)	52
none	< 30	2 (100.0%)	0 (0.0%)	2
	>= 30	10 (55.6%)	8 (44.4%)	18
	total	12 (60.0%)	8 (40.0%)	20
total	< 30	55 (87.3%)	8 (12.7%)	63
	>= 30	36 (60.0%)	24 (40.0%)	60
	total	91 (74.0%)	32 (26.0%)	123

If it is true that men tend to identify objects based more on shapes than on colors and women vice versa, the number of respondents who select "apple in orange color" is more in men and less in women. However, Table 1 shows that it is not true; The number of men who selected "apple in orange color" (40.0%) is less than those who selected "orange in red color" (60.0%), although the ratio of those who selected "orange in red color" is higher in women (82.1%) than in men (60.0%). According to Tables 2 and 3, there is almost no difference between color or item preferences.

Tables 4 and 5 show the results of the experiments of showing the illustrations of "clover in pink" and "cherry blossom in green" to the respondents and asked, "Which is identified as a cherry blossom?" It is

not observed any significant difference in gender or in color preference. The ratio of those who selected "cherry blossom in green," i. e. identified by shape, is even higher in women (52.6%) than in men (40.0%).

Table 4. Which is identified as a cherry blossom? (by gender)

gender	age	clover in pink	cherry blossom in green	total
men	< 30	8 (80.0%)	2 (20.0%)	10
	>= 30	19 (54.3%)	16 (45.7%)	35
	total	27 (60.0%)	18 (40.0%)	45
women	< 30	27 (50.9%)	26 (49.1%)	53
	>= 30	10 (40.0%)	15 (60.0%)	25
	total	37 (47.4%)	41 (52.6%)	78
total	< 30	35 (55.6%)	28 (44.4%)	63
	>= 30	29 (48.3%)	31 (51.7%)	60
	total	64 (52.0%)	59 (48.0%)	123

Table 5. Which is identified as a cherry blossom? (by color preference)

preference	age	clover in pink	cherry blossom in green	total
pink	< 30	18 (64.3%)	10 (35.7%)	28
	>= 30	7 (63.6%)	4 (36.4%)	11
	total	25 (64.1%)	14 (35.9%)	39
green	< 30	17 (48.6%)	18 (51.4%)	35
	>= 30	22 (44.9%)	27 (55.1%)	49
	total	39 (46.4%)	45 (53.6%)	84
total	< 30	35 (55.6%)	28 (44.4%)	63
	>= 30	29 (48.3%)	31 (51.7%)	60
	total	64 (52.0%)	59 (48.0%)	123

Tables 6 and 7 show the results of the experiments of showing the illustrations of "Mario with the green cap" and "Luigi with the red cap" to the respondents and asked, "Which is identified as Mario?", by gender and by color preference. It is observed that Mario is identified by its shape, not depending on gender or color preference. It suggests that Mario and Luigi are remembered by their faces because they are famous video game characters.

Tables 8 and 9 show results in the case of Elmo / Cookie Monster. In this case, Elmo is identified by its color, not depending on gender or color preference. It suggests that Elmo and Cookie Monster are remembered by their colors, differently from Mario / Luigi, maybe because they are simple animation characters and the colors are more informative than the shapes.

Table 6. Which is identified as Mario? (by gender)

gender	age	Mario with the green cap	Luigi with the red cap	total
men	< 30	10 (100.0%)	0 (0.0%)	10
	>= 30	29 (82.9%)	6 (17.1%)	35
	total	39 (86.7%)	6 (13.3%)	45
women	< 30	44 (84.6%)	8 (15.4%)	52
	>= 30	22 (84.6%)	4 (15.4%)	26
	total	66 (84.6%)	12 (15.4%)	78
total	< 30	54 (87.1%)	8 (12.9%)	62
	>= 30	51 (83.6%)	10 (16.4%)	61
	total	105 (85.4%)	18 (14.6%)	123

Table 7. Which is identified as Mario? (by color preference)

preference	age	Mario with the green cap	Luigi with the red cap	total
green	< 30	25 (92.6%)	2 (7.4%)	27
	>= 30	32 (86.5%)	5 (13.5%)	37
	total	57 (89.1%)	7 (10.9%)	64
red	< 30	29 (82.9%)	6 (17.1%)	35
	>= 30	19 (79.2%)	5 (20.8%)	24
	total	48 (81.4%)	11 (18.6%)	59
total	< 30	54 (87.1%)	8 (12.9%)	62
	>= 30	51 (83.6%)	10 (16.4%)	61
	total	105 (85.4%)	18 (14.6%)	123

Table 8. Which is identified as Elmo? (by gender)

gender	age	Elmo in blue	Cookie Monster in red	I don't know either	total
men	< 30	3 (30.0%)	6 (60.0%)	1 (10.0%)	10
	>= 30	12 (34.3%)	13 (37.1%)	10 (28.6%)	35
	total	15 (33.3%)	19 (42.2%)	11 (24.4%)	45
women	< 30	16 (30.8%)	36 (69.2%)	0 (0.0%)	52
	>= 30	10 (38.5%)	10 (38.5%)	6 (23.1%)	26
	total	26 (33.3%)	46 (59.0%)	6 (7.7%)	78
total	< 30	19 (30.6%)	42 (67.7%)	1 (1.6%)	62
	>= 30	22 (36.1%)	23 (37.7%)	16 (26.2%)	61
	total	41 (33.3%)	65 (52.8%)	17 (13.8%)	123

Table 9. Which is identified as Elmo? (by color preference)

preference	age	Elmo in blue	Cookie Monster in red	I don't know either	total
men	< 30	7 (28.0%)	18 (72.0%)	0 (0.0%)	25
	>= 30	6 (27.3%)	11 (50.0%)	5 (22.7%)	22
	total	13 (27.7%)	29 (61.7%)	5 (10.6%)	47
women	< 30	12 (32.4%)	24 (64.9%)	1 (2.7%)	37
	>= 30	16 (41.0%)	12 (30.8%)	11 (28.2%)	39
	total	28 (36.8%)	36 (47.4%)	12 (15.8%)	76
total	< 30	19 (30.6%)	42 (67.7%)	1 (1.6%)	62
	>= 30	22 (36.1%)	23 (37.7%)	16 (26.2%)	61
	total	41 (33.3%)	65 (52.8%)	17 (13.8%)	123

CONCLUSIONS

We have investigated in this paper whether the gender difference in the style of visual object identification is true or not through experiments of identifying one of two objects whose colors are interchanged. The experimental results do not support the statement that men tend to identify objects based more on shapes than on colors and women vice versa. The results suggest that the difference of identification styles by gender and color preference may appear more clearly in natural items than in characters in video games and TV series. It is expected to carry out more experiments in various conditions.

ACKNOWLEDGEMENT

REFERENCES

1. Abramov, I., Gordon, J., Feldman, O., & Chavarga A. (2012). Sex and Vision II: Color Appearance of Monochromatic Lights. *Biology of Sex Differences* 3 (1): 21. https://doi.org/10.1186/2042-6410-3-21
2. Asano, A., Deguchi, A., & Muraki Asano C. (2018). Preference of colors and colors of products, and its gender differences – survey on consumer electronics products. *Journal of the Color Science Association of Japan* 42 (6): supplement 37-39. [in Japanese]
3. *Mario Bros.,* https://www.nintendo.co.jp/n08/mariobros/ [in Japanese]
4. *Sesame Street,* https://www.sesamestreet.org/

BASIC COLOR NAME IN THAI: INVESTIGATION OF REGIONS AND GENDER

Nischanade Chitapanya[1]* Chanprapha Phuangsuwan[2], and Mitsuo Ikeda[2].

[1]Graduated School, Faculty of Mass Communication Technology, Rajamangala University of Technology Thanyaburi, Thailand.
[2]Color Research Center, Rajamangala University of Technology Thanyaburi, Thailand.

*Corresponding author: Nischanade Chitapanya, nischanade_p@mail.rmutt.ac.th

Keywords: Thai color names, Color categories, World color survey, Munsell color samples.

ABSTRACT

The varieties of color name can be influenced by cognitive process and linguistic-specific. Due to the diversity of Thai cultures, dialects, and environments that varied according to the regions, causing questions about the basic color name in Thai. Here we investigated the use of color name from 161 Thai-native speakers (89 females and 72 males) who live in 4 regions of Thailand; North, Northeast, central, and South. We employed 330 Munsell color chips taken from the Munsell Book of Color Glossy Edition: 320 chromatic chips, Munsell Value ranging from 2 to 9 with 40 equally spaced of Munsell Hue (2.5 R to 10 RP, in hue steps of 2.5) at the maximum chroma of each value in each hue, and 10 achromatic chips of Value from 1.5 to 9.5. The subjects were asked to name the color chips using monolexemic color term. Although there are diversity of cultures and dialects among 4 regions, we found pattern of color names used are similar in all regions, also number of color names are not significantly different (F=0.246, p=0.864): mean number of color name in all regions are about 19. We also noticed that in all regions the subjects used the least number of color names of 12. However, the t-test revealed gender difference that reflected the significant difference in color naming. Females use non-basic color term (non-BCTs) more significantly than males (t=2.65, p=0.004), mean number of non-BCTs in females is 20 and 17 in males. We also found that females use more non-BCTs to identify warm colors than males.

INTRODUCTION

Humans can perceive a wide range of colors, and to communicate about the colors people have invented various of color names. The names of colors can be influenced by cognitive processes as well as language and gender differences [1], [2], [3]. There is a variety of accents and dialects spoken in different regions of Thailand. Beside the interlingua/common Thai language which is mainly used in Central region of Thailand and used as the official Thai language, other regions also have their dialects: Northern dialect, Southern dialect, Isan dialect (Northeastern dialect), etc. According to the different dialect spoken in each region, we questioned whether it would affect the use of color names in different regions or not. In addition, we also examined the differences in the use of color names among different genders.

METHODOLOGY

Subjects

There were 161 Thai native speakers participated in this study, 89 females and 72 males, age ranges from 18 to 60 years-old, the average age was 21.95 ± 5.93. The subjects have domiciled in different provinces of Thailand, which in this study we divided the provinces into four regions: North (42 subjects), Northeast (38 subjects), central (50 subjects), and South (31 subjects) according to cultural characteristics. All subjects were tested for their normal color vision by using the Farnsworth Munsell D-

15 Color Vision Test before starting experiment, only the subject who pass the test could participate the experiment.

Color stimuli

We employed 330 color chips taken from the Munsell Book of Color Glossy Edition which were almost the same as was used in the World Color Survey [4]. The color chips composed of 320 chromatic chips, Munsell Value ranging from 2 to 9 with 40 equally spaced Munsell Hue (2.5 R to 10 RP, in hue steps of 2.5) at the maximum chroma of each value in each hue, and 10 achromatic chips of Value from 1.5 to 9.5 (see Fig. 1). The color chips have the size of 2 x 2.1 cm, each chip was mounted on a square cardboard of the size 7 x 7 cm covered by gray matte paper of approximately N5.
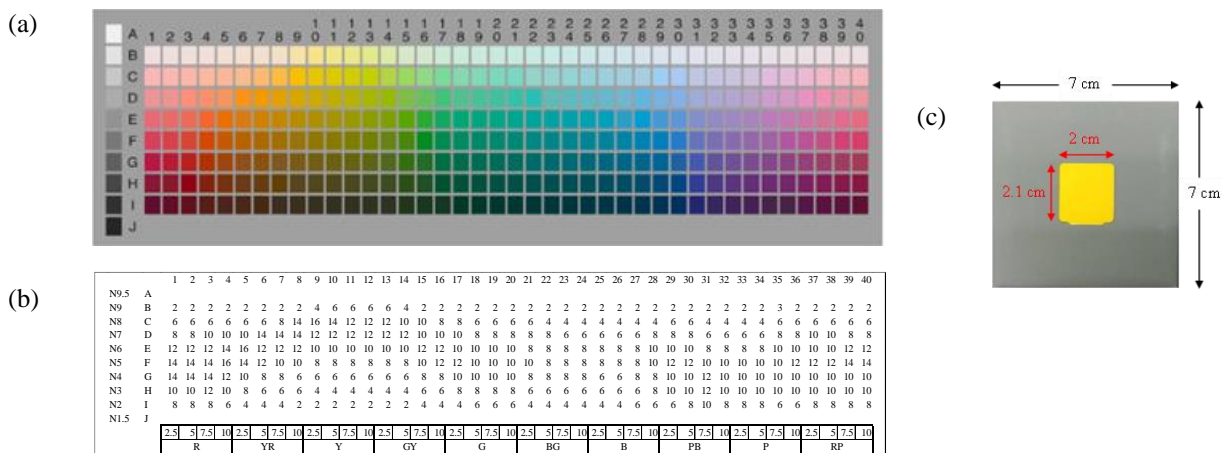
Figure 1. (a) World color survey color space. (b) Attribute of the Munsell color chips, two lowest horizontal rows indicated 40 hues with a step of 2.5 start from 2.5R to 10RP. The left most vertical column shows Munsell values from 1.5 to 9.5. Number inside the graph shows Munsell chroma of each chip. (c) Example of color chips.

Experimental booth

This study was conducted under control experiment using experimental booth. The booth has the size of 150 cm (L) x 180 cm (H) x 60 cm (W) illuminated by 6 fluorescent lamps provided illuminance at 2,509 lx, correlated color temperature 5,859 Kelvin, color rendering index (RI) was 97. The color samples were presented on a gray background surrounded by white walls of the booth.

Procedure

Before starting experiment, a subject was asked to fill a questionnaire to give his/her information about region, and dialect. After that, each of color chips was presented to a subject one by one with a fixed pseudorandom order. The subject was asked to give a color name by using a monolexemic color term; the color name without mixed colors (no combination of two or more colors, such as yellow-green) or modified colors (no word that specifies the darkness or brightness, such as dark green). However, the subject was allowed to use object names if they felt that those are commonly used in their daily life, such as coffee or banana, etc.

RESULTS

There was no statistically significant difference for the number of color names used per subject among four regions (F = 0.246, p = 0.864). The mean number of color names used per subject in North is 19.19, Northeast 18.58, Central is 19.50, and South is 19.03. The total number of color names obtained from all subjects in North was 72, Northeast was 56, Central was 74, and South was 67 color names. Figure 2 shows the color categories pattern used by the subjects in each region. We can see the color categories patterns in the four regions are very similar. Although there is difference in the shape of the categories, the number of color categories and location of those categories are the same.

Twenty highly frequent color names used by subjects in each region are shown in Figure 3. The subjects used similar color names in all four regions, *bai-tong* 'banana leaves' and *kram* 'indigo' found in the highly frequent list of color names in North. While *seat* 'orange trumpet' was found in the highly frequent list of color names in Northeast, and *mint* was found in the highly frequent list of color names in South. But none in the highly frequent list of other regions. This finding suggested that the subjects in the four regions have shared the same color names despite the dialects, cultural, and natural environment among the four regions are different.
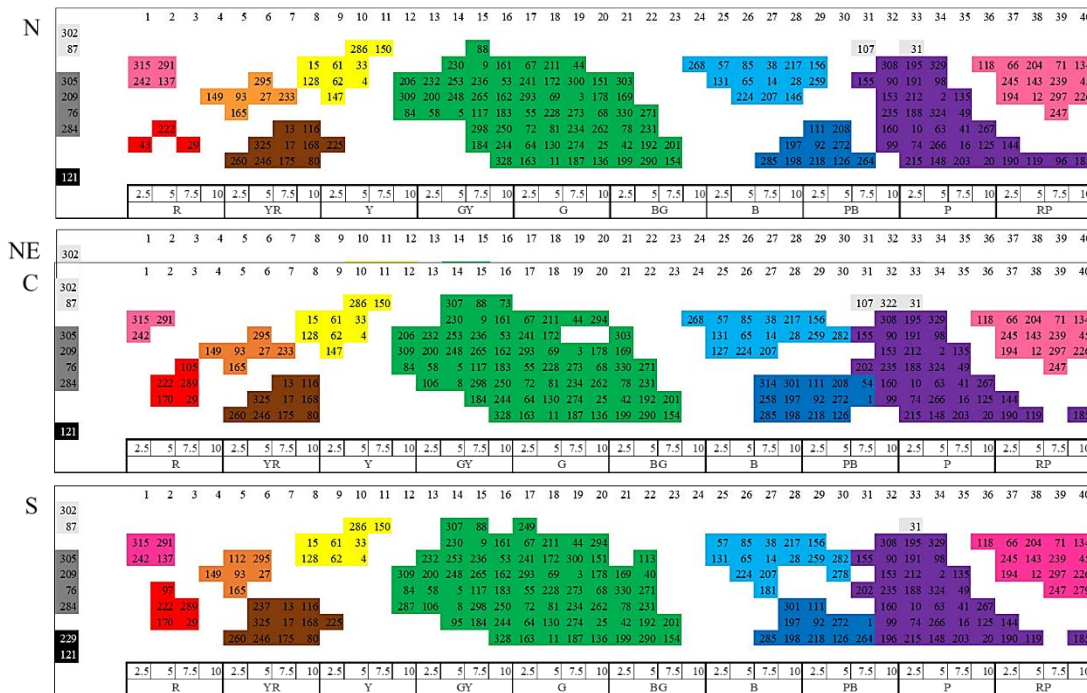

Figure 2. Color categories pattern for each region plotted on WCS color chart with the consistency of response ≥80% in each color chip, obtained from free-naming.
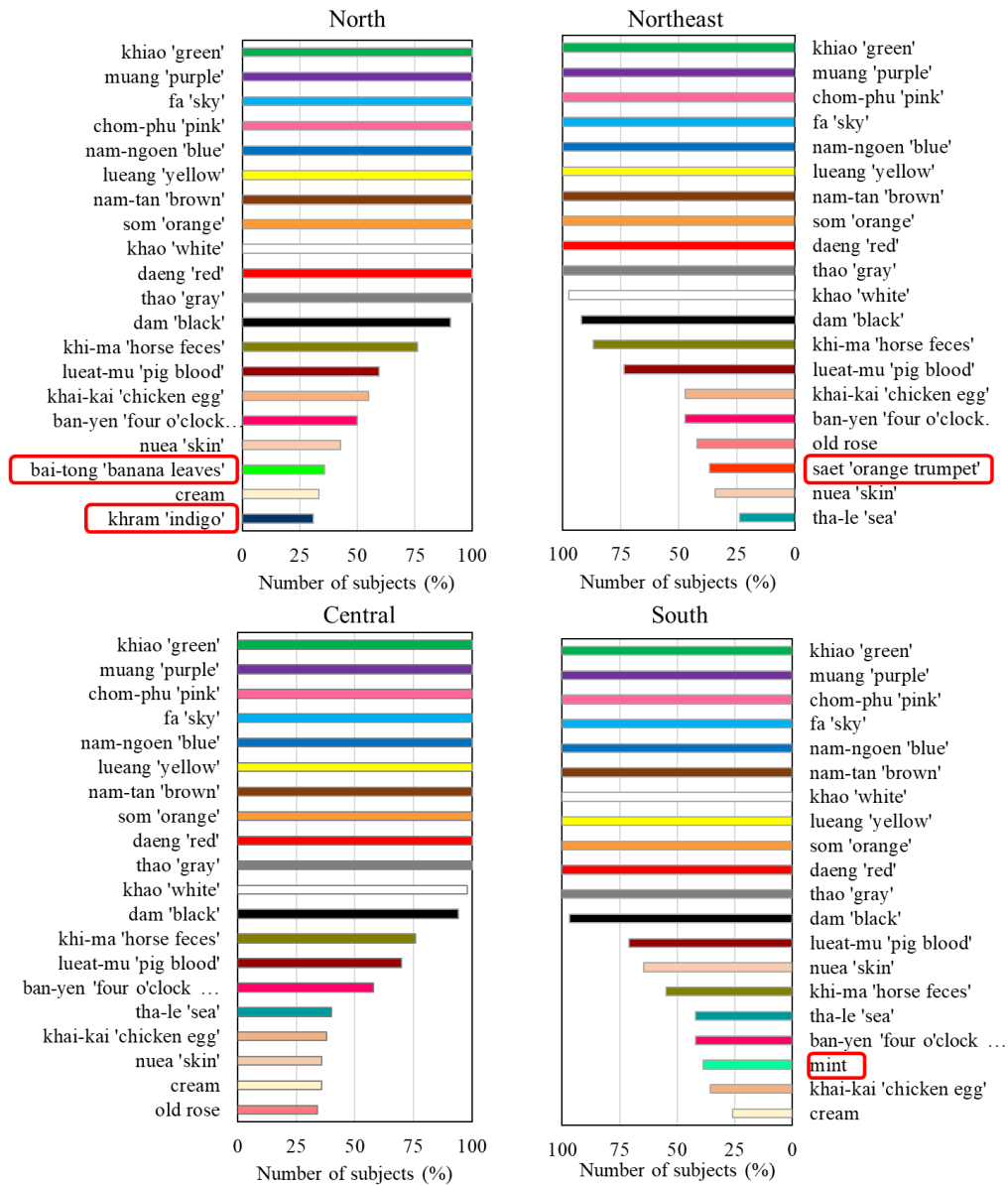
Figure 3. Twenty highly frequent color names used by subjects in each of four regions. The red rectangles indicated color names which highly frequent use in only that region, but not in other regions.

We also examined differences in the use of color names between females and males. There was a statistically significant difference in the number of color names used per subject among the two genders, which females used slightly more non-BCTs than males (t=2.65, p=0.004), see Figure 4. Total number of color names used by female was 89 and used by male was 80. The mean number of color names used per female subjects is 20.11 ± 5.45 and 17.88 ± 4.58 for male subjects. Figure 5 illustrated the color categories patterns used by females and males with ≥80% consensus of responses, the patterns appear quite same for both genders, especially the shape of *lueang* 'yellow' category, and all categories were in the same location.
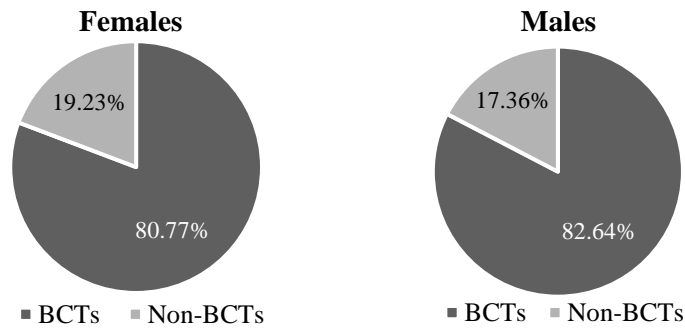
Figure 4. The proportion of use BCTs and non-BCTs in females and males.
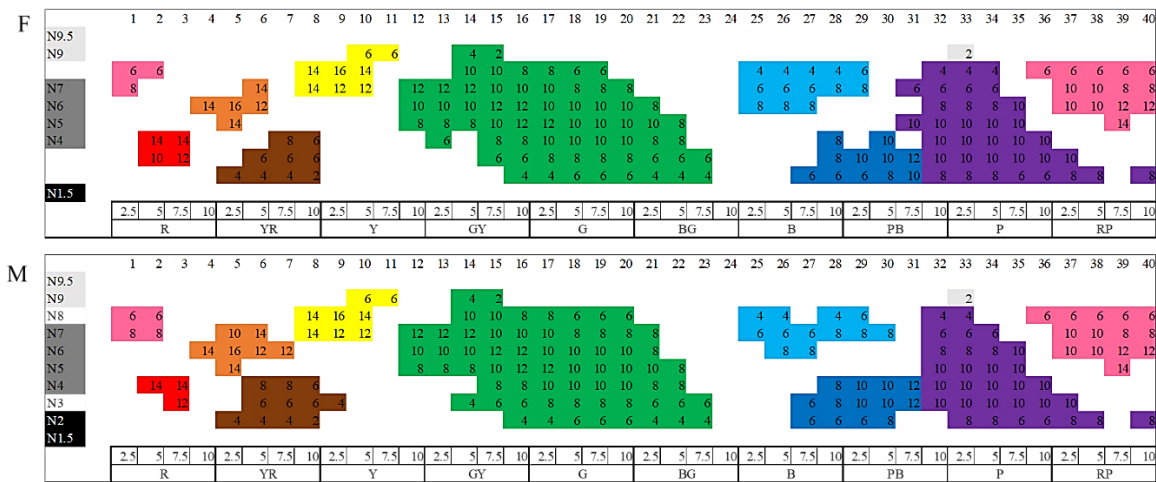

Figure 5. Color categories pattern for difference gender plotted on WCS color chart with the consistency of response ≥80% in each color chip, obtained from free-naming.

Figure 6 shows twenty color names that are frequently used for males and females, and there were similar trends in both genders. Both females and males used quite the same color names, but different in order and percent of use. It also reveals gender differences that some color names; *old rose* and *bai-tong* 'banana leaves' were frequently used for females but not in the males' frequent color names. Conversely, *cream*, and *saet* 'orange trumpet' were frequently used for males, but not among the females' frequent color names. In addition, we also found that females use more non-BCTs to identify warm colors than males, whereas males more refine in the use of more non-BCTs in cool colors, this is consistent with the finding of Mylonas et al. [1]. The color names in warm colors that were given by females but not by males are *chi-won* 'yellow robe of Buddhist monk', *klip-bua* 'petal of the lotus blossom', *kha-min* 'turmeric', *phlai* 'zingiber cassumunar', *ma-miao* 'pomerac', *pun-haeng* 'dry mortar', *cha-nom* 'milk tea', *khlon* 'mud', *sa-nim* 'rust', *thian* 'candle', *khrang* 'shellac', *thap-thim* 'ruby', *caramel*, *chat* 'crimson', *dok-khun* 'golden shower', *dao-rueang* 'marigold', and *fak-thong* 'pumpkin'. The color names in cool colors that were given by males but not by females are *tha-han* 'military color', *sa-rai* 'seaweed', *turquoise*, *cantaloupe*, *khi-pet* 'duck feces', *ton-kluai* 'banana tree', *ton-mai* 'tree', *phrik-yuak* 'bell pepper', *taeng-kwa* 'cucumber', *khi-nok* 'bird feces', and *fak* 'winter melon'.
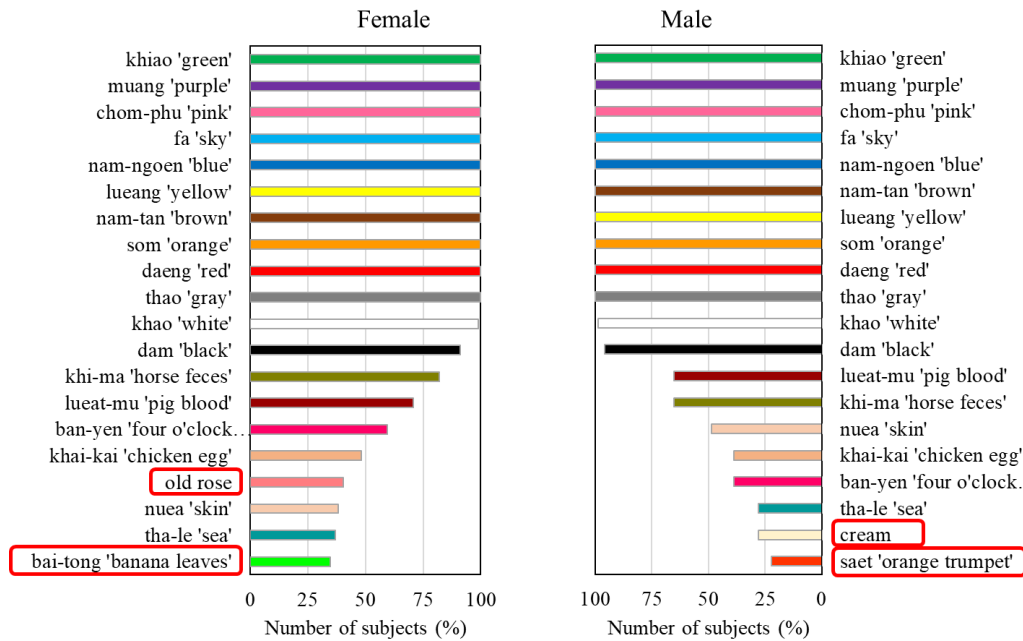
Figure 6. Proportion of use BCTs and non-BCTs in females and males. The red rectangles indicated color names which highly frequent use in only that gender, but not in another.

ACKNOWLEDGEMENT

REFERENCES

1. Mylonas, D. Paramei, G.V. MacDonald, L. (2014). Gender Differences in Colour Naming. In: Anderson W, Biggam CP, Hough CA, Kay CJ, editors. *Colour Studies: A Broad Spectrum.* Amsterdam/Philadelphia: John Benjamins, 225–239.

2. Lindsey, D. T., Brown, A. M. (2014). The color lexicon of American English. *Journal of Vision*, 14(2), 1-25.

3. Paramei GV, Griber YA, Mylonas D. (2017). An online color naming experiment in Russian using Munsell color samples. *Color Research & Application.* 43(3), 358– 374.

4. Cook RS, Kay P, Regier T. (2005). The World Color Survey Database. *Handbook of Categorization in Cognitive Science.* 223–241.

RESPONSE OF THE ORBITOFRONTAL AREA TO HARMONY BETWEEN COLOR AND FRAGRANCE IN A LIGHTING ENVIRONMENT

Gaku Yamashita[1], Midori Tanaka[2] and Takahiko Horiuchi[1]*

[1]*Graduate School of Science and Engineering, Chiba University, Japan.*
[2]*Graduate School of Global and Transdisciplinary Studies, Chiba University, Japan.*

*Corresponding author: Takahiko Horiuchi, e-mail horiuchi@faculty.chiba-u.jp

Keywords: Cross-modal effect, Sensitivity, LED, Harmony, NIRS

ABSTRACT

We use various senses to obtain information from the outside world. It is known that a plurality of senses act simultaneously, fusing the information gathered from multiple senses. In this study, we focused on the sense of sight and smell. Many studies have investigated the harmony between these two senses using colored objects, such as patches. In this study, we considered the relationship between the two using lighting colors. Conventional studies have shown that these differences in harmony occur in the orbitofrontal area. Thus, we investigated the response of the orbitofrontal area using NIRS. For fragrance, 20 types of aromas were prepared, and observers were asked to select the aromas that they felt was most pleasant and most unpleasant. Cotton wool was then soaked with these two aromas and placed in a light-shielding brown bottle to be used as a fragrance stimulus. For the lighting environment, we designed six types of lighting with different colors of different saturations using a programmable LED device, consisting of 14 types of LEDs. In the experiment, the observers wearing NIRS were instructed to sniff the stimulus in the light. Upon analysis, more activation was observed in oxyHb during the cross-modal condition as compared to that during the single-modal condition. Additionally, the left orbitofrontal area was found to be significantly activated compared to the right orbitofrontal area. Furthermore, a greater harmony between the lighting color and fragrance was attributed to a smaller orbitofrontal area activity cycle.

INTRODUCTION

In our daily lives, we obtain information from the five senses (sight, hearing, smell, taste, and touch) and make action selections. We use multisensory modalities to receive external stimuli and perceive the outside world. As such, a comprehensive judgment is made from that information. Therefore, in recent years, studies on the five senses, which have been conducted independently in the past, are been conducted in the form of multi-sensory research considering the fusion of all or some of the senses called the cross-modal or multi-modal condition.

Previous studies in the cross-modal of sight and smell have used "color" and "fragrance" to suggest that their harmony tends to additively enhance the original impression of the fragrance [1-3]. However, in these studies, object colors such as color patches have been used for "color," which is a visual stimulation. There have been few spatial verifications using lighting. Furthermore, the color of the target object itself was often defined according to the harmony color (strawberry fragrance: red, lemon fragrance: yellow), and it is possible that the subjectivity of the observers had a significant influence on the results. In recent years, studies that objectively analyze the cross-modal effect from the physiological

aspect have increased. Devices that measure brain waves, such as functional magnetic resonance imaging (fMRI) and near-infrared spectroscopy (NIRS), have become easier to use, enabling more objective verification. In particular, there are wearable devices that incorporate NIRS, which can measure oxyheamoglobin (oxyHb) concentration; with these devices it is easier to perform physical experiments than with conventional devices, and reproducibility has also been confirmed [4-5].

In this study, we used NIRS to measure the activity of the orbitofrontal area (cortex) and perform a physiologically cross-modal analysis of sight and smell, aiming for its application in space design in real life. The orbitofrontal area is the ventral surface of the prefrontal cortex of the brain and plays an important role in regulating cognitive and social behaviors associated with reward and punishment. In this paper, we analyze the cross-modal effect of harmony between color and fragrance in a lighting environment, based on the activity of the orbitofrontal area.

EXPERIMENTS

Smell stimulation

Essential oils were used for smell stimulation. In this study, we compared the cross-modal effect of the lighting color that humans recall when they hear the name of the fragrance, as well as the lighting color when they actually smell it. Therefore, the smell stimulation used must be such that the observer can easily recall the lighting color simply by hearing the name. Therefore, in these experiments, we used five essential oils, vanilla, mint, lime, grapefruit, and cypress, which are familiar to Japanese observers. We soaked cotton wool cut into 1 cm squares with the essential oil and placed it in a 20 ml brown light-shielding bottle to stimulate the sense of smell. At this time, we adjusted the intensity of the fragrance to approximately 100 in the odor meter (OMX-SRM, Shinei Technology Co., Ltd.) near the opening of the brown light-shielding bottle.

Visual stimulation

We used a spectral tunable lighting product (LEDCube, Thouslite) for visual stimulation. In these experiments, we referred to the practical color coordinate system (PCCS) when designing the lighting. We have 12 types of color names defined by PCCS at regular intervals (A: Poppy Red, B: Vermilion, C: Tanjarin, D: Dandelion, E: Fresh Green, F: Emerald Green, G: Peacock Green, H: Cyan, I: Ultra Marine, J: Bellflower, K: Mauve, L: Magenta). We calculated the CIE xy values from the RGB values of each color and provided them as an input to the LEDCube to reproduce the lighting color. We also considered differently saturated lighting for each color to verify a more harmonious cross-modal effect. We set white light $(x, y) = (0.33, 0.33)$ as the origin. The lighting colors that each chromaticity coordinate reduced to two-thirds is A' to L', and the lighting colors that each color reduced to one-third is A" to L". It was decided that these 36 types of lighting colors would be used for visual stimulation. We fixed the illuminance at 50 lx. The lighting colors of the stimuli on the chromaticity coordinates are shown in Fig. 1.

Experiment environment

The experimental setup is illustrated in Fig. 2. The LEDCube was installed on a gray-walled viewing booth. The viewing booth with the LED cube was placed on the table and covered with a blackout curtain. The observers sat on a chair and were presented with experimental stimuli. The temperature in the room where the experiments were conducted was fixed at 25 °C.

Selection of smell stimulation and investigation of harmonized lighting colors

To select which of the five smell stimulations were used in the experiment and which lighting color was used to compare the cross-modal effects, we conducted three preliminary surveys for five observers. First, we asked the observers to select one of the five types of smell stimulation that they was most

"pleasant" and one that they felt most was "unpleasant", and decided to use those two in a cross-modal experiment as smell stimulation. Next, we investigated the harmony between the fragrance and the lighting colors when the observers actually smelled the fragrance. The observers observed 36 types of lighting colors while sniffing the fragrance and evaluated the degree of harmony for each lighting color on a 10-point scale. This process was performed for each of the "pleasant" and "unpleasant" fragrances selected by the observers. Finally, we investigated the closeness between the colors that the observers recall from the name of the fragrance and the lighting colors. The observers were presented with 36 types of lighting colors for the names of the five essential oils, and they evaluated the closeness between the image color recalled from the names of the essential oils and lighting colors on a 10-point scale. The following eight lighting colors were used as visual stimuli in the cross-modal experiment: (1) a and b were most in harmony with the "pleasant" and "unpleasant" scents, respectively, when the subjects actually smelled the scents, (2) c and d were most dissonant with them, (3) a' and b' were most similar to the "pleasant" and "unpleasant" image colors recalled from the name of the scent, respectively, and (4) c' and d' were the most distant from them. According to these preliminary surveys, the smell and visual stimulation used in the cross-modal experiments were different among the five observers.
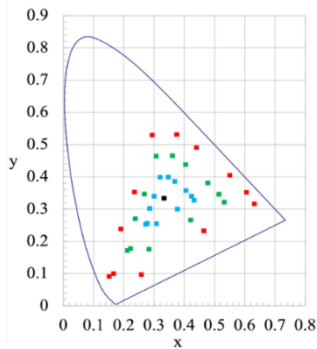

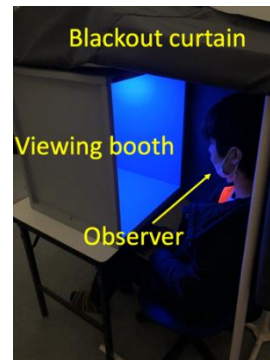**Figure 1. XY chromaticity distribution of lighting colors**

Figure 2. Experiment environment

Experimental method

These experiments consisted of three types: an experiment in which the smell stimulation was presented alone, an experiment in which the visual stimulation was presented alone, and a cross-modal experiment in which the smell and visual stimulations were presented simultaneously. In the smell stimulation experiments, two patterns of "pleasant" and "unpleasant" smells selected by the observers were performed. In the visual stimulation experiment, eight lighting colors described in the previous subsection were used. In the cross-modal experiments, we used two lighting colors for each condition: a and a' that were harmonious or similar to the pleasant fragrance (condition α), b and b' that were harmonious or similar to the unpleasant fragrance (condition β), c and c' that were dissonant or the images were separated with a pleasant fragrance (condition γ), and d and d' that were dissonant or the images were separated with a unpleasant fragrance (condition θ). These 18 trials were performed in one day. The process was performed for 2 days per observer. The observers were five male students aged 21–23 years.

For the smell stimulation experiment, observers sat on chairs in the viewing booth and wore a device equipped with NIRS technology (HB133, ASTEM). The lighting color in the viewing booth was set to white light (0.33, 0.33), to act as the reference light. The observers held a brown light-shielding bottle containing the smell stimulation in their hands. Sixty seconds after the start of NIRS measurement, we gave a voice signal, and the observers confirmed it and immediately sniffed the smell stimulation for 30 seconds. The observers waited for 120 s. For the visual stimulation experiments, similar to the smell stimulation experiment, the observers wore NIRS and sat in a chair. The lighting was set to the reference light. At 60 s after the NIRS measurement started, we changed the lighting of the viewing booth from the

reference light to a lighting color that was the visual stimulation. Thirty seconds after the presentation of the visual stimulation, we returned the lighting to the reference light and asked the observers to wait 120 seconds. For the cross-modal experiments, similar to the smell stimulation experiment, the observers wore NIRS and sat in a chair, and the lighting was set to a reference light. The observers then had smell stimulation in their hands in advance. Sixty seconds after the start of NIRS measurement, we changed the lighting of the viewing booth from the reference light to the lighting color, which was the visual stimulation. After confirming this, the observers immediately sniffed the smell stimulation for 30 s. Thirty seconds after the lighting was changed, we returned the lighting to the reference light again, and the observers finished sniffing the smell stimulation and waited for 120 seconds.

RESULTS

We calculated the average oxyHb of the two-day experiments with five observers and analyzed the results. The difference between the peak value until the end of the measurement in NIRS and immediately before the presentation of the stimulation was defined as the amount of change in oxyHb. Figure 3 shows the calculated values for each stimulation experiment. Comparing each stimulation experiment, it was found that the amount of change in oxyHb in the smell stimulation experiment was the largest. There was not much difference between the visual stimulation experiment and the cross-modal experiment. It was also found that there was a difference in the amount of change in oxyHb between channels. The NIRS used in these experiments was able to measure the orbitofrontal area on the two channels. Ch1 and Ch2 indicate the left and right sides, respectively. Comparing the amount of change in oxyHb between the channels, it was found that the left orbitofrontal area changed significantly in all stimulation experiments.
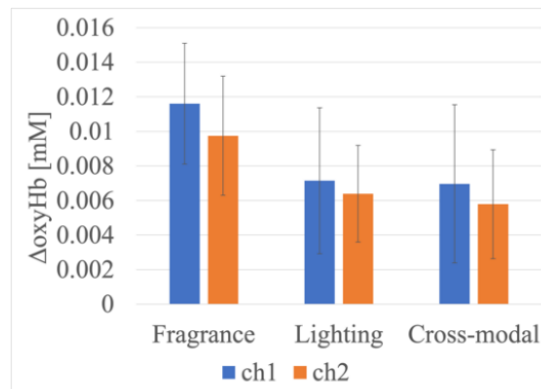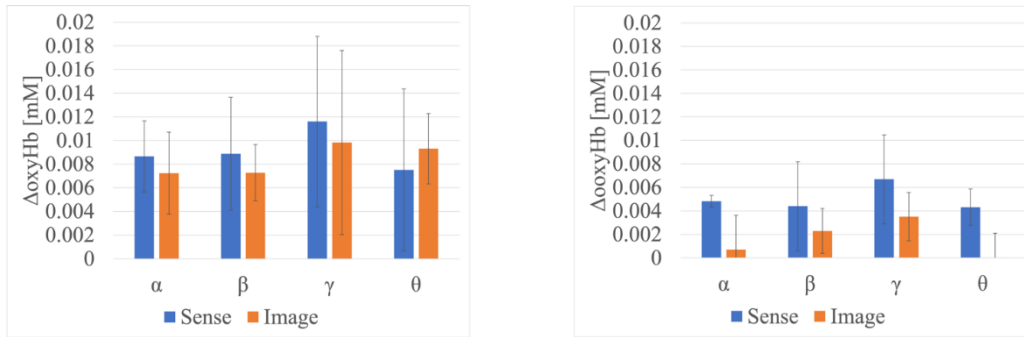

Figure 3. Amount of change in oxyHb for each experiment

Figure 4 shows the amount of change in oxyHb for each condition in the cross-modal experiments. Figure 4(a) shows the difference between the peak value until the end of the NIRS measurement and immediately before the presentation of the stimulation, and Fig. 4(b) shows the difference between the peak value at 30 s during the presentation of the stimulation and immediately before the presentation of the stimulation. At the time of the preliminary survey, the lighting colors that the observers actually sniffed and judged to be in harmony or dissonance is expressed as "Sense." The lighting colors that the observers judged to be the closest to or far from the image color recalled from the name of the fragrance is expressed as "Image." From the results, it was found that the amount of change in sense is larger than that in the image under most conditions. Furthermore, it was found that the difference between sense and image was more remarkable in Fig. 4(b) than in Fig. 4(a). From this, it can be said that greater the harmony between the fragrance and the lighting colors, faster is the response speed of the observers in the orbitofrontal area.

(a) Peak value until the end of the measurement   (b) Peak value during stimulus presentation

Figure 4. Amount of change in oxyHb in cross-modal experiment

DISCUSSION

Number of stimulation and orbital prefrontal cortex reaction

The smell stimulation activated the orbitofrontal area of the observers more than visual stimulation and the cross modal. It is probable that the orbitofrontal area was activated more because the observers carefully sniffed the essential oils that they were not accustomed to sniffing in the white light, which was set as the reference light. We have previously conducted experiments in which observers were made to wear eye masks and presented with smell stimulation and compared the results with that of complete obstruction of visual information and cross-modal experiments. At that time, the amount of change in oxyHb was larger in the cross-modal experiment. This is consistent with previous studies showing that the higher the number of stimulations taken by the observers, the more active the orbitofrontal area [3].

Left–right difference in orbital prefrontal cortex activation

The left side of the orbitofrontal area was more activated than the right side in all the experiments. However, in previous studies that analyzed the response of the orbitofrontal area to smell stimulation, opinions were divided based on laterality [2, 6, 7]. Conversely, studies analyzing four brain regions that were the neural basis of "love" [8] showed that the left side of the orbitofrontal area correlates with positive emotions and the right side with negative emotions. As the smell stimulations used in these experiments were essential oils that produce relaxing effects, it is possible that positive emotions were promoted, and the left side of the orbitofrontal area was more activated.

Effect of harmony between scent and lighting color

The cross-modal (sense) with the lighting colors selected by the observers by sniffing the fragrance activates the orbitofrontal area more than the cross-modal (image) with the lighting colors selected by the observers while recalling the name of the fragrance. In other words, it can be seen that the cross-modal combination that the observers felt was in harmony with the senses was more pleasant than preconceptual combinations. Previous studies have confirmed that greater the degree of harmony between fragrance and color stimulation, such as color patches, the more active the part of the brain, including the orbitofrontal area [2, 3]. This tendency is also obtained with lighting color, which is the visual stimulation of this study, and suggests that it can be applied to space design in real life. Conversely, as Sense is more active even under dissonant conditions, it can be said that the orbitofrontal area is activated even when it is more dissonant. Furthermore, it was found that greater the degree of harmony, faster is the reaction speed of the orbitofrontal area. Studies have mentioned the effects of harmony between fragrance and color on human task processing speed [1]. It can be said that this study was able to verify the relationship between

the degree of harmony and human reaction speed from the viewpoint of brain waves, which is a physiological aspect.

CONCLUSIONS

In this study, we analyzed the cross-modal effect of the harmony of color and fragrance in a lighting environment based on the activity of the orbitofrontal area. As a result of simultaneously presenting two types of fragrances and eight types of lighting colors selected by our preliminary surveys, we concluded that the left orbitofrontal area was significantly activated compared to the right orbitofrontal area. Furthermore, there was a tendency for greater harmony between the fragrance and the lighting color. The more active the activity of the orbitofrontal area, faster is the response speed to the stimulation.

In our experiments, the observers were asked to sniff from a brown light-shielding bottle as the smell stimulation. In order to verify the results in real life, it is a future task to expand the scale of the experiment, fill the entire room with a fragrance, and conduct the experiment in an indoor space.

ACKNOWLEDGMENT

REFERENCES

1. Luisa, D., Daniel S. & Charles S. (2006). Cross-Modal Associations Between Odors and Colors. *Chemical Senses, 31*, 531-538. https://doi.org/10.1093/chemse/bjj057

2. Robert, A., Paul., M. Mark, J., Christian, F., Beckmann, Peter, C., Hansen & Gemma, A. (2005). Color of Scents: Chromatic Stimuli Modulate Odor Responses in the Human Brain. *Journal of Neurophysiology*. https://doi.org/10.1152/jn.00555.2004

3. Danja, K., Christina, R., Janina, S., Jessica, F. & Johan, N. (2019). Multisensory Enhancement of Odor Object Processing in Primary Olfactory Cortex. *Neuroscience, 418*, 254-265. https://doi.org/10.1016/j.neuroscience.2019.08.040

4. Kono, T., Matuo, K., Tsunashima, K., Kasai, K., Takizawa, R., Mark, A., Yamasue, H., Yano, T., Taketani, Y. & Kato, N. (2007). Multiple-time replicability of near-infrared spectroscopy recording during prefrontal activation task in healthy men. *Neuroscience Research, 57*(4), 504-512. https://doi.org/10.1016/j.neures.2006.12.007

5. Kakimoto, Y., Nishimura, Y., Hara, N., Okada, M., Tanii, H. & Okazaki, Y. (2009). Intrasubject reproducibility of prefrontal cortex activities during a verbal fluency task over two repeated sessions using multi-channel near-infrared spectroscopy. *Psychiatry and Clinical Neurosciences, 63*(4), 491-499. https://doi.org/10.1111/j.1440-1819.2009.01988.x

6. Sara, I., Roberta, M., Vincenzo, C., Irene, V., Giulia, F. & Michela, B. (2019). Smell and 3D Haptic Representation: A Common Pathway to Understand Brain Dynamics in a Cross-Modal Task. A Pilot OERP and fNIRS Study. *Frontiers in Behavioral Neuroscience*. https://doi.org/10.3389/fnbeh.2019.00226

7. Ishimaru, T., Yata, T., Horikawa, K. & Hatanaka, S. (2004). Near-infrared spectroscopy of the adult human olfactory cortex. *Acta Oto-Laryngologica, 124*(553), 95-98. https://doi.org/10.1080/03655230410017751

8. Noriuchi, M., Kikuchi, Y & Senoo, A. (2008). The Functional Neuroanatomy of Maternal Love: Mother's Response to Infant's Attachment Behaviors. *Biological Psychiatry, 63*(4), 415-423. https://doi.org/10.1016/j.biopsych.2007.05.018

THE INFLUENCE OF LIGHTING DIRECTION FOR FOOD PHOTOGRAPHY ON ATTRACTIVENESS

Chatchai Nuangcharoenporn[1], Waiyawut Wuthiastasarn[1], and Uravis Tangkijviwat[1]*

[1]*Department of Color Technology and Design, Faculty of Mass Communication Technology, Rajamangala University of Technology Thanyaburi, Thailand.*

Keywords: attractiveness, food photography

ABSTRACT

Nowadays online food delivery is very popular. One of the factors that help consumers make decisions to buy food is pictures. Food photography is important to catch customers' attention that they desire to order more because it looks appetizing. Food photographs also could increase sales volume. However, the photographs could be affected by various factors for instance photography equipment, the color of lighting, art composition, and so on. These factors were found to influence attractiveness in food photography. A direction of light is one of the photography procedures lighting setups. It would be interesting to investigate how the direction of light affects consumers' attractiveness. This study, hence, aimed to investigate a relationship between the direction of light setting and the attractiveness of food photography. Thai dessert was selected for taking a photograph with different directions of lighting, consisting of a combination of four vertical elevation angles (0°, 30°, 60°, and 90°) and twelve horizontal side angles of dessert dish from 0 to 330 degrees. Fifty-two participants were asked to judge their feelings on thirty-seven pictures by using an attractiveness scale. Results showed the higher a vertical elevation angle, the higher an attractiveness score with a significant difference at 0.001, whereas it was not found in a horizontal side angle. This experimental result will be used as a practical tool for the lighting setup, especially for dessert photography.

INTRODUCTION

Nowadays, a sharing of photography through social media, websites, and blogs becomes very popular, in particularly a food photograph [1,2]. A variety of food photographs published on cooking or restaurant website aims at to catch a customer's attention and to be appetite [3]. Many factors have an influence over customer's attention for instance an expensive ingredient, food decoration, and food composition [4]. In addition, photography techniques such as lighting setup, special effect, and camera angle are also arouse our taste sensation [5]. Food photographs, hence, are published on social media, websites, and other media for increasing a sale volume [6].

In a previous study, Kazuma et. al. [3] proposed an attractiveness prediction model for food photographs by using a machine learning system. A camera angle, an appearance of the entire food, and the appearance of the main ingredients are variables in the model. Furthermore, they also found that food photo attractiveness on customers could be affected by a lighting technique. A lighting setup not only is concerned with color temperature, but also lighting direction. Illuminants for lighting setup consist of a main light and a fill light. The main light is a primary illuminant that uses for exposing light to objects. It's located at an angle of 45° to the object. The fill light located at the opposite angle to the main light. To reduce shadows that are created from the main light and the fill light illuminance is always weaker than the key light [7]. Moreover, the direction of main light affects to direction and intensity of object's shadow. When the main light changes direction and intensity, a shadow of object could be changed. This change might affect customer's attention. This study, therefore, aimed to investigate a relationship between a lighting direction and an attractiveness of food photography.

METHODOLOGY

Participants

Fifty-two subjects with age ranging from 21 to 31 years (23 men and 29 women) participated in this experiment. All subjects were a normal or corrected to normal vision and passed a Ishihara's color blindness test vision.

Stimuli

Photographs of Thai dessert fruit-shaped mung bean, namely Luk Chup, were taken as a stimulus (figure 1). The intensity of illuminants was fixed at 11000 lux for main light and 5500 lux for fill light. Figure 2 (a) and (b) showed the position of a main light with moving a vertical elevation angle from 0 (●), 30° (■), 60° (◆) to 90° (○) and a horizontal side angle of the dish from 0°, 30°, 60°, 90°, 120°, 150°, 180°, 210°, 240°, 270°, 300° to 330°. The fill light and camera were fixed at 45° of a vertical elevation angle (▲) and 0° of a horizontal side angle. Thirty-seven photographs were obtained from a combination of a vertical elevation angle and a horizontal side angle.

Figure 1. Thai dessert fruit-shaped mung bean "Luk Chup"
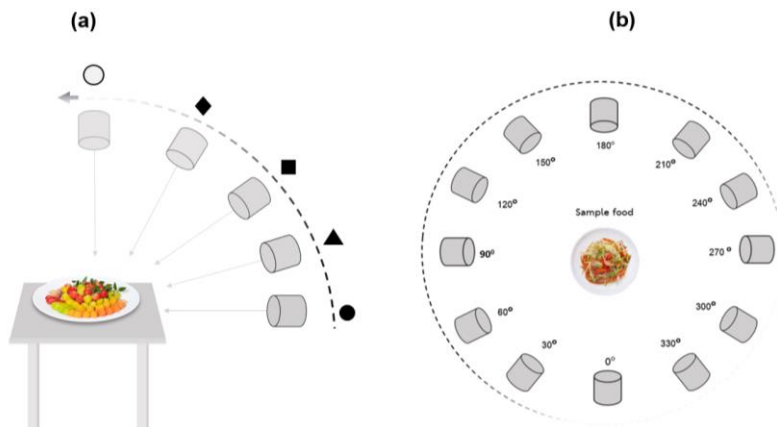

Figure 2. (a) A position of a vertical elevation angle from 0° (●), 30° (■), 60° (◆) to 90° (○) and (b) a position of a horizontal side angle from 0°, 30°, 60°, 90°, 120°, 150°, 180°, 210°, 240°, 270°, 300° to 330°.

Procedure

This study was conducted on an online questionnaire. The first part of the questionnaire was general information and opinions in deciding to order food. All participants were asked to rate their current hunger/fullness status on five point of Likert scales (1 = extremely hunger to 5 = extremely full) and they were asked to rate liking of Thai fruit-shaped mung dessert on two Likert scales which are like and dislike. We asked them about "Do you think food photos are important in deciding to order food?" on five-point of Likert scales (1 = strongly agree to 5 = strongly disagree) and we also asked subjects which factor they

consider first when deciding to order online food delivery by using choice that we prepare choice to them (i.e. price, food photo, promotion, review and brands).

In experiment, 37 photographs were randomly presented. Each participant was asked to rate their feeling in an attractiveness scale for given photography. The attractiveness scale was ranged from 1(extremely unattractiveness) to 6(extremely).

RESULT

All participants had reported common information on hunger/fullness that they were not hungry (mean = 2.67, SD.=1.043) and most of the participants liked Thai fruit-shaped mung desserts, Participants were strongly agreed with the question of would you think a photograph is important in deciding to order food (mean =4.40, SD.= 0.634). In a question of the factor that their considered to order food, the first-three factors were a photograph, prices, and promotion in respectively.
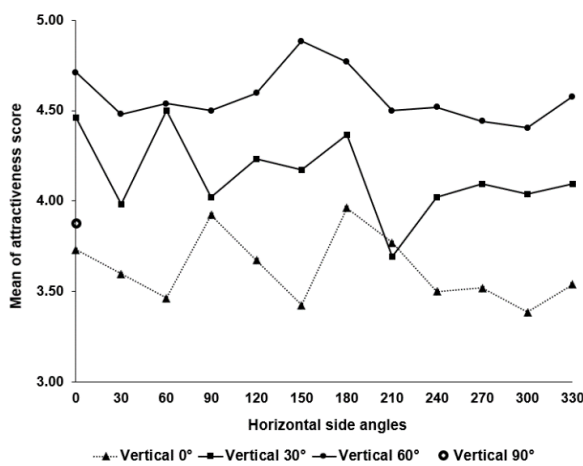

Figure 3. The difference of attractiveness score in each vertical elevation angles of 0°-90° classified by horizontal side angles of 0° - 330° of food photography.
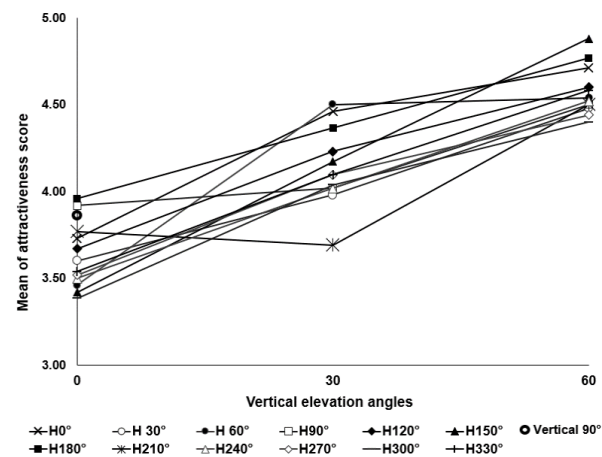
Figure 4. Comparison of mean attractiveness scores of food photos on vertical elevation angles.

Influences of lighting direction on horizontal side angles

Data of attractiveness score obtained from all participants were performed by means of SPSS 25.0 for Window. Figure 3 demonstrated a mean of attractiveness scores for dessert photography in a difference of horizontal side angles. An abscissa axis represented a horizontal side angle from 0° to 330°, whereas a vertical axis represented the mean of attractiveness score. In addition, vertical elevation angle 0° (▲), 30° (■) and 60°(●) displayed a set of mean of attractiveness scores on different horizontal side angles, respectively. Moreover, the mean score of the photograph was taken on vertical 90° displayed by opened circle (O).

Results showed that dessert photography with vertical elevation angle 0° (▲) had the highest mean attractiveness score at horizontal side angles 180° (Mean =3.96, SD.= 1.441), and photograph with the lowest mean attractiveness was horizontal side angles of 300° (Mean = 3.38, SD.= 1.457). For vertical elevation angles of 30° (■), the dessert photograph with the highest mean attractiveness score was horizontal side angles 60° (Mean = 4.50, SD.=1.163), and the lowest mean attractiveness was found in a horizontal side angle of 300° (Mean = 3.69, SD.= 1.528). In a 60° degree (●) vertical elevation angle, the

dessert photograph with the highest mean attractiveness score was horizontal side angle 150° with the mean 4.88 (SD.= 1.114). A dessert photograph with the lowest attractiveness averages was horizontal side angle of 300°, with mean 4.40 (SD.= 1.225).

In addition, the participants assessed their attractiveness to dessert photographs taken on the vertical angle of 90° (○) with mean = 3.87 (SD.=1.519). However, when compared the results of horizontal side angles to a difference of vertical elevation angles, the result was not clear. In addition, a significant difference was tested with One-Way ANOVA. Table 1 showed the mean attractiveness of dessert photograph in horizontal side angles was not statistically significant difference at p - value 0.05.

Table 1. One-way ANOVA analysis on mean attractiveness in each a vertical elevation angle and a horizontal side angle.

		Sum of squares		df	F	Sig.
Vertical 0, Horizontal 0 -330	Between Group	20.63		11	0.825	0.615
	Within Group	1391.86		612		
Vertical 30, Horizontal 0 -330	Between Group	29.23		11	1.482	0.134
	Within Group	1097.63		612		
Vertical 60, Horizontal 0 -330	Between Group	11.65		11	0.812	0.628
	Within Group	798.65		612		

Influences of lighting direction on vertical elevation angles

Figure 4 showed the mean attractiveness score of dessert photograph in each horizontal side angle from 0° to 330° classified by a vertical elevation angle 0°, 30° and 60°, where vertical axis represented the mean of attractiveness score and an abscissa axis represented the vertical elevation angle from 0°, 30° to 60°. For mean value of photograph with vertical elevation angles 90° was shown by a opened circle (○).

Results showed when the vertical elevation angles increase, the mean attractiveness of food photographs increased. For example, dessert taken under lighting at horizontal side angle 150° with vertical elevation angles 0°, 30° and 60° had mean attractiveness score 3.42 (SD.=1.649), 4.17 (SD.=1.324) and 4.88 (SD.=1.114), respectively. This result occurred in all horizontal side angle except 210° (∗), the mean attractiveness decreased when the vertical elevation angle increased.

Furthermore, dessert photographs at horizontal side angle 60° (●) in vertical of 0°, 30° and 60° had mean attractiveness 3.46 (SD.=1.488), 4.50 (SD.=1.163), and 4.54 (SD.=1.111), respectively. It was found that when vertical elevation increased from 30° to 60°, the mean score was stable and then a bit increased. With the mean attractiveness increasing trend, vertical affects the attractiveness of dessert photography. Therefore, we tested with one-way ANOVA to find significance.

Table 2. One-way ANOVA of mean attractiveness score of dessert photograph in each horizontal side angles on vertical elevation angle of 0°, 30°, 60° and 90°

Food photo on horizontal angles of dish and vertical angles													
		H0	H30	H60	H90	H120	H150	H180	H210	H240	H270	H300	H330
df	BG:	3	3	3	3	3	3	3	3	3	3	3	3
	WG:	204	204	204	204	204	204	204	204	204	204	204	204
SS	BG:	34.42	21.38	42.36	13.03	26.01	58.94	26.72	21.24	27.86	23.53	27.96	29.73
	WG:	353.88	388.53	364.90	401.73	387.25	411.50	365.26	415.36	443.01	426.38	380.80	390.19
F		6.61	3.74	7.89	2.20	4.56	9.74	4.973	3.47	4.27	3.75	4.99	5.18
P		.000**	.012*	.000**	0.88	.004*	.000**	.002*	.017*	.006*	.012*	.002*	.002*

*Notes: * p<0.05, **p<0.001, H: Horizontal side angle, BG: Between Group - WG: Within Group*

As shown in Table 2, the results of One-Way ANOVA of mean attractiveness in dessert photograph in each horizontal side angle on a vertical elevation angle of 0°, 30°, 60° and 90°. There was a statistically significant difference between vertical elevation angle and horizontal side angle with mean attractiveness score at p<0.001 (F = 52.73, p = .000).

It was found that the dessert photograph taken under vertical 60° of lighting could have the greatest impact on the attractiveness of dessert photography. The result indicated that increasing the height of vertical elevation angles of lighting tends to increase the attractiveness. This tendency was occurred in all condition. However, the mean of attractiveness was not significantly different at horizontal angles of 90° (□) and all vertical angles (F = 2.21, p = 0.88).

DISCUSSION

Influences of lighting direction on vertical elevation angles of food dish on attractiveness

Our finding showed that increased vertical elevation angles from 0° to 60°. This leaded to an increased sense of attractiveness on dessert photography as well. The dessert photographs (b) Vertical 0°-Horizontal 0°, (c) Vertical 30°- Horizontal 0° compared with the (d) Vertical 60° - Horizontal 0° degrees. We found that the intensity of shadows in the dessert on the dish can be clearly reduced. The higher of a vertical elevation angle may provide a high illuminance level to convey a bright photograph. This result implied that the level of shadow intensity could reduce the feeling of attractiveness on customers.

(a)　　　　**(b)**　　　　**(c)**　　　　**(d)**
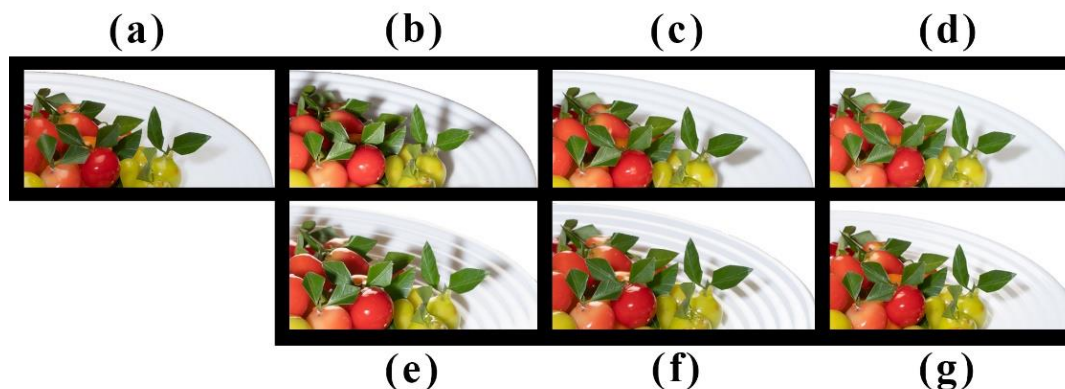

(e)　　　　**(f)**　　　　**(g)**

Figure 5. An example of a comparison of vertical angle food photos in shadow areas (a) V90°, (b) V0°-H0°, (c) V30°-H0°, (d) V60°-H0°, (e) V0-H180°, (f) V30°- H180° and (g) V60°-H180°

Lighting horizontal side of dish not affected on attractiveness of food

Lighting direction of horizontal side angles does not affect to the attractiveness of dessert photography. Kazuma et al. studied of estimation of the attractiveness of food photography based on image features [3]. They suggested that a camera angle was an important factor in enhancing attractiveness. In addition, their research also was found that the type of the food including the shape and position of the appearance of main ingredient in that dish could increase the level of attractiveness. In this study, the dessert was used as the stimulus. It does not contain the main ingredient and no exact direction. Therefore, the changes in the type of dessert or food stimuli to other categories of foods, the horizontal side of angles might be affecting to attractiveness on consumers. It implies that a changing type of foods would be required to understand the direction of lighting on horizontal angle change attractiveness in future experiments.

We concluded that the direction of lighting on vertical elevation angles can modulate the attractiveness of dessert photography. whereas horizontal angle did not statistically significant difference in attractiveness.

REFERENCES

1. Cai, W., Richter, S. and McKenna, B. (2019), "Progress on technology use in tourism", Journal of Hospitality and Tourism Technology, Vol. 10 No. 4, pp. 651-672.

2. Oliveira, B. and Casais, B. (2019), "The importance of user-generated photos in restaurant selection", Journal of Hospitality and Tourism Technology, Vol. 10 No. 1, pp. 2-14, available at: https://doi.org/10.1108/JHTT-11-2017-0130

3. Kazuma T, Tatsumi H, Keisuke D, Yasutomo K, Takatsugu H., Ichiro I, Daisuke D, & Hiroshi, M. (2019) Estimation of the attractiveness of food photography based on image features. IEICE TRANS. INF. & SYST., VOL.E102–D, NO.8 AUGUST 2019

4. Chen, X., Ren, H., Liu, Y., Okumus, B. and Bilgihan, A. (2020), "Attention to Chinese menus with metaphorical or metonymic names: an eye movement lab experiment", International Journal of Hospitality Management, Vol. 84, p. 102305

5. Martin, C.K., Nicklas, T., Gunturk, B., Correa, J.B., Allen, H.R. and Champagne, C. (2014), "Measuring food intake with digital photography", Journal of Human Nutrition and Dietetics, Vol. 27, pp. 72-81.

6. Liu, I., Norman, W.C. and Pennington-Gray, L. (2013), "A flash of culinary tourism: understanding the influences of online food photography on people's travel planning process on Flickr", Tourism Culture and Communication, Vol. 13 No. 1, pp. 5-18.

7. Rea MS (2000). The IESNA lighting handbook, 9th edn. New York: Illuminating Engineering Society of North America.

8. Hasenbeck, A., Cho, S., Meullenet, J. F., Tokar, T., Yang, F., Huddleston, E. A., et al. (2014). Color and illuminance level of lighting can modulate willingness to eat bell peppers. Journal of the Science of Food and Agriculture, 94, 2049–2056.

EFFECT OF NATURAL SKIN COLOR CHANGE ON FACIAL EXPRESSION RECOGNITION

Masahiro Kato[1]*, Yoko Mizokami[2] and Hiromi Sato[2]

[1] *Department of Imaging Sciences, Graduate School of Science and Engineering, Chiba University, Japan.*
[2] *Department of Imaging Sciences, Graduate School of Engineering, Chiba University, Japan.*

*Corresponding author: Masahiro Kato, masahiro18@chiba-u.jp

Keywords: Facial expression, Skin color, Emotion, Hemoglobin, Melanin

ABSTRACT

Face color is known to affect the perception of facial expressions. For example, Nakajima et al. showed that reddish and bluish faces enhance the perception of anger and sadness, respectively. However, the effect of facial color on the perception of facial expressions in the range of natural skin color changes has not been verified. In the previous study, we showed that skin color change in the direction of melanin-hemoglobin increase or decrease affects the perception of negative facial expressions such as anger and sadness. However, we did not examine the effect of facial color on the perception of positive facial expressions in the range of natural skin color change. Here, we investigate the effect of skin color change due to the increase or decrease of melanin and hemoglobin on the perception of positive facial expressions, such as happiness. We prepared five different skin color conditions. The average skin color of Japanese females was used as the skin color of the standard condition, and the skin color of the other four conditions were modulated to either of hemoglobin or melanin decrease/increase direction (H-, H+, M-, M+). We created a series of male or female face images which shifted from neutral expression to happy expression in 11 steps each for each face color. We used the method of constant stimuli for the facial expression evaluation. Participants judged whether a face stimulus appeared to be "happy" or "not happy." The results showed that the H- and M- conditions promoted the perception of happiness. This result was different from that for anger, but partially consistent with that for sadness. It was suggested that skin color change affected the perception of positive as well as negative facial expressions. The combination of facial expression and facial color would affect expression recognition.

INTRODUCTION

Facial expression is a major cue for predicting and understanding the physiological and psychological states of others and their emotions [1]. Facial color is also important information for facilitating human relationships by influencing our assessment of others' health and attractiveness [2, 3]. Experiments examining the effect of facial color on facial expression recognition showed that reddish faces enhanced the recognition of anger [4, 5, 6]. However, these studies only performed color modulation in the CIELAB $a*$ direction and did not examine the effect of facial color on facial expression recognition in physiological skin color changes. Physiological responses such as heart rate and blood pressure affect facial color, and mental and physical states are reflected in physiological responses [7]. Therefore, skin color is tied to emotional states, and we may use skin color to recognize facial expressions. It is critical to examine how skin color changes that may occur in daily life affect facial expression recognition. The purpose of this study is to investigate the effect of facial color with increase/decrease modulation of melanin and hemoglobin on both negative and positive facial expression recognition.

Hamada et al. used Monte Carlo simulations of a nine-layer skin model to accurately reproduce the spectral reflectance when the pigment components of melanin and hemoglobin change [8, 9]. These studies allow us to simulate physiological changes in human skin by modulating skin color in the direction

of increases and decreases in melanin and hemoglobin. In this study, we conducted an experiment on facial expression recognition using face images with skin colors that reproduced changes in the pigment components of melanin and hemoglobin. We examined the facial expressions of "happiness" and analyzed the results in comparison with those of "anger" and "sadness" in the previous study [10]. We then compared the threshold of judgment for each expression among each skin color to verify whether the difference in face color makes a difference in expression recognition.

METHOD

Environment

The experiment was conducted in a dark room. The stimuli were displayed on a color-calibrated LCD monitor (EIZO Corporation, ColorEdge CG247) with a maximum luminance of 107 cd/m^2 and a white point of D65. A participant's head was fixed on a chin rest to maintain a viewing distance of 60 cm, and responses were made using a response keyboard. The program for the experiment was written in the Matlab environment (R2018b, The Mathworks, Inc.) using Psychtoolbox-extensions [11, 12, 13].

Observers

Nine participants (ages 21-26) were enrolled in the experiment of the happy face condition, The participants had a normal color vision, and visual acuity was normal or corrected to normal.

Stimuli

The face stimulus was displayed with a visual angle of 17.0° × 13.0° in the center of a neutral gray background. We used face images in the ATR Facial Expression Image Database (DB99) (ATR-Promotions, Kyoto, http://www.atr-p.com/face-db.html). We created the average faces of six male Japanese images for neutral and happy expressions by using morphing software. We made the average faces of four female images, too. The neck, ears, and hairline of the face images were cropped to extract only the face. In addition, to modulate the skin color area only, an adjustment mask was created to extract skin color regions other than the eyes, mouth, and eyebrows. An example of the morph continuum is shown in Figure 1 ("Anger" and "Sadness" are adopted from the previous study for comparison [10]). Five face color conditions were prepared for each expression (Figure 1D). The standard face color was adjusted to $L* = 65.598$, $a* = 8.9832$, and $b* = 17.788$ using the spectral reflectance data of 694 Japanese women (aged 20-78 years) measured under D65 [14]. We prepared skin color conditions with different hemoglobin and melanin concentration calculated from the absorption coefficient of the skin layer by Monte Carlo simulation. We chose the absorption coefficient to equate the distance from the average color in -/+ directions: 0.1 (H-) and 1.9 (H+) for hemoglobin absorption coefficient, 0.7 (M-) and 1.3 (M+) for melanin absorption coefficient as shown in Table1. The color of each pixel in the face area was shifted the same distance as the shift of average color while keeping the color distribution of the face the same. For happiness conditions, we morphed between neutral and happy expressions in 10 steps, creating 11-levels of angry rate: 20, 27, 34, 41, 48, 55, 62, 69, 76, 83, and 90% under each face color condition. Therefore, 110 stimuli (male and female faces, 5 skin color types, 11 levels of expression rate) are used in total.

Table 1. Absorption coefficient and chromaticity data of five different face color conditions

	Hemoglobin absorption coefficient	Melanin absorption coefficient	L^*	a^*	b^*	ΔE^*_{ab}
Standard	1.0	1.0	65.598	8.9832	17.788	-
H-	0.1	1.0	68.941	5.4766	17.985	4.849
H+	1.9	1.0	63.243	11.626	16.788	3.678
M-	1.0	0.7	69.595	8.2815	15.670	4.578
M+	1.0	1.3	62.117	9.6145	19.172	3.799
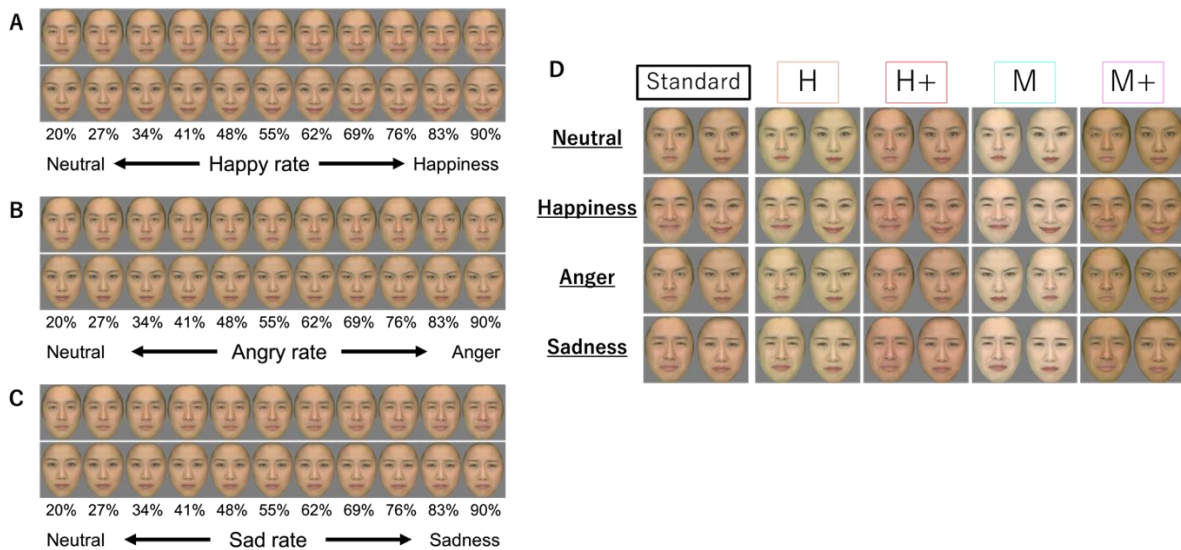
Figure 1. Eleven-levels of expression rate for Happiness (A), Anger (B), and Sadness (C), and five face color conditions for each expression (D)

Procedure

We measured the matching point between neutral and three facial expressions (the point of subjective equality, PSE) using the constant method of stimuli. Following dark adaptation, light adaptation, and background adaptation for 30 seconds each, the fixation point was presented for 5000 ms. Then, the first facial stimulus was presented for 1000 ms. Participants judged the facial expression of the stimulus using a keyboard while the fixation point was presented. The participants answered whether the face appeared as "happy" or "not happy" for each condition by a two-alternative forced choice. When the response was complete, the next facial stimulus was presented 1000 ms later. All stimuli were presented in a random order, and each session consisted of five consecutive trials. Each participant conducted three sessions.

Analysis

The probability of happiness response to each facial stimulus was calculated for each participant. The probability of each participant was fitted by a psychometric function using a generalized linear model with a binomial distribution in Matlab. From the psychometric function, we calculated the point of subjective equality (PSE), at which the probability of responding as happy is 50%. Repeated measures ANOVA (analysis of variance) was used to explore possible contributions of skin color conditions on the PSEs. For post-hoc pairwise comparisons, Ryan's method was used.

RESULT

Happiness condition

We calculated the PSEs of happiness perception in each skin color condition. Figure 2 shows the average PSE of each skin color modulation relative to the PSE of standard skin color, including both male and female stimuli. There are individual differences in criteria on how angry the face is. Therefore, we normalized the PSE of each skin color modulation condition by the PSE of standard skin color for each observer to eliminate the effect of the individual difference. Thus, M- and H- with the normalized PSE under one show enhanced perception of happiness, whereas M+ and H+ with the normalized PSE over one show suppressed perception of happiness (Fig. 2A). We conducted A two-way ANOVA with repeated measures for the gender of the facial stimuli (male and female) and normalized four skin color conditions. The results showed a significant main effect for the skin color condition ($F(3, 5) = 16.488$, $p < 0.001$). There was no significant main effect of stimulus gender and the interaction between skin color and stimulus gender.

Anger and Sadness condition (from the previous study)

As in the happiness conditions, we normalized the PSE of each skin color modulation condition by the PSE of standard skin color for each observer (Fig. 2B). M+ and H+ with the normalized PSE show enhanced perception of anger, whereas M- and H- with the normalized PSE show suppressed perception of anger. We conducted A two-way ANOVA with repeated measures for the gender of the facial stimuli (male and female) and normalized four skin color conditions. The results showed a significant main effect for the skin color condition ($F(3, 13) = 9.511$, $p < 0.001$). There was no significant main effect of stimulus gender. However, the interaction between skin color and stimulus gender was significant ($F(3, 13) = 5.984$, $p < 0.0015$).

In the sadness conditions, we also normalized the PSE of each skin color modulation condition by the PSE of standard skin color for each observer (Fig. 2C). We conducted A two-way ANOVA with repeated measures for the gender of the facial stimuli (male and female) and normalized four skin color conditions. The results showed no significant main effect for the skin color condition ($F(3,9) = 3.067$, $p = 0.0401$). Post-hoc pairwise comparisons showed no significant pairs of differences between skin colors, and a significant difference was obtained in the interaction ($F(3,9) = 3.084$, $p < 0.0394$). Therefore, we conducted a one-factor analysis of variance on the results of the male and female facial stimuli. For male facial stimuli, the main effect of quantified skin color was significant ($F(3, 9) = 3.949$, $p < 0.05$). For female facial stimuli, the quantified main effect of skin color was not significant ($F(3, 9) = 0.967$, $p = 0.419$). These results suggest that H- and M- faces were judged to be sadder only in the male face stimuli used in the experiment.
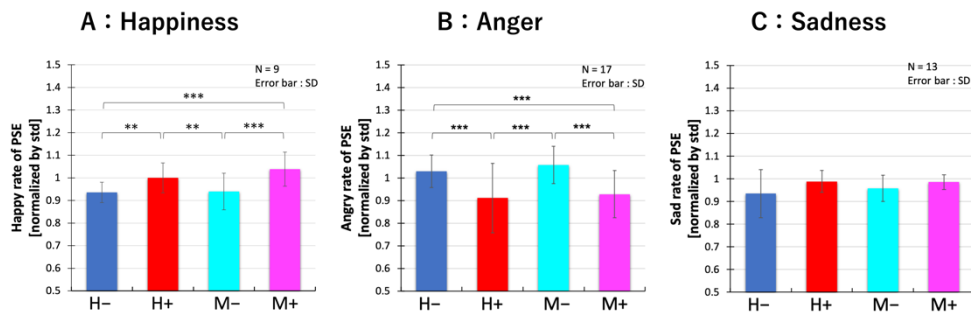
Figure 2. PSE of each skin color on each condition normalized by each PSE of standard face

DISCUSSION

In this study, skin color change with increased hemoglobin or melanin was associated with an enhanced perception of anger. And skin color change with decreased hemoglobin or melanin was associated with enhanced perception of happiness and sadness. The results that reddish faces facilitated the recognition of anger were consistent with the previous studies. Faces with relatively brighter skin colors have been shown to be more attractive [15, 16, 17], and attractive faces are more likely to be perceived as happy [18]. Therefore, it is conceivable that many light skin colors may promote a positive impression. Compared to the standard skin color, the skin with increased hemoglobin or melanin is less bright, and that with decreased hemoglobin or melanin is brighter (Table 1). In our result, anger perception was suppressed, and happiness perception was promoted in the light skin color condition. The opposite trend was shown in the darker skin color condition. These suggest that lighter skin colors gave a more positive impression, enhanced the perception of happiness, and suppressed the negative impression of anger. However, lighter skin colors may also promote a slightly negative impression of sadness in male stimuli. It was reported that an unattractive face with a positive expression was judged more attractive than an attractive face with a neutral expression [18]. Therefore, facial expression may take precedence in facial expression recognition even if the skin color gives cues of a positive and an attractive impression. It would not be possible to predict the effect on all facial expression recognition solely from facial color. The combination of facial expressions and facial colors would influence facial expression recognition.

ACKNOWLEDGEMENT

REFERENCES

1. Jack, R. E., Garrod, O. G., & Schyns, P. G. (2014). Dynamic facial expressions of emotion transmit an evolving hierarchy of signals over time. *Current Biology*, 24(2), 187-192.

2. Re, D. E., Whitehead, R. D., Xiao, D., & Perrett, D. I. (2011). Oxygenated-blood colour change thresholds for perceived facial redness, health, and attractiveness. *PloS one*, 6(3), e17859.

3. Langlois, J. H., Kalakanis, L., Rubenstein, A. J., Larson, A., Hallam, M., & Smoot, M. (2000). Maxims or myths of beauty? A meta-analytic and theoretical review. *Psychological Bulletin*, 126(3), 390.

4. Nakajima, K., Minami, T., & Nakauchi, S. (2017). Interaction between facial expression and color. *Scientific Reports*, 7(1), 1-9.

5. Thorstenson, C. A., Pazda, A. D., Young, S. G., & Elliot, A. J. (2019). Face color facilitates the disambiguation of confusing emotion expressions: Toward a social functional account of face color in emotion communication. *Emotion*, 19(5), 799.

6. Young, S. G., Thorstenson, C. A., & Pazda, A. D. (2018). Facial redness, expression, and masculinity influence perceptions of anger and health. *Cognition and Emotion*, 32(1), 49-60.

7. Kreibig, S. D. (2010). Autonomic nervous system activity in emotion: A review. *Biological Psychology*, 84(3), 394-421.

8. Hamada, K., Mizokami, Y., Kikuchi, K., Yaguchi, H. & Aizu, Y. (2018). Discrimination threshold of skin color in skin image. *Journal of the Color Science Society of Japan*, 42(2), 50-58. (In Japanese)

9. Maeda, T., Arakawa, N., Takahashi, M., & Aizu, Y. (2010). Monte Carlo simulation of spectral reflectance using a multilayered skin tissue model. *Optical Review*, 17(3), 223-229.

10. Kato, M. & Mizokami, Y. (2020). Effects of skin color change due to melanin and hemoglobin increase/decrease on recognizing facial expressions. *2020 Summer Meeting of the Vision Society of Japan*, *Vision*, 32, 146 (1S12). (In Japanese)

11. Brainard, D. H., & Vision, S. (1997). The psychophysics toolbox. *Spatial Vision*, 10(4), 433-436.

12. Pelli, D. G., & Vision, S. (1997). The VideoToolbox software for visual psychophysics: Transforming numbers into movies. *Spatial Vision*, 10, 437-442.

13. Kleiner, M., Brainard, D., Pelli, D., Ingling, A., Murray, R., & Broussard, C. (2007). What's new in Psychtoolbox-3? *Perception*, 36 ECVP Abstract Supplement 14.

14. Kikuchi, K., Katagiri, S., Yoshikawa, T., Mizokami, Y. & Yaguchi, H. (2018). Long-term changes in Japanese women's facial skin color. *Color Research & Application*, 43(1), 119-129.

15. Yamamoto, M., Lim, Y., Wei, X., Inui, M. & Kobayashi, H. (2003) On the preferred flesh colour in Japan, China and South Korea. *Imaging Science Journal*, 51(3), 163-174.

16. Han, C., Wang, H., Hahn, A. C., Fisher, C. I., Kandrik, M., Fasolt, V., ... & Jones, B. C. (2018). Cultural differences in preferences for facial coloration. *Evolution and Human Behavior*, 39(2), 154-159.

17. Coetzee, V., Greeff, J. M., Stephen, I. D., & Perrett, D. I. (2014). Cross-cultural agreement in facial attractiveness preferences: The role of ethnicity and gender. *PloS one*, 9(7), e99629.

18. Golle, J., Mast, F. W., & Lobmaier, J. S. (2014). Something to smile about: the interrelationship between attractiveness and emotional expression. *Cognition and Emotion*, 28(2), 298–310.

PILL CLASSIFICATION BASED ON MACHINE LEARNING

Areerat Pathomchaiwal[1]*

[1]*Department of Printing Engineering, Faculty of Engineering,
Institute of Printing Engineering, Siam University, Thailand.

*Corresponding author: Areerat Pathomchaiwal, areerat.pathom@gmail.com

ABSTRACT

Pill image classification has been widely used in commercial applications. In this paper, we propose a deep learning for pill image classification. The proposed pill dataset into separate training and testing sets. We find that neural networks need significantly less training data to obtain the state-of-the-art performance than previously proposed methods. This method is based on a residual neural network for pill image classification. The results show that the proposed classification model yields an accuracy of 97.27% in classification performance.

INTRODUCTION

Image identification and life-saving medical improvements are all powered by recent advances in artificial intelligence (AI). Machine learning, particularly reinforcement learning, scientists and medical personnel in analyzing medical data in order to better treat diseases. Deep learning improves clinicians' capacity to estimated medical images, and AI advances personalized medicine's future.

Nowadays, there are a lot of elderly recipients who take medicine every day. The recognition of pill is a difficult task for low vision elderly based on information from imprint. The elderly can avoid mistaking pills and keep a safe medication. These recognition tools [1, 2] require elderly to classify pills images using shape, color and imprint.

In this study, we proposed and developed a computer vision technique based on convolutional neural networks [3, 4, 7]. In addition to shape features of pill images. We compare our proposed and convolutional neural networks (CNNs) architectures: VGG16 [5], VGG19 [5], InceptionV3 [6], Resnet 50 [7], Densenet [8], Xception [9], and MobileNet [10]

METHODS

In this study, we proposed convolutional neural networks based on the ResNet model. As shown in Fig 1., The stacked layers perform a residual mapping by creating shortcut connections which perform identity mapping (x). Their outputs were added to the output of the stacked layers' residual function F(x). The residual learning structure composed of several layers in a network as in Eq. (1).

$$y_l = h(x_l) + F(x_l + W_l)$$
$$x_{l+1} = f(y_l)$$

(1)

when $h(x_l)$ is the identity mapping, F is the residual function, x_l is the input, and W_l is the weight coefficient. The identity mapping can be written as $h(x_l) = x_l$. $f(x)$ is ReLU of the activation layer.
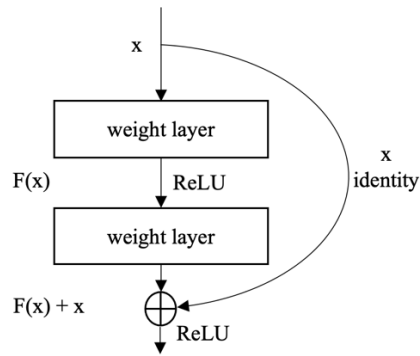
Figure 1. Residual learning: a building block

We used the publicly available NLM dataset [11] consisting of 1,000 reference pill images were used to train model and 2,000 consumer-grade pill images were used to test the performance our model. As show in Fig 2., we performed training on eight classes that had different pills' shapes of classes and images: Three-sided (3 sided), Four-sided (4 sided), Five-sided (5 sided), Six-sided (6 sided), Capsule, Oval, Round, and Other.

The training dataset is divided into two out of which the first one contains 90% training images 10% of images are used for validation and testing dataset. The images are resized to $224 \times 224 \times 3$ (224 pixels by 224 pixels by 3 channels) before they are applied to various networks. Then we perform data augmentations including random rotation, random cropping and random horizontal flipping were used on the training, validation and testing dataset. We normalize all the image pixel values to between [-1,1] for training dataset.
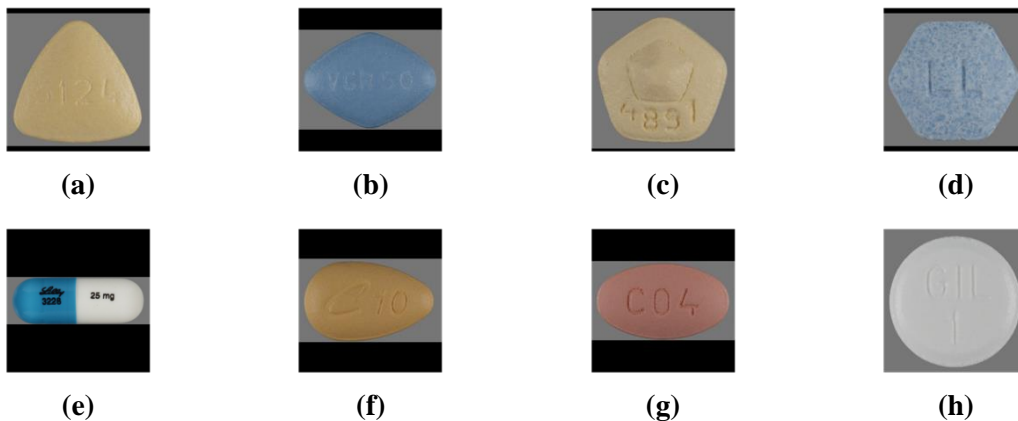
Figure 2. Example images of eight classes; (a) Three-sided. (b) Four-sided.
(c) Five-sided. (d) Six-sided. (e) Capsule (f) Oval. (g) Round. (h) Other.

The classification model is implemented by Python on Google Colab Pro with NVDIA Teala P100. We train the model with a batch size 32 using Adam with learning rate of 0.0001 without weight decay or dropout. The accuracy of the model has not been improved when the number of epochs exceeds 10.

We use the trained models to classify the test images and calculate the overall classification accuracy. The classification accuracy is the ability to predict correctly and guess the value of predicted attribute for new data. The accuracy is calculated as in Eq. (2), It is defined as the ratio of sum of true positives (TP) and true negatives (TN) to the total number of trials.

$$Accuracy = \frac{TP + TN}{TP + FP + FN + TN} \times 100 \qquad (2)$$

where TP and TN are outcomes produced when the model correctly classifies the positive class and the negative class, respectively. While FP and FN are outcomes produced when the model incorrectly classifies the positive class and the negative class, respectively.

RESULTS

We evaluate the classification performance using the eight trained models and summarize our results in Table 1. The proposed has better performance as it achieved an accuracy of 97.27% and loss of 0.0650 on validation data. We compare our proposed and convolutional neural networks architectures: VGG16, VGG19, InceptionV3, Resnet 50, Densenet, Xception, and MobileNet. Figure 3 show accuracy and loss performance for the proposed model.
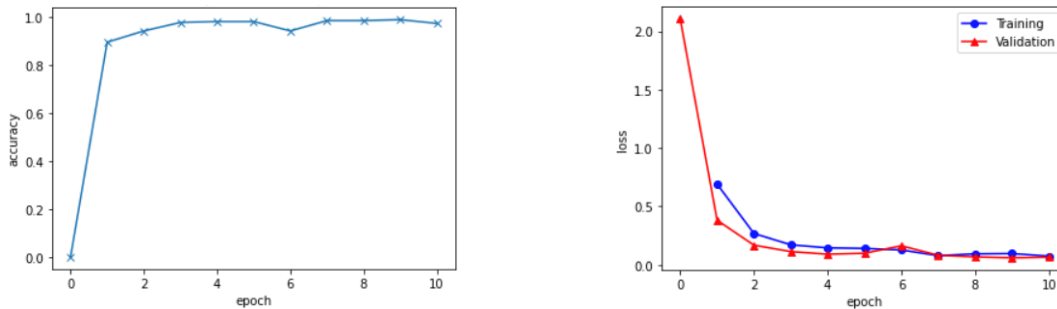
Figure 3. Accuracy and Loss of the proposed model.

Table 1. The compare between proposed and some other models.

Models	Accuracy (%)
Our proposed	97.27
VGG16	90.90
VGG19	87.44
InceptionV3	90.14
Resnet 50	89.65
DenseNet	90.53
Xception	90.07
MobileNet	90.87

CONCLUSIONS

We presented a study pill classification based on residual networks. The residual networks are several times faster to train. Pill classification allows pharmacist to verify the pill before dispensing them and allows the elderly patient to verify it before taking it. The pill shape analysis can be used in the Pharmaceutical Industry for classification and crack detection. In the future, it will be important to extend

the usability of the application to the general population, and to update the database to increase its accuracy.

REFERENCES

1. LeCun, Y., Bottou, L., Bengio, Y., & Haffner, P. (1998). Gradient-based learning applied to document recognition. In Proceedings of the IEEE, 86(11), (pp. 2278-2324).
2. Lu, W. (2012). Method for Image Shape Recognition with Neural Network. In Advances in Computer Science and Information Engineering (pp. 547-551). Springer, Berlin, Heidelberg.
3. Alom, M. Z., Taha, T. M., Yakopcic, C., Westberg, S., Sidike, P., Nasrin, M. S., Hasan, M., et al. (2019). A State-of-the-Art Survey on Deep Learning Theory and Architectures. *Electronics*, 8(3), 292. MDPI AG. Retrieved from http://dx.doi.org/10.3390/electronics8030292.
4. Krizhevsky, A., Sutskever, I., & Hinton, G. E. (2012). Imagenet classification with deep convolutional neural networks. *Advances in neural information processing systems*, 25, 1097-1105.
5. Simonyan, K., & Zisserman, A. (2014). Very deep convolutional networks for large-scale image recognition. arXiv preprint arXiv:1409.1556.
6. Szegedy, C., Vanhoucke, V., Ioffe, S., Shlens, J., & Wojna, Z. (2016). Rethinking the inception architecture for computer vision. In Proceedings of the IEEE conference on computer vision and pattern recognition (pp. 2818-2826).
7. He, K., Zhang, X., Ren, S., & Sun, J. (2016). Deep residual learning for image recognition. In Proceedings of the IEEE conference on computer vision and pattern recognition (pp. 770-778).
8. Huang, G., Liu, Z., Van Der Maaten, L., & Weinberger, K. Q. (2017). Densely connected convolutional networks. In Proceedings of the IEEE conference on computer vision and pattern recognition (pp. 4700-4708).
9. Chollet, F. (2017). Xception: Deep learning with depthwise separable convolutions. In Proceedings of the IEEE conference on computer vision and pattern recognition (pp. 1251-1258).
10. Sandler, M., Howard, A., Zhu, M., Zhmoginov, A., & Chen, L. C. (2018). Mobilenetv2: Inverted residuals and linear bottlenecks. In Proceedings of the IEEE conference on computer vision and pattern recognition (pp. 4510-4520).
11. Pill Image. National Library of Medicine. https://www.nlm.nih.gov/databases/download/pill_image.html

EFFECT OF LIGHT COLOR ON EYES-CLOSED EEG

Jun Mukondo[1]* and Hiroshi Takahashi[1]

[1]*Department of Electrical & Electronic Engineering, Kanagawa Institute of Technology, Japan.*

*Corresponding author: Jun Mukondo. s1812003@kait.jp

Keywords: Light color, Eyes-closed EEG, α wave, Alertness, Sleeping environment

ABSTRACT

Sleep is an essential part of peoples' daily lives. Thanks to electric lighting being commonplace, most people adjust the room lighting before sleeping. Numerous studies have shown that light affects alertness and work efficiency; however the effects of exposure to light when the eyes are closed, such as during sleep, is still unclear. Therefore, in this study we examined the effect of lighting on Electroencephalograms (EEG) in the setting of a person closing their eyes and falling asleep.

The experiment was conducted in a dark room using red, green, and blue light and three types of illuminance per color: 1 lx, 10 lx, and 100 lx. Using these factors, 10 condition patterns were prepared, including the "Dark" condition. Four men and one woman in their twenties were selected to participate in this experiment. EEGs in each subject were obtained at each of four different times. The first EEG was obtained in an environment of 300 lx of white light (reference EEG) the second in a dark room under the experimental lighting conditions (EEG before adaptation); and the third after adaptation to the same lighting environment as the second, but after acclimatizing to the experimental conditions for 10 minutes (EEG after adaptation). Each subject was then asked to close their eyes; after the eyes had been closed for 5 minutes, a fourth EEG was obtained (eyes-closed EEG). Brain wave activity was compared among the four different timing.

The rate of change in spectral content in each frequency band fluctuated among the EEGs obtained under the different conditions. Moreover, it was clarified that the rate of change of α waves due to illuminance differed depending on the light color.

INTRODUCTION

In the field of nursing, the sleeping environment is reviewed daily to improve the quality of sleep for patients. According to a study by the Nursing Society, the sleep illuminance preferred by the participants shortens the time to fall asleep, and the light environment is also one of the factors of sleep [1]. Past studies have shown that lights affect people [2][3][4]. However, little research has been done on the effects of light when humans close their eyes [1]. Therefore, the purpose of this study is to investigate how lights affect humans when the eyes are closed. It investigated the illuminance and light color based on physiological indicators using brain waves.

EXPERIMENT

Table 1 shows the experimental conditions. Each of 100lx, 10lx, 1lx surface lights were prepared respectively for this experiment. The light color is red, green and blue LEDs. And the Dark color was prepared assuming the darkness. In the experiment, Electroencephalograph (EEG) was used as a physiological index. Electrodes were placed on C3 and C4 of the subject's scalp by the International 10-20 system. An additional electrode was attached to the A1 that served as a reference electrode for the

electrode attached to the scalp. The data are 3 to 3.5 Hz (delta), 4 to 7.5 (theta), 8 to 12.5 Hz (alpha), and 13 to 30 Hz (beta).

Eight people in their twenties were chosen to be the subject of the experiment. The subjects were asked to refrain from alcohol intake the previous day and caffeine intake on the experiment day, make sure to have a good (quality of) sleep before the experiment Immediately

After the start of the experiment, subjects were given the first EEG measurements(EEG①) before entering the darkroom. After EEG ①, the subjects were asked to adapt to the light conditions in a dark room, and the adaptation was performed for 10 minutes. During the 10-minute adaptation, a second EEG measurement(EEG②) was performed in parallel for the first minute. A third EEG measurement(EEG③) was performed after adaptation for 10 minutes. After EEG③ , participants then were instruction to close their eyes . Five minutes after the subject closed his eyes, a fourth EEG measurement(EEG④) was performed. This is the end of the experiment.

In this experiment, To observe the Effect of Light color on Eyes-closed EEG, two brain waves of EEG③ and EEG④ were compared.

Table 1. Experimental condition

Light source	LED
Surface illuminance	1lx, 10lx, 100lx
Light source height	1.2m
Chromaticity	Red: (0.70, 0.30) Green: (0.22, 0.73) Blue: (0.14, 0.06)

RESULTS AND DISCUSSION

Figure 1 shows the fluctuation of the content rate of each frequency band. First of all, the content rate is a numerical value of the ratio of the four types of brain waves contained in the brain. This will be a graph of them. What can be seen from Figure 1 is that the content rate fluctuates before and after closing the eyes.

Figure 2 is a graph of the ratio of alpha waves before and after closing the eyes under each condition. In this experiment, the alpha waves of each light before and after closing the eyes were compared to examine the rate of change. The increase in the rate of change indicates the calmness of the participants due to the light color. From now on, this numerical value is considered the "calmness ratio".

And, in Figure 2, it can be seen that red 100lx showed the highest calmness ratio and red 10lx showed the lowest calmness ratio.

In addition, Dark color did not show any change in alpha waves before and after closing the eyes. Also, since 100lx has highest illuminance, the color effect is most likely to appear. As a result, red has the highest calmness ratio among the three colors.

According to a study by Mariana G. Figueiro, "red showed suppression of alpha waves compared to Dark"[2]. However, the opposite result was obtained in this study. In the future, the results should be continuously examined, including the possibility of "the effect that the subject receives from the light color during adaptation".
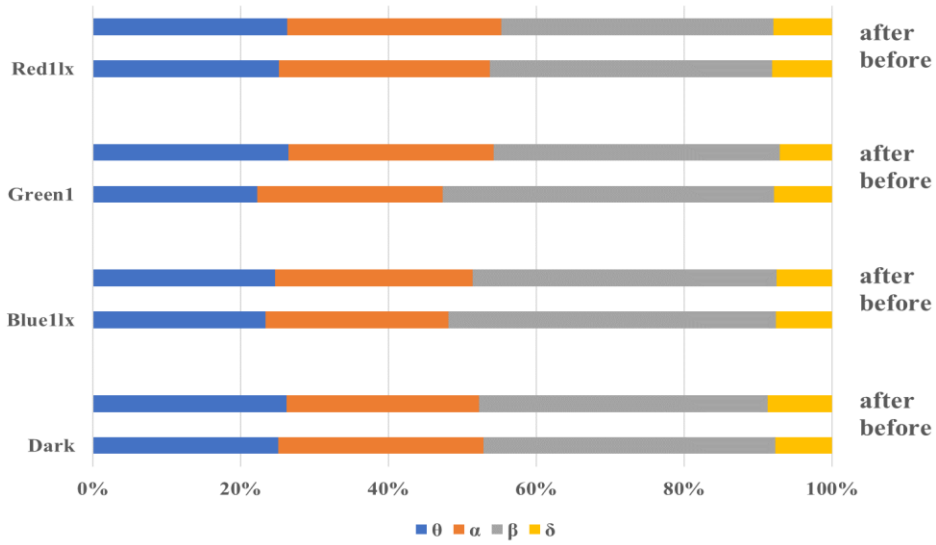
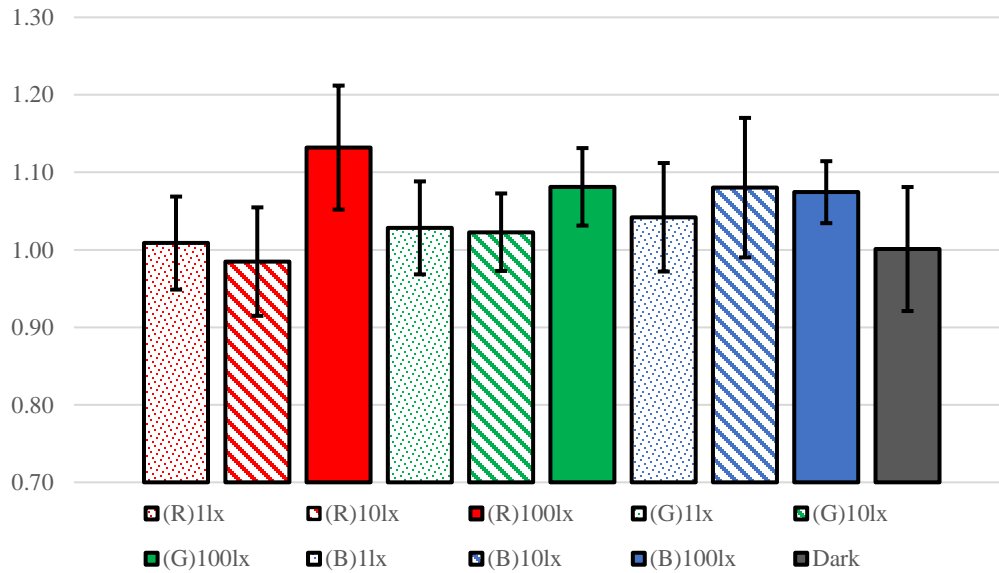**Figure 1.** Fluctuation of the content rate of each frequency band

Figure 2. Ratio of alpha waves before and after closing eyes under each condition

CONCLUSION

In this study, an experiment was conducted on the effect of light color on closing the eyes. The results can be summarized as follows:

(1) EEG fluctuations were observed when the eyes were closed in the light.

(2) Since 100lx has highest illuminance, the color effect is most likely to appear.

(3) Comparing 100lx of red, green and blue, red has the most calmness ratio.

REFERENCES

1. N Yoshinaga, M Fujita & Yuji L. Tanaka (2011). Fundamental Research about Individual Variation in Illuminance Prefarence during Hypnagogic Stage and Biological Responsiveness: Influence on Physiological Function and Subjective Evaluation. Japanese Journal of Nursing Art and Science.
2. Levent Sahin, Mariana G. Figueiro (2013). Alerting effects of short-wavelength (blue) and long-wavelength (red) lights in the afternoon. Lighting Research Center, Rensselaer Polytechnic Institute, 21 Union Street, Troy, NY 12180, United States.
3. Hiroki Noguchi (2001). A research into improvements in lighting environment for more comfortable sleep. Kyushu University Institutional Repository.
4. Takahashi, H. and Watanabe, S. (2019). Effects of light colour on work efficiency and alertness. Proceedings of the 29th Session of the CIE, 1031-1034.

OBSERVATION OF COLOR AND GLOSS CHANGE DURING THAWING OF FOODS USING A NON-CONTACT 2D MEASUREMENT SYSTEM WITH A DIGITAL CAMERA

Ayumu Kinugawa[1*], Hiroyuki Iyota[2], Shimpei Fukagawa[2], Hayato Masuda[2] and Hideki Sakai[3]

[1]*Faculty of Mechanical Engineering, Osaka City University, Japan*
[2]*Graduate School of Mechanical Engineering, Osaka City University, Japan*
[3]*Graduate School of Human Life Science, Osaka City University, Japan*

*Corresponding author: Hiroyuki Iyota, e-mail: iyota@eng.osaka-cu.ac.jp

Keywords: Dome-shaped illumination, non-contact colorimetry, rough surface

ABSTRACT

The appearance of food, including surface color and glossiness, is a major factor in the evaluation of food quality and its conditions. When the color of an object is recognized, it is judged by the diffuse reflection of the material surface, excluding the specular light of the object. Additionally, the glossiness is recognized by the specular reflections. In general, the gloss can be determined from the difference in the strength of the specular reflected light to the diffused light. A non-contact two-dimensional (2D) image recording system using a digital camera was developed and dome-shaped illumination was applied to measure the color and glossiness of the object. Uniformly irradiating lighting was generated using this illumination system. In addition, a light trap was inserted between the inner wall of the dome and the object. When the light trap was rotated at a certain angle, the images without the partially specular reflected light were captured by a digital camera. Through image processing, the images with the specular component included (SCI) and excluded (SCE) were obtained. Further, a 2D glossiness mapping image was obtained using the difference in the $L*$ values of each pixel between the SCI and the SCE in the $L*a*b*$ color system. This study was focused on thawing frozen foods. The glossiness, color, weight, and internal temperature of each object were continuously measured during the thawing process and the effects of the air temperature and humidity on the process were further investigated.

INTRODUCTION

As the appearance elements of an object are greatly influenced by the color and glossiness, the quantitative evaluation of color and glossiness is required. A non-contact 2D image recording system using a digital camera was developed and dome-shaped illumination was applied to measure the color and glossiness of the object [1][2]. It can record for several hours, and it is possible to monitor the weight of the object. Using this equipment, Fukagawa *et al.*[3] reported changes in the color and glossiness during the drying process of specific samples, such as, black beans and silica gel. In this study, the gloss, weight, and core temperature of frozen blueberries was measured during the thawing process.

COLOR MESUREMENT SYSTEM

Figure 1 shows an overview of the developed equipment. The dome imitated an integrating sphere, through which a constant lighting condition could be obtained. By reflecting the light multiple times in the integrating sphere, it was possible to uniformly irradiate the sample with a non-uniform surface without generating any shadows. The placements of the equipment parts included a light source of high color rendering white LED, average color rendering index Ra90 of 29 W with a correlated color

temperature of 6200 K at the bottom of the dome, an electronic balance under the sample table, and a light trap with a width of 30° every 60° in the upper half of the white dome. The weight of the sample was measured using an electronic balance. The measurement of the temperature and humidity inside the dome was made feasible by employing a temperature and humidity sensor using a single board computer, Arduino Uno.
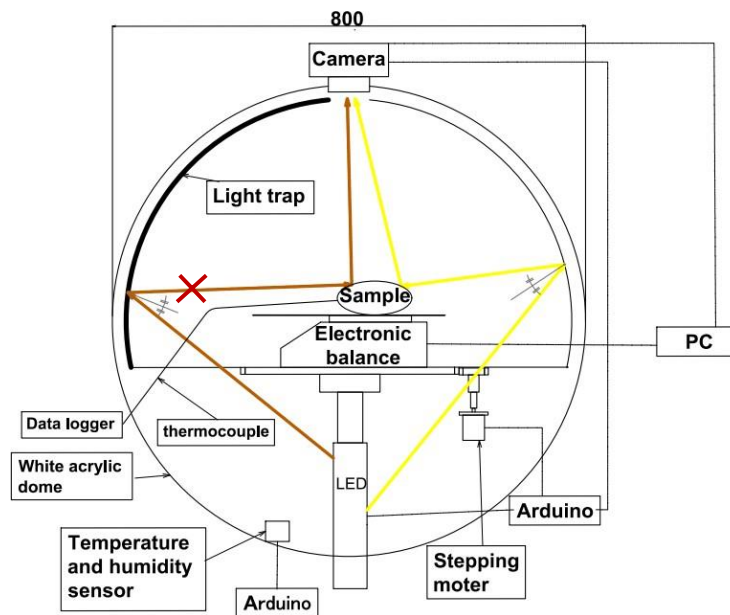

Figure 1. Dome-shaped illumination to measure the color and glossiness of the object.

The measurement principle is described as follows. The light trap was rotated 30° under the control of a stepping motor, and the sample was photographed each time automatically controlled by the Arduino Uno computer. The light reflected from the light trap' direction was not included. Therefore, the captured image does not include specularly reflected light components. By using image processing on the 12 images obtained after one round of photographing, the SCI that collects solely the pixels with the highest brightness and the SCE that collects solely the pixels with the lowest brightness are obtained. The SCI is an image that collects the pixels that contain a specular light component, and the SCE is an image that collects the pixels that do not contain a specular light component. Although the colors are recorded as RGB in a digital camera, it depends on the camera used and the lighting environment. Therefore, in this study, the brightness and color were quantitatively evaluated using the *CIE-L* a* b** color system that does not depend on them. In the CIE-*L* a* b** color system, the *L** value represents lightness, the *a** value, and the *b** value represents color. The color of the object can be determined from the *a** and *b** values of the SCE, which does not include the specularly reflected light component. The difference in the brightness can be obtained from the difference in *the L** values between the SCI and SCE. In this study, the glossiness was calculated from the difference in brightness. Therefore, using achromatic drawing paper in black, dark gray, light gray, and white, the relationship between the glossiness obtained by the conventional contact-type glossiness measuring device (GM-268 plus made by Konica Minolta) and the brightness difference obtained by the proposed equipment was investigated. Furthermore, the glossiness calculation formula to compute the glossiness from the brightness difference was derived [3]. In the proposed equipment, 20 degree mirror gloss was used for evaluating glossiness unit.

EXPERIMENT

In this study, frozen blueberries of the Dole brand purchased from the market, were used as samples. The photographing intervals of the device were 3 min and 108 min (37 times). The weight of each sample was measured every 10 s and the initial weight was 0 g. A thermocouple was inserted at the center of the sample to measure the internal temperature change. The frozen blueberries were thawed at room temperature and relative humidity of approximately 26-30 °C and 53-60 %, respectively. Figure 2(a) shows one of the 12 images taken. Figures 2(b) and 2(c) show the SCI and SCE obtained by the image processing of the 12 images per lap, respectively. Further, the L^*, a^*, and b^* values of the sample were checked.
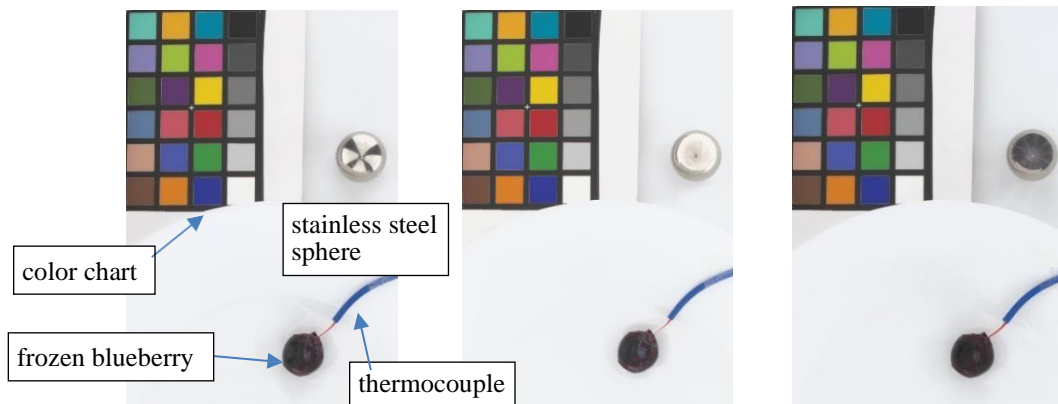
Figure 2(a). An example of a photograph taken

Figure 2(b). SCI image image

Figure 2(c). SCE

EXPERIMENTAL RESULTS AND CONSIDERATIONS

Figure 3(a) shows the time change of the temperature and the humidity inside the dome and the internal temperature of the object. Figure 3(b) shows the changes in the weight and the glossiness over time. The graph in Figure 3(b) shows that the glossiness increased sharply immediately after starting the experiment, reached the maximum value at 6 min after starting, and decreased thereafter. The internal temperature of the blueberries was 0° C and - 3 °C around 8 min and 6 min after starting the experiment, respectively, as shown in Figure 3(a). Thus, from the beginning of the experiment, the glossiness increased, the frost on the surface thawed as the internal temperature rose, and water condensed on the surface of the blueberries, which further increased the glossiness. The reason for the glossiness starting to decrease after 6 minutes was because the frost that formed in the room air after the blueberries were removed from the freezer at -18 °C had finished melting and the condensed water on the surface had begun to evaporate. In addition, it can be seen from Figure 3(a) that the internal temperature of the blueberries exceeds 20 °C and approaches the dome temperature approximately 20 min after starting the experiment. At this time, the weight and glossiness change in the same manner.
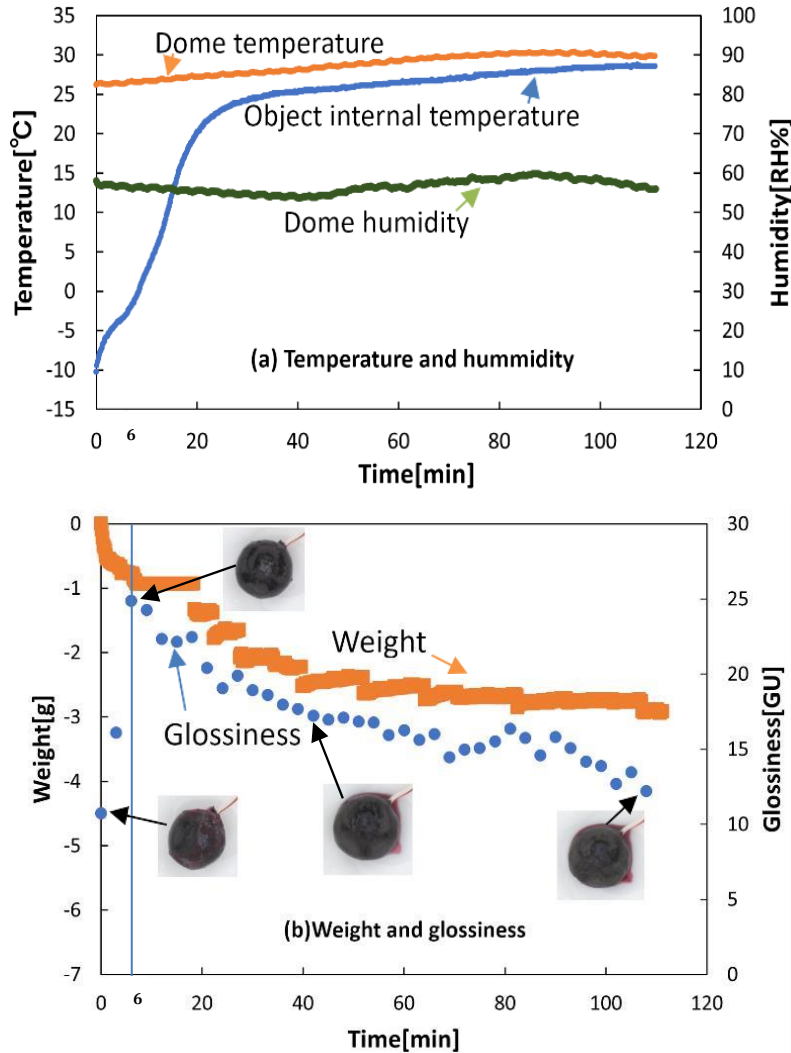
Figure 3. Time variation of the dome temperature and humidity, internal temperature, weight and glossiness of the blueberries

CONCLUSION

Using this equipment, the changes in the color and gross color were investigated during the thawing process of frozen foods. As the internal temperature of the blueberries approached 0 °C, the frost melted and the glossiness increased. After that, the water on the surface evaporated, the glossiness decreased with the decrease in weight.

Future studies will include further exploration of the relationship between the presence or absence of water on the food surface and the gross, and the effect of the thawing conditions on the color and gross color of the food. For this purpose, the current equipment requires further enhancements, such as, introducing the capacity to control the temperature and humidity inside the dome.

REFERENCES

1. Sakai, H., Isomi, M. & Iyota, H. (2018). Non-contact colorimetric measurement using dome illumination for complex shape objects. *Proceedings of the 4th Asia Color Association Conference*: 183-186.
2. Hirouchi, A., Iyota, H., Isomi, M., Yamamoto, H. & Sakai H. (2019). Automatization of 2D-image recording system for analysis of change in food appearance using dome illumination with digital camera. *Proceedings of the 5th Asia Color Association Conference:* 462-465.
3. Shimpei Fukagawa, Hiroyuki Iyota, Hideki Sakai and Mai Isomi (2021). Development of color and gloss measurement system with wide-range temperature and humidity control unit. *Proceedings of the 14th Congress*: (on-line in press)

ADAPTIVE HISTOGRAM ADJUSTMENT TONE MAPPING BASED ON BLOCK SEGMENTATION AND FUSION

Hao Jiang, Haisong Xu[1]*, Jiaxun Zhang[1], Yiming Huang[1]

[1]State Key Laboratory of Modern Optical Instrumentation, College of Optical Science and Engineering, Zhejiang University, Hangzhou 310027, China

*Corresponding author: Haisong Xu, chsxu@zju.edu.cn

Keywords: High dynamic range, Tone mapping, Histogram adjustment, Block segmentation, Image fusion

ABSTRACT

The tone mapping operators (TMOs) aim at reproducing the visual perception of high dynamic range (HDR) scenes on the low dynamic range media. In this study, an adaptive histogram adjustment tone mapping algorithm was proposed based on block segmentation and fusion. Traditional histogram-based TMOs may lead to excessive contrast enhancement, so we adopted a novel histogram adjustment method inspired by K-means clustering algorithm. In this algorithm, the HDR images are segmented to several blocks and the histogram adjustment is applied separately to improve the image quality further. Then we designed an image fusion scheme with the form of a bilateral filter to deal with the artefacts on block boundaries. The proposed TMO was evaluated on a number of HDR images using tone-mapped image quality index (TMQI), indicating better image quality than the representative tone mapping methods. Meanwhile, a good balance between the global and local contrast can be achieved with this algorithm.

INTRODUCTION

High dynamic range (HDR) imaging technologies have achieved great progress recently. With the sources of HDR images being more accessible, there comes the need of reproducing HDR images on traditional low dynamic range (LDR) displays. And tone mapping operators (TMOs) can fulfill the demand, aiming to reproduce the visual impressions and feature details of the original real scenes faithfully.

Traditional histogram-based TMOs tend to be related with the histogram equalization or the perceptual characteristics of human vision system [1-2]. This may lead to excessive stretching of contrast in highly populated bins, whereas the pixels in sparse bins can suffer from excessive compression of contrast. Considering of these drawbacks, we propose an adaptive adjustment tone mapping algorithm based on block segmentation and fusion.

ADAPTIVE HISTOGRAM ADJUSTMENT TONE MAPPING

Pipeline of the proposed tone mapping

In the proposed algorithm, the weighted sum of the channels of HDR image is calculated to get the luminance channel. Then the luminance image is divided into non-overlapping blocks evenly. Inside each block, the histogram is adjusted based on K-means clustering, which results in an appropriate detail-preserving curve. Finally, a scheme of image fusion is done by weighted mean of a bilateral filter form. The main procedure of the proposed algorithm is shown in Figure 1.
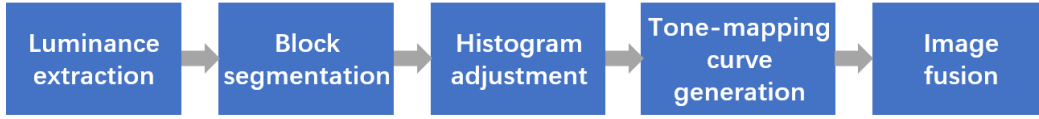
Figure 1. The pipeline of the proposed algorithm

Luminance extraction and block segmentation

Given an HDR image in RGB format, the luminance channel is extracted as Eq. (1).

$$I = 0.2627R + 0.6780G + 0.0593B \qquad (1)$$

The luminance extraction makes it possible that the hue and chroma information is generally maintained in final output.

Then the luminance image is divided into non-overlapping regular rectangular blocks. With this step, the tone-mapped images would have better local contrasts and so preserve more details.

Histogram adjustment

In each divided block, we apply a histogram-adjustment algorithm inspired by *K*-means clustering, which is detailed introduced by Oskarsson *et al.* [3]. With the algorithm implemented, the subimages are mapped as Eq. (2).

$$F(u): \{u_1, \dots, u_N\} \rightarrow \{c_1, c_2, \dots, c_K\} \qquad (2)$$

where $u_1, u_1, \dots, u_N$ are intensity levels of a subimage, $c_1, c_2, \dots, c_K$ are cluster centers, N refers to the number of intensities, K is set as 256 to match up with the bit depth of LDR images and so each cluster corresponds to an LDR intensity value, and F means the mapping curve generated.

Tone-mapping curve generation

In this session, a global tone-mapping curve is utilized to suppress excessive enhancement or compression. According to Weber-Fechner's law, the perceptual lightness versus logarithm of radiance is linear. In literature, there are a number of global TMOs taking the form of logarithm. Similarly, we build another mapping curve as Eqs. (3)-(4).

$$G(u): \{u_1, \dots, u_N\} \rightarrow \{l_1, l_2, \dots, l_K\} \qquad (3)$$

where the mapping curve is denoted as G and for $i = 1, \dots, n$,

$$l_i = \exp\left(\log(u_1) + i \cdot \frac{\log(u_N) - \log(u_1)}{K + 1}\right) \qquad (4)$$

In combination of $F(u)$ and $G(u)$, we derive a balanced mapping curve. Considering excessive contrast enhancement or compression often occur in uniform regions, a uniformity measure β is induced to tune proportions. The blended mapping curve is presented in Eqs. (5)-(7).

$$H(u): \{u_1, \dots, u_N\} \rightarrow \{v_1, v_2, \dots, v_K\} \qquad (5)$$

$$v_i = (1 - \beta)c_i + \beta l_i, i = 1, \dots, n \qquad (6)$$

$$\beta = 0.5 * (1 - e^{a-\eta}) \qquad (7)$$

where H is denoted as the blended curve. The subimages' histograms need to be calculated again with the number of bins being 20. In the case, a is then the number of bins which have larger density than the average and η serves as a constant controlling balance power. Notice that v_i is not the final LDR values. There needs also another step to map v_i to LDR values.

Image fusion

After the complementation of block segmentation and curve generation, we propose an image fusion scheme taking the form of a bilateral filter. Without image fusion, subimages would have an appealing contrast but distort in block boundaries apparently. It is considered that a block is related to its neighbouring blocks, as is mapped values. Given an input HDR image I, the image fusion scheme of the output image p is given in Eq. (8).

$$p(\text{x,y}) = \frac{\sum_{i=1}^{i=B} H_i(I(x,y)) \cdot w_d(i) \cdot w_s(i)}{\sum_{i=1}^{i=B} w_d(i) \cdot w_s(i)} \tag{8}$$

(where x, y are pixel coordinates, w_d is the distance weighting factor, w_s is the intensity similarity weighting function, and B is the number of neighbouring blocks considered. In detail, the calculations of w_d and w_s are shown in Eqs. (9-11).

$$w_d(i) = e^{-(d_i/\sigma_d)} \tag{9}$$

$$w_s(i) = e^{-(s_i/\sigma_s)} \tag{10}$$

$$s_i = \frac{|\log(I_t + 1) - \log(I_i + 1)|}{\log(I_{max} + 1)} \tag{11}$$

where d_i is the Euclidean distance between the current pixel $I(x,y)$ and the centres of each of the neighbouring blocks, σ_d controls the smoothness of the image, s_i measures the difference of average values between the target block I_t and surrounding blocks I_i, and σ_s tunes the influence of neighbouring blocks.

Finally, the colour channels of HDR images are transformed to LDR values according to Eq. (12).

$$c(x,y) = C(x,y)/I(x,y) \cdot p(x,y) \tag{12}$$

where $C(x,y)$ denotes one of the colour channels (red, green and blue), and $c(x,y)$ is the output LDR values.

EVALUATION

The proposed algorithm was compared with 5 typical tone mapping algorithms, including Drago *et al*., Ferwerda *et al*., Kim *et al.*, Mai *et al.* and Reinhard *et al.* [4-8].

Implementation details

The parameter selection plays a vital role in our algorithm. We attempt to achieve a balance between the local contrast and overall lightness. The involved parameters are listed in Table 1.

Table 1. The parameters' selected in the proposed algorithm

Parameters	Values
Number of blocks	16*12
N	512
K	256
B	5*5
σ_s	32
σ_d	245.4

Considering that the resolution of HDR images used is up to 3930*2941, the images are all segmented into 16*12 blocks. The division makes sure that there are efficient pixels in each individual block to implement histogram adjustment, while it keeps pleasant local contrast simultaneously.

As to histogram adjustment, the bins of input image histogram is set as 512, with clusters' amount (K) being kept as 256. K corresponds to the bit depth of LDR images and N is twice the number of K to ensure histogram details preserved.

Heuristically, we set the neighbouring blocks as 5*5 grids, i.e., B holds the value of 25. Meanwhile, σ_s is set to 32 and σ_d is calculated as Eq. (13).

$$\sigma_d = (H_0 + W_0)/2 \tag{13}$$

where H_0 and W_0 are the height and width of an individual block respectively.

Objective Assessment

The desirable characteristics of a TMO are that it should produce artefacts-free natural-looking results and preserve the structure. The tone-mapped image quality index (TMQI) calculates the structural similarity and naturalness indices and then combines them to give an overall quality index [9]. Researches show that TMQI has great correlation with the visual preference of images. Therefore, we utilize TMQI to implement the objective evaluation on the tested algorithms.

The tested HDR images are from LVZ-HDR dataset, including indoor and outdoor scenes [10]. TMQI scores for the 9 test images are given in Table 2, with the highest scores being bold. The proposed algorithm shows the best performance for most images, which meanwhile gets best scores for the statistical indexes listed.

Table 2. TMQI scores of tone-mapped images for the tested algorithm

Image Number	Drago	Ferwerda	Kim	Mai	Reinhard	Proposed
1	0.76	0.59	0.74	0.82	0.73	**0.85**
2	0.70	0.52	0.69	**0.80**	0.67	0.79
3	0.77	0.64	0.79	**0.86**	0.74	**0.86**
4	0.76	0.64	0.79	0.84	0.75	**0.85**
5	0.88	0.73	0.88	0.94	0.82	**0.95**
6	0.85	0.71	0.85	0.84	0.79	**0.89**
7	0.91	0.76	0.90	0.86	0.84	**0.92**
8	0.86	0.74	0.89	0.92	0.83	**0.94**
9	0.72	0.66	**0.83**	0.79	0.71	0.82
Mean	0.80	0.67	0.82	0.85	0.76	**0.87**
Min	0.70	0.52	0.69	**0.79**	0.67	**0.79**
Lower quartile	0.76	0.64	0.79	0.82	0.73	**0.85**
Median	0.77	0.66	0.83	0.84	0.75	**0.86**
Upper quartile	0.86	0.73	0.88	0.86	0.82	**0.92**
Max	0.91	0.76	0.90	0.94	0.84	**0.95**

Subjective comparison

A typical visual comparison of the competing methods is demonstrated in Figure 2. The presented images are based on a representative HDR scene, with both indoor and outdoor contents. The results

in (a), (b), (c) and (e) show good global contrast. Whereas there are lacks of indoor details more or less. (d) presents vivid indoor details while the outdoor scene looks like suffering from over-exposure. By comparison, it can be seen from (f) that the proposed algorithm guarantees impressive local contrast from outdoor scenes to indoor details.
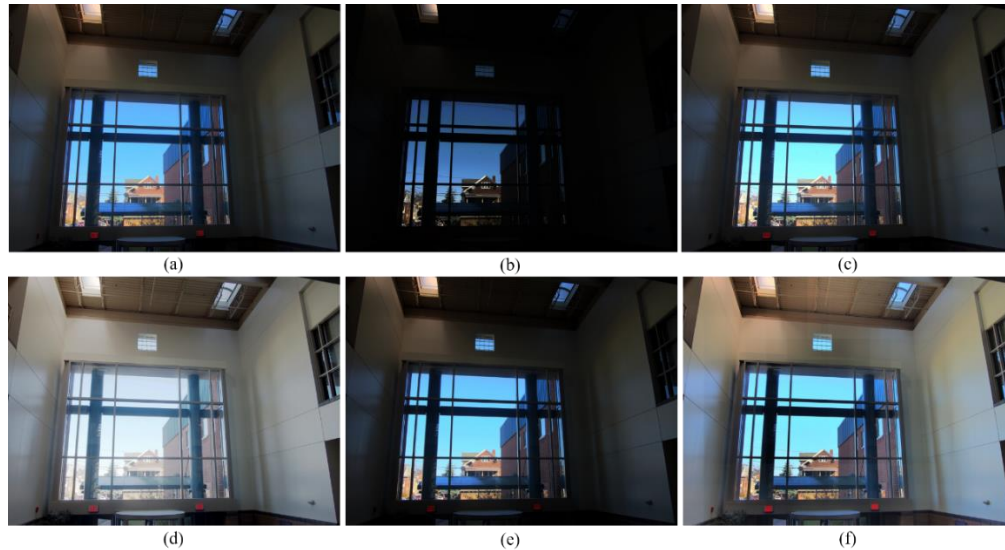

Figure 2. Tone mapping results of a test image. (a)Drago *et al*. (b)Ferwerda *et al*. (c)Kim *et al*. (d)Mai *et al*. (e) Reinhard *et al*. (f)Proposed.

CONCLUSION

In this paper, a histogram-adjustment-based tone mapping algorithm is presented. We proposed a strategy of segmenting an image into several blocks to improve local contrast. Moreover, an image fusion scheme taking the form of a bilateral filter was adopted heuristically. Both subjective assessment and objective evaluation indicate that our algorithm gives comparable results to the typical tone mapping algorithms and achieves a balance between overall lightness perception and detail preserving.

REFERENCES

1. Duan, J., Bressan, M., Dance, C., & Qiu, G. (2010). Tone-mapping high dynamic range images by novel histogram adjustment. *Pattern Recognition*, 43(5), 1847-1862.

2. Khan, I. R., Rahardja, S., Khan, M. M., Movania, M. M., & Abed, F. (2017). A tone-mapping technique based on histogram using a sensitivity model of the human visual system. *IEEE Transactions on Industrial Electronics*, 65(4), 3469-3479.

3. Oskarsson, M. (2017). Temporally consistent tone mapping of images and video using optimal k-means clustering. *Journal of mathematical imaging and vision*, 57(2), 225-238.

4. Drago, F., Myszkowski, K., Annen, T., & Chiba, N. (2003, September). Adaptive logarithmic mapping for displaying high contrast scenes. In *Computer graphics forum,* 22(3), 419-426.

5. Ferwerda, J. A., Pattanaik, S. N., Shirley, P., & Greenberg, D. P. (1996, August). A model of visual adaptation for realistic image synthesis. In *Proceedings of the 23rd annual conference on Computer graphics and interactive techniques* (pp. 249-258).

6. Kim, M. H., & Kautz, J. (2008, February). Consistent tone reproduction. In *Proceedings of the Tenth IASTED International Conference on Computer Graphics and Imaging* (pp. 152-159).

7. Mai, Z., Mansour, H., Mantiuk, R., Nasiopoulos, P., Ward, R., & Heidrich, W. (2010). Optimizing a tone curve for backward-compatible high dynamic range image and video compression. *IEEE transactions on image processing*, 20(6), 1558-1571.

8. Reinhard, E., Stark, M., Shirley, P., & Ferwerda, J. (2002, July). Photographic tone reproduction for digital images. In *Proceedings of the 29th annual conference on Computer graphics and interactive techniques* (pp. 267-276).

9. Yeganeh, H., & Wang, Z. (2012). Objective quality assessment of tone-mapped images. *IEEE Transactions on Image Processing*, 22(2), 657-667.

10. Panetta, K., Kezebou, L., Oludare, V., Agaian, S., & Xia, Z. (2021). TMO-Net: A Parameter-Free Tone Mapping Operator Using Generative Adversarial Network, and Performance Benchmarking on Large Scale HDR Dataset. *IEEE Access*, 9, 39500-39517.

INFLUENCE OF SUBSTRATE PROPERTIES ON COLOR APPEARANCE OF THAI CURRY PRODUCT LABELS IN UV INKJET PRINTING

Somporn Nilmanee[1]*, Vorachet Juntiya[2] , and Meechai Luddee[3]

[1]*Packaging and Material Technology Program, Center of Excellence in Bio-Based Materials and Packaging Innovation, Faculty of Agro-Industry, Prince of Songkla University, Hatyai, Songkhla, 90110, Thailand*

[2]*School of Health Science, Mae Fah Luang University, Thasud Muang, Chiang Rai, 57100, Thailand*

[3]*Faculty of Agro-Industry, King Mongkut's University of Technology North Bangkok, Prachinburi campus, 25230, Thailand*

*Corresponding author: Somporn Nilmanee, e-mail: somporn.ni@psu.ac.th

Keywords: Color appearance, Digital printing, Labeling, Substrate

ABSTRACT

The aim of this study is to evaluate the influence of different substrate properties with color appearance and image color perception on Thai curry product labels in UV inkjet printing. Three commercial substrates of pressure sensitive (PS) label were selected to use in this study. Graphic design of three Thai curry patterns was printed on the substrate differences of thickness and whiteness in setting up the LED-UV curable inkjet printer for speeds, print directions and resolutions. Through the measurement of color appearance on printing quality was discussed by CIE L*a*b*, ΔE^*_{ab} (color difference) and gloss. The related influence of UV digital printing system has not only label cost but also ability of barcode reader application. However, the preference of image color perception on suitable substrates should be considered by designer or manufacturer.

INTRODUCTION

Current usages of digital printing have become a mainstream process to expect growth in the commercial print area. The adoption of digital printing is widespread to a variety of products into the various market sectors. For packaging industry, digital printing applications are self-adhesive labels, prototyping of package promotion, batch number, print and apply labels, point-of sale items and digital proofing. The digital printing advantages for labels process can make on demand in limited order quantity, short run of production speed, cost consideration, and printing onto a variety of substrates under inkjet or toner printing system. Majority of digital work process of packaging is label category to meet the inkjet printing. If digital printing is to expand into other packaging areas, toner-based systems may not be able meet the demands of printer. Because of higher cost toner-based system, digital inkjet is expected to grow at a fast rate [3].

In addition to UV-curable ink and solvent ink, color and adhesion of ink are important commercial applications to direct product labeling. Solvent-based inks dry by evaporation and UV-curable inks are solidified by brief exposure to UV source [2]. In this study focused on digital printing with LED-UV curable inkjet printer on three surfaces of labels at different printing speed condition. In figure 1 shows UV-LED print mechanism of UV ink property of immediate curing upon UV light irradiation, no drying time is required.
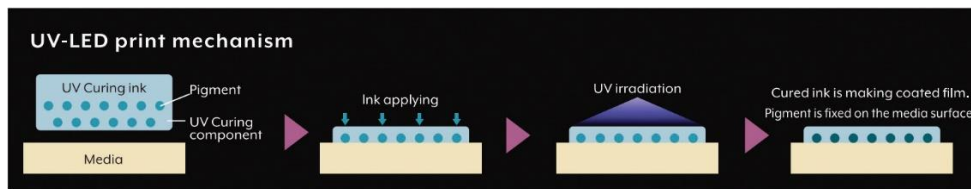
Figure 1. UV-LED print mechanism of UV ink property
source: www.mimaki.com

Additional considerations of label material selection with suitable product include substrate properties such as opacity, stiffness, smoothness, brightness, whiteness and thickness. These factors are based on ensuring quality, consumer compliance of agreement as well as good color appearance. The most common film materials are used in package labels. According to substrate for digital printing, Bugner, 2002 [2] described the intended application of the substrate forms for digital printing. The inkjet receivers of substrate compose of uncoated papers, coated paper, composites, films and synthetic paper. UV ink process is printable to PVC, PET, PP, paper, fabric and more varied applications. For the substrate types of print modes, it can choose from depending on work purpose or consumer satisfaction. In term of color measurement, spectrophotometer has ability to measures transmitted, reflected, or emitted light from an object at many different wavelengths. Typically, the measurement is made in spectral radiance or colors perceived emittance values from 400 to 700 nanometers [1]. The CIE adopted three - dimension color model is called CIE-LAB in which the distances do correspond to perceived color differences. It can be useful for work at understanding Lab (CIE-Lab). Therefore, the objective of this study is to evaluate the influence of different substrate properties with color appearance and image color perception on Thai curry product labels in UV inkjet digital printing.

MATERIAL AND METHOD

Material and sample preparation

Graphic design of labels was created with Adobe Illustrator program which program can be determined cyan (C), magenta (M), yellow (Y) and black (K) equivalent for choosing in subtractive system. Thai curry Pressure Sensitive (PS) labels of three product types under Anurux brand were designed with Adobe Illustrator CC. Graphic of the labels were designed to compost of food pictures, information of product and brand name. The UV- curable ink of inkjet printing was provided onto the three commercial substrates of pressure-sensitive adhesive materials (Avery Dennison supplier). Three products were collected background spaces of the printed label samples for measuring colors as shown in Figure 2 (green: instant green curry power, red: instant massaman curry power, and yellow: instant yellow curry power). Accordance with printer parameter setting up, the label samples were printed with digital inkjet printer (Mimaki, UCJV 155-160, Japan). It was determined scan speed in both normal and high speed level at the same uni-print direction and resolution setting for 600 x 1200 dpi of all printed substrate samples.

Color measurement and microscopic images

CIE L* a* b* and color difference (ΔE) value of the printed label samples were measured according to ISO 12647-6: 2020 standard using spectrophotometer X-Rite eXact™, USA) at D50 illuminant, 2 observer, 0°/45 geometry). The evaluation of the printed surface is based on comparing the color appearance between different printing speeds and printing substrate materials.

Digital microscope (1000x, China) used optics system and a digital camera to capture and magnify images. These images were displayed computer monitor with camera software through USB

port which can be attached to microscope for printed photo quality of 0.1 MP. They were visually assessed. The substrates without printing image were measured by using a gloss meter. Gloss was measured at the angle of 60°.

| Product a | Product b | Product c |

Figure 2. Thai curry label design features

RESULT AND DISSCUSSION

CIE L*a*b*, Color difference and Microscopic Analysis

As shown in Table 1 and Table 2, L*, a* and b* values of printing color onto three substrates at labeling three products (Instant yellow curry powder, instant massaman curry powder and instant green curry powder) exhibited a similar graphical trend for both printing speeds. The effect of label color with L* values was found that instant yellow curry powder and instant green curry powder higher than instant massaman curry powder. This indicated that yellow and green were vivid pigment color as lightness. Parmod & Sharma, 2017[8] applied the ultraviolet (UV) curing process to be coated the substrate with properties of high-gloss hardness. Effective photoinitator has to be adjusted to a special region and the special absorbance. Seipel *et al.*, 2019 [9] studied color effect of switching speeds by inkjet printing and UV-LED curing based on photochromic dry.

Table 1. The color specifications of normal speed printing onto three different substrates

Materials	Thickness (um)	CIE L*a*b			Gloss (GU)
		Instant yellow curry powder	Instant Massaman Curry powder	Instant Green curry Powder	
Substrate 1	97	L =87.95	L =35.49	L =73.64	100.33
		a = -3.07	a = 35.07	a = -31.89	
		b = 88.21	b = 20.08	b = 65.03	
ΔE S1-S2		3.96	1.50	1.19	
Substrate 2	262	L = 87.86	L = 37.16	L = 74.49	88.66
		a = -4.15	a = 37.59	a = -32.30	
		b = 88.45	b = 20.95	b = 65.96	
ΔE S2-S3		10.11	.3.20	7.47	
Substrate 3	200	L = 81.79	L =35.52	L =70.34	78.90
		a = -4.52	a = 35.21	a = -31.67	
		b = 80.69	b = 18.74	b = 61.70	
ΔE S3-S1		7.96	4.93	5.77	

Table 2. The color specifications of high speed printing onto three different substrates

Materials	Thickness (um)	CIE L*a*b*			Gloss (GU)
		Instant yellow curry powder	Instant Massaman Curry powder	Instant Green curry Powder	
Substrate 1	97	L = 87.74 a = -3.56 b = 83.23	L = 40.54 a = 35.77 b = 20.33	L =76.06 a = -28.47 b = 63.94	100.33
ΔE S1-S2		3.50	1.45	1.11	
Substrate 2	262	L = 88.20 a = -3.28 b = 85.13	L = 39.81 a = 35.25 b = 18.80	L = 75.87 a = -29.40 b = 64.32	88.66
ΔE S2-S3		10.30	3.22	6.31	
Substrate 3	200	L = 82.54 a = -4.27 b = 77.03	L = 38.31 a = 33.12 b = 16.82	L = 71.89 a = -28.34 b = 58.84	78.90
ΔE S3-S1		8.37	4.33	6.24	

This study can conclude that the print color was affected by its corresponding whiteness and lightness. The result of this study was consistent with the description of Li *et al*., 2020 [7] that investigated the effect of UV-curable inkjet printing on the heat- sensitive PP substrate. The influences of printing parameters such as the printing distance, number of overprints, color of ink. The physical size of the area shown in each image is 11 mm x 9 mm as indicated in Table 2 - 4. When comparing the printer speed with black letter printed samples and negative letter without printed samples were performed clearly sharpness difference between high speed printing and normal speed printing at the same trend of three substrates. Furthermore, the results showed that gloss values of each substrate were small color differences with in most visible to the human eye. On the other hand, color difference (ΔE) of each condition exhibited closely 1 ΔE for substrate 1 and substrate 2 of instant massaman curry powder and instant green curry powder. In study of Hajipour & Shans-Nateri [4] analyzed a color tolerance of the color gamut between reference and printed sample with UV- inkjet printing. The maximum acceptable color difference was obtained 2 CIE L*a*b* of CMYK target. Additionally, this could be due to the fact that affected the comparison of color difference (ΔE) before and after transfer of the dot area in UV- curable inkjet printing [7].

High speed printing of yellow curry label	High speed printing of massaman curry label	High speed printing of green curry label
Normal speed printing of yellow curry label	Normal speed printing of massaman curry label	Normal speed printing of green curry label
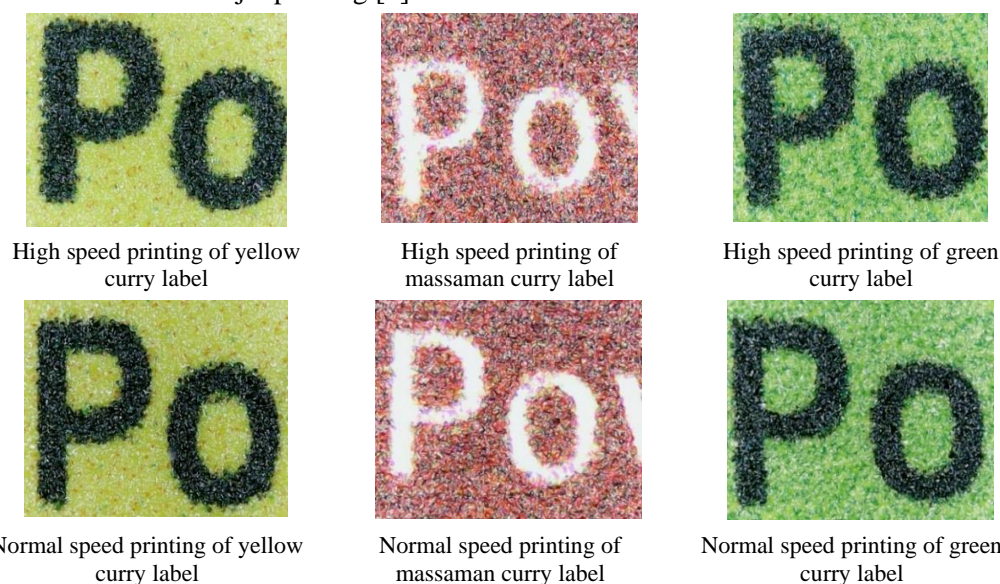
Figure 2. Microscopic surface of the printed labels at normal speed and high speed of printer operating onto substrate 1

High speed printing of yellow curry label

High speed printing of massaman curry label

High speed printing of green curry label

Normal speed printing of yellow curry label

Normal speed printing of massaman curry label

Normal speed printing of green curry label

Figure 3. Microscopic surface of the printed labels at normal speed and high speed of printer operating onto substrate 2

High speed printing of yellow curry label

High speed printing of massaman curry label

High speed printing of green curry label

Normal speed printing of yellow curry label

Normal speed printing of massaman curry label

Normal speed printing of green curry label

Figure 4. Microscopic surface images of the printed labels at normal speed and high speed of printer operating onto substrate 3

CONCLUSION

The print color appearances were affected by its corresponding substrate color and printing parameter switching speed level. Gloss value of all substrates was slightly presented ink color difference of label background in this study. It can be important color appearance of image which reveals negative letter background as bare white of each substrate. Printing speed and vivid ink color had effected sharpness of distinguish of dot area of images and also L* value. The labeling preference of image color perception onto suitable substrates should be considered by designer and manufacturer agreement.

REFERENCES

1. Ashe, T. P. (2014). *Color management & quality output: Working with color from camera to display to print*. New York and London. Focal Press: Taylor & Francis group.

2. Bugner, D. E. (2002). *Handbook of imaging materials, Papers and Films for Ink Jet Printing. 2nd Edition*: New York, USA: CRC Press.

3. Casatelli, L. M. (2011). *Digital printing technologies for packaging*, *Digital print trends by packagetype*, England: Pira International Ltd.

4. Hajipour, A, & Shans-Nateri, A. (2021). Expanding the color gamut of inkjet textile printing during color matching. *Color research & applicati*on, 46, 1218-1226. doi 10.1002/col.22681

5. Hu, Guichun Hu,. Fu, Shiyu,. Chu, Fuqing,. & Lin, Maohai. (2017). Relationship between paper whiteness and color reproduction in inkjet printing. *BioResources*, *12*(3)4854-4866.

6. Li, G. W., Ho, C. P., Yick, K. I. & Zhou, J. Y. (2020). Effect of UV-Curable inkjet printing parameters on physical, low-stress mechanical, and aesthetic properties of polypropylene knitted fabric. *Fibers and polymers*, *21*(12) 2788-2798. doi10.1007/s12221-020-1295-5

7. Lu, X. & Chen, C. 2020. A study on print quality attributes variance of OMR between PET and ABS by digital inkjet printing. *IOP Conference Material Science and Engineering*. 964. doi:10.1088/1757-899X/964/1/012019

8. Parmod & Sharma, S. (2017). Curing and drying technology in printing and packaging substrate. *International Journal of Science, Engineering & Computer Technology*, *7*(1), 41-43.

9. Seipel, S., Yu, J., Viková, M., Vik, M., Koldinská, M., Havelka, A. & Nierstrasz, V. (2019). Color performance, durability and handle of inkjet-printed and UV-cured photochromic textiles for multi-colored application. *Fibers and polymers*, *20*(7), 1425-1435. doi 10.1007/s12221-019-1039-6

EVALUATION OF CONSISTENT COLOR APPEARANCE

Yuta Terashima[1]*, Yukiya Konta[1] and Yasuki Yamauchi[1]

[1]*Department of Informatics, Graduate School of Science and Engineering, Yamagata University, Japan.*

*Corresponding author: Yuta Terashima, twd04048@st.yamagata-u.ac.jp

Keywords: Consistent color appearance, Color reproduction, Psychophysical evaluation

ABSTRACT

The colors attainable on devices vary tremendously as their gamut differ. Therefore, images reproduced on different devices have different colors. However, it is desirable for the images reproduced on various devices, such as a company logo, to have a similar color impression/appearance. The degree of similarity in color appearance among this set of images can be defined as consistent color appearance (CCA). If the CCA is high, the colors appear similar (or consistent). To evaluate whether the colors have CCA, it is necessary to develop a metric to describe CCA. Although several color difference metrics, such as CIEDE2000, have been often used to evaluate color difference, they do not necessarily represent subjective differences in color impression/appearance. To solve this problem, a new concept of "trendline" has been proposed. Consistent colors were expressed as a trendline. Thus, the degree of deviation from a trendline might be used to evaluate CCA, i.e., a set with a smaller deviation from the trendline would have more consistent colors. In this study, we conducted psychophysical experiments to verify this approach. We created 25 sets of color patches for six hues (red, green, blue, cyan, magenta, and yellow). Each set consisted of 7 patches. Some of the colors were chosen to be on the trendline, while the others were off-trendline. Subjects were presented with two sets of the color patches, selecting the one with higher CCA. The sum of the color differences between all pairs of adjacent patches was calculated. A good correlation was found between the selection rate and the total sum of the color difference. This result indicates that the trendline approach can be used to develop a good metric to describe CCA.

INTRODUCTION

In order to reproduce an image on different color reproduction devices, such as a company logo, it is important to match their color appearance. The degree of similarity in color appearance among a set of images on such devices can be defined as consistent color appearance (CCA). Metric describing such as CIE76 [1] and CIEDE2000 [2,3] have been widely used to evaluate color difference and color reproducibility. They are suggested to use when the color differences are relatively small. When it comes to evaluating large color differences and consistent color appearances, we would need a new metric to which can well express them. The International Commission on Illumination (CIE) has established the TC8-16 committee and is currently working to develop a method for evaluating the consistency of color appearance in a single reproduction medium. A technical committee (TC8-16) has been just working on standardization activities in CIE, aiming to develop this metric.

Evaluating the difference in appearance of two sets would be equivalent to evaluate how close those two sets are. Instead of comparing the color difference/closeness directly, it would be also possible to compare colors with some intervening color. Our final goal in this study is to propose a new metric based on the hypothesis mentioned above. As the first step, we have proposed a new approach of "trendline" in our previous study [4-6]. We conducted psychophysical experiments to find consistent colors for a reference color and, as a result, consistent colors were expressed as a

trendline (Fig. 1). The next step is to verify whether our concept, the degree of deviation from a trendline is applicable to predict CCA, i.e., a set with a smaller deviation from the trendline would have more consistent colors. In this study, we conducted psychophysical experiments to verify this approach and investigated how the degree of deviation from the trendline affects the consistency evaluation.
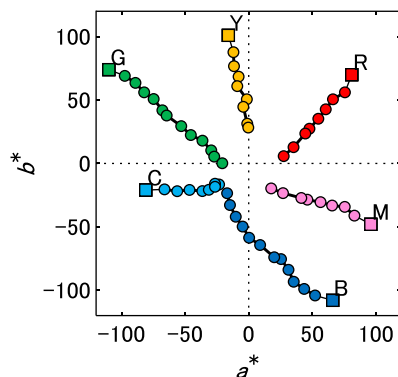

Figure 1. The trendline 2019 in *a*-b** plane

METHOD

Apparatus

The experiment was conducted in a viewing booth whose walls were covered with black velvet. Fluorescent light with a CCT of approximately 5000K (FL20SS ENW/18HF, Panasonic, Japan) lit the inside the booth to prevent observers from dark adaptation. The illumination of the booth was approximately 100 lx. The experiment was performed with an LCD monitor (24.1-inch ColorEdge CX241-CNX, EIZO, Japan; $1,920 \times 1,200$ pixels) for stimulus presentation. The monitor was calibrated with a spectral photometer (SR-3AR, Topcon Technohouse Corporation, Japan) to allow accurate reproduction of colors, based on their colorimetric values. The display had a CCT of 4984 K with a peak white luminance of 119.4 cd/m^2. The CIE1931 xy chromaticity of the R, G, and B primaries were (0.642, 0.329), (0.204, 0.704), and (0.152, 0.060), respectively. All experimental procedures were controlled using MATLAB R2021a (MathWorks, United States) and Psychtoolbox 3 [7,8] on a PC (Vostro 470, Dell, United States; Intel Core i7-3770; NVIDIA GeForce GT 620; 64-bit Windows 10 Pro). The observers' responses were obtained using a mouse connected to the computer. Observers were able to move their heads freely and viewed the stimuli binocularly.

Stimuli

An example of the stimulus is shown in Fig. 2a. The stimuli, defined as a "color group", consisted of a set of seven different color patches, from left to right, R, A, B*i*, C, D*i*, E and F. The patches distribution of red hue condition is shown in Fig. 2b. The patch R, A, C, E, and F are the "trendline colors" on the trendline 2019, while the patch B*i* and D*i* are test colors with five different colors. The test colors are apart from the trendline 2019. The patch B is selected from one of the 5 color test colors, either B3 (on the trendline), B1, B2, B4, or B5 (off- trendline), and so is the patch D (either D3, D1, D2, D4, or D5). The saturation of the test colors B1 to B5 is the same as that of the B3, and similarly the saturation of the test colors D1 to D5 is the same as that of the D3. The color difference of the test colors was 5, 10 degrees in CIELAB metric hue-angle from the trendline 2019 in both directions, respectively. The hue-angle parameters of the test colors are also defined by the following equation:

$$h_{Bi} = h_{B3} \pm \Delta h, \tag{1}$$

$$h_{Di} = h_{D3} \pm \Delta h, \tag{2}$$

where h_{Bi} and h_{Di} are the hue-angle of the test colors B1-5 and D1-5, respectively. The hue-angles of the test colors B3 and D3, which locate on the trendline 2019 are represented as h_{B3} and h_{D3}, respectively. In these equations, Δh is a hue-angle difference parameter from the hue-angles h_{B3} and h_{D3} of the B3 and D3 colors, with three levels of $\Delta h = 0$, 5 and 10 degrees.

As mentioned above, the color groups consisted of a combination of five trendline colors (R, A, C, E, F on the trendline) and the two test colors (Bi, Di). A total of 25 color groups were created. Since we have defined the trendlines for six colors (Red, Green, Blue, Cyan, Magenta, Yellow), the color group was also created for those colors. Figure 2c shows an example pair of stimuli on screen. It consisted of two-color groups, which were presented simultaneously on a gray background. The color groups were separated and colored with the gray background.
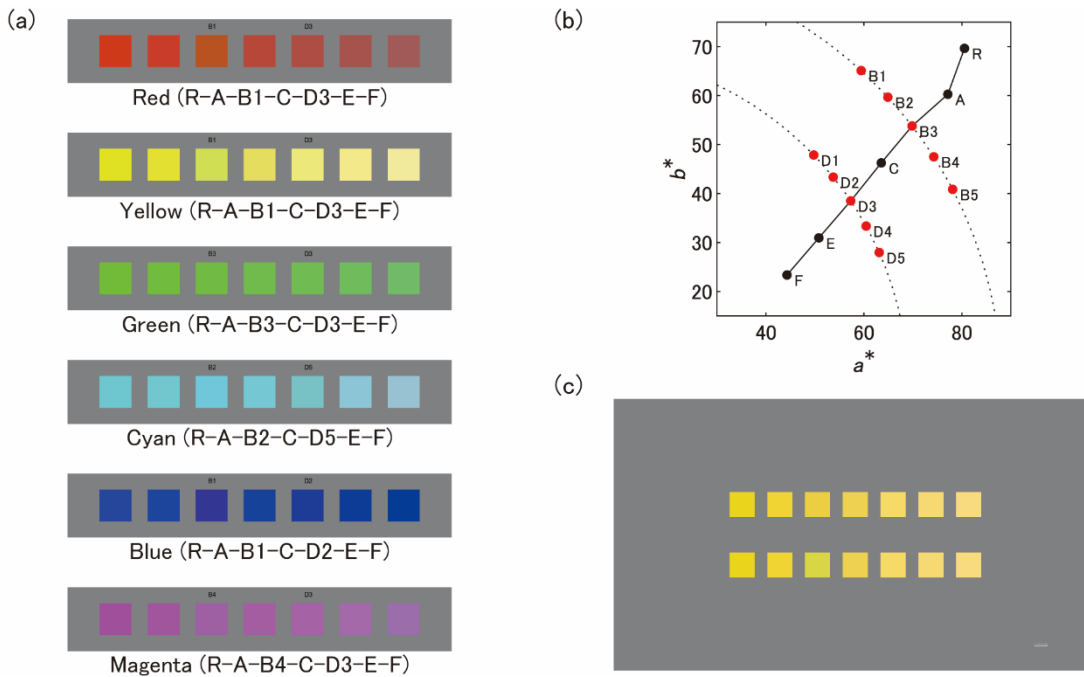
Figure 2. (a) Example of the stimuli in six hue conditions used in the experiment. (b) Test patches distribution of red hue condition in the CIELAB a^*-b^* plane. The black circular plots and line fitting represent the trendline 2019, and the red circular plots are test patch colors. (c) Example of the presented stimulus pair on display.

Procedure

The degree of color similarity of a set of color patches was measured using the Thurstone's paired comparison method. The experimenter explained the general procedure of the experiment and specifically explained the concept of "consistent color appearance" to the observer. Each observer received a training session prior to the experiment. In the experiment, each observer was asked to sit approximately 80 cm from the display. They required to adapt to the viewing conditions for 1 min prior to each session and viewed the grey background on the screen. After the adaptation, a stimulus pair was displayed for evaluation. A stimulus pair was presented on the monitor during each trial (Figure 2b). The combination of the stimulus set and the order of presentation of the stimulus pairs were randomly determined for each trial. During stimulus presentation, the observer responded

which of the two (upper or lower set) appeared to be more consistent by clicking the mouse button in a two-alternative forced-choice (2AFC) task. The stimulus was presented on the screen until the observer made a response. After the observer's response to the mouse click, a mask with a gray background was presented on the screen for 0.8 s, followed by a uniform gray screen to avoid dark adaptation. The next stimulus was presented after the mask.

The number of stimulus pairs was 1,800 ([$_{25}C_2$ = 300 stimulus pairs] × [6 hue conditions]), and each observer responded three times for each pair. The experiment was divided into 18 sessions for each observer, and it took approximately 16.5 min to complete a session, on average. Observers performed three sessions per day (some observers performed up to six sessions), with at least approximately 5 min of rest between sessions.

Five male graduate and undergraduate students in their twenties from Yamagata University, including the author, participated in the experiment as observers. All observers had normal or corrected-to-normal visual acuity, and they were naïve for the purpose of the research except the author.

RESULTS AND DISCCUSION

Figure 3 shows the selection ratios calculated for all the observers' responses. The vertical axis shows ratios of stimuli choice in z-score. The horizontal axis shows the three categories of all stimuli, which are TL, Category I, and Category II. Each symbol represents the selection ratio for each stimulus, where squares denote TL, circles denote Category I, and triangles denote Category II. In this figure, the higher ordinate values indicate that the stimulus is more consistent. As a description of each category, TL is the stimulus on the trendline (R-A-B3-C-D3-E-F), Category I is the positional relationship where the patches B and D deviated to the same side of the trendline, either +Δh or -Δh, and Category II is the opposite side. Two clear tendencies are observed in this figure. First, the overall selection ratios varied from high to low values in each condition. It can be suggested that the degree of consistency differs greatly across the stimuli. In particular, the selection rate for Category I resulted in a relatively higher value than that for Category II. Furthermore, as can be seen from the blue, we found high and low ratio groups even in the same category. It can be suggested that the blue trendline is not hue linear, which may have caused this result. Second, as an overall result, TL had the highest or second highest ratio of selection, with the highest ratios in the red, green, blue, and magenta conditions and the second highest in the yellow and cyan conditions. This result suggests that the trendline 2019 proposed in the previous study hold sufficient consistent color appearance.

We then investigated the tendency of consistent color groups, focusing on the degree of deviation from the trendline. The degree of deviation was defined by calculating the sum of the hue-angle differences from the trendline 2019 for B and D colors. For instance, the degree of deviation of stimulus R-A-B2-C-D5-E-F is calculated as 15 from the sum of the hue angle difference $\Delta h = 5$ for B2 and $\Delta h = 10$ for D5. Figure 4 illustrates the relationship between selection ratios and the degree of deviation from the trendline. The symbols indicate the stimulus categories described above, and Category I was further classified into two sub-categories (I-α and I-β), which are indicates by colored symbols. I-α means the test color in the direction of +Δh, and I-β means the direction of -Δh. The x-axis indicates the degree of deviation, and the y-axis indicates the selection ratio. The solid lines represent the linear regression lines. As a result, stimuli with a large degree of divergence tended to have a lower selection rate. In addition, the overall results for subcategories α and β show that stimuli in the +Δh direction had a lower selection rate than stimuli in the -Δh direction and this trend was particularly pronounced in the blue condition. Even the degree of deviation from the trendline were the same, however, they did not necessary give the same closeness/appearance evaluation in terms of consistency of color.
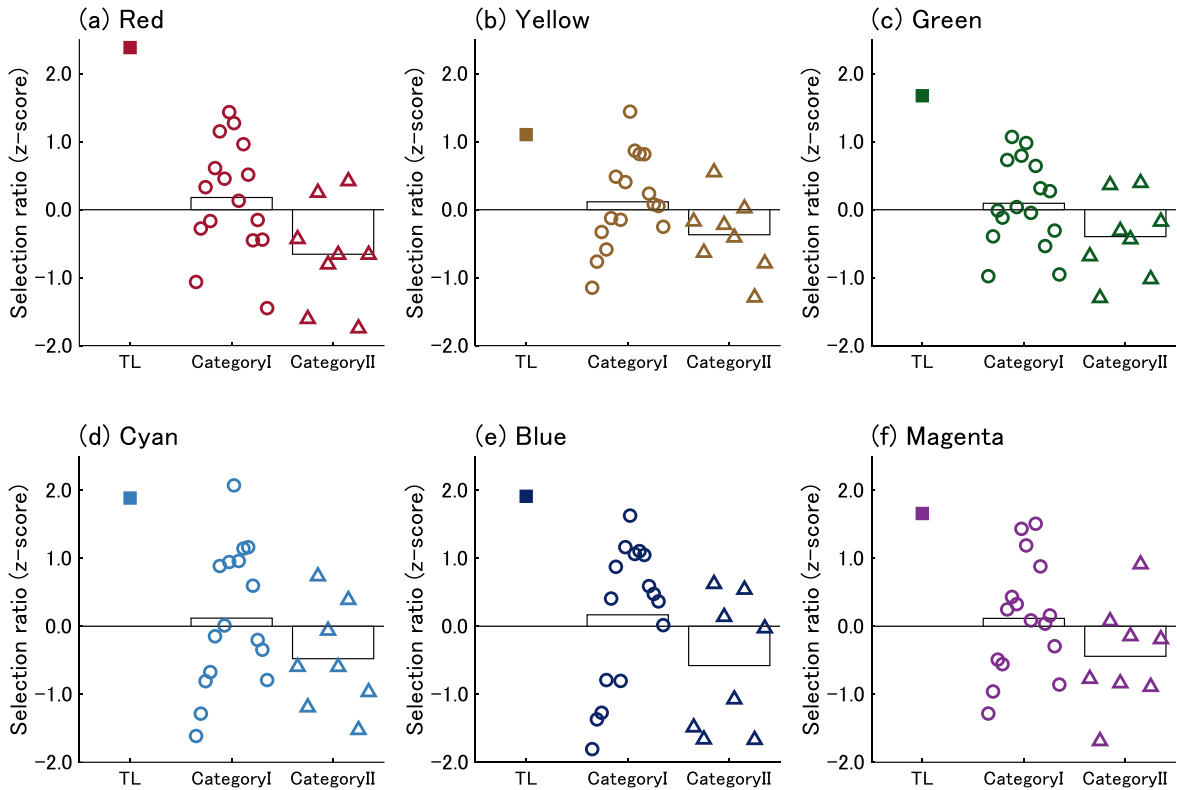
Figure 3. Selection ratios averaged across observers for all stimuli. (a) to (f) are red, yellow, green, cyan, blue, and magenta hue conditions, respectively

CONCLUSION

In our study, we conducted experiments to evaluate consistent color appearance for various set of color patches. In addition, we examined the validity of a new approach for evaluating CCA proposed in previous studies and investigated how the degree of deviation from the trendline affects the consistency evaluation. In conclusion, it was found that the color groups evaluated as highly consistent had a small deviation from the trendline or were located near the trend line. In addition, the color groups on the trendline had a high selection rate, suggesting that the approach of using the trendline to evaluate color consistency may allow quantitative evaluation of the degree of consistency. However, actual images do not consist of only a single color, but a variety of colors. Therefore, it is necessary to investigate how to apply our trendline concept to evaluate the CCA of multi-color images in the future.
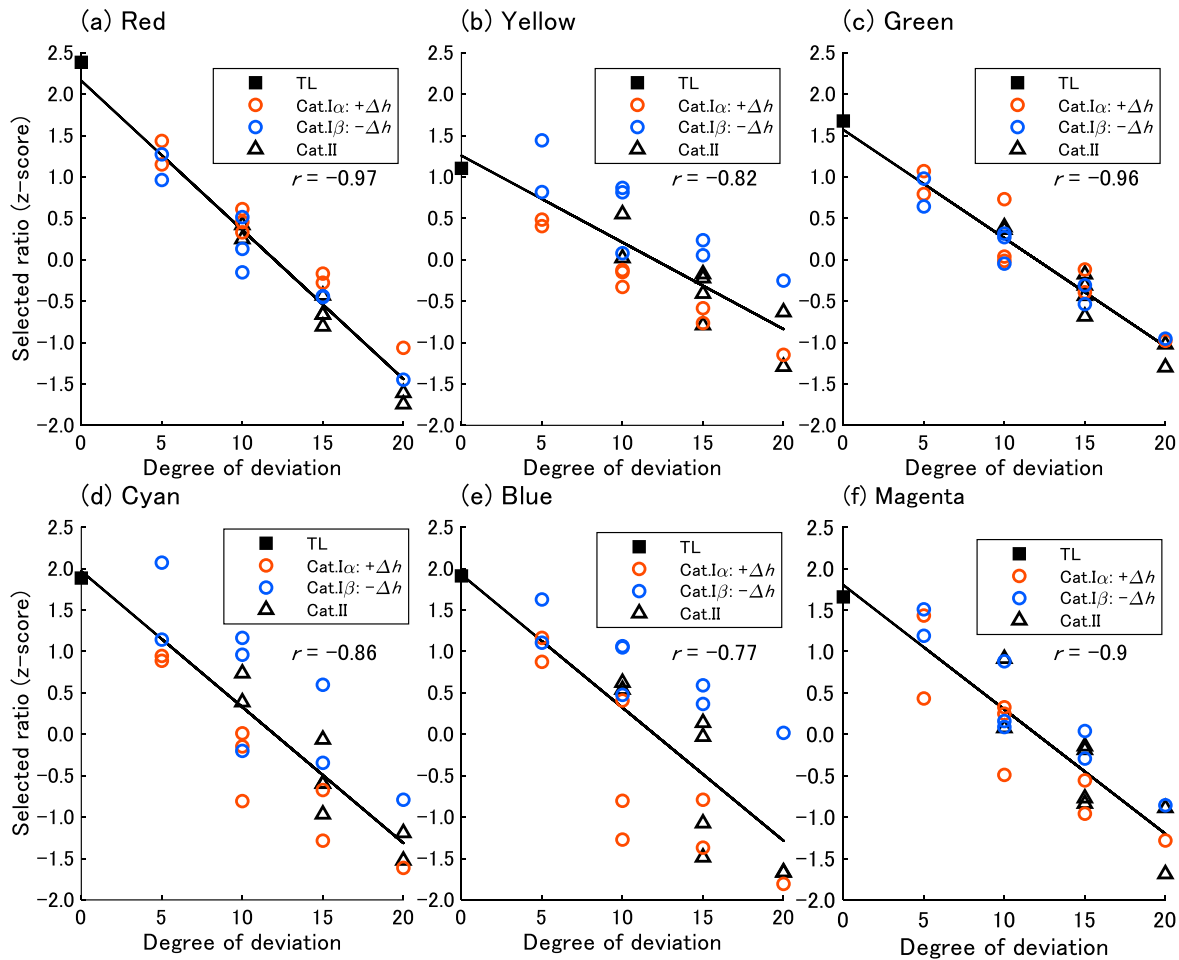
Figure 4. Relationship between selection ratios and the degree of deviation from the trendline

REFERENCES

1. CIE. (2018). Colorimetry, 4th Edition. CIE 015: 2018. doi: 10.25039/TR.015.2018
2. Luo, M. R., Cui, G., & Rigg, B. (2001). The development of the CIE 2000 colour-difference formula: CIEDE2000. *Color Research & Application*, *26*(5), 340-350.
3. ISO and CIE. (2014). Colorimetry-Part 6: CIEDE2000 colour-difference formula. ISO/CIE 11664-6:2014(E), 11664-11666.
4. Yamauchi, Y., Iida. Y., Kawashima. Y., & Nagai, T. (2015). A New Metric for Evaluating the Closeness of Two Colors. *Proceedings of AIC2015*, 680-684.
5. Iida, Y., Kawashima, Y., Nagai, T., & Yamauchi. Y. (2015). A novel metric to evaluate the closeness of the two colors. *Proceedings of CIE2015*, 1086-1092.
6. Terashima, Y., Yamada, S., Tashiro, T., & Yamauchi, Y. (2020). Examination of corresponding colors for consistent color reproduction independent of color gamut (in Japanese), *Vision, 32*(1), 33.
7. Brainard, D. H. (1997). The psychophysics toolbox. *Spatial Vision, 10*, 433-436.
8. Kleiner, M., Brainard, D. H., & Pelli, D. G. (2007). What's new in Psychtoolbox-3? *Perception, 36* (ECVP Abstract Supplement).

METHODS FOR COMPUTING CONE RESPONSES LMS AND CONE FUNDAMENTAL BASED TRISTIMULUS VALUES

Meiyue Liu[1], Cheng Gao[1] and <u>Changjun Li</u>[1]

[1]School of Computer Science and Software Engineering, University of Science and Technology Liaoning, Anshan, China

*Corresponding author: Changjun Li, cjliustl@sina.com

Keywords: colorimetry, cone fundamentals, tristimulus values

ABSTRACT

In this paper we compared the direct selection (DS), CIE recommended (CIE-R), ASTM table 5 (ASTM T5), LLR and LWL methods for computing tristimulus values (TSV) XYZ, $X_F Y_F Z_F$, and LMS. 2393 1nm reflectance set, three continuous, three fluorescent and nine LED illuminants are used for the comparison. It was found that the LWL performs the best in terms of CIELAB colour difference, then followed by the LLR method. The ASTM T5 method forms the third. CIE-R and DS methods perform the worst. It is therefore, the LWL method is recommended for computing TSVs XYZ, $X_F Y_F Z_F$, and LMS.

INTRODUCTION

Tristimulus values (TSV) for the current CIE colorimetry [1] is defined by

$$V = \int_a^b W_V(\lambda) R(\lambda) d\lambda, \text{ with } V = X, Y \text{ and } Z \quad (1)$$

where

$$W_X(\lambda) = \kappa_X E(\lambda)\overline{x}(\lambda), \ W_Y(\lambda) = \kappa_Y E(\lambda)\overline{y}(\lambda), \ W_Z(\lambda) = \kappa_Z E(\lambda)\overline{z}(\lambda). \quad (2)$$

Here, $\overline{x}(\lambda)$, $\overline{y}(\lambda)$, and $\overline{z}(\lambda)$ are CIE 1931 or 1964 colour matching functions (CMF), and κ_X, κ_Y, and κ_Z are scaling factors, and they are all the same and is defined by

$$\kappa_X = \kappa_Y = \kappa_Z = \kappa = 100 / \int_a^b E(\lambda)\overline{y}(\lambda) d\lambda \quad (3)$$

Note that when $\overline{x}(\lambda)$, $\overline{y}(\lambda)$, and $\overline{z}(\lambda)$ are CIE 1964 CMFs, normally a subscript "10" is used. However, the integrands involved in Eq. (1) has no analytical expressions, hence CIE [1] recommended that the integrations should be carried out by 1nm numerical summations:

$$V = \sum_{i=0}^n W_V(\lambda_i) R(\lambda_i)\Delta\lambda, \text{ with } V = X, Y \text{ and } Z \quad (4)$$

at wavelength intervals $\Delta\lambda = 1$ nm.

However, 1nm data are rarely available in practice, since reflectance values are typically measured by a spectrophotometer at an interval much larger than 1nm such as 10nm. Thus, for

practical applications, there is still a problem for how to compute TSVs. CIE has no precise recommendation up to now. Hence there are many methods available for computing TSVs. Different methods lead to different results and the differences obtained using different methods can be large, which can cause problems in current industrial application practice. Li et al. [2] compared available methods such as DS (direct selection), CIE-R (CIE recommended), ASTM table 5 (ASTM T5), Optimum wights (known as LLR method) and Least Square weights (known as LWL method) methods under the continuous (CIE D65, A, and D50) and fluorescent (CIE F2, F7 and F11) illuminants and found that the LLR method is the best.

In 2006 and 2015 CIE [3,4] recommended 2° and 10° of cone fundamentals (CF): $\bar{l}(\lambda), \bar{m}(\lambda)$, and $\bar{s}(\lambda)$. CIE also recommended two sets (2° and 10°) of CMFs $\bar{x}_F(\lambda), \bar{y}_F(\lambda)$, and $\bar{z}_F(\lambda)$ associated with the two sets of CFs: $\bar{l}(\lambda), \bar{m}(\lambda)$, and $\bar{s}(\lambda)$.

Note that when we replace CMF $\bar{x}(\lambda), \bar{y}(\lambda)$, and $\bar{z}(\lambda)$ by $\bar{l}(\lambda), \bar{m}(\lambda)$, and $\bar{s}(\lambda)$ in Eqs. (1) and (2), we have the cone response TSV LMS. In this case the scaling factors κ_L, κ_M, and κ_S are different and may have different choices for different applications since the CFs $\bar{l}(\lambda), \bar{m}(\lambda)$, and $\bar{s}(\lambda)$ were normalized to have a maximum value of 1 for each of them; When we replace CMF $\bar{x}(\lambda), \bar{y}(\lambda)$, and $\bar{z}(\lambda)$ by $\bar{x}_F(\lambda), \bar{y}_F(\lambda)$, and $\bar{z}_F(\lambda)$ in Eqs. (1) and (2) we have the TSV $X_F Y_F Z_F$, and in this case the associated scaling factors $\kappa_{X,F}, \kappa_{Y,F}$, and $\kappa_{Z,F}$ are all equal, and they can be similarly defined using Eq. (3). Note also that subscript "10" is also introduced for the 10° CF and CMF based on 10° CF. Here in this article, we omit the subscript "10" and only mention 2° or 10° CMF or CF.

CIE launched 10 key research areas four years ago and application of CIE 2015 CF-based CIE colorimetry is part of them. The objective of this proposal by the CIE is to conduct field trials that compare the results of the use of the CIE 1931 (2°), CIE 1964 (10°) and CIE 2006 2° and 10° CMFs $\bar{x}_F(\lambda), \bar{y}_F(\lambda)$, and $\bar{z}_F(\lambda)$, especially when applied to LED lighting and in imaging applications. Recently, CIE set up a technical committee TC1-98 to investigate the roadmap for establishing future colorimetry based on CIE 2006 2° and 10° CFs : $\bar{l}(\lambda), \bar{m}(\lambda)$, and $\bar{s}(\lambda)$.

No matter colorimetry based on $\bar{x}_F(\lambda), \bar{y}_F(\lambda)$, and $\bar{z}_F(\lambda)$ or $\bar{l}(\lambda), \bar{m}(\lambda)$, and $\bar{s}(\lambda)$, TSV space $X_F Y_F Z_F$ or LMS are important space since all other spaces will be transformed from the TSV space. Hence, accurate compute TSVs are also important. In this article, we will use the available DS, CIE-R, ASTM T5, LLR and LWL methods used for computing TSVs XYZ for the current colorimetry as the methods for computing TSV $X_F Y_F Z_F$, and TSV LMS, and find out which method is the best for computing them.

EVALUATION PROCEDURE

Illuminants

Three sets of illuminants are used. They are the three continuous (D65, D50 and A), three fluorescent (FL02, FL07 and FL11) and nine LED (B1, B2, B3, B4, B5, BH1, RGB1, V1 and V2) [1] illuminants respectively.

CMFs and CFs

CIE 1931 and 1964 CMFs, CIE 2006 2° and 10° CMFs, and CIE 2006 2° and 10° CFs are used for computing TSVs combined with any of the illuminants used.

Methods for computing TSVs

　　DS, CIE-R, ASTM T5, LLR and LWL methods [2] are used.

Standard 1nm reflectance set

　　1124 reflectance functions measured from Pantone samples and 1269 reflectance functions measured from matt Munsell color chips [2] are used. All were measured between 380nm and 780nm at 1nm interval. This set of reflectance is considered as standard and accurate (or standard) TSVs can be computed using 1nm summation (see Eq. 4).

Measured 10nm reflectance set

　　Using the standard 1nm reflectance set, 10nm reflectance set can be obtained using the simulation model [2].

Computed TSVs

　　Based on the measured 10nm reflectance set, TSVs can be computed using any of the methods under any of the viewing conditions (illuminant plus observer).

Performance measure

　　Similar to CIELAB space can be transformed from the TSV XYZ space, we also can transform the computed TSVs and standard TSVs to the corresponding CIELAB space, and then CIELAB colour difference can be computed. The smaller the CIELAB color difference is, the more accurate the corresponding method is. For each combination of illuminant and color matching function, five statistical measures are used to evaluate the performance of each method. They are the average (Average), median (Median), 80-percentile (denoted as ΔE_{80}), 95- percentile (denoted as ΔE_{95}) and maximum (Max) of CIELAB color difference.

PERFORMANCE FOR EACH METHOD

　　Firstly, weight tables were available for the ASTM T5 under continuous and fluorescent illuminants and CIE 1931 and 1964 CMFs, but not available for LED illuminants, and CIE 2006 2° and 10° CMFs, and CIE 2006 2° and 10° CFs. Hence, we used the ASTM E2022 procedure to compute the TSVs for the ASTM T5.

　　All test results are shown in Figures 1-7 respectively. Figure 1 (A) shows the 3-dimensional bar chart for the performance of the five methods under the 9 LED illuminants and CIE1931 and 1964 CMFs. The left side of the horizontal axis we are facing labels with each of the five methods, the right side of the horizontal axis we are facing labels with each of the five measures. The higher the bar is, the worse the corresponding method preforms under the corresponding measure. It can be seen the DS method performs the worst among any measure. The second worst method is the CIE-R method. LWL, LLR and ASTM E2022 methods are better than CIE-R and DS methods. Figure 1(B) further shows the performance of the LWL, LLR and ASTM E2022 methods. Overall, LWL method performs the best, then followed by LLR and ASTM E2022 preforms the third. Note that Li et al. [2] already showed the LWL performs the best under the continuous and fluorescent illuminants.
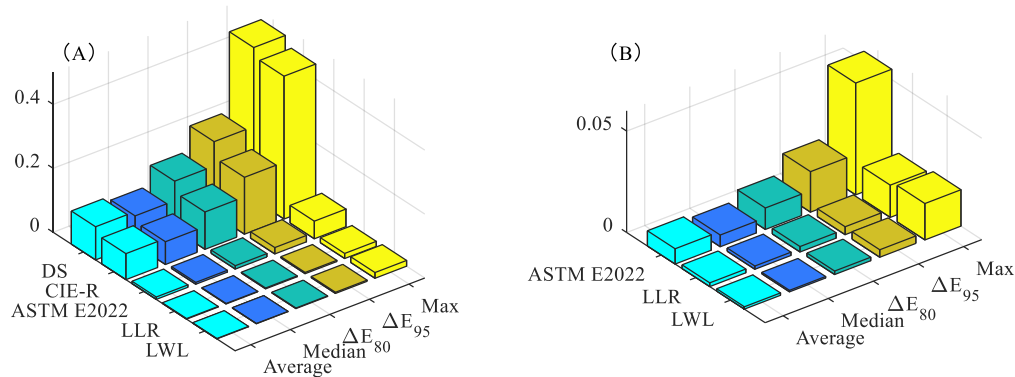
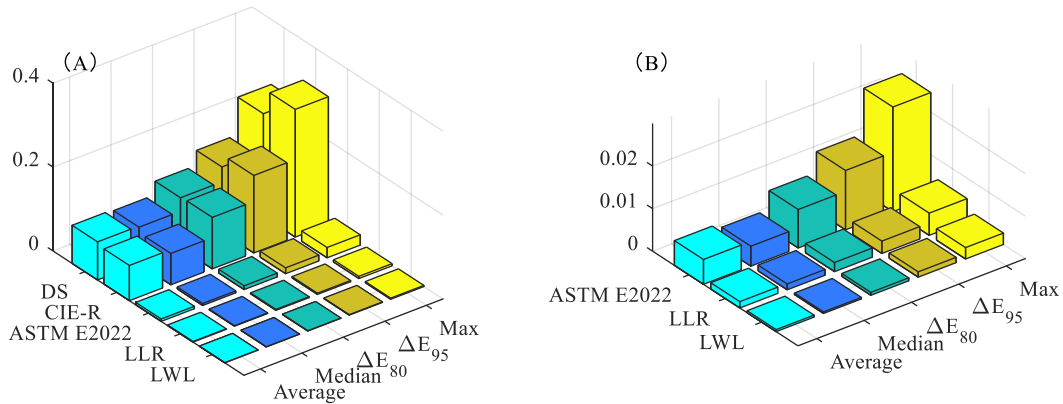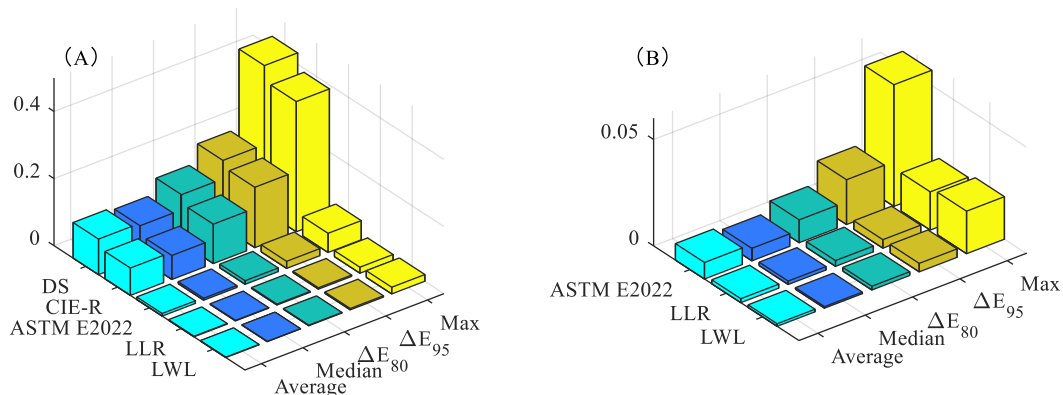**Figure 1. The performance of each method using the combination of nine CIE LED illuminants and two CMFs (CIE 1931 and CIE 1964)**

Figures 2-4 show the performance for all methods under the three continuous, three fluorescent, and nine LED illuminants respectively combined with CIE 2006 2° and 10° CFs. It can be seen again that LWL method performs the best, then followed by LLR and ASTM E2022 preforms the third. The CIE-R and DS performs the worst. Also it can be seen that all methods perform worse under the fluorescent illuminants than under continuous and LED illuminants.
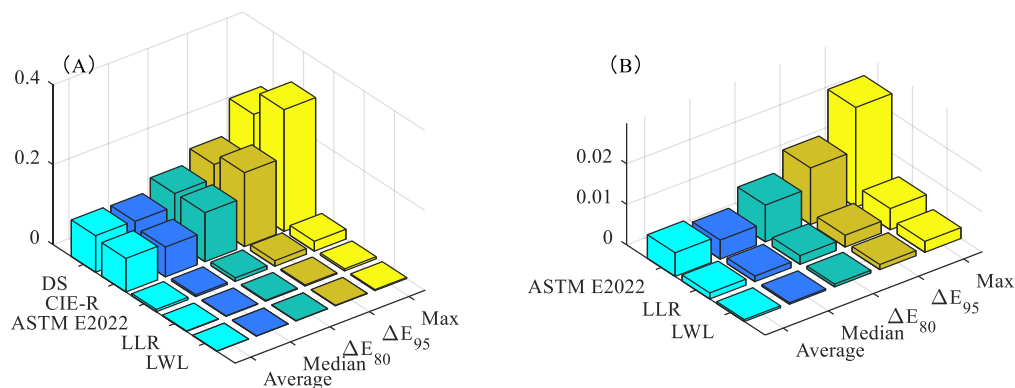
Figure 2. The performance of each method using the combination of three CIE continuous illuminants and two CFs (CIE 2006 2° and 10° CFs)
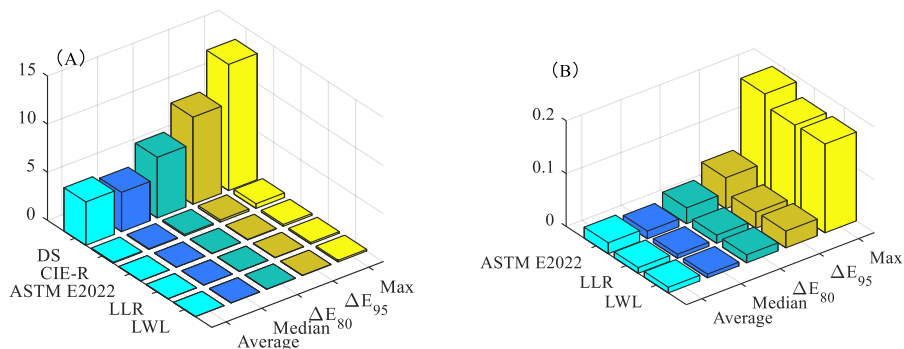
Figure 3. The performance of each method using the combination of three CIE fluorescent illuminants and two CFs (CIE 2006 2° and 10° CFs)

Figures 5-7 show the performance for all methods under the three continuous, three fluorescent, and nine LED illuminants respectively combined with CIE 2006 2° and 10° CMFs. It can be seen again that LWL method performs the best, then followed by LLR and ASTM E2022 preforms the third. The CIE-R and DS performs the worst. All methods perform worse under the fluorescent illuminants than under continuous and LED illuminants.
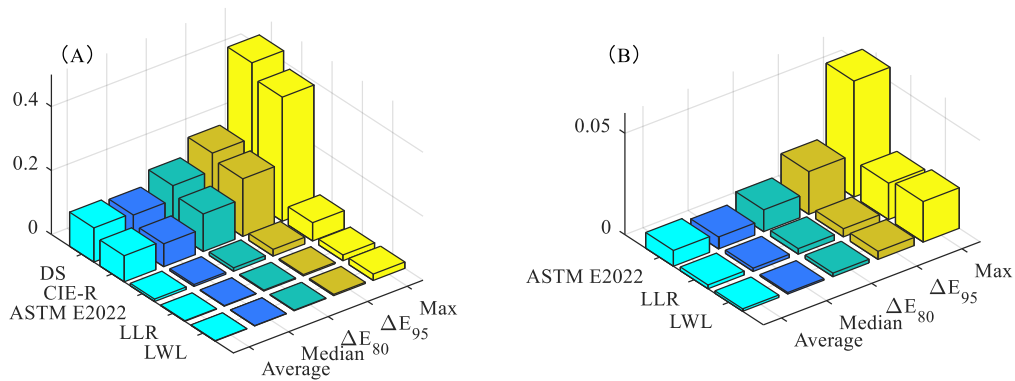
Figure 4. The performance of each method using the combination of nine CIE LED illuminants and two CFs (CIE 2006 2° and 10° CFs)

Figure 5. The performance of each method using the combination of three CIE continuous illuminants and two CMFs (CIE 2006 2° and 10° CMFs)
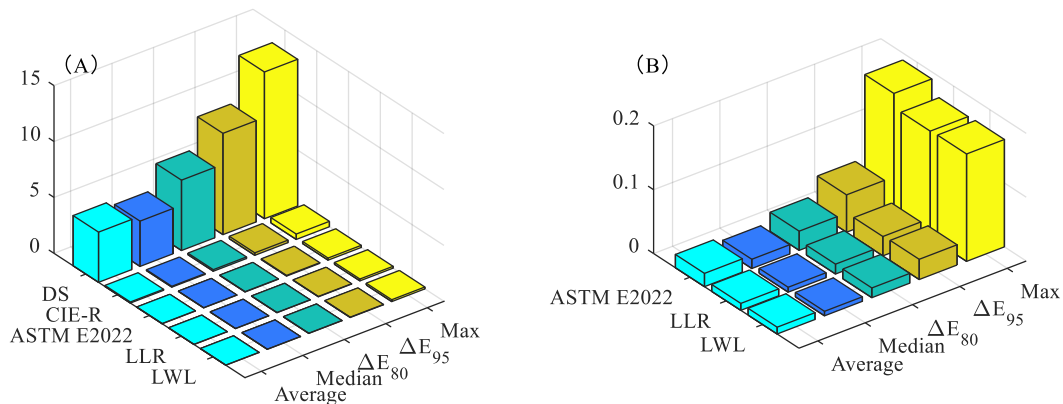
Figure 6. The performance of each method using the combination of three CIE fluorescent illuminants and two CMFs (CIE 2006 2° and 10° CMFs)

Figure 7. The performance of each method using the combination of nine CIE LED illuminants and two CMFs (CIE 2006 2° and 10° CMFs)

CONCLUSION

In this paper, the DS, CIE-R, ASTM E2022, LLR, and LWL methods for computing CIE TSVs are compared. No matter which colour matching function or cone fundamentals is used, it was found that all methods perform worse for CIE fluorescent illuminants than for CIE continuous and LED illuminants and the LWL method performs the best among all methods for 10nm measuring interval length. Therefore, it is proposed that the LWL method should be used for computing TSVs XYZ, $X_F Y_F Z_F$, and LMS.

ACKNOWLEDGEMENT

REFERENCES

1. CIE 015:2018. (2018). *Colorimetry, 4th Edition*. Vienna: CIE. https://doi.org/10.1002/col.22387
2. Li, C., Ming, R. L., Melgosa, M., & Pointer, M. R. (2016). Testing the accuracy of methods for the computation of cie tristimulus values using weighting tables. *Color Research & Application*, 41(2), 1-41. https://doi.org/10.1002/col.21951
3. *CIE Publication 170-1: 2006 Fundamental Chromaticity Diagram with Physiological Axes - Part 1: Definition of CIE 2006 Cone Fundamentals, Vienna, CIE*
4. CIE 170-2:2015(2015). *Fundamental chromaticity diagram with physiological axes - Part 2: Spectral luminous efficiency functions and chromaticity diagrams*. Vienna: CIE. https://doi.org/10.1002/col.22020

THE INVESTIGATE COLOR OF THAI ICED TEA FOR ADVERTISING

Chanida Saksirikosol[1] Jarunee Jarernros[1]* and Kitirochna Rattanakasamsuk[2]

[1] *Department of Advertising and Public Relations Technology, Faculty of Mass Communication Technology, Rajamangala University of Technology Thanyaburi, Thailand.*
[2] *Color Research Center, Rajamangala University of Technology Thanyaburi, Thailand.*

*Corresponding author: Jarunee Jarernros, e-mail: jarunee_j@rmutt.ac.th

ABSTRACT

Individuals' interpretation of Thai tea color might vary based on their experiences because each area's color range of Thai tea has a different color shade. The Thai tea color is distinctive, which may provide communication issues if employed in the design or creation of advertisements. Therefore, this research aims to investigate the color of Thai tea color for advertising. The subjects were students and staff of the Faculty of Mass Communication Technology. They were all tested for color vision deficiency using the Ishihara Tests. The experiment was divided into two parts. The first part was to identify the hue of Thai tea color by selecting the color chips from Munsell hue ring. The second part was to select the color chips from the Munsell color chart of the hue obtained from experimental part I. According to the results of experiment part I, six Munsell hues were selected by at least one subject (i.e., 5YR, 2.5YR, 7.5YR, 10R, 10YR and 2.5Y). In the second experimental part, the subjects selected the colors from 241 color chips that had the hue from the first experimental part. Eight Munsell colors that were consistently selected by at least 20 percent of the subjects were 3.75YR 6/12, 3.75YR 5/12, 5YR 5/12, 1.25YR 5/12, 2.5YR 5/12, 5YR 6/10, 2.5YR 6/12 and 2.5YR 5/14. All colors appeared orange.

INTRODUCTION

Color is an important part that is used in various fields and for the benefits of communication in human daily life, such as to classify the clarity, to convey the meaning, to be used as a symbol [1]. In the advertising field, color has a significant impact on creative works because the colors chosen to be used in the work arise from human's learning to interpret what they perceive naturally. These processes occur automatically in all humans [2]. Nowadays, the names of natural objects or objects of a particular color are often used as references to name colors in order to reduce communication errors and to enable those who are communicating to imagine and visualize the object.

Nowadays, tea beverages are becoming popular among Thai people [3]. For Thailand, there is a famous and unique tea drink both Thais and foreigners known as "Thai Iced tea", which is used as a name instead of the color name. Due to the unique color characteristics of tea leaves, when brewing through hot water, the tea turns orange-red. The flavoring process is with various ingredients such as sugar, sweetened condensed milk, regular condensed milk and fresh milk resulting in the color of Thai tea that is in orange tone. The ingredients in tea brewing in each region are different. As a result, the color of Thai iced tea is various [4].

There was very little research that tried to investigate the representative color of Thai iced tea based on our survey. Saksirikosol et al. (2020) conducted an experiment to establish the

representative hue of Thai iced tea [5] and discovered that perception of Thai iced tea color varies depending on an individual's field of experience. By mixing colors through a computer screen, the color choosing process was from the memory of the subject. The result of mixing color for Thai Tea was showed in CIEL*a*b* color space. The boundary of Thai iced tea color was identified widely in the orange region. The averaged of Thai iced tea color was L* = 52.61, a* = 19.36, b* = 52.81. However, there is a limit of color gamut shown by the computer screen, so it may not be able to display the colors that the subject wants.

In this study, the researchers used the Munsell color system in an experiment to allow the subjects to select a color from the color chip they saw. This covered the colors that our eyes see more than the colors on the monitor. The objective is to investigate the color of Thai iced tea for advertising.

METHODOLOGY

This experiment was divided into two parts. The samples were students and staff of the Faculty of Mass Communication Technology, Rajamangala University of Technology Thanyaburi who have normal vision and pass the Ishiharas Tests plates. There were 400 subjects in experimental part 1 and 144 subjects in experimental part 2.

Experimental part I

The researchers created the Hue Ring using 40 Munsell color chips covering all hue colors in the Munsell Book (Munsell Book Glossy Collection X-rite). Each color chip had chroma 8 and value 5. These colors are arranged in circles on a gray background, as shown in figure 1. Then the Munsell hue ring was installed in a laboratory. The subjects were asked to choose a color that represents the color of Thai iced tea from Munsell hue ring with no limit on the number of choices.
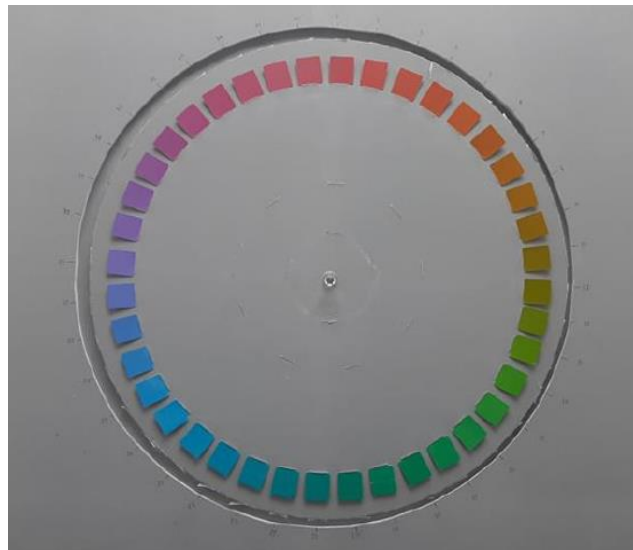
Figure 1. Munsell hue ring used in this experiment

Experimental part II

The other color chips that are in the same color chart as the hue from Experiment part 1 were randomly arranged on a gray board. Then the subjects chose a color chip that represents the color of Thai iced tea based on their field of experience with no limitation on the number of choices in a

laboratory. The illuminance in the experimental room was set between 1000-1200 lux. Figure 2 show the schematic diagram of the set up in the experimental room.
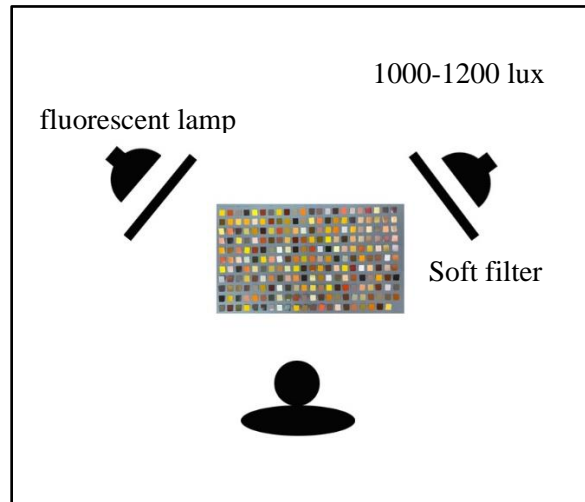
Figure 2. Schematic diagram of the experimental room (Top view)

RESULT AND DISCUSSIONS

Experimental result part I

Result of the selected hue representing the Thai iced tea color was shown in Figure 3. The abscissa represented Munsell hue. The ordinate represented the number of selections. The result showed that there were 6 selected hues. The most selected hue is 5YR which was selected 336 times, followed by 2.5YR, 229 times; 7.5YR, 182 times; 10R, 33 times; 10YR, 26 times, and 2.5Y, 14 times respectively. All selected hue was in an orange shade which relating to an identity color of Thai iced tea.
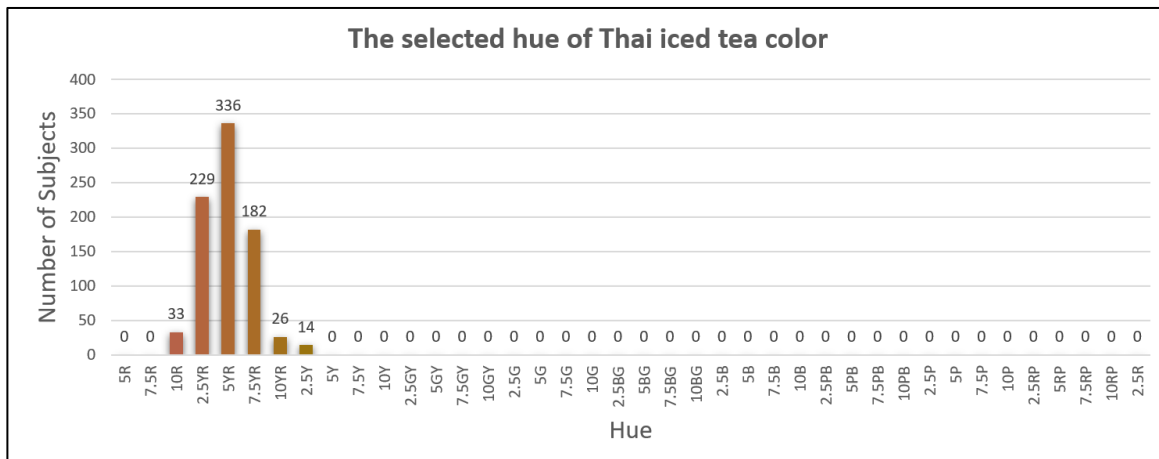
Figure 3. Representative hue selected by all subjects

Experimental result part II

The total of 241 color chips randomly arranged on gray paper was in Munsell 6 hue, 217 color chips, and 24 additional supplementary colors in the same color hue. From the experiment, it was

found that the colors that were selected more than 20% from 144 subjects consisted of 8 colors, as shown in Figure 4. The area of the color represents the frequency of the selection.   The 8 colors representing Thai iced tea colors are 3.75YR 6/12 (43.75%), 3.75YR 5/12 (57.00%), 5YR 5/12 (36.81%), 1.25YR 5/12 (30.56%), 2.5YR 5/12 (26.39%), 5YR 6/10 (22.92%), 2.5YR 6/12 (21.53%), and 2.5YR 5/14 (20.83%). Table 1 shows the color values in the CIEL*a*b color space to be used in the printing industry.
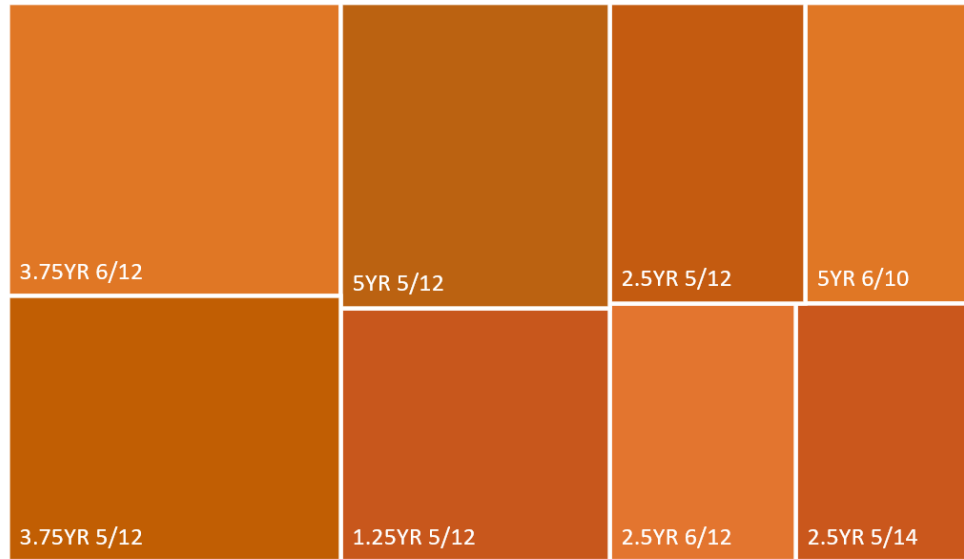
Figure 4. Top selected Munsell color for Thai iced tea color
(Note: color might not present the exact color appearance to subjects)

Table 1. CIEL*a*b* of Thai tea color

Munsell	L*	a*	b*
1.25YR 5/12	51.45	43.70	54.37
2.5YR 5/12	51.70	40.95	63.21
2.5YR 5/14	54.16	44.79	72.04
2.5YR 6/12	61.20	41.98	63.76
3.75YR 5/12	50.52	36.70	64.33
3.75YR 6/12	61.32	37.40	63.97
5YR 5/12	52.84	32.94	64.50
1.25YR 6//10	62.32	29.00	55.70

According to Saksirikosol et al. (2020), the average CIE L*a*b* color value of the Thai iced tea color is (52.61, 19.36, 52.81) [5]. In this experiment, the average of 8 CIE L*a*b* colors is (55.69, 38.43, 62.74). When compared, it was found that the CIE L*a*b* color value had a color difference (ΔEab) of 21.72. Color differences occur as a result of differences in a* and b* values. The large color differences may be caused by the limitation of the monitor' color gamut. As a result, it was unable to display the colors that the subjects want.

CONCLUSION

This research suggested a color that can be used to define or represent the color of Thai iced tea to be used as a guideline for designing advertisements. According to the Munsell color system, the colors that represent the color of Thai iced tea are 8 colors, which are 3.75YR 6/12, 3.75YR 5/12, 5YR5/12, 1.25YR5/12, 2.5YR5/12, 5YR6/10, 2.5YR6/12, and 2.5YR5/14.   All color was high chroma orange.

ACKNOWLEDGEMENT

REFERENCES

1. Srithong N. (2019, August 2). Thaitone – See Thaitone "Attaluk hang tone Thai Roo wai mai tok trend". [Thaitone - Thaitone color "Identity of Thaitone know that not out of trend"] Retrieved from https://www.baanlaesuan.com/58106/design/lifestyle/thaitone-2.
2. Supaporn N. (2013). Perception of People on Well-being in Bang Pai Community. Nontaburi: Rajapruk University.
3. Ongjarit C. (2011). Evaluating Colour Images of Espresso. The 1st National and International Graduate Study Conference 2011. Bangkok.
4. Tim Cheung. (2018). World's 50 Most Delicious Drinks. Retrieved from https://edition.cnn.com/travel/article/most-delicious-drinks-world.
5. Saksirikosol, C., Rattanakasamsuk, K., Jarernros, J. and Phuangsuwan, C. (2020). Color of Thai Iced Tea. Journal of the Color Science Association of Japan, Vol.44, No.3 Supplement. Kyoto, Japan, pp.180-181.
6. Jankeaw, K., Rattanakasamsuk, K., Kihara, R. and Kawazumi, M. (2019). Representative Color of Grape. The 5th Asia Color Association Conference: Color Communication. Nagoya, Japan, pp.283-287.

EVALUATION OF COLOR SPACE FOR HIGH DYNAMIC RANGE AND WIDE COLOR GAMUT IMAGE SIGNALS

Yiming Huang, Haisong Xu[1]*, and Hao Jiang[1]

[1]*State Key Laboratory of Modern Optical Instrumentation, College of Optical Science and Engineering, Zhejiang University, Hangzhou 310027, China*

*Corresponding author: Haisong Xu, chsxu@zju.edu.cn

Keywords: Color space, High dynamic range, Wide color gamut, Image processing

ABSTRACT

High dynamic range (HDR) and wide color gamut (WCG) images are now commonly available, challenging the property of the existing color spaces, which play an important role in color image processing and color vision applications. In this study, the performance of several state-of-the-art HDR and WCG encoding color spaces, namely IC_TC_P, $J_za_zb_z$, and Non-Constant Luminance (NCL) $Y'C_B'C_R'$, was investigated. First, just-noticeable-difference (JND) uniformity and hue linearity were compared visually and numerically via the existing visual datasets. Then, the crosstalk characteristics of each color space were analyzed by conducting chroma sub-sampling to both standard dynamic range (SDR) and HDR image databases. The results indicate that IC_TC_P and $J_za_zb_z$ present better perceptual uniformity and hue linearity compared to $Y'C_B'C_R'$, while better JND-uniformity and hue-linearity would not mean better crosstalk characteristics.

INTRODUCTION

The media industry is continuously striving to improve image quality and to enhance the overall viewing experience. Currently there is significant emphasis on high dynamic range (HDR) and wide color gamut (WCG) imaging. As an indispensable part of color image processing, color space plays a vital role in the performance of the algorithm. Specifically, the uniformity of the just noticeable difference (JND) could improve the coding efficiency. In addition to JND-uniformity, hue-linearity helps the tone balance of the image implemented by color gamut mapping. Furthermore, the achromatic axis and the chromatic axes of the color space should be de-correlated as far as possible to ensure the performance of chroma sub-sampling and tone mapping algorithm. The popularity of HDR and WCG images has challenged the above-mentioned characteristics of traditional color spaces. In this context, a series of color spaces for HDR and WCG signals have been developed, while the research on color space would also promote the development of HDR and WCG imaging technology.

In this paper, a comparative study was carried out in three state-of-the-art HDR and WCG encoding color spaces, i.e., IC_TC_P [1], $J_za_zb_z$ [2], and Non-Constant Luminance (NCL) $Y'C_B'C_R'$ [3], to explore the advantages of these color spaces, so that the appropriate color space could be selected for specific applications.

METHODS

Several criteria were considered to investigate the performance of the HDR and WCG color spaces from multiple dimensions, which are described in details below.

JND-Uniformity

The main goal of image coding is to minimize the color distortion with a limited bit depth. The uniformity of a color space relates directly to its coding efficiency. In order to avoid visible quantization artifacts, the step of each coding value should be below the JND. That is, the more regular and uniform the JND ellipses are throughout the color space, the more efficient the coding would be.

The JND-uniformity of the three tested color spaces was compared both visually and numerically. For the visual comparison, the MacAdam JND ellipses [4] were plotted in the three color spaces. And the numerical comparison for the JND-uniformity (C_{JND}) is shown in Eq. (1).

$$C_{JND} = \frac{1}{2n} \sum_{i=1}^{2} \sum_{j=1}^{n} \left(\frac{l_{i,j}}{\frac{1}{2n} \sum_{i=1}^{2} \sum_{j=1}^{n} l_{i,j}} - 1 \right)^2 ,$$
(1)

where $l_{i,j}$ represents the length of the major or minor half axis of the j-th JND ellipse, and n denotes the total number of the JND ellipses. For the MacAdam ellipses, n is 25.

Hue-Linearity

Since the human visual system (HVS) is more sensitive to the changes in hue than those in chroma, the linearity of the constant hue is very important in saturation adjustment of the image, such as the color gamut mapping operation. A completely hue-linear color space would not introduce any hue shift with the changes of the saturation of the image.

Equations (2)-(3) calculate the linearity (C_{hue}) of the Hung and Berns [5] data set in the three tested color spaces. In addition, iso-hue lines were also be plotted in these color spaces for visual evaluation.

$$h_{i,j} = \tan\left(b_{i,j} / a_{i,j}\right),$$
(2)

$$C_{hue} = \frac{1}{mn} \sum_{i=1}^{m} \sum_{j=1}^{n} \left(h_{i,j} - \frac{1}{n} \sum_{j=1}^{n} h_{i,j} \right)^2 ,$$
(3)

where $h_{i,j}$ represents the hue value of the j-th point in the i-th iso-hue line of the data set, by calculating the tangent angle of the achromatic axes $a_{i,j}$ and $b_{i,j}$ of the corresponding color space. There are 12 iso-hue lines in total in the Hung and Berns data set and each line has 4 data points, that is, m and n in Eq. (3) are 12 and 4, respectively.

Color Crosstalk

In this paper, the crosstalk characteristics refer specifically to the correlation between the achromatic axis and the chromatic axes of the color space. To test the crosstalk characteristics of the three color spaces, chroma sub-sampling was conducted in standard dynamic range (SDR) and HDR images from TID2013 [6] and HdM-HDR-2014 [7] databases, respectively.

RESULTS AND DISCUSSION

JND-Uniformity and Hue-Linearity

Figures 1-2 both show the Rec.2100 color gamut hull with 1000 cd/m^2 peak white in the three color spaces with an orthographic view along the achromatic axes. For the visually verification of the JND-uniformity and hue-linearity of the tested color spaces, the MacAdam ellipses and Hung and Berns iso-hue lines were also plotted in the two sets of figures, respectively, where the JND ellipses were amplified by a factor of 10. Note that PQ instead of HLG curve was adopted for the non-linear transfer function of Y'C$_B$'C$_R$', in order to be consistent with IC$_T$C$_P$ and J$_z$a$_z$b$_z$. The results of Eqs. (1)-(3) in the three color spaces are listed in Table 1, indicating that the JND-uniformity of IC$_T$C$_P$ and J$_z$a$_z$b$_z$ is better than that of Y'C$_B$'C$_R$'. J$_z$a$_z$b$_z$ has the best hue-linearity, especially in the blue region, which benefits from the pre-adjustment of CIE XYZ tristimulus values before being converted to the corresponding color space.
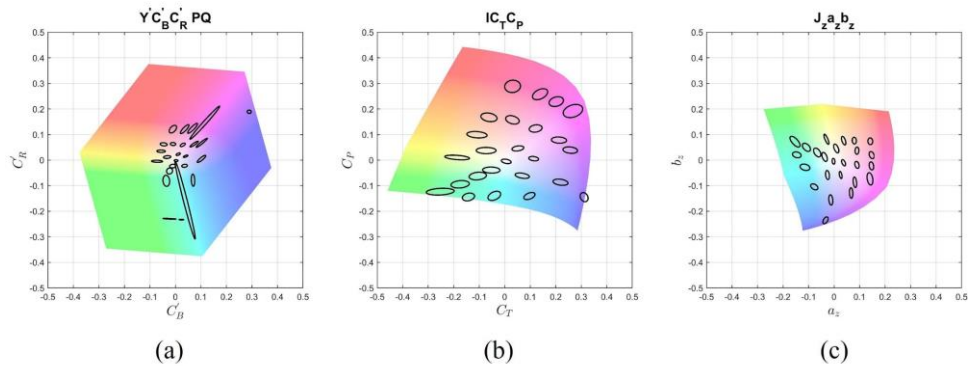
Figure 1. Visual comparison of JND-uniformity among the current state-of-the-art HDR and WCG color spaces: (a) Y'C$_B$'C$_R$', (b) IC$_T$C$_P$, and (c) J$_z$a$_z$b$_z$.
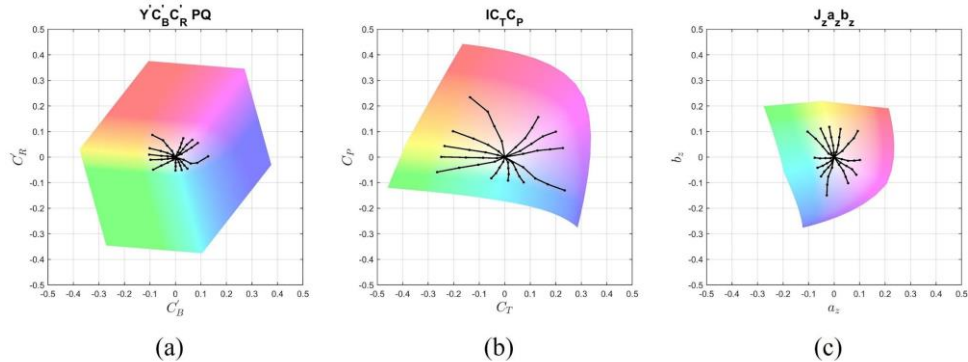
Figure 2. Visual comparison of hue-linearity among the current state-of-the-art HDR and WCG color spaces: (a) Y'C$_B$'C$_R$', (b) IC$_T$C$_P$, and (c) J$_z$a$_z$b$_z$.

Table 1: Numerical comparison of JND-uniformity and hue-linearity of the three tested color spaces.

	C_{JND}	C_{hue}
Y'C_B'C_R'	2.4670	0.0089
IC_TC_P	0.2340	0.0080
$J_za_zb_z$	**0.1734**	**0.0058**

Crosstalk Characteristics

Table 2 presents the reproduction accuracy of the SDR and HDR images after conversion to 4:2:0 and back in the three color spaces. 4 metrics were implemented for the quantitative evaluation, i.e., PSNR, SSIM, CIEDE2000, and ꟻLIP [8]. We can see that the reproduction accuracy of HDR images is better than SDR images, because these three color spaces are designed specifically for HDR and WCG images. Y'C_B'C_R' performs better on SDR images, indicating that the traditional color space format with the PQ non-linear transfer function is still applicable to SDR images. For HDR images, IC_TC_P have the best performance in the color metrics (CIEDE2000 and ꟻLIP). The results of Tables 1 and 2 also suggest that better JND-uniformity and hue-linearity would not mean better crosstalk characteristics. In order to improve the de-correlation between the achromatic axis and the chromatic axes of a color space, further scientific optimization methods are expected to be developed.

Table 2: The reproduction accuracy of the SDR and HDR images after chroma sub-sampling in the three tested color spaces.

	SDR				HDR			
	PSNR	SSIM	DE00	ꟻLIP	PSNR	SSIM	DE00	ꟻLIP
Y'C_B'C_R'	**39.6898**	0.9936	**1.24**	**0.0232**	**40.8235**	**0.9676**	0.53	0.0041
IC_TC_P	38.7959	**0.9938**	1.31	0.0296	40.0952	0.9667	**0.46**	**0.0034**
$J_za_zb_z$	38.8149	0.9929	1.39	0.0420	38.2474	0.9502	0.46	0.0044

CONCLUSION

The performance of three state-of-the-art HDR and WCG color spaces was investigated from multiple dimensions. The results demonstrate that $J_za_zb_z$ has the best JND-uniformity and hue-linearity. Crosstalk characteristics do not have a strong correlation with JND-uniformity and hue-linearity of the color space. For SDR images, Y'C_B'C_R' has better crosstalk characteristics compared to IC_TC_P and $J_za_zb_z$, while the de-correlation between the achromatic axis and the chromatic axes of IC_TC_P is the best for HDR images.

REFERENCES

1. Dolby Laboratory. (2016). IC_TC_P Dolby White Paper. https://professional.dolby.com/siteassets/pdfs/ictcp_dolbywhitepaper_v071.pdf
2. Safdar, M., Cui, G., Kim, Y. J., & Luo, M. R. (2017). Perceptually uniform color space for image signals including high dynamic range and wide gamut. *Optics Express*, *25*(13), 15131-15151.
3. ITU-R BT.2100-2. (2020). Image parameter values for high dynamic range television for use in production and international programme exchange.
4. MacAdam, D. L. (1942) Visual sensitivities to color differences in daylight. *Journal of the Optical Society of America*, *32*(5), 247-274.

5. Hung, P. C. & Berns, R. S. (1995). Determination of constant hue loci for a CRT gamut and their predictions using color appearance spaces. *Color Research & Application*, *20*(5), 285-295.
6. Ponomarenko, N., Jin, L., Ieremeiev, O., Lukin, V., Egiazarian, K., Astola, J., …Kuo C. (2015). Image database TID2013: Peculiarities, results and perspectives. *Signal Processing: Image Communication*, 30, 57-77.
7. Froehlich, J., Grandinetti, S., Eberhardt, B., Walter, S., Schilling, A. & Brendel, H. (2014). Creating cinematic wide gamut HDR-video for the evaluation of tone mapping operators and HDR-displays. *Digital Photography X*, International Society for Optics and Photonics, 90230X.
8. Andersson, P., Nilsson, J., Akenine-Möller, T., Oskarsson, M., Åström, K. & Fairchild, M.D. (2020). ꟻLIP: A Difference Evaluator for Alternating Images. *Proceedings of the ACM on Computer Graphics and Interactive Techniques*, *3*(2), 15:1-15:23.

OPTIMIZATION OF SPECTRAL SENSITIVITY FOR MULTISPECTRAL IMAGING SYSTEM

Peng Xu[1]* and Haisong Xu[2]

[1]*School of Engineering and Technology, Jiyang College of Zhejiang A&F University, China*
[2]*State Key Laboratory of Modern Optical Instrumentation, College of Optical Science and Engineering, Zhejiang University, China*

*Corresponding author: Peng Xu, xsjzxp@163.com

Keywords: Multispectral imaging, Spectral sensitivity, Optimization

ABSTRACT

The spectral sensitivity of multispectral imaging system influences the accuracy of recovered spectral image and colorimetric image, so optimizing the spectral sensitivity is necessary to maintain the compact structure of multispectral imaging system and high performance. The existing optimization methods neglect the uniformity of the target samples, therefore the optimized channels are not applicable for any object. The uniform target samples are first selected in this paper, and the optimizing is implemented based on the uniform target samples through simulation. The genetic algorithm is adopted to optimize the spectral sensitivity of channels. The shape of the spectral sensitivity is formulated as the Gaussian curve, and the full width of half maximum of the Gaussian curve is optimized with respect to different number of channels. The optimized spectral sensitivities achieving best spectral and colorimetric accuracy are obtained, respectively.

INTRODUCTION

Multispectral imaging can obtain more accurate colorimetric and spectral image than traditional color imaging due to the increased number of spectral channels. The spectral sensitivity of spectral channels influences the generation of multichannel responses and further the reconstructed spectral reflectances. So it is necessary to optimize the spectra sensitivity of multispectral imaging system to gain high accuracy and keep compact structure. The existing methods of optimizing spectral sensitivity can be divided to two categories, i.e. the data-driven method[1,2] and the non-data-driven method[3,4]. The non-data-driven method only considers the spectral characteristics of the filter and the optimization objective based on a certain assumption, and usually obtains the optimization results under that assumption. With the increase of open spectral databases, various data-driven optimization methods are gradually proposed. In the data-driven method, the appropriate target samples are firstly selected, and then the spectral reflectances of target samples are reconstructed based on the corresponding multichannel responses. Besides, the accuracy of reconstructed spectral reflectances of the target samples is taken as the optimization objective. The data-driven method can add the spectral characteristic data of imaging factors such as light source, sensor and color filter into the optimization process to simulate the multispectral imaging mechanism more truly. However, such existing methods neglect the uniformness of the target samples, and the peak wavelength and bandwidth of the spectral sensitivity are not optimized simultaneously. In this paper, the data-driven method is adopted, and the uniform target samples are firstly selected. Then the real-coded genetic algorithm (RCGA) is employed to optimize the peak wavelength and bandwidth of the spectral sensitivity together. Finally, the optimized spectral sensitivities achieving best spectral and colorimetric accuracy are obtained, respectively.

SELECTION OF UNIFORM TARGET SAMPLES

Uniform color samples were selected from the spectral reflectances of 114120 real object samples[5]. The provider collected samples from a large number of spectral reflectance databases and spectral image databases, and then combined some highly similar samples through clustering, and eliminated samples containing impulsive noise. The sampling range of spectral reflectance is 400nm to 700nm, with 10nm interval. In the chroma-hue plane, the hue angle is evenly divided from 0° to 350° with 10° intervals, and 36 hue angles are thus obtained. All samples are scattered in the chroma-hue plane. According to the statistics, the hue angle containing the least samples is 130°, and the number of samples at this hue angle is 59. After selecting samples with color difference between two pairs greater than 1, the number of samples to be selected is 54, so the number of samples to be selected at each hue angle is 54. Moreover, 54 neutral samples are also added. As a result, the number of selected uniform target samples is 1998 = 36×54+54, as shown in Fig. 1.
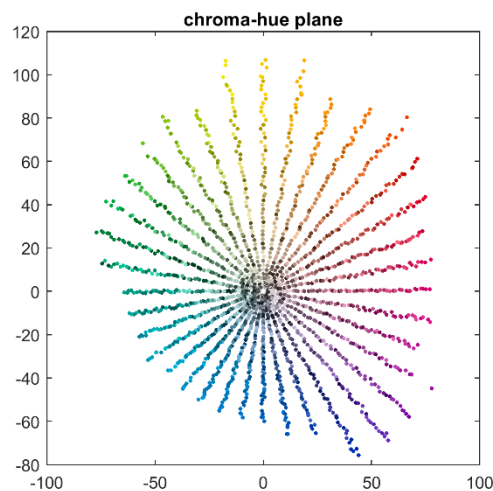
Figure 1. Uniform target samples

OPTIMIZATION OF SPECTRAL SENSITIVITY BASED ON RCGA

The type of spectral sensitivity is formulated as the Gaussian curve, as illustrated in Fig. 2. The main parameters of the Gaussian curve are peak wavelength and bandwidth. So the variables to be optimized in the RCGA are the peak wavelengths and bandwidths of spectral channels.
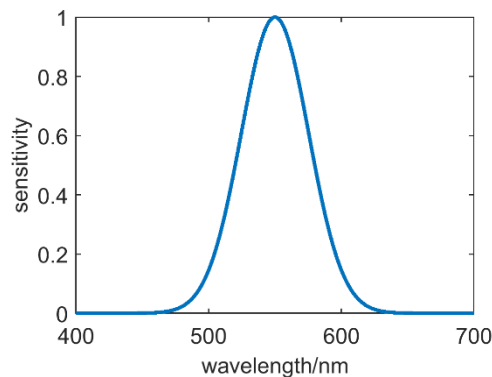
Figure 2. Spectral sensitivity of Gaussian type

Since the bandwidth of each channel is individually optimized, the number of variables is twice that of channels. The number of channels to be optimized is 3 to 16. The range of the bandwidth is 5nm to 120nm, with 1nm interval. The objective functions are the CIE DE2000 color difference and RMSE spectral difference of the uniform target samples, respectively. The peak wavelength and bandwidth of each channel achieving best colorimetric and spectral accuracy are obtained simultaneously through RCGA. Besides, a conventional method called even is compared with the proposed method. In this method, the peak wavelengths of all the channels of certain number are evenly spaced within the spectral range. The color accuracies of optimized channels with the two methods are displayed in the Fig. 3(a). The red dash line and green solid line individually represent the results of the even method and the proposed method labeled with optimized.

(a)   (b)   (c)

Figure 3. The results of colorimetric optimization

When the number of channel is less, the optimized channels have better performance than the even method. For instance, the color difference of the 3 optimized channels is much less than that of the even method. Moreover, the performance between the two methods is very close when the number reaches 5. Therefore, the spectral sensitivities of the 3 and 5 optimized channels are displayed in Fig. 3(b) and Fig. 3(c), respectively, as plotted color curves. Besides, in the two subgraphs, the spectral sensitivities of the channels obtained with the even method are also plotted, shown as gray curves. Meanwhile, the peak wavelengths of color matching functions are marked as 3 green dots in each subgraph. As indicated, the peak wavelengths of optimized channels are almost within the spectral range of those of color matching functions. So the derived channels through colorimetric optimization gather in the spectral range determined by the peak wavelengths of color matching functions.

The peak wavelengths and bandwidths of 3 optimal channels through colorimetric optimization are given in Table 1. Besides, the two parameters of obtained channels with even method are shown as well. Since the bandwidth of each channel is optimized simultaneously, each optimized channel has respective bandwidth. The peak wavelengths of the first and third channel are less than those of even method, and the second one is very close. What's more, the bandwidths of optimized channels are less than those of even method.

Table 1: The peak wavelengths and bandwidths of 3 optimal channels

	peak wavelength (nm)			bandwidth(nm)		
even	475	550	625	113	113	113
optimized	452	551	590	56	90	86

As shown in Fig.4(a), the performance of derived channels through spectral optimization is compared with that of even method. As can be seen, the performance of the two methods is very alike regardless of the number of channels. And the proposed method is slightly better than the even method. The spectral sensitivities of 3 and 5 optimized channels are plotted as color curves in Fig.4(b) and Fig.4(c), respectively. The gray curves still represent the spectral sensitivities obtained

with the even method. As can be seen, the peak wavelengths of optimized channels almost distribute evenly within the whole spectral range. What's more, the peak wavelength of last optimized channel is closer to the end of the spectral range, indicating the more covering of the whole spectral range is more beneficial for recovering the spectral reflectance.

(a)   (b)   (c)

Figure 4. The results of spectral optimization

As shown in Table 2, the optimized bandwidths are narrower than those obtained with the even method, indicating narrow bandwidths are helpful for reconstructing the spectral reflectance. Moreover, the optimized peak wavelength of the first channel is 441nm, and the last one is 694 nm. The corresponding ones of even method are 450 nm and 650 nm. So the optimized channels occupy more spectral space within the spectral range.

Table 2: The peak wavelengths and bandwidths of 5 optimal channels

	peak wavelength (nm)					bandwidth(nm)				
even	450	500	550	600	650	120	120	120	120	120
optimized	441	530	571	629	694	96	91	73	72	63

CONCLUSION

The spectral sensitivities of multispectral imaging system are optimized based on RCGA. The peak wavelengths and bandwidths are optimized simultaneously with respect to colorimetric objective and spectral objective. When the number of channel is small, the optimized channels have better colorimetric performance than the even method. And the peak wavelengths gather within the spectral range determined by the color matching functions. For spectral optimization, the derived channels are slightly better than the even method. And the optimized channels cover wider spectral space within the spectral range.

ACKNOWLEDGEMENT

REFERENCES

1. Shinoda, K., Kawase, M., Hasegawa, M., Ishikawa, M., Komagata, H., Kobayashi, N. (2018). Joint optimization of multispectral filter arrays and demosaicking for pathological images, *IIEEJ Transactions on Image Electronics and Visual Computing*, 6, pp. 13-21.

2. Wu, R., Li, Y., Xie, X., Lin, Z. (2019). Optimized Multi-Spectral Filter Arrays for Spectral Reconstruction, *Sensors*, 19, pp. 2905.
3. Shinoda, K., Yanagi, Y., Hayasaki, Y., et al. (2017). Multispectral filter array design without training images. *Optical Review*, 24(4):554-571.
4. Li, S. (2018). Filter selection for optimizing the spectral sensitivity of broadband multispectral cameras based on maximum linear independence. *Sensors*, 18(5):1455.
5. https://ridiqulous.com/spectral-reflectance-database/

INVESTIGATION OF CIE UGR AND VISUAL CHARACTERISTICS INDUCED BY HIGH LUMINANCE LEDS

Hung-Chung Li[1]*

[1] *Department of Cosmetic Science, Chang Gung University of Science and Technology, Wenhua 1st Rd., Guishan Dist., Taoyuan City 33303, Taiwan (R.O.C.)*

*Corresponding author: Hung-Chung Li, hcli01@mail.cgust.edu.tw

ABSTRACT

In recent years, the white LED's light efficiency has been gradually increased with the rapid development of solid-state lighting technology. It could widely be seen in our daily lives. Three psycho-visual experiments are carried out in the study to obtain the visual responses, including afterimage's duration time, the color difference between stimulus and background, and visibility. Totally twelve observers participate in the experiment to assess 60 test patterns with different colors, exposure time, the luminance level of LEDs, and the background for each evaluation item. The experimental setup and procedure will be described in detail in the full paper. Besides, the quantification of glare is determined by the CIE UGR formula to calculate the value. As a result, it shows that the color difference between stimulus and background and visibility is highly correlated to the CIE UGR values, whereas the correlation of afterimage's duration time isn't significant. The correlation coefficient are 0.95, -0.84, and 0.72, respectively. Moreover, it presents a similar trend in both 1 and 3 seconds of exposure time. In summary, the study reveals that the CIE UGR value can express the degree of the visual afterimage characteristics.

INTRODUCTION

With the rapid development of solid-state lighting technology, white LED light efficiency has gradually increased in recent years. LED lighting technology can be seen widely in our daily life, such as in LED backlight modules, information boards and lighting applications. However, the LED dot matrix's high luminance characteristics might easily cause a dazzling glare, disturbing human vision and damaging the visual system, especially the retina. When looking directly toward the high luminance LED, humans would initially perceive a glare, and it was removed with an afterimage that appeared [1, 2].

Gazing at the high luminance stimulus might bring about a visual afterimage. Depending on the duration time, there were two types of visual afterimage presented. As the stimulus was removed, a brief positive afterimage was displayed which then gradually changed to a negative one in a relatively slow process [3]. For the positive afterimage, the light and dark parts corresponded to those of the object, whereas complementary colors appeared in the negative one [4]. In general, with a longer fixation duration, a significant negative afterimage is perceived. However, the afterimage's intense influence was determined by the positive one and was slightly colored. Due to the disadvantages of afterimage on visual performance, many studies have contributed to investigating afterimage characteristics which result from a high luminance stimulus.

Glare can be divided into two classes, discomfort and disability glare, respectively. The significant difference is that the latter can strongly obstruct visual performance. Although lots of previous works have investigated the influence of glare [5, 6], the evaluation methods [7], and glare recovery [8]

induced by LED lighting, there still were few studies focusing on how it relates to the visual afterimage. Therefore, the study discusses the relationship between the unified glare rating (UGR) and the visual afterimage characteristics.

METHODS

To obtain the visual response of the visual afterimage characteristics induced by high luminance LEDs from the observers, three psychophysical experiments are conducted. Three experiments acquire the data of duration time of the afterimage, the color difference between the afterimage and the background, and the visibility of the afterimage.

Totally 60 test patterns are evaluated for each item, including duration of the afterimage, color difference, and visibility with two luminance levels of illumination, five colors, three luminance levels of background and two exposure times. Figure 1 shows an example of a viewing field seen in a completely dark environment. An RGB LED spotlight presents all the stimuli with an IR remote control, enabling the adjustment of colors, transitions, and luminance levels. A half-silvered mirror (50% reflection and 50% transmission) is placed 70 cm in front of the observers to simultaneously acquire the stimulus and different luminance of the background, presented by a 47-inch narrow-bezel transparent display (47TS50MF, LG). The circular stimulus viewing angle is about 1.35° at the subject's position, and a cross mark is placed at the center of the half-mirror as a fixation point. Tables 1 and 2 show the parameter settings. Figures 2 (a) and Figures 2 (b) illustrate the CIE1976 u', v' chromaticity coordinates of the LED color stimuli and the detail of viewing conditions, respectively.

Figure 1. An example of the viewing field.

Table 1: Parameters of the afterimage experiment.

Stimulus Color	Red	Green	Blue	Yellow	White
Background (grayscale)	Black (0)		Gray (128)		White (255)
Exposure time	1 s			3 s	

Table 2: Luminance (cd/m²) of five colors (through a half-mirror).

cd/m²	Red	Green	Blue	Yellow	White
Level 1	4376	7101	1308	12,031	10,365
Level 2	18,165	29,095	5163	47,416	40,579
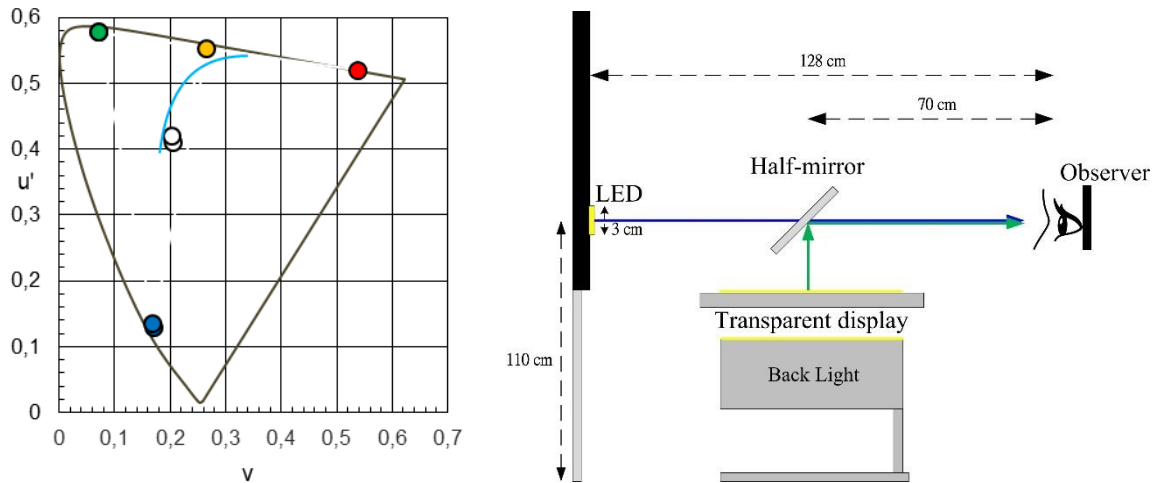
Figure 2. (a) The CIE 1976 u', v' chromaticity coordinates of the LED color stimuli (b) Illustration of the viewing conditions.

Before starting the experiments, a 20-min dark adaptation is required. During the experiment, each observer is seated in front of a half-silvered mirror in a completely dark environment. An experimenter sitting next to the blackout system controls the display of stimuli in the same order and records the observer's assessments. Twelve observers with normal vision, including seven males and five females, participate in each experiment. The observers are around 26 years of age. Each observer assesses two-fifths of the patterns twice for verification and adapt to the background for 10 s before the stimulus is presented.

For measuring the afterimage duration, a Graphical User Interface (GUI) is developed to switch the background luminance and automatically calculate the duration, utilizing a timer to record the start and end times. The start time is the moment the high luminous stimulus is turned off. After the perceived negative afterimage disappeared, the observer is asked to click the mouse button as the end time. In the grading of the color difference between the afterimage and background, a series of color difference grayscale images is displayed with the background on the half-mirror simultaneously after the stimulus is presented. After 1 s and 5 s from stimulus removal, the observer have to judge the grayscale level and ascertain the relative color difference. The grayscale series from left to right are assigned as follows: level 0 to 8 for black, −4 to 4 for gray and −8 to 0 for a white background, respectively. The negative rating values signify the afterimage is relatively darker than the background. Moreover, levels 9, 5, and 1 are allowed for estimating an over bright afterimage in each background. The assessment of visibility is conducted by evaluating the rating scale to understand the impact of afterimage on visibility. The low-contrast characters appeared in 3 s at the center of the half-mirror as the stimulus is removed. The observers need to estimate the visibility with a rating level from 1 (unclear) to 8 (clear). Similar to the duration time task, two GUI applications are individually applied to the experiment for color difference and visibility and to simulate the background with grayscale and characters.

RESULTS

The experimental parameters and the test patterns are adopted to calculate the CIE UGR values following Eq. 1, where the L_b is the background luminance (cd/m²), L is the luminance of the luminous parts of each luminaire in the direction of the observer's eye (cd/m²), ω is the solid angle

of the luminous parts of each luminaire at the observer's eye (sr), and ρ is the Guth position index for each luminaire. Two luminance levels of five colors and the luminance of three backgrounds are considered as the parameters of L and L_b to calculate the UGR value, and ω is 0.001726. Because the observer straightly gazes at color stimuli, the parameter ρ is set as 1. Two exposure times inclusive of 1 and 3 seconds are discussed to investigate the relationship between the UGR values and the visual characteristics of afterimage, and the results are shown in Figures 3 and 4, respectively. The correlation coefficient of 1 second and 3 seconds is 0.72, 0.95, and -0.84, and 0.67, 0.93, -0.83 for duration time, the color difference between the background and visual afterimage, and visibility. Accordingly, a similar trend is presented in both 1 and 3 seconds. The color difference between visual afterimage and background and visibility is highly correlated to the CIE UGR values. In contrast, the afterimage's duration time shows a poor correlation with the UGR value. Based on the finding, the visual characteristics of the afterimage can be well described by the UGR value expect for the duration time, which needs further studies.

$$UGR = 8\log\left[\frac{0.25}{L_b} \times \sum \frac{L^2\omega}{\rho^2}\right] \tag{1}$$
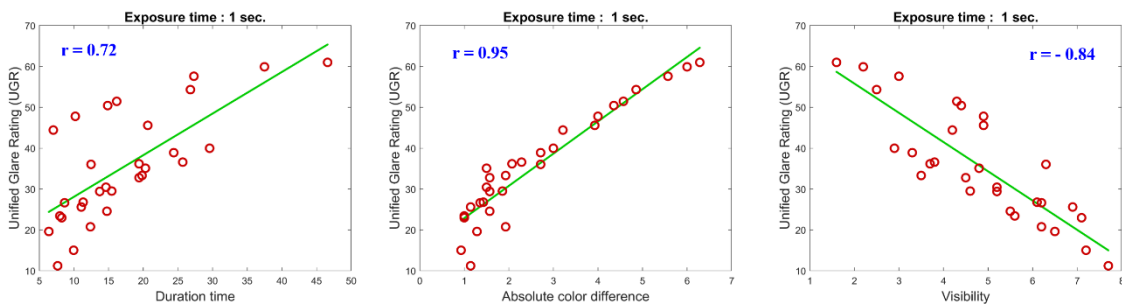
Figure 3. The scatter plot of the correlation coefficient of 1 second for duration time, the color difference, and visibility.
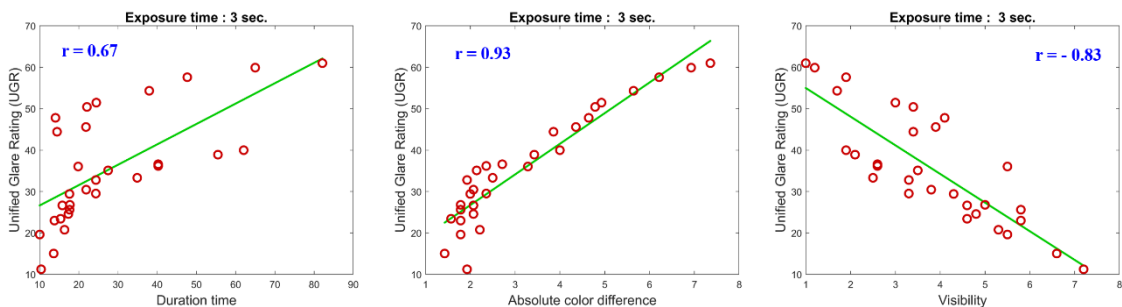
Figure 4. The scatter plot of the correlation coefficient of 3 second for duration time, the color difference, and visibility

CONCLUSIONS

In conclusion, the study explores the relationship between the visual characteristics of afterimage and the CIE UGR values induced by high luminance LEDs. To carry out the research, three psycho-visual experiments are conducted to obtain the visual responses, including duration time, the color

difference between the visual afterimage and the background, and visibility, from the observers. The CIE UGR values are calculated by use of the test pattern and the experimental parameters, such as luminance levels of the stimuli and the luminance of the background. The results indicate that the color difference and the visibility of visual afterimage are highly correlated to the CIE UGR values, and both 1 and 3 seconds have a similar trend. However, the relationship between the duration time and UGR value isn't ideal, which requires intensive study. In addition, the study suggests that the visual afterimage's characteristics can be described by using the CIE URG value as a factor.

ACKNOWLEDGEMENT

REFERENCES

1. Akinsanmi, O., Ganjang, A. D., & Ezea, H. U. (2015). Design and development of an automatic automobile headlight switching system. *International Journal of Engineering and Applied Sciences*, *2*(8), 257837.
2. Reidenbach, H. D. (2009). Prevention of Overexposure by Means of Active Protective Reactions and Magnitude of Temporary Blinding from Visible Laser Radiation. In *World Congress on Medical Physics and Biomedical Engineering, September 7-12, 2009, Munich, Germany* (pp. 41-44). Springer, Berlin, Heidelberg.
3. Roeckelein, J. E. (2004). *Imagery in psychology: A reference guide*. Greenwood Publishing Group.
4. Schreuder, D. A. (2020). Correspondence: Disturbance of vision by after-images from LED light sources. *Lighting Research & Technology*, *52*(1), 159-161.
5. Tyukhova, Y., & Waters, C. E. (2019). Subjective and pupil responses to discomfort glare from small, high-luminance light sources. *Lighting Research & Technology*, *51*(4), 592-611.
6. Tyukhova, Y., & Waters, C. E. (2018). Discomfort glare from small, high-luminance light sources when viewed against a dark surround. *Leukos*, *14*(4), 215-230.
7. Chen, P. L., Liao, C. H., Li, H. C., Jou, S. J., Chen, H. T., Lin, Y. H., ... & Lee, T. X. (2015, July). A portable inspection system to estimate direct glare of various LED modules. In *International Conference on Optical and Photonic Engineering (icOPEN 2015)* (Vol. 9524, p. 95241X). International Society for Optics and Photonics.
8. Collins, M. (1989). The onset of prolonged glare recovery with age. *Ophthalmic and Physiological Optics*, *9*(4), 368-371.

COLOR APPEARANCE OF COLOR CHIPS UNDER VIVID COLORED LEDS

Phubet Chitapanya[1], Chanprapha Phuangsuwan[2], and Mitsuo Ikeda[2]

[1] *Color science and Human vision, Mass Communication Technology, Rajamangala University of Technology Thanyaburi, Thailand.*
[2] *Color Research Center (CRC), Mass Communication Technology, Rajamangala University of Technology Thanyaburi, Thailand.*

*Corresponding author: Phubet Chitapanya, phubet_c@mail.rmutt.ac.th

Keywords: Color appearance, color constancy, vivid illumination, elementary color naming, RVSI

ABSTRACT

The ability to stably perceive the color appearance of objects under various colored lights is called color constancy. Color Constancy Index (CCI) is a measure to quantify the efficacy of the phenomena. This index was commonly calculated based on a color space that used a physical color object as a reference. It varies from 0 to 1 to show poor color constancy to perfect color constancy. Whereas the index is usually based on a magnitude of distance shift between observation's judgment and ideal value, in this study, the color appearance of color chips was investigated by using perception color space. In the first experiment, there were 100 persons participated. An observer sat in the experimental booth and judged color appearance by the elementary color-naming method for each of 26 color chips under 13 RGB-LED illuminations of six hues: red, yellow, green, cyan, blue, and magenta, plus a white light, D65. The light of each hue had two saturations, dull and vivid. In the second experiment, the booth was extended into test rooms and subject rooms. There was a small hole in a wall between those rooms. A participant sat in the subject room illuminated by White LEDs to see a color chip placed on a stand holder in the test room. Using this two-room technique, participants reported that they could perceive a color chip placed on a wall in the subject room, even originality it placed under the test room. As a result, color constancy was poor under yellow, cyan, and green light more than the others. Moreover, color constancy was usually low when the color chip was complementary to the colored light.

INTRODUCTION

Inside our brain, there is a mechanism whose ability is to control our perception. Color constancy is a phenomenon that makes a human stably perceive the same color under various colored illuminations. This statement is applicable only when illumination is located near the white illumination or not vivid colored illumination. To see the same color, researchers predicted that the mechanism should understand or know the color of illumination [19] in the first place. Therefore, lack of clue of illuminations or initial visual information (IVI) [20-21] under vivid colored illumination can be expected to be a poor color constancy or be difficult for the mechanism to understand the original surface color.

There were many ways to measure color constancy. The most famous method was color matching [22] which the participant has to match the test color to appear to be the same as the reference color, and in an achromatic setting [23] which the participant must adjust the test under a circumstance to appear to be neutral or gray. These methods were claimed to be valuable and accurate. Still, they required lots of time to match, and sometimes participants hardly obtained a satisfactory setting since there was a range in adjusting a step depending on the experimental design. Another method was categorical color naming. By naming color, which a participant judged what color he or she was

seeing allowed the researcher to expand various test color stimuli with the advantages of a fast tasking and familiar to human behavior. Even there was a good point. This method limited participant's answers by only a certain number, for example, eleven colors as the basic color naming [24].

In the present experiment, we used elementary color naming, which is quantitative judgment and allowed us to study a variety of color chips under vivid color illuminations. We proposed a modified color constancy index which ranged from 0 to 1 as poor color constancy to perfect color constancy, respectively, to be appreciated to the polar diagram, which is a perceptual color space.

METHODOLOGY

The first experiment done inside a room-size was 172×82×132 cm, as shown in Figure 1. The room was decorated with a flower vase, a picture on the wall, and a collection of books to stimulate a participant's daily life situation. The room was illuminated by only RGB-LED light, a Phillips product as Kinetics color cover MX power core model. The light was put on the left ceiling of the room and covered by translucent white paper to obtain a uniform illumination. In front of a subject's chair, there was a small table which a rectangular paper (Munsell N6) of 33×33 cm. dimensions giving 22.5° arc of visual angle with a viewing distance of a subject position. A test patch which size was 6×6 cm. giving 5.7 °, was placed on the paper.

Figure 1. Apparatus of experiment 1

In the second experiment, the room was extended to be a test room on the left side in Figure 2, and the right room is called a subject room. The test room was illuminated by the same RGB-LED light, which can be changed colored light depending on illumination conditions. On the other hand, the subject room was illuminated by only D65 LED light. Between the test and subject room, there was a small square hole on the wall in which the subject sits in the subject room could see a color chip placed on the holding stand in the test room. This procedure is called the two-room technique, in which the subject adapts to only the white light, while the color appearance of color chips is not affected by the color light of the illumination conditions.

There were thirteen illuminations, including white as D65, in this experiment. The illuminations are composed of 6 colors: red, yellow, green, cyan, blue, and magenta. There were two saturation steps: a dull or less vivid color light group and a high saturation color light group, as shown in Figure 3 as connected by the dashed line and solid line, respectively. In our experiment, the illuminant was controlled in all lighting as 100 ± 5 lx except the B2 condition, which is limited to blue diode capacity in our experiment, for the B2 condition was 80 ± 5 lx. The coordinate of each light in Figure 3 was plotted on u'v' graph, which is almost a uniform color space.

Figure 2. Apparatus of experiment 2
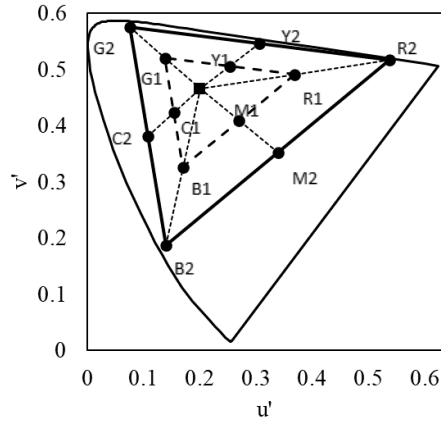
Figure 3. Illumination conditions

In Figure 4, 26 color chips were produced by Konica Minolta printer C83HC. The chips can be divided into three groups as 15 chips based on the Test color sample [25], which used to measure color constancy index as shown in a solid circle symbol, 8 chips which represented as the color gamut of the printer shown as an open circle symbol, and 3 chips as achromatic chips which is a square symbol in the figure.

There were 100 subjects who participated in experiment 1, and 30 subjects participated in experiment 2. They were students from Rajamangala University of Technology Thanyaburi and had a normal color vision tested by Ishihara test and got a score credit in return. Before participating, they had taken a color vision class and were trained to judge color appearance by the elementary color-naming method.
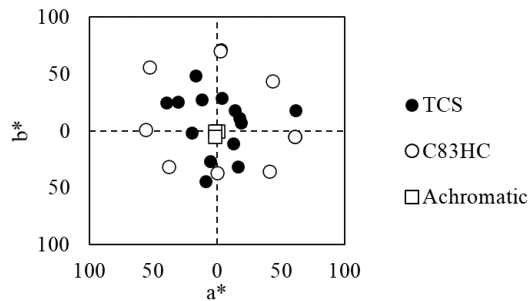
Figure 4. 26 Color chips printed by Konica Minolta C83HC

Every changing illumination, a subject had to adapt the light for 3 minutes. During the time, he or she has to look around the room without seeing the RGB-LED instrument. Each color chip would be placed in front of the subject's chair on the grey paper as a background. The subject had to judge color appearance of color chips by assessed how much percentage of chromaticness, whiteness, and blackness. Then, the percentage of red, yellow, green, and blue. The second judgment was based on the opponent color theory. A subject could not judge red and green together, and vice versa. Totally, one subject had to be named 26 color chips × 13 illuminations for one repetition. A subject could participate in only 3-4 illuminations to prevent exhaust, not exceeding 4 hours per day, including relaxing time.

RESULT

The average result of elementary color naming can be transformed and plotted on the polar diagram as shown in Figure 5 and Figure 6. The color area in each figure represents color perception under each test illumination, while the behind area as dash area is the color perception under D65 illumination. This figure shows that color perception under less vivid color light was not much different from the reference light compared to the vivid light condition. The color perception under the vivid case was narrow and even reversed shape in some conditions, such as Y2.

Color constancy index was calculated based on Eq. (1-3). Ordinary color constancy index (OCCI) is an index measurement based on the different magnitude between a distance of color appearance under D65 to the appearance under the test illumination, as shown in Figure 7. While the hue color constancy (HCI) can be calculated as a hue angle as blur arc line compared to the red arc line in the same manner as OCCI. Finally, the modified color constancy index (MCCI) was calculated based on the multiplication of those previous indexes to show the color constancy index performance under test illumination.

$$OCCI = 1 - \frac{a}{b} \qquad (1)$$

$$HCI = 1 - \frac{\theta a}{\theta b} \qquad (2)$$

$$MCCI = OCCI \times HCI \qquad (3)$$
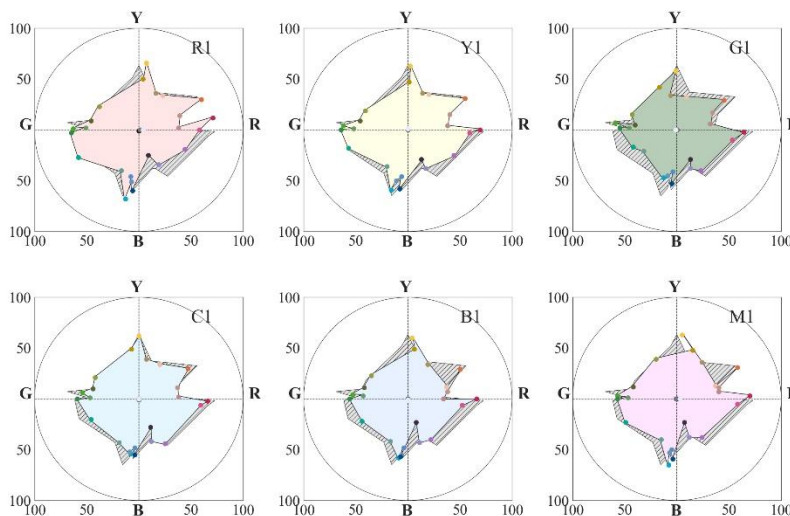
Figure 5. The average result of dull color light condition group
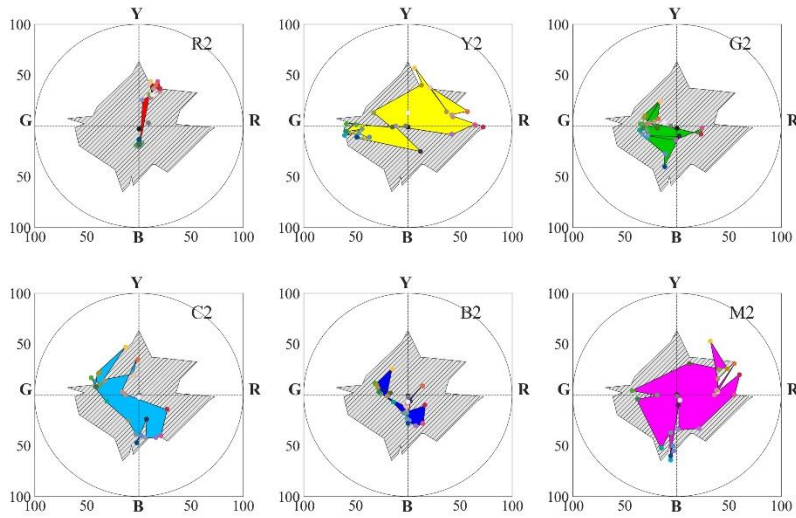
Figure 6. The average result of vivid color light condition group
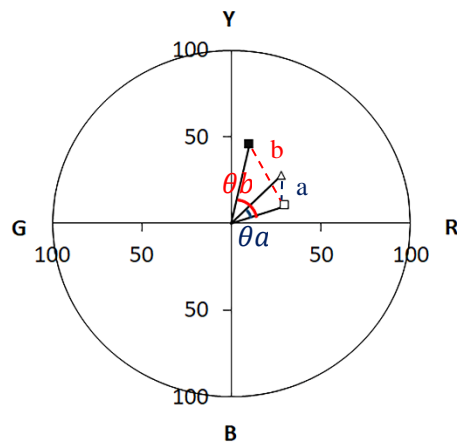
Figure 7. The color constancy index in the polar diagram.
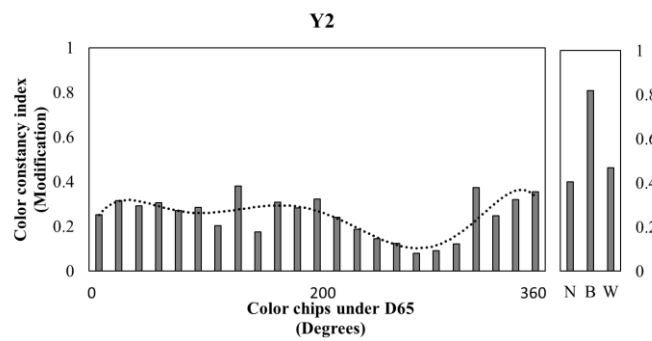
Figure 8. The result of color constancy index under Y2

The example of the color constancy index result under the Y2 condition is shown in Figure 8. The result showed that the lowest color constancy index was around the color chip, which appeared to be blue. Similar results also occurred in another colored illumination. Figure 9 shows the color constancy index on the ordinate and light condition distance from D65 on the abscissa. The result showed color constancy was poor as early dropped under cyan, yellow, and green illumination more than the others.
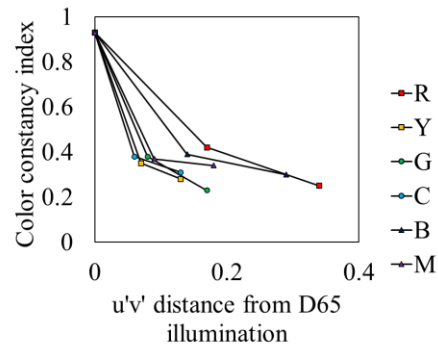
Figure 9. The average result of vivid color light condition group

ACKNOWLEDGEMENT

REFERENCES

19. Morimoto, T., Kusuyama, T., Fukuda, K., & Uchikawa, K. (2021). Human color constancy based on the geometry of color distributions. *Journal of Vision*, *21*(3), 7. https://doi.org/10.1167/jov.21.3.7
20. Ikeda, M. (2004). Color Appearance Explained, Predicted and Confirmed by the Concept of Recognized Visual Space of Illumination. *Optical Review, 11*(4), 217–225. https://doi.org/10.1007/s10043-004-0217-x
21. Yamauchi, R., Ikeda, M., & Shinoda, H. (2003). Walls Surrounding a Space Work More Efficiently Construct a Recognized Visual Space of Illumination than Do Scattered Objects. *Optical Review, 10*(3), 166–173. https://doi.org/10.1007/s10043-003-0166-9
22. Arend, L. E., Reeves, A., Schirillo, J., & Goldstein, R. (1991). Simultaneous color constancy: papers with diverse Munsell values. *Journal of the Optical Society of America A, 8*(4), 661. https://doi.org/10.1364/josaa.8.000661
23. Rajendran, S. S., & Webster, M. A. (2020). Color variance and achromatic settings. *Journal of the Optical Society of America A, 37*(4). https://doi.org/10.1364/josaa.382316
24. Berlin, B., & Kay, P. (2000). *Basic color terms: Their universality and evolution*. California, USA: CLSI Publ.
25. Hunt, R. W. G., & Pointer, M. R. (2011). *Measuring colour*. West Sussex, UK:John Wiley & Sons.

EFFECT OF ROOM ILLUMINANCE ON SIMULTANEOUS COLOR CONTRAST DISPLAYED ON AN ELECTRIC DISPLAY WITH OR WITHOUT A PAPER TISSUE

Janejira Mepean[1]*, Mitsuo Ikeda[2] and Chanprapha Phuangsuwan[2]

[1] Faculty of Mass Communication Technology, Rajamangala University of Technology Thanyaburi, Thailand.
[2] Color Research Center Rajamangala University of Technology Thanyaburi, Thailand.

*Corresponding author: Janejira Mepean, janjira672@gmail.com

Keywords: Electric display, Elementary color naming, Simultaneous color contrast, Room illuminance, Tissue paper.

ABSTRACT

It is known that the simultaneous color contrast SCC is a phenomenon to show the chromatic adaptation. Stimulus pattern of SCC is a colored field with an achromatic patch at the center. It was pointed out that the colored surrounding field works as an adapting color and the color appearance of the central gray test patch is a result of the chromatic adaptation to the surrounding color. In the case of paper stimulus, the test patch does not appear vivid color but if it is observed through a tissue paper the SCC effect is much enhanced and the central gray test patch appears vivid in color. The phenomenon is explained that the tissue blurs the gray test patch contours reducing the object recognition of the stimulus and only the colors remain to give a stronger chromatic adaptation. We investigate if the tissue also works for an electric display, a self-luminous display, in case of simultaneous color contrast. Luminance of four surrounding colors, red, yellow, green, and blue, was kept constant at 46, 128, 88, and 15 cd/m^2, respectively, and the room illuminance was adjusted to 10 levels ranging from 3 to 1600 lx. Subjects judged color appearance of the test and the surround by the elementary color naming with or without a white tissue paper. A ratio of chromaticness of test patch to the chromaticness of surround suddenly increased from the room illuminance 200 lx despite of decrease of the surrounding chromaticness.

INTRODUCTION

One of the phenomenon of color appearance is the simultaneous color contrast or SCC to show mechanism of the chromatic adaptation to the surrounding color, a gray test patch at the center appeared cyan if surrounded by red, for example. In the case of paper stimulus, the phenomenon is not strong and the cyan color is not vivid, but if the SCC stimulus is covered by a white tissue the SCC effect is much enhanced and the central gray test patch appears more vivid in color [1, 2] we can explain by the recognized visual space of illumination RVSI theory [3]. A subject adapts to the color of illumination of a space constructed over the surrounding surface [4, 5]. In the case of the paper stimulus, one of the major effects is the level of ambient lighting in viewing condition. But nowadays many researchers present stimulus by using an electronic display that is self-luminous which gives a stronger adaptation than object stimulus and the experiments are mostly performed in a dimly illuminnated room to avoid the effect of reflections of the room illumination on the surface

of display. We are interested if the tissue still works in the SCC effect for an electric display with existence of room illuminance.

EXPERIMENT

To obtain effect of room illumination, the illuminance was changed at ten levels, 3, 6, 13, 25, 50, 100, 200, 400, 800, and 1600 lx on the display by using six ceiling fluorescent lamps. The surrounding luminance was kept constant for all four colors of surrounds, red, yellow, green, and blue at 41.3, 124, 83.5, and 9.5 cd/m^2, respectively, the central gray patch at 41 cd/m^2. Their xy chromaticities are shown in Figure 1 for without-tissue (a) and for with-tissue (b).
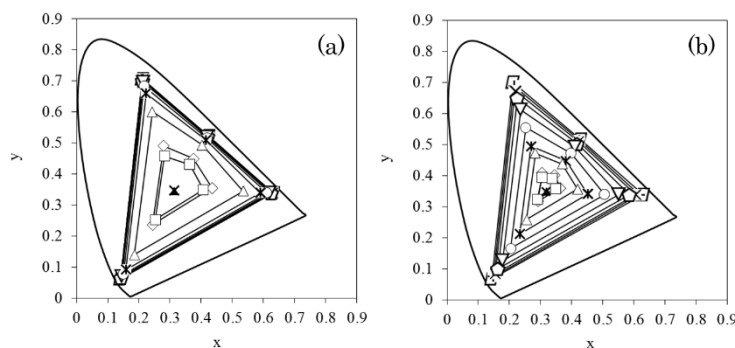
Figure 1. The surrounding colors under ten levels of illuminance without-tissue (a), with-tissue (b) (▱ , 3 lx; □, 6 lx;□, 13 lx; ⬠, 25 lx;▽, 50; ◯, 100; □, 200 lx; △, 400 lx; ◇, 800 lx; ▢, 1600 lx;, ▲, white, and r, gray

A 24.1″ EIZO LCD display was used to present the SCC stimulus. The display was placed horizontally on a table and was masked with black paper. The size of the surround was 23x23 cm^2 (25.9° of visual angle) and the gray patch was 3x3 cm^2 (3.4° of visual angle). We use the one sheet of commercially available white tissue stretched flat on the frame to cover the stimulus in with-tissue condition, the size of the tissue within the frame was 13x14 cm^2. The transmittance was constant at 56 % for visible wavelength and the haze value was 80 %. The physical effect of a tissue is to blur the image and to reflect the white ceiling light toward a subject reducing the contrast of the image and desaturating color of the image on the display.

Ten subjects with normal color vision participated in the experiment. Subjects were asked to judge the color appearance of surround and gray patch by the elementary color naming method, namely, to estimate chromaticness, whiteness, and blackness in percentage and unique hues, red, yellow, green, and blue in percentage also if there was perceived chromaticness. The judgment was repeated for five times in different days.

RESULTS

Figures 2 and 3 show examples of results of red surround for subject JM and PC, respectively. The amounts of chromaticness at ten levels of room illuminance are shown for the surround in (a) and for the gray test patch in (b), open circles for the with-tissue and filled circles for the without-tissue. The abscissa shows the room illuminance and the ordinate the amount of

chromaticness. The subject JM perceived quite constant chromaticness for surrounding without tissue (2a), but the chromaticness clearly reduced for higher illuminance with tissue. The chromaticness of test patches stayed constant at all of illumination both with and without-tissue (2b). As we are interested in the power of surround to induce color at the test patch, we took ratio of chromaticness of test patch to the chromaticness of surround, and the results are shown in (2c) of Figures. 2 and 3, the ordinate giving the chromaticness ratio. The effect of tissue is quite apparent at the higher room illuminances of 200 lx in both subjects.
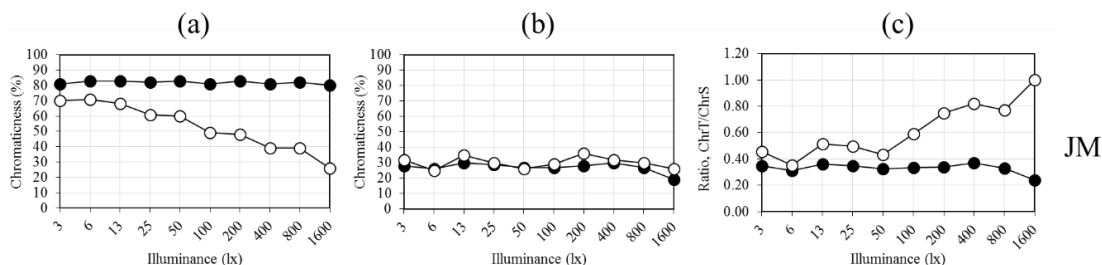
Figure 2. a, Amount of chromaticness of red surrounding with ten levels of illuminance surrounding, (b) test patch. The chromaticness ratio red stimulus (c), compared between without tissue (=) and with tissue (◯). Subject, JM
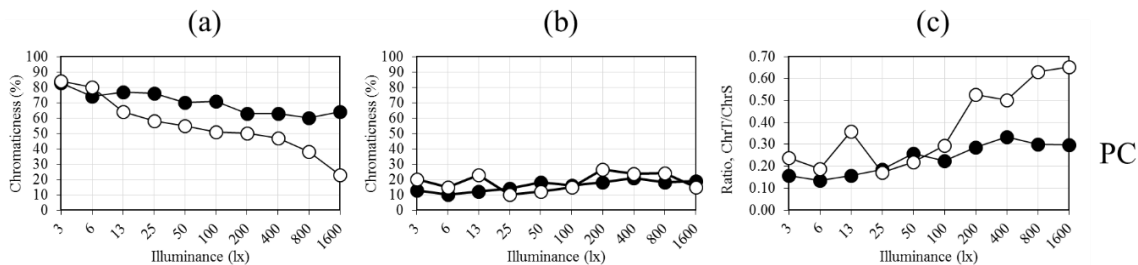
Figure 3. Amount of chromaticness of red surrounding with ten levels of illuminance (a) surrounding, (b) test patch. The chromaticness ratio red stimulus (c), compared between without tissue (=) and with tissue (◯). Subject, PC
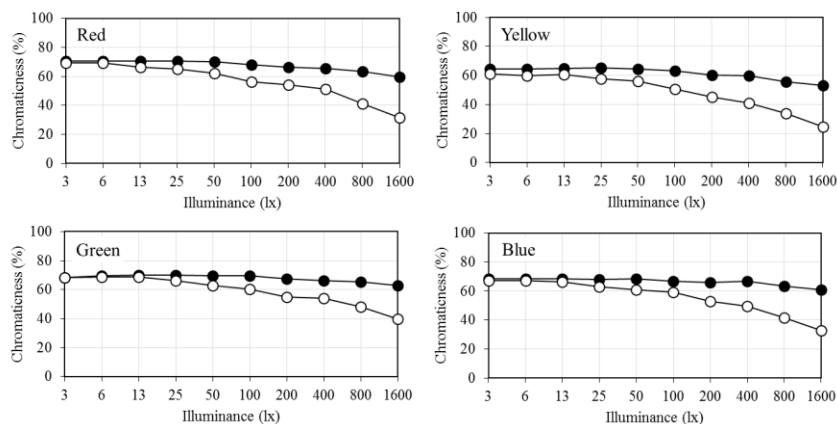
Figure 4. Amount of chromaticness of four surrounding colors with ten levels of illuminance compared between without-tissue (●) and with-tissue (✦)

We averaged the results of color perception of four surrounds for ten subjects and showed the result in Figure 4, the chromaticness of four surrounds is quite constant without tissue, but it clearly decreased with tissue as the illuminance increased. Figure 5 shows the chromaticness of the test patches without-tissue (●) and with-tissue (○). It shows a relatively similar and relatively constant value of chromaticness at all the illuminance levels, except green surround, where the chromaticness reduces slightly higher illuminance.

Figure 6 shows the chromaticness ratios that were obtained from Figures 4 and 5. It seems to be constant under room illumination level from 3-100 lx, but at the illuminances over 200 lx it increased, except with the green surround. Finally, their averages of all four surrounding colors are shown in Figure 7.
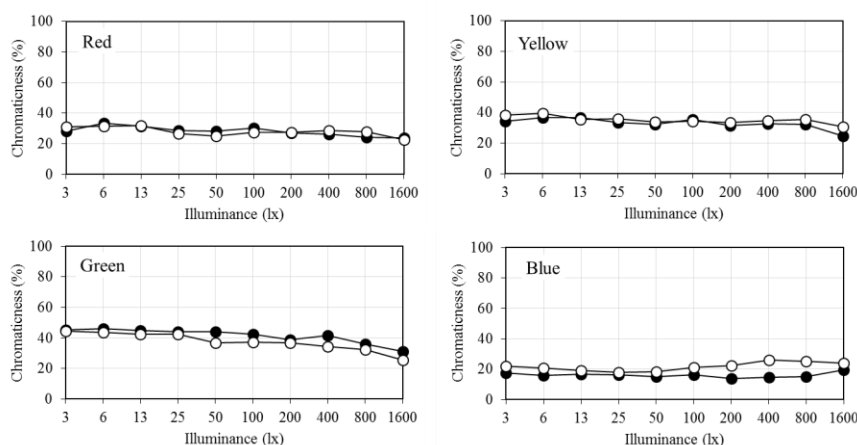
Figure 5. Amount of chromaticness of test patch in each surrounding color with ten levels of illuminance compared between without-tissue (●) and with-tissue (✦)
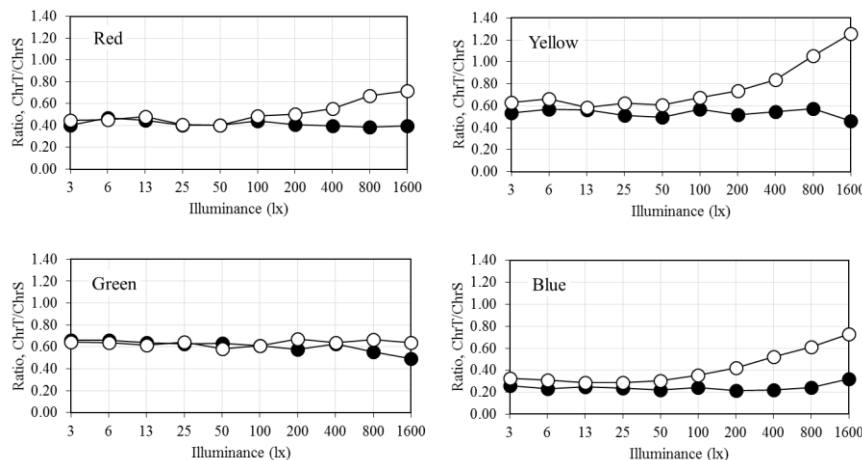
Figure 6. Chromaticness ratio of four surrounding colors with ten levels of illuminance compared between without-tissue (●) and with-tissue (✦)
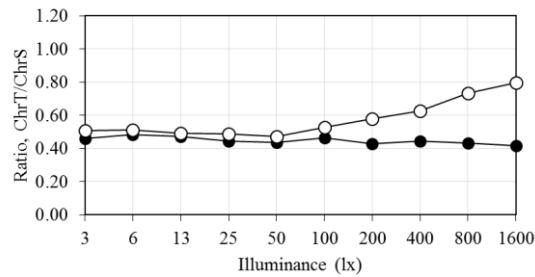
Figure 7. Averaged results from four surrounding colors compared between without-tissue (●) and with-tissue (✦).

Finally, the apparent hue of test patch of four surrounding colors in all levels of illuminance is shown in Figure 8 by hue angle of test patch for the without-tissue by solid lines and for the with-tissue by dashed lines. It is shown that the hue angle does not change for all levels of illuminance. And overlaps for both without and with-tissue, except the test patches of red appearance with-tissue.
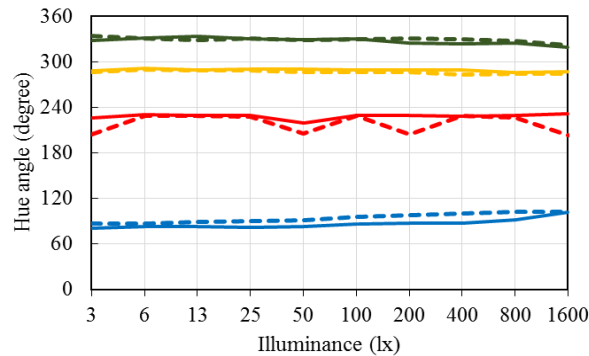
Figure 8. Apparent hue changes for test patch in each surrounding color with ten levels of illuminance compared between without-tissue (——) and with-tissue (- - -).

CONCLUSION AND DISCUSSION

Room illuminance did not affect the amounts of chromaticness of the simultaneous color contrast viewed through tissue paper. But when expressing them in the ratio of test patch chromaticness to surrounding chromaticness, the effect showed stronger at illuminance over 200 lx. We found that the ratio continued to increase from the illuminance 200 lx and beyond. Higher room illuminance increases the reflection of white light from the tissue surface and the subjects seen a reduced surrounding color through the tissue paper but still perceived the occurrence of simultaneous color contrast as same as without-tissue. A more reflection of the ceiling light at the stimulus reduced the image contrast and reduced the sharpness perception of the edges of the test patch and increased the color induction by the same token as the image blurring effect.

We can understand these results by taking account of the tissue effect of the image blurring and the reflection of white light. The image blurring effect reduced an object recognition of the test patch leaving only color or light which caused higher illuminance perception of vertical space (or vertical RVSI) constructed over the surface of the stimulus causing the test patch color to appear more vivid. [4]

ACKNOWLEDGEMENT

REFERENCES

1. Graham, H. C. & Brown, L. J. (1965). *Vision and visual perception:* Color contrast and color appearance: Brightness constancy and color constancy. USA: John Wiley & Sons.
2. Ikeda, M. & Phuangsuwan, C. (2020). The effect of tissue paper on the color appearance of colored papers. *Journal of the Optical Society of America A*, *37*(4), A114-A121.
3. Ikeda, M. (2004). Color Appearance Explained, Predicted and Confirmed by the Concept of Recognized Visual Space of Illumination. *Optical Review,* 11(4), 217–225.
4. Phuangsuwan, C. & Ikeda, M. (2017). Chromatic adaptation to illumination investigated with adapting and adapted color. *Color Research and application*, 42, 571–579.
5. Phuangsuwan, C. & Ikeda, M. & Mepean, J. (2018). Color appearance of afterimages compared to the chromatic adaptation to illumination. *Color Research and Application,* 43(3), 349–357.

DESIGN OF SAFETY COLORS CONSIDERING AGING COLOR VISION

Hung-Shing Chen[1*], Shih-Chieh Chang[2]

[1]*Graduate Institute of Electro-Optical Engineering, National Taiwan University of Science and Technology /*
[2]*Graduate Institute of Electro-Optical Engineering, Taiwan.*

*Corresponding author: Hung-Shing Chen, bridge@mail.ntust.edu.tw

Keywords: CIE 2006 physiological observer, Safety color, Age-dependent vision model

ABSTRACT

The aim of this study attempts to provide an age-related computational color simulation method for designing industrial safety colors. Three types of age-related vision models were test to present color appearances of the elderly, which are CIE 2006 physiological observer (CIEPO06 model), Okajima model based on the transmittances of aged human lens, and Yaguchi model based on the anomalous trichromacy transformation to explore color changes at different ages. The 18 chromatic colors and 6 achromatic colors on X-rite ColorChecker are adopted as the test colors. Referring to the guideline of the safety colors in Japanese Industrial Standards (JIS), the simulated blue colors at the ages of 20 and 80 are judged whether they belong safety colors.

INTRODUCTION

During the aging process of human beings, visual function will gradually decline, and the eyes, retina and visual nervous system will change, and the vision changes that are usually associated with age will occur in the aging process, rather than diseases. The decline in visual function also leads to difficulties in recognizing colors. In 2006, CIE launched a cone-shaped cell sensitivity curve model that takes age and different viewing angles as variables. The visible light wavelength range can be converted into this model corresponding to the long, medium and short wavelengths of the human eye [1]. Because it is aiming at simulating the physiological changes of the human eye, it is also known as CIE 2006 physiological observer (CIE 170-1:2006, denoted "CIEPO06"). CIEPO06 model quantifies the process of forming the human eye in the visual system. The red, green and blue three-color sensitivity curves are converted into cone fundamentals sensitivity curves. The present study basically adopts an extension of the CIEPO06 model that was modified by Asano [2].

Okajima et al. adopted "two-factor model" based on the transmittances of aged human lens to simulate the color visions of older people [3, 4]. Because the human eye's transmittance spectra can be changed by different ages, it is possible to simulate the age-dependent color visions. Because the initial two-factor model did not consider color adaptation mechanism, it is reasonable to perform perfect color adaptation in the computation of Okajima et al. to match the practical vision system (denoted "Okajima model"). Besides, Yaguchi et al. proposed a vision model based on anomalous trichromacy transformation (denoted "Yaguchi model") [5]. In their study, it was proposed to convert the original CIEPO06 model into $y'(\lambda)$ (luminance channel), $r/g'(\lambda)$ (red / green opponent color channel), $y/b'(\lambda)$ (yellow / blue opponent color channel). This model adopted the cone spectral sensitivity of the CIEPO06 model, where the equal-energy-white ratio was set to 1. Then converted to the tristimulus values of the opponent colors. Finally, the tristimulus values of the opponent color were again transformed into the tristimulus values by linear conversion.

EXPERIMENTAL DESIGNS

To evaluate the performances of the three vision models, the common conditions are described as follows: 2° fundamental observer (2° color matching functions) is adapted to provide a framework for calculating average cone fundamentals for an age between 20 and 80. Meanwhile, the spectral power distribution of CIE D65 illuminant was adopted to calculate the CIE tristimulus values of the color samples. This study designed two experiments to simulate visual changes of the elderly. Experiment 1 named "Designing *safety color (chromatic colors)*". The 18 chromatic colors of X-Rite ColorChecker color chart, which numbered in order from No.1 to No.18, were adopted as the experimental samples (Figure 1). The CIE tristimulus values of the 18 color samples were computed according to the age-related CMFs derived from the three vision models. Furthermore, CIE $u'v'$ chromaticity values with the ages of 20 and 80 were plotted to analyze chromaticity directions and color differences. The JIS safety color drawn on CIE u'v' chromaticity diagram is shown in the gray regions of Figure 2, which includes the colors of red, orange, yellow, green, blue, purple and achromatic colors [6]. The experimental procedure of Experiment 1 is described as follows:

Step 1: Calculate CIE tristimulus values of the 18 chromatic samples for the 3 test vision models.

Step 2: Transform into CIE u'v' chromaticity values and CIE $L^*a^*b^*$ values of the chromatic samples at the ages of 20 and 80.

Step 3: Plot the chosen chromatic samples on CIE u'v' chromaticity diagram to judge whether they locate inside the safety color area according to the guideline of JIS safety color.

Step 4: Compute color differences between the ages of 20 and 80 for the chromatic samples using the 3 vision models respectively.

Experiment 2 named "Designing *safety color (achromatic colors)*". It is hoped to understand whether color adaption mechanism is designed in the 3 test vision models by means of the computation for a series of achromatic colors. Totally 6 achromatic colors of X-Rite ColorChecker color chart, which numbered in order from No.19 to No.24, were adopted as the experimental samples (Figure 1). The reflectance spectra of 6 achromatic colors were measured through the spectrophotometer (X-Rite i1 Pro2). The experimental procedure is similar to Experiment 1, and it is described as follows:

Step 1: Calculate CIE tristimulus values of the 6 achromatic samples for the 3 test vision models.

Step 2: Transform into CIE u'v' chromaticity values and CIE $L^*a^*b^*$ values of the achromatic samples at the ages of 20 and 80.

Step 3: Plot the chosen chromatic samples on CIE u'v' chromaticity diagram to judge whether they locate inside the safety color area according to the guideline of JIS safety color.

Step 4: Compute color differences between the ages of 20 and 80 for the achromatic samples using the 3 vision models respectively.
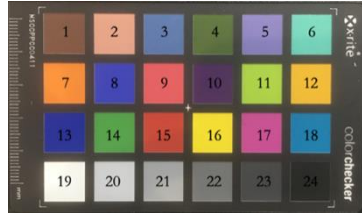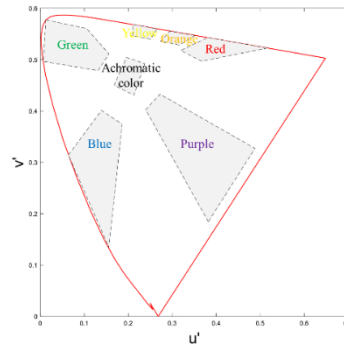
Figure 1. X-Rite ColorChecker   **Figure 2. Chromaticity ranges of JIS safety colors.**

RESULTS AND DISCUSSIONS

The CMFs simulation result of CIEPO06 model ranging the ages of 20 to 80 is shown in Figure 3. It indicated when the age becomes higher, the spectral curve tends to move slightly towards the longer wavelength. Furthermore, two kinds of experiments are designed in this study as following:
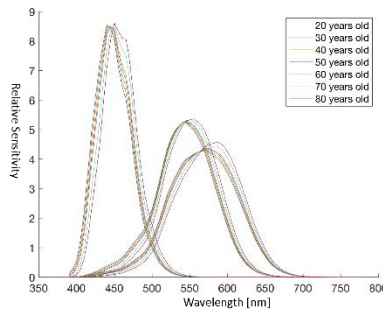

Figure 3. Color Matching Functions of CIEPO06.

Experiment 1: Designing Safety Colors (Chromatic Colors)

This experiment attempts to determine whether the chromatic color samples are within the safety color range. Figure 4 shows the chromaticity plots of the 16 color samples via CIEPO06, Okajima, and Yaguchi models. Note that the predicting colors corresponding to 20-year-old and 80-year-old are represented by the arrows. The arrow directions in the figure represent the chromaticity tends from 20-year-old to 80-year-old for three age-dependent vision models. The results indicated that the three models have similar trends of the overall u' v' chromaticity shifting directions from 20-year-old to 80-year-old are counterclockwise. Notice that most colors in Yaguchi model have a little blue shift.

(a)   (b)   (c)
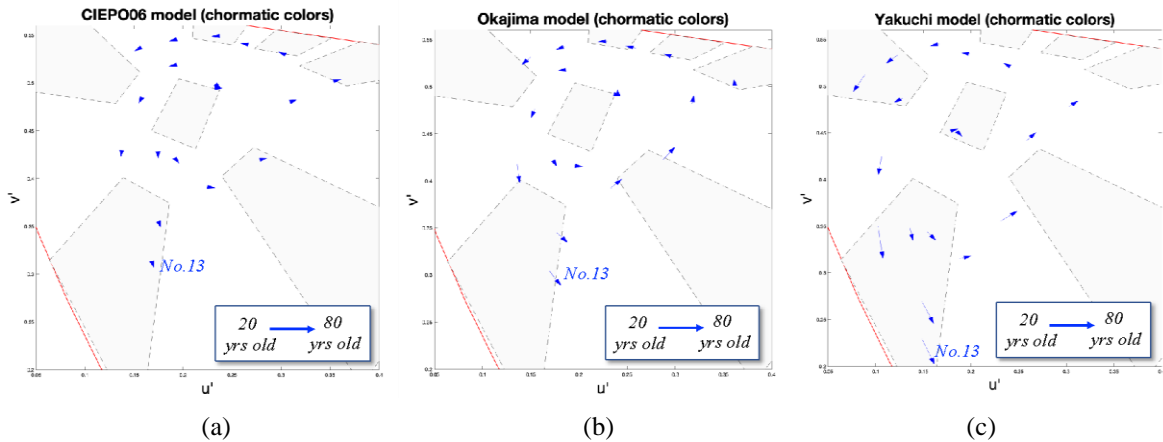
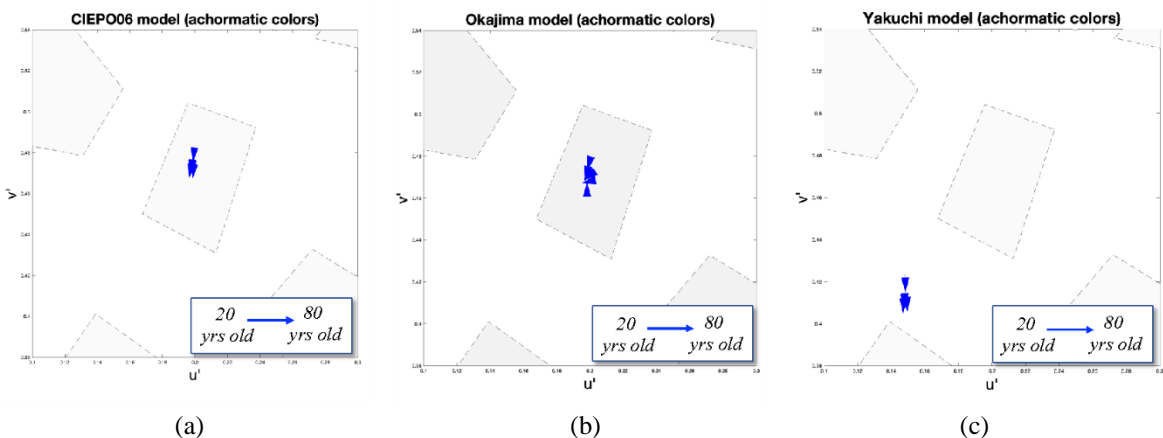**Figure 4. Chromatic color shifts (No.1~No.18) between 20 and 80 years old: (a) CIEP006 model, (b) Okajima model and (c) Yaguchi model.**

Experiment 2: Designing Safety Colors (Achromatic Colors)

The 6 achromatic color shifts between 20 and 80 years old for the 3 test models are shown in Figure 5. The results indicated that the slight color shifts of CIEPO06 model and Okajima model are found within the JIS safety color range. However, the achromatic color tracks of Yakuchi model are located outside the JIS safety color range.

Table 1 lists the color differences (ΔE_{00}) between 20 years old and 80 years old, which is used to evaluate the chromatic colors and achromatic colors of ColorChecker using the test color vison models. For 18 chromatic colors, CIEPO06 model achieved the minimum color difference (mean $\Delta E_{00}=0.3$), while Okajima model achieved the maximum color difference (mean $\Delta E_{00}=7.9$). The achromatic color also has a similar tendency. For 6 achromatic colors, CIEPO06 model achieved the minimum color difference (mean $\Delta E_{00}= 0.2$), while Okajima model achieved the maximum color difference (mean $\Delta E_{00}=7.0$).

(a)   (b)   (c)

Figure 5. Achromatic color shifts (No.9~No.24) between 20 and 80 years old: (a) CIEP006 model, (b) Okajima model and (c) Yaguchi model.

TABLE 1. Color differences of ColorChecker (20 years old vs. 80 years old).

ΔE_{00} Model	18 chromatic colors		6 achromatic colors	
	Mean	Standard deviation	Mean	Standard deviation
CIEPO06 model	0.3	0.1	0.2	0.1
Okajima model	7.9	1.6	7.0	2.3
Yakuchi model	4.6	1.8	1.8	0.6
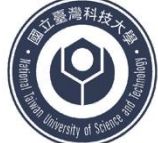
The color conversion algorithm was applied to perform coloring the university badge of Taiwan Tech (termed "Badge") at the ages of 20 and 80. Here, the assigned color was selected to No.13 (blue) of the ColorChecker. The simulation results using the three vision models are arranged in Table 2. It can be seen that the colors simulated by CIEPO06 model is relatively close to the reference color of ColorChecker, which were redrived from CIE 1931 2-degree CMFs and approximately responds to 32 years old of CIEPO06 model.

The Badge's color at the age of 20 using Okajima model was similar to that of CIEPO06. However, both colors at the age of 80 are quite different. Okajima model produced darker blue than CIEPO06's one at the age of 80. Besides, Yakuchi model resulted in more vivid blue appearance at the age of 20 and 80 among the three models. Consequently, for the Badge's coloring results, the color difference values (ΔE_{00}) between 20 years old and 80 years old are 0.3 for CIEPO06 model, 14.1 for Okajima model, 6.1 for Yakuchi model.

CONCLUSIONS

This study provides an age-related computational simulation method to design indusial safety colors, and discussed color appearances using different age-related vision models. Three types of vision models are tested to present color appearances of the elderly, which are CIE 2006 physiological observer (CIEPO06), Okajima model based on the transmittances of aged human lens, and Yaguchi model based on the anomalous trichromacy transformation. The 18 chromatic colors and 6 achormatic colors on the ColorChecker are discussed as test colors. Two types of experiments are designed to compare the predicting colors between 20 years old and 80 years old. Referring to the guideline of the safety color in Japanese Industrial Standards (JIS), the chromatic colors and achromatic colors are tested to analyze the color changes between the young and elderly people. It can be thought that the age-related Color Matching Functions (cone fundamentals) possibly affect color appearances at different ages. CIEPO06 model model has introduced highly perfect color adaptation mechanism to compensate the visual system due to the brightness of color changes of age factors. Consequently, CIEPO06 can be regarded as an appropriate age-dependent vision model applying to design industrial safety colors.

Table 2: Examples of university badge's coloring/
(Blue of ColorChecker, No.13)

ColorChecker Blue (32 years old)		
Age Model	20 years old	80 years old
CIEPO06		
Okajima model		
Yaguchi model		

REFERENCES

1. CIE. Fundamental Chromaticity Diagram with Physiological Axes - Part 1. In: CIE Publication No.170 (2006).
2. Asano, Y. (2015). Individual Colorimetric Observers for Personalized Color Imaging. (PhD), Rochester Institute of Technology (2015).
3. Joel Pokorny and Vivianne C. Smith. Evaluation of single-pigment shift model of anomalous trichromacy. J. Opt. Soc. Am. 67, 1196-1209 (1977)
4. Okajima, K., Takase, M. Computerized Simulation and Chromatic Adaptation Experiments Based on a Model of Aged Human Lens. OPT REV 8, 64–70 (2001). https://doi.org/10.1007/s10043-001-0064-y
5. Yaguchi H., Luo J., Kato M., Mizokami Y. Computerized simulation of color appearance for anomalous trichromats using the multispectral image. Journal of the Optical Society of America A., 35(4), B278-B286 (2018).
6. Introduction to the modification of JIS safety color (JIS Z 9103) (in Japanese). http://safetycolor.jp/kaisetsu/. Accessed September 7 (2021).

DEVICE DEPENDENT SIMULTANEOUS COLOR CONTRAST

Chanprapha Phuangsuwan[1]*, Mitsuo Ikeda[1], Janejira Mepean[2] and Akaradet Tongsawang[3]

[1]Color Research Center, Faculty of Mass Communication Technology; MCT
Rajamangala University of Technology Thanyaburi; RMUTT, Thailand
[2]Department of Color Technology and Design, MCT, RMUTT, Thailand.
[3]Department of Digital Printing and Packaging Technology, MCT, RMUTT, Thailand.

*Corresponding author: Chanprapha Phuangsuwan, phuangsuwan@gmail.com

ABSTRACT

The simultaneous color contrast was investigated with two different devices, a printed paper, an electronic display. In all two devices a stimulus was made of a small gray patch surrounded by a color. The color appearance of the gray patch was measured by the elementary color naming method, namely amounts of chromaticness, whiteness, and blackness in percentage, and amounts of four unique hues, red, yellow, green, and blue, in percentage. Stimulus conditions such as chromaticities, luminance and sizes are made similar between the two devices. Results showed that the color appearance of the gray patch was most vivid with the electric display and the paper which gave the least amount of chromaticness. The results indicate that the simultaneous color contrast phenomenon is device dependent.

INTRODUCTION

Simultaneous color contrast is a phenomenon that occurs when one color is influenced by a surrounding color. The color changes both in hues and brightness. In the case of brightness change it is called simultaneous brightness contrast. Many researchers used the simultaneous color contrast to investigate how our visual mechanism works. [1-4] A concept of recognized visual space of illumination RVSI proposed by Ikeda [5] asserts that the chromatic adaptation takes place to the illumination of the space where the simultaneous color contrast experiment is done. The most common and traditional pattern is a paper stimulus as demonstrated on textbooks [6, 7], which we call object color mode experiment. Currently, many researchers employed electric display, with which they can manipulate stimulus easily and present complicated patterns to meet various experimental conditions [1, 2, 8]. The previous studies on the topic suggested that the simultaneous color contrast is device dependent. [9,10] However, in this experiment, the size and luminance of the stimuli were not precisely controlled. And we noticed that the environment light was not same. In the electronic display subjects judged the simultaneous color in a dark room while in the printed paper they did in the bright room. In the present study we aim to demonstrate whether the color appearance of the simultaneous color contrast is device dependent under precise control of chromaticities, luminance and size of stimuli and of the room illuminance. Two devices are investigated printed papers and an electronic display. This study is important because as in the printing industry or graphic design, proof of the color is normally done on a monitor instead of paper. However, the final reproduction will be on the paper or other materials which found that they were often disappointed by the colors that are produced.

EXPERIMENT

Table 1. Chromaticities and luminance

Surround Colors/test patch	Paper			Display		
	Y	u′	v′	Y	u′	v′
Gray	83	0.193	0.492	84	0.193	0.489
Red	47	0.357	0.519	48	0.359	0.518
Orange	86	0.277	0.538	86	0.276	0.540
Yellow	197	0.203	0.557	198	0.203	0.551
Greenish yellow	110	0.173	0.549	111	0.174	0.548
Green	52	0.141	0.535	52	0.141	0.534
Cyan	70	0.142	0.416	70	0.146	0.416
Blue	23	0.160	0.385	21	0.162	0.380
Purple	28	0.251	0.419	27	0.251	0.415
Gray patch	99	0.192	0.419	99	0.194	0.491

A common stimulus for the simultaneous color contrast experiment was prepared. There is a large colored field with a small gray patch at the center as shown on the left of Figure 1. Surrounds were made of nine colors and one color for the gray patch. The chromaticites u′v′ and luminance Y were controlled almost the same between devises as shown in the table 1.

The surrounding colors were printed on the matt paper 230 g/m^2 by digital printing. The gray patch was printed by the same printer but on a matt paper 210 g/m^2 to avoid the shadow while putting it on the surrounds. The size was 31□44.5 cm (34.5° □48°) and gray patch was 4□4 cm (4.6° □4.6°), when viewed at the distance 50 cm.

The EIZO LCD display 27inches, model: ColorEdge CX271, Color mode sRGB, CCT 5500K was employed in the experiment.
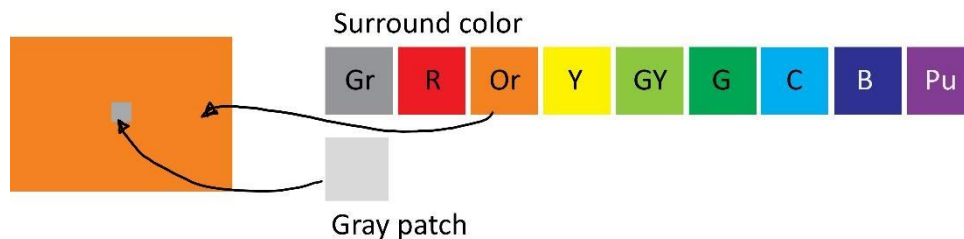
Figure 1. Simultaneous color stimulus, surrounding colors and a gray test patch

Procedure

The color appearance was judged by the elementary color naming method. That is to estimate the amounts of chromaticness, whiteness, and blackness in percentage, and the apparent hue by the amounts of two or one unique hues also in percentage, where that red and green and yellow and blue cannot be answered at the same time. The stimulus was presented in the experimental room (110□215□200 cm), where the illuminance was kept constant at 900 lx, chromaticities at x = 0.339, y = 0.377, and CCT at 5500K both in the paper and display conditions. The viewing distance was 50 cm. When a stimulus was presented, a subject adapted to the surrounding field for about one minute and judged the color appearance of the surround, and then the central patch. Nine surrounding colors

were pseudo-randomly presented. The judgement was repeated for 3 times on different day or time. Figure 2 shows the atmosphere of the experiment.

Participants

Three subjects, CP, MI and JM participated in the experiment. The age range is from 25 to 88 years old. CP and JM were Thai females and MI was a Japanese male. They were experienced subject and have a normal color vision checked by 100 hues test and Ishihara test.

Figure 2. Simultaneous color pattern, surrounding colors and gray patch

RESULT AND DISCUSSION
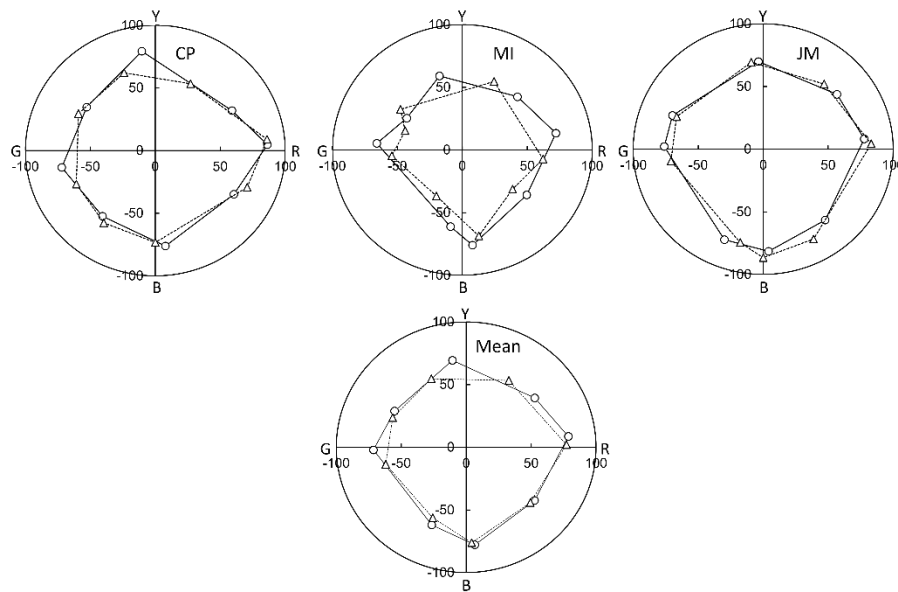
Figure 3. The results of the surrounding colors compared between printed paper and electronic display. □; printed paper, △; electronic display

The color appearance of surrounding colors is plotted on a polar diagram used in the opponent colors theory. The unique red and green appearance are taken along the horizontal direction, red being positive and green negative and unique yellow and blue along the vertical direction, the former being positive and the latter being negative. The distance from the origin along the radial direction gives the amount of chromaticness, the circumference giving 100% of the chromaticness. Apparent hue is expressed by the angle from R-axis in the counterclockwise direction and it is determined by the ratio of amounts of unique hues. Upper three graphs in Figure 3 show the mean results within

individual subject, CP, MI and JM and the bottom diagram is there. Open circles show the results of printed paper condition and open triangles show for electronic display condition. The amount of chromaticness of the surround is almost same in all surrounding colors, but the apparent hue showed difference. There is no difference in red, greenish yellow, cyan, blue, and purple, but in orange, yellow and green there is found difference. Before seeing the difference, the apparent hue angle was defined as the angle of a line connecting the origin of the graph to the concerned point measured from R axis. Then △θ was obtained by (θdisplay - θpaper) and the results are shown at the last column of the table attached in Fig. 4. Orange, yellow, green gave large values of △θ.

Sur	θ display	θ paper	dis-pa △θ
Gr	162	162	0
R	5	6.5	-1.5
Or	59	38	21
Y	118	99	19
GY	157.5	151.5	6
G	192.5	182	10.5
C	244	247	-3
B	273.5	275	-1.5
P	319	322	-3
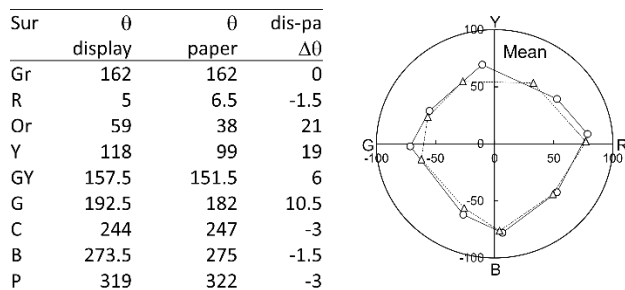
Figure 4. Hue difference △θ (θdisplay−θpaper).
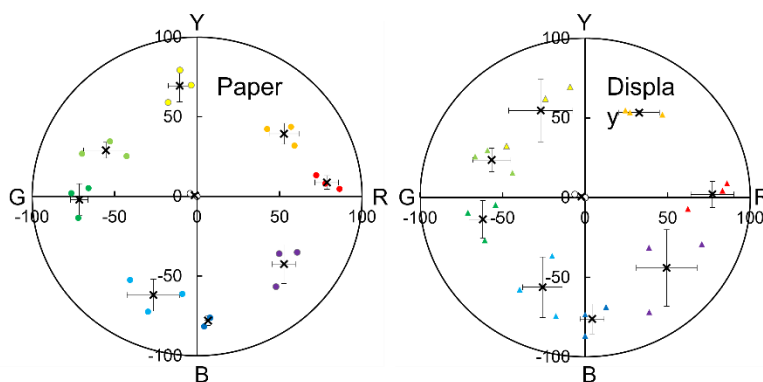
Figure 5. The standard deviation among 3 subjects for apparent color surrounding

Figure 5 shows the standard deviation among subjects for color appearance of surrounds. SD in the case of paper is smaller than that in the case of display to imply more difficult to judge the color on display. In other words, the color appearance on papers is more stable than on display, a self-luminous surface.

The upper figure of Figure 6 shows by dotted contours the mean result of simultaneous color contrast of gray test patch under 8 surrounding colors in the case of paper in each subject (the gray surround is not shown). The solid contours show the color appearance of test patch in the case of display. The illustration shows much difference in the amount of chromaticness between the electronic display and the paper stimuli. The amount is much larger in the display, implying device dependency. There is also seen difference among individuals. Particularly the contours of the subject MI, who is the oldest, are very small compared with other subjects, particularly with the subject JM who is the youngest among three subjects. When MI and JM started to look at the display at the same instance the subject JM immediately perceived a vivid color at the gray test patch, but MI did not perceive color at all or had to wait for a while until to perceive slight color. The effect of the age on the simultaneous color contrast effect should be investigated more in the future. The bottom figure of Fig. 6 gives the mean result of the three subjects. The colored lines connect points of same color

pairs. For example, the red colored line connecting the solid contour to the dotted contour indicates the color appearance of simultaneous color contrast of gray test patch when it is surrounded by red color and the line locates in the cyan area(area between unique green and blue).The fact that these lines do not necessarily converge to the origin in the graph indicates that the apparent hues of the test patch are not necessarily same in the paper stimuli and the display stimuli, again implying the device dependency. Disagreement of apparent hues between the display and the paper is also shown by variance in △θ defined as (θdisplay−θpaper), which is shown in Table 2.
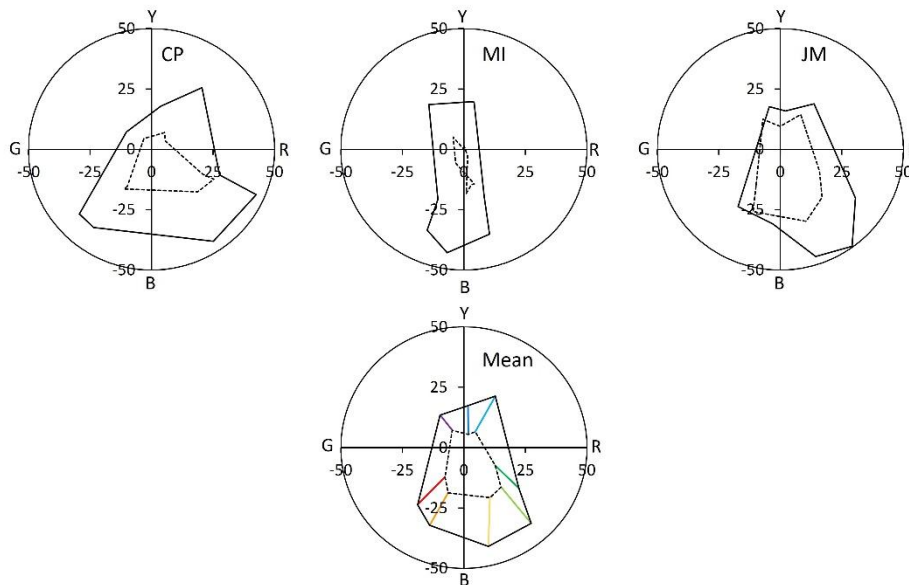
Figure 6. The results of the simultaneous colors contrast compared between printed paper; dotted line and electronic display; solid line

Table 2. Hue difference △θ (θdisplay−θpaper) of gray test patch inducted

	θ Display	θ Paper	$\Delta\theta$ dis-pa
Gr	0	0	0
R	233.5	238	-4.5
Or	248	256	-8
Y	284	296.5	-12.5
GY	309.5	305.5	4
G	319.5	320.5	-1
C	61	78	-17
B	81	44	37
P	124	121	3
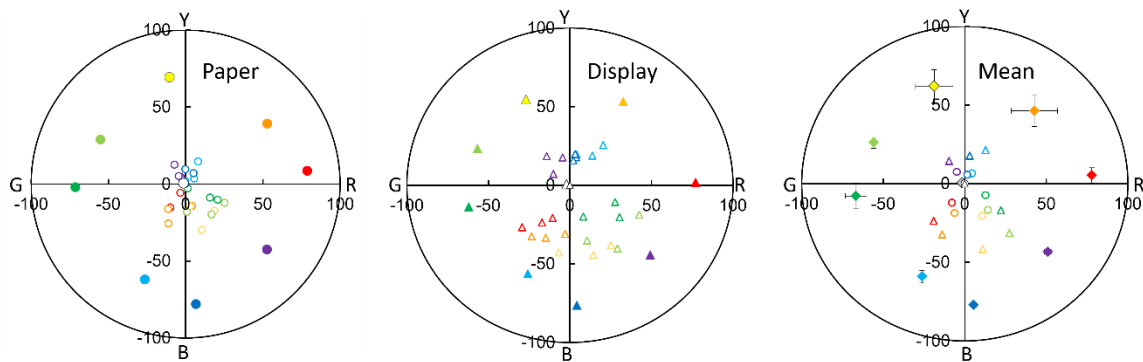
Figure 7. Color appearance variances among 3 subjects of gray test patch inducted

The results of this experiment agree well with the phenomenon adapting and adapted color, which was explained by RVSI theory. It said that the simultaneous color contrast is a mechanism of chromatic adaptation to illumination of a space.[11] Figure 7 shows the color appearance variances among subject for simultaneous color contrast at gray test patch. There are three points with same symbols that correspond to the three subjects. Colors of the symbols indicate the surrounding colors and large filled circles with colors indicate the color appearance of the surrounds. It is seen that the variance among subjects is larger in display.

CONCLUSION

We conclude that the simultaneous color contrast demonstrated under printed paper and electronic display were device dependent. The chromatic adaptation works strongly with the electronic display. To the electronic display subjects recognized the color of light stronger than to the paper even though the physical colors were kept same in both devices. On the other hand, the subjects recognized the paper stimuli as objects, not light and the chromatic adaptation did not work strongly.

In the printing industry they do proofing the printed color mostly through the display (soft proof). The most important process to set the color proofing is called Color Management System [12] which assumes the device independence. Our results confirmed that our color appearance is device dependent but cannot draw the systematic conclusion at the moment we need to do further experiment by investigating more factors such as the proper luminance of color which give the lowest device dependent.

ACKNOWLEDGEMENT

REFERENCES

1. Ekroll, V. and Faul, F. (2013). Transparency perception: the key to understanding simultaneous color contrast. *J. Opt. Soc. Am. A 30*(3), 342-352.
2. Wu, R.C. and Wardman, R. H. (2007). Lightness and Hue Contrast Effects in Surface (Fabric) Colours. *Col. Res. Appl. 32*(1), 55-64.
3. Takahashi, S. and Ejima, Y. (1982). The Study on Simultaneous Color Contrast Effect by the Opponent Color Responses. *Kogaku (Optics).11*, 478-484. [in Japanese]

4. Brown, R.O. and MacLeod, D. I.A. (1997). Color appearance depends on the variance of surround colors. *Current Biol. 7*(11), 844-849.
5. Ikeda, M. (2004). Color appearance explained, predicted, and confirmed by the concept of recognized visual space of illumination. *Opt. Rev. 11*, 217-225.
6. Hurvich, L.M. (1981). *Color Vision*. Plate 2-2 and 13-1, Sinauer Assoc. Inc.
7. Boynton, R.M. (1979). *Human Color Vision*. Fig. 2.4 P37, Holt, Rinehart, and Winston.
8. Ekroll, V., Faul, F. and Niederée, R. (2004). The peculiar nature of simultaneous colour contrast in uniform surrounds. *Vision Research, 44*(15), 1765-1786.
9. Phuangsuwan, C. and Ikeda, M. (2018). Simultaneous Color Contrast Demonstrated on Different Devices. *Proceeding of CSAJ, Osaka, Japan, Supplement in Journal of the Color Science Association of Japan. 42*(3), 2-3 June 2018, 54-56.
10. Phuangsuwan, C., and Ikeda, M. (2019). Device dependent simultaneous color contrast. *Proceeding of CSAJ, Osaka, Japan, Supplement in Journal of the Color Science Association of Japan. 43*(3), 121-124.
11. Phuangsuwan, C. and Ikeda, M. (2017). Chromatic adaptation to illumination investigated with adapting and adapted color. *Color Research and Application, 42*, 571-579.
12. Kipphan, P.K. (2001). Handbook of print media. Verlag Berlin Heidelberg, Springer.

VALIDATION OF CONE SENSITIVITY-SHIFT MODEL FOR THE PERCEPTUAL COLOR DIFFERENCE OF COLOR VISION DEFICIENCY

Onozaki, Y.[1*], Sato, H.[2], and Mizokami, Y.[2]

[1]*Department of Imaging Sciences, Graduate School of Science and Engineering, Chiba University, Japan.*
[2]*Department of Imaging Sciences, Graduate School of Engineering, Chiba University, Japan*

*Corresponding author: Onozaki, Y., afna7218@chiba-u.jp

Keywords: Color deficiency, Color discrimination, Cone sensitivity-shift model

ABSTRACT

It has been considered that anomalous trichromats possess longer or shorter wavelength-shifted photopigments instead of normal L- or M-photopigments. The amount of the cone sensitivity shift would correspond to the severity of color deficiency. Yaguchi et al. (2018) developed a cone sensitivity-shift model that assumes spectral sensitivity shifts in the L and M cones of the color vision deficiencies. This study investigated whether the cone sensitivity-shift model can predict the perceptual color difference of color vision deficiency. We conducted experiments to evaluate the appearance of color-patch pairs by observers with color vision deficiencies. Twenty protan or deutan observers evaluated the color discrimination of color-patch pairs under white illumination with the correlated color temperature of 5000K. The stimuli consisted of twenty color pairs with different degrees of discrimination difficulty. We tested conditions with the naked eye and the five types of color-correcting glasses with different spectral transmittances. Observers rated the difficulty of color discrimination using a 10-point scale. The discriminability of some color pairs was improved using color-correcting glasses, and others were not. We calculated the chromaticity difference, luminance difference, and color difference for all color pairs predicted by the cone sensitivity-shift model. Then, we analyzed the correlation between the observer's score and those predicted differences. The evaluation data showed the highest correlation with the chromaticity difference, whereas it showed little correlation with the luminance difference. Our results suggest that the chromaticity difference based on the color-shift model can considerably predict the color discrimination of color vision deficiency.

INTRODUCTION

It has been considered that anomalous trichromats possess longer or shorter wavelength-shifted photopigments instead of normal L- or M-photopigments. The amount of the cone sensitivity shift would correspond to the severity of color deficiency. Yaguchi et al. proposed a computational simulation of the color appearance for anomalous trichromats assuming spectral sensitivity shifts in the L and M cones of the color vision deficiencies using the spectral absorbance of cone pigments based on the CIE 2006 XYZ tristimulus values (from now on called the cone sensitivity-shift model) [1, 2]. It employed the low-optical density spectral absorptances of the pigments and the peak optical densities of L-, M-, and S-cones defined in the CIE 170-1 [2], assuming a standard adaptation condition, such as an equal-energy white. This study investigated whether the cone sensitivity-shift model can predict the perceptual color difference of color vision deficiency. We also examined the effectiveness of the color-correcting glasses, which were developed to overcome the limitations of color vision deficiency.

EXPERIMENT

To quantify the predictability of the cone sensitivity-shift model and verify the effect of color-correcting glasses, we conducted experiments to evaluate the appearance of color-patch pairs by observers with color vision deficiencies. In the experiment, an observer with or without color-correcting glasses judged the discriminability of the color-patch pairs under white illumination.

Methods

The experiment was conducted in an environment illuminated by a white LED light stand (Yamada Shomei Co., Ltd. Z-208PROB) with an illuminance of about 500 lx and a correlated color temperature of about 5000 K ($R_a = 97$). The relative spectral power of the illumination is shown in Fig. 1.
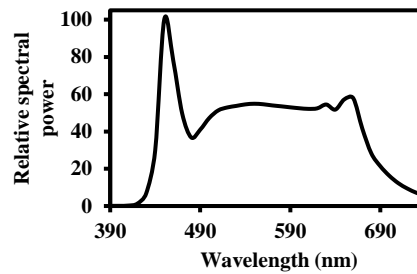
Figure 5. Relative spectral power of the illumination

We tested five types of commercially available color-correcting glasses (glasses A-E) with different spectral transmittances, as shown in Fig. 2. For glasses E, observers selected the appropriate glasses from among ten levels of glasses with different spectral transmittance (Fig. 2 (b)).

(a) Glasses A-D
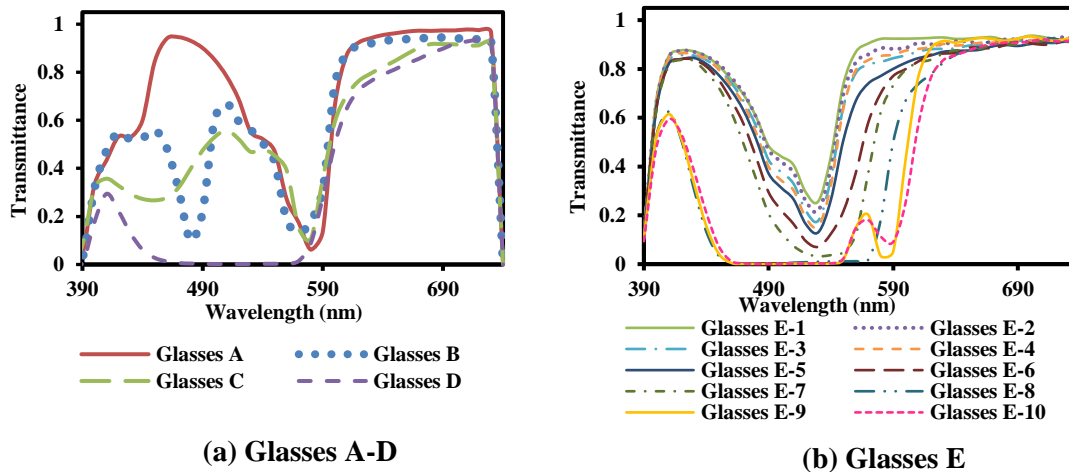
(b) Glasses E

**Figure 6. Spectral transmittance of color-corrective glasses**

Stimulus

We made the stimuli consisted of twenty color pairs with different degrees of discrimination difficulty for observer evaluation as shown in Fig. 3 (a) PCCS: easily confused color [3], (b)-1 Color Universal Design: easily confused colors [4], (b)-2 Color Universal Design: easily identifiable colors [4], (c) black and red, (d) Japanese Industrial Standard: safety color [5]. The chromaticity coordinates of color patches are shown in Figure 4.
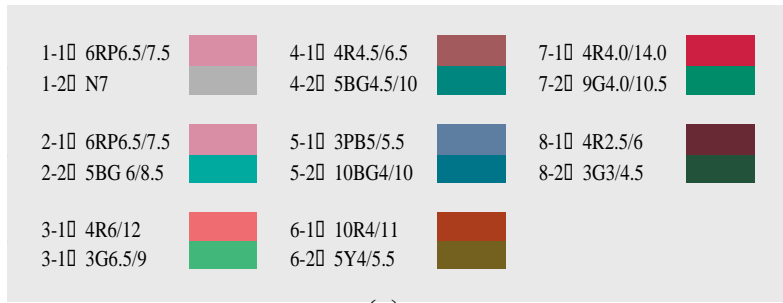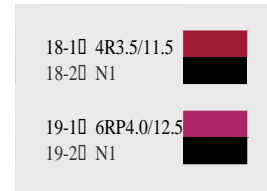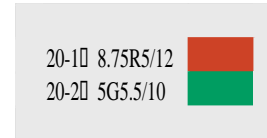
(a)
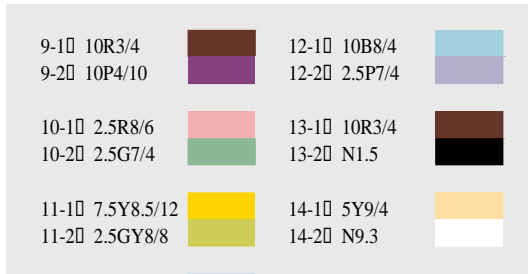
(b)-1
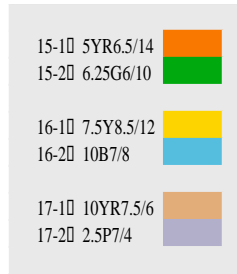
(b)-2

(c)

(d)

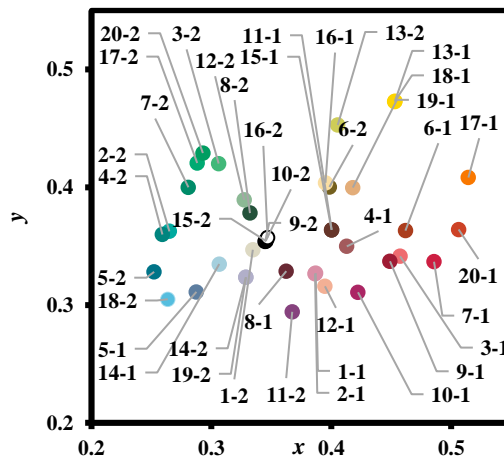**Figure 3. Color-patch pairs for evaluation**

Figure 4. Chromaticity coordinates of color patch on CIE1931 *xy* chromaticity diagram (See Fig. 3 for numbering)

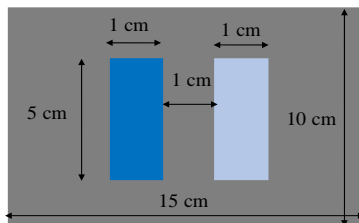The pair of color patches were attached to the center of a gray mount as shown in Fig. 5.

Figure 5. Examples of color-patch pair

Procedure

Observers evaluated the discriminability of color-patch pairs on the desk with the naked eye and the five types of color-correcting glasses (glasses A-E) by using a 10-point scale (1, not discriminable; 5, discriminable; 10, very discriminable).

Observers

Twenty observers (nineteen males and one female) took part in the experiments. Their color vision type was classified based on several tests, including an Ishihara test, SPP, PANEL D15. They were sixteen deuteranopes (deutan), three protanopes (protan), and one observer with an unknown color vision type. Therefore, we analyzed the results of nineteen observers whose color vision type was identified.

RESULTS AND DISCUSSION

Fig. 6 shows the average scores of (a) sixteen deutan observers and (b) three protan observers for each color-patch pair. The scores were highly variable depending on the color-patch pairs or the type of color vision. Also, the discriminability of some color pairs was improved using color-correcting glasses, while others were not.

Fig. 7 (a)-(c) shows the correlations between the score with no glasses of sixteen deutan observers and the model predictions calculated from the simulations of deuteranomaly with M cones shifted by a wavenumber of 500 cm^{-1} (D (M-500)) as the moderate intensity of deutan. Fig. 7 (d)-(f) shows the correlations between the score with no glasses of three protan observers and the model predictions calculated from the simulations of protanomaly with L cones shifted by a wavenumber of 500 cm^{-1} (P (L+500)). The model-predicted chromaticity difference, luminance difference, and color differences of the color-patch pairs were calculated. CIELUV based on the CIE 2006 $X_F Y_F Z_F$ tristimulus values is not defined formally, but we used it for convenience.

The black dashed line shows the linear approximation line, and the upper R^2 shows its coefficient of determination. The results of both deutan and protan showed the highest correlation with the chromaticity difference, whereas it showed little correlation with the luminance difference. The results for glasses showed the highest correlation with chromaticity difference, except for glasses D, which showed the highest correlation with luminance difference. Moreover, the solid red line in Fig. 7 shows the quadratic approximation curve, and the lower R^2 shows its coefficient of determination. In all conditions, the coefficient of determination of the quadratic approximation was slightly better than that for the linear approximation.
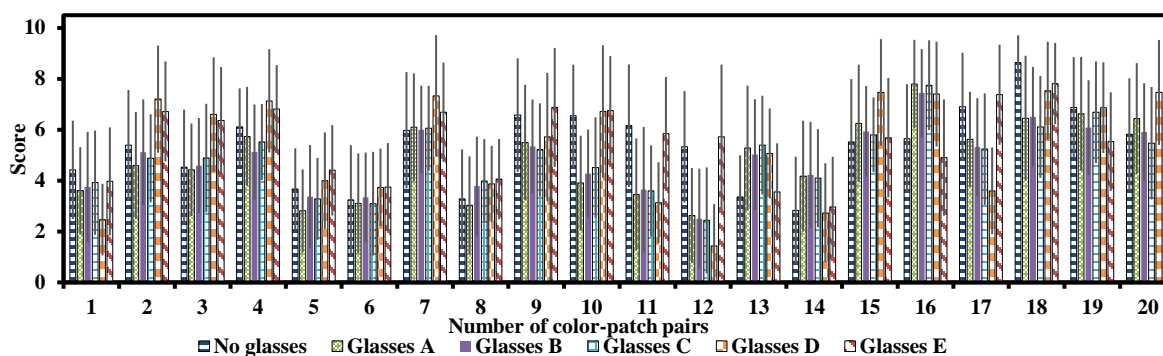
(a) Deutan
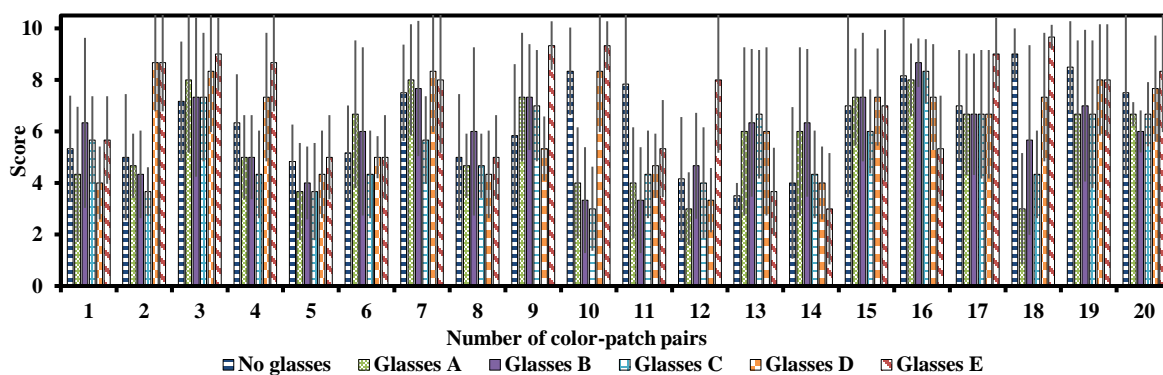
(b) Protan

Figure 6. The average score for each color-patch pair. Error bar shows standard deviations

The results suggest that people with color vision deficiency discriminate colors based on chromaticity differences. The chromaticity differences based on the cone sensitivity-shift model could predict color discrimination of color vision deficiency. The low correlation between the model prediction of luminance differences and the score assigned by the observers suggested that the observers were unlikely to discriminate colors based on luminance differences. Since this result is not consistent with the commonly known results that luminance is an important cue for discrimination for color deficiency, we need further investigation under a condition controlling luminance carefully. Additionally, the discriminability of some color pairs was improved using color-correcting glasses, while others were not, probably because the color-correcting glasses cut some wavelengths of the color-patch pair. However, factors such as the individual difference in the optical density of photopigment and the different adaptation states to various illumination colors could also influence the results of the simulation and should be considered for a more precise simulation.
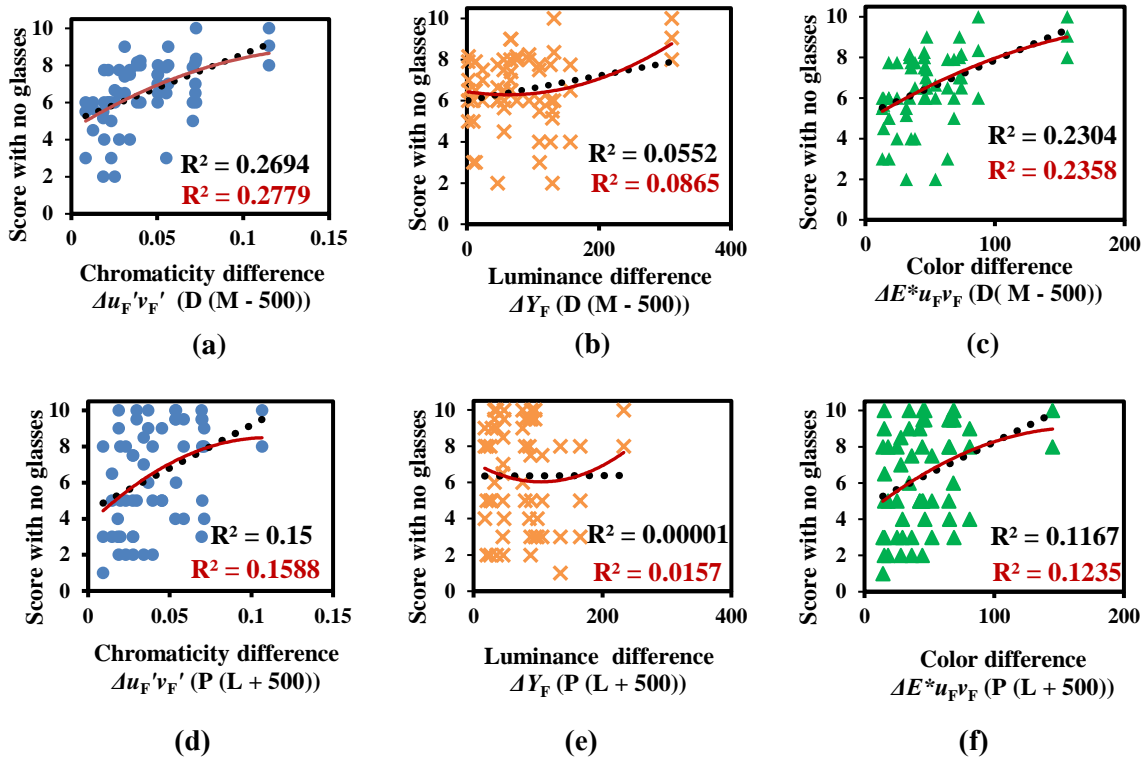
Figure 7. The correlations between the score results for no glasses and the model predictions of deutan (a-c) and protan (d-f)

CONCLUSION

Although we need further investigation, our results suggest that the chromaticity difference based on the color-shift model can considerably predict the color discrimination of color vision deficiency. Also, it is important to consider the reflectance of patches, the transmittance of glasses, and cone sensitivity and their combination for the discriminability of color deficiency.

REFERENCES

1. Yaguchi, H., Luo, J., Kato, M., & Mizokami, Y. (2018). Computerized simulation of color appearance for anomalous trichromats using the multispectral image. *JOSA A*, 35(4), B278-B286.
   https://doi.org/10.1364/JOSAA.35.00B278

2. *CIE. (2006). CIE 170-1:2006 Fundamental chromaticity diagram with physiological axes–Part 1. CIE Central Bureau: Vienna, Austria.*

3. Japan Color Research Institute (2021). Prototype of Mixed Color Chart for People with Color Blindness. COLOR No. 154. (In Japanese), Retrieved October 10, 2021 from
   https://www.jcri.jp/JCRI/hiroba/COLOR/buhou/154/154-5.htm.

4. Ito, K. (2012). Color universal design: Towards barrier-free design for diverse color visions. *Journal of Information Processing and Management*, 55(5), 307-317. (In Japanese)
   http://dx.doi.org/10.1241/johokanri.55.307

5. Japanese Stadards Association (2018). JIS Z 9101:2018. (In Japanese)
   https://www.jsa.or.jp/

QUALITY CLASSIFICATION OF SIAM ORANGE (Citrus nobilis) BASED ON COLOR IMAGE AND DEFECT PARAMETERS USING DIGITAL IMAGE PROCESSING METHODS AND ARTIFICIAL NEURAL NETWORKS

Ananda Sekar Bhawono Bagaswoto[1], Atris Suyantohadi[1], <u>Anggoro Cahyo Sukartiko</u>[1]*

[1]*Department of Agro-Industrial Technology, Faculty of Agricultural Technology, Universitas Gadjah Mada, Indonesia.*

*Corresponding author: Anggoro Cahyo Sukartiko, cahyos@ugm.ac.id

Keywords: Artificial neural network, siamese citrus quality, digital image processing

ABSTRACT

The quality of citrus fruits is often based on the color or appearance on the surface of the fruit. Assessment or classification of citrus fruit quality is usually done manually by human labor which is done visually using the sense of sight. This method has several limitations, one of which is operator subjectivity which can be caused by differences in their knowledge, abilities, and fatigue. This study aims to classify fruit quality using digital image processing methods and Artificial Neural Networks (ANN) with backpropagation architecture. Quality assessment of citrus was done using components or color parameters and defects on the surface of citrus fruits. Siamese oranges (Citrus nobilis) with various grades of quality were used as samples consisting of 80 fruits, 60 of which were used as training samples, while the rest were used for testing. All samples were taken from plantations located in Jatinom, Klaten. Samples were divided into three classes according to the quality standards regulated in SNI 3165:2009, which are superclass, class A, and class B. Fruit images were taken using a Logitech C525 webcam installed in the Color Assessment Cabinet (CAC) and a D65 18W light bulb as a source lamp. Digital image processing and ANN were created and run using MATLAB software. The results showed that the parameters of the defect area and entropy had high correlation interpretation ($r=0{,}6 - 0{,}8$), and color component a* (from the L*a*b* color space) had sufficient correlations ($r=0.4 - 0.6$) to be used in the classification of citrus fruit quality. The ANN consists of 3 inputs (parameters with sufficient correlation), 18 hidden layer neurons, and 3 outputs (super quality, class a, and class b). The accuracy results are 91.67% in the training/validation process, while in the testing process gets an accuracy of 75%.

INTRODUCTION

Orange (Citrus L.) is one of the largest commodities in Indonesia. According to [1], oranges were the commodity with the third-largest production volume in 2017, with a total of 2,165,189 tons. The total harvest in 2017 was 150,978 tons, 7.5% higher than the previous year. The quality of the fruit is often based on the color or appearance on the surface of the fruit. Author [2] stated that color is still the main quality parameter in determining oranges consumer's demand.

The main problem of postharvest processing of citrus observed by [3] is the quality based on external appearances such as texture, color, and size. Assessment or classification of citrus fruit quality is usually done manually by human labor which is done visually using the sense of sight. This

method has several limitations, one of which is operator subjectivity which can be caused by differences in their knowledge, abilities, and fatigue.

From these problems, a classification method that can distinguish the quality of citrus fruits with color and appearance parameters non-destructively is needed. The image processing method is one way that can be used to identify quality by assessing the area of physical disability and the size of citrus fruits. According to [4], image processing and artificial neural networks can improve the fruit quality classification process according to the established standards. An artificial neural network is used as a system that is expected to be able to recognize differences in quality based on image features resulting from image processing. According to [5], using image processing techniques, uniform classification results will be obtained. This study aims to classify fruit quality using digital image processing methods and Artificial Neural Networks (ANN) with backpropagation architecture.

MATERIAL AND METHOD

Sample Preparation

Siamese oranges (Citrus nobilis) with various grades of quality were used as samples consisting of 80 fruits, 60 of which were used as training samples, while the rest were used for testing. All samples were taken from plantations located in Jatinom, Klaten from September to December 2020. Samples were divided into three classes according to the quality standards regulated in SNI 3165:2009, which are superclass, class A, and class B. The classification was carried out by people who have the knowledge and experience needed to determine the quality of citrus fruits.

Image Acquisition and Processing

Quality assessment of citrus was done using components or color parameters and defects on the surface of citrus fruits. Fruit images were taken using a Logitech C525 webcam installed in the Color Assessment Cabinet (CAC) with a resolution of 640x480 pixels and a D65 18W light bulb as a source lamp. The material used as the background for sampling is dark blue cardboard. The choice of background color in image capture is very influential on whether or not the image is clear to be processed. The selected background color should contrast with the sample color so that it is easy to distinguish. According to Widodo, et al (2018), the blue background has a color value that is quite contrasting with oranges so that it can facilitate the segmentation process. The sample image was taken three times on each side (top, side, and bottom). Digital image processing and ANN were created and run using MATLAB software. The data obtained were the image's color components (RGB, L*a*b*, and HSV), the image texture components (contrast, correlation, energy, homogeneity, and entropy), and the area of defects in the sample image.

The defect was detected using texture feature analysis, such as contrast, energy, homogeneity, and their correlation values. A grayscale image which was then adjusted for intensity to highlight the defect area in the sample to facilitate the segmentation process was used in the analysis. The result of the segmentation process was a binary image, showing the area of the defect in the sample. The defect area was compared with the sample area, resulting in a percentage of the defect area in the sample.

Sample dimension was measured by calibrating the pixel length of the image. Calibration was carried out to obtain a pixel constant so that it can be converted into millimeters (mm). The results were then grouped based on the size and level of citrus defects following the SNI 3165:2009 and then used as a reference because at this stage the calculation and analysis of the accuracy of measurements using an artificial neural network have not been carried out.

Artificial Neural Network (ANN)

The ANN architecture was developed using Matlab software and the neural network toolbox. Backpropagation, which consists of three stages, i.e., the provision of input patterns during the training process, the backpropagation process from errors, and setting the weighting value, was used. The weighting value was based on the quality parameters that have been determined in the previous stage. Mean Squared Error (MSE) was chosen for evaluating the ANN architectural design. The training process was carried out to train the artificial neural network to be able to identify differences in the quality of each sample. The training variables were hidden neurons, learning rate, momentum constant, epoch, and activation function. The determination of hidden neurons/layers was based on the number of input neurons and output neurons. Validation was done by comparing the results of the artificial neural network architecture training in which the highest and consistent accuracy was then used to predict the sample image. The level of accuracy was the percentage comparison between the number of objects that match reality with the total number of objects tested. Artificial neural testing was carried out using different samples with the training and validation process of ANN because the network had not yet recognized the new sample so that the classification of the network test was not influenced by the reading of the previous sample. The ANN testing process was the final quality classification process to determine the level of accuracy of the citrus quality classification from the network that has been made.

RESULTS AND DISCUSSION

Image Processing and Features Extraction

The image that has been obtained is an RGB image, which needs to be converted into a Grayscale image (Figure 1.a) to perform texture analysis using the Gray-Level Co-occurrence Matrix (GLCM) method and an HSV image (Figure 1.b-d) for threshold and conversion functions to a binary image, before returning it to the original color (Figure 1.e). The extraction process was then carried out to obtain the value of a component in the image that can be used to identify characteristics or patterns in the image. In this process, the components that be used for the identification process were the color component values of red, green, blue, hue, saturation, value, L*, a*, and b*. In addition to the color component, the value of texture features was also needed composing of contrast, correlation, energy, homogeneity, and entropy.
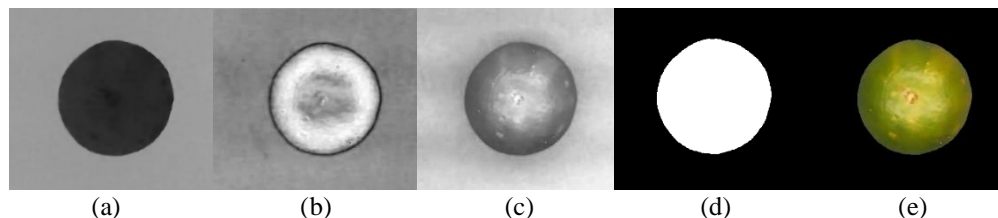

(a)   (b)   (c)   (d)   (e)

Figure 1. Image Segmentation and Processing. (a) Hue; (b) Saturation; (c) HSV; (d) Post-binary conversion segmentation image; (e) Final image

At the first trial, samples were classified based on their defect area and diameters, using image processing only, without combination with ANN. All image feature extraction results from the top, bottom, and other sides were averaged. From the results of image processing using MATLAB, the average value of extraction data and the results of quality classification were obtained. Based only on appearance using the above method, the accuracy value was 65%, therefore, cannot provide high accuracy results. Several things may affect the accuracy level of the detection of the defective area in the sample. One of them was the way of segmenting the defect area in the sample. From Figure 2, it can be seen that the segmentation results cannot detect the defect area as expected, resulting in the detection of a smaller defect area than it was (Figure 2.a-b) or vice versa, the defect area exceeded the actual defect area (Figure 2.c-d).
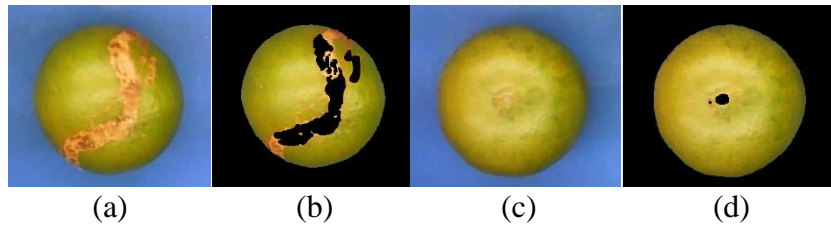
Figure 2. Defect Area Segmentation. (a) Real image sample 1; (b) Detected defect area sample 1; (c) Real image sample 2; (d) Defect area fault detection sample 2

A correlation analysis between image parameters and the quality level of the fruit was conducted to determine which parameters will be used as ANN input. The results of the correlation test were obtained with the highest correlation and significance values in three parameters, including defect area, entropy, and a* value, respectively, with a $r_{defect\ area} = 0.618$, $r_{entropy} = 0.608$, and $r_{a*\ value} = 0.411$, all three with a value significance 0.00. These three parameters were then used as input in the ANN in the next steps.

Artificial Neural Network Architecture

The ANN was constructed using a backpropagation training algorithm. The first step in the preparation of the ANN was to determine the value of the output target on the network. The training target was made with a combination of binary numbers (0 and 1) two combinations with three quality class outputs. The network was typed with the command syntax as follow

$$Net=newff\ (PR, [S_1\ S_2… Sn], \{TF_1\ TF_2… TFn\}, BTF, BLF, PF) \qquad (1)$$

where Net is the name of the backpropagation network; PR is a matrix of order R x 2 containing the max and min values of R for the input elements; Sn is the number of layers in the nth unit; TFn as an activation function used in the nth layer (default=tansig); BTF is a network training function (default=traingdx); BLF is a weight/bias change function (default= learngdm), and PF is a calculation error (default = MSE).

In determining the training function, experiments were carried out with five different functions, namely *traingd, traingda, traingdm, traingdx, and trainrp*. Of the five functions, the *trainrp* function produced the lowest MSE value (MSE=0.155, the highest is *traingd* 0.209). In determining the number of hidden layers, experiments were carried out on the number of 10 up to 34 hidden layers with multiples of two. The results of determining the hidden layer with the lowest MSE value criteria were produced with a total of 18 hidden layers (MSE = .0.112, the highest 28 layers 0.140). Learning rate (*lr*) is a variable that can be changed which has implications for the size of the learning step, while the momentum constant (*mc*) is a weight change based on the direction of the last gradient pattern and the previous pattern. The determination of the *lr* and the *mc* was carried out at a value of 0.10 to 0.90 with an interval of 0.05. Learning with the lowest MSE value was obtained at 0.45 (MSE=0.107, the highest rate was 0.90 at 0.152). while mc with the lowest MSE was at mc 0.45 (MSE=0.113, the highest was at mc 0.25 at 0.166). The epoch or the number of iterations aims to reduce the MSE value if it is still large enough by increasing the iteration limit, set from 1000 to 8000, with the lowest MSE value at epoch 5000 (MSE=0.06). The final step in compiling the network was to determine the combination of neuron activation functions in the artificial neural network using the components that have been obtained previously, namely the *trainrp* training function, 18 hidden layers, a learning rate of 0.45, a momentum constant of 0.45, and an epoch of 5000 iterations. The activation functions tested were *tansig, logsig*, and *purelin* with a total number of combinations of 27 trials, with the best combination of activation functions at *tansig-tansig-logsig* (MSE=0.026, the highest *tansig-tansig-tansig* 0.764).

Validation and Testing

Validation is the process of measuring the level of network accuracy that has been made on the input data. Validation was carried out to determine the level of network learning and the introduction of quality classes from training data which will be used as a network in the testing process. The level of accuracy was measured by comparing the output value generated by the network with the target network. The validation results are shown in Table 1. The results of the artificial neural network validation test in this study were 91.67%.

Table 1. Classification Results of Trained Samples

Grade	ANN-based Classification			Sample number	Correct classification	Accuracy (%)
	Superclass	Class A	Class B			
Superclass	19	1	0	20	19	95.00
Class A	3	17	0	20	17	85.00
Class B	1	0	19	20	19	95.00
Total				60	55	91.67

ANN testing was carried out to find out ANN performance to classify the quality of citrus fruits. The process was carried out using different data from the training and validation processes. The number of samples used in the testing process was 20 samples which were divided into 3 quality groups. The summary of the results of the artificial neural network testing is in Table 2. The level of accuracy generated in the ANN testing process is 75%. The level of accuracy obtained indicates that the ANN can detect samples quality. The accuracy of the classification model that has been made can be considered quite good.

Table 2. Classification Results of Untrained Samples

Grade	ANN-based Classification			Sample number	Correct classification	Accuracy (%)
	Superclass	Class A	Class B			
Superclass	3	2	1	6	3	50,00
Class A	0	8	0	8	8	100.00
Class B	1	1	4	6	4	66.67
Total				20	15	75.00

ANN-based quality classification in our study still resulted in relatively low accuracy (less than 80%). The samples have various peel colors (green and yellow parts), which may affect the results of the image extraction value, a basis for image-based classification. Besides, a visible reflection of the light produced by the CAC tool on the sample may also influence the extraction. Because the surface texture of citrus fruits is quite glossy, the surface of the fruit can reflect light quite easily. The reflection is more visible in the orange sample with green color, while in the yellow-orange sample the reflection looks fainter. These problems will make the orange image taken to be affected by external factors. The result can affect the color of the original image on the sample surface which makes the extraction of sample color inaccurate.

In a study that measured texture defects in images using the pixel classification method, [6] found the problem that lighting could affect the measurement results. Lighting affects the intensity of the defect, causing an error in the detection of the defect area. Author [6] stated that the pixel classification method requires good lighting because the method cannot detect defects in shiny areas.
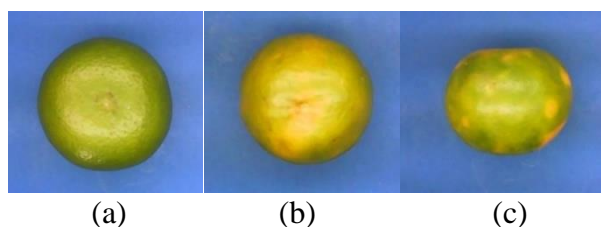
(a) (b) (c)

Figure 3. Various peel colors on samples. (a) Green-dominant peel; (b) Yellow-dominant, and (c) Yellowish green

In this study, the effect of color on the quality classification of citrus fruits based on the image cannot be the main determinant of whether or not the quality of citrus fruits. In the SNI and UNECE standards, the quality classification of citrus fruits refers to the presence or absence of irregularities or defects on the surface of the citrus. These deviations can be in the form of irregularities in fruit shape, skin color, and defects in the skin due to mechanical damage. The two standards do not classify the quality of oranges based on the color (green-yellow) of the fruit, but rather lead to damage that can affect the original color on the surface of the citrus fruit.

CONCLUSION

The results showed that the parameters of the defect area and entropy had high correlation interpretation (r=0,6 – 0,8), and color component a* (from the L*a*b* color space) had sufficient correlations (r=0.4 - 0.6) to be used in the classification of citrus fruit quality. The ANN consists of 3 inputs (parameters with sufficient correlation), 18 hidden layer neurons, and 3 outputs (super quality, class a, and class b). The accuracy results are 91.67% in the training/validation process, while in the testing process gets an accuracy of 75%.

ACKNOWLEDGEMENT

REFERENCES

1. Statistics Indonesia 2017 Production of Fruits 2017
2. Muthmainnah H, Poerwanto R and Efendi D 2015 Perubahan Warna Kulit Buah Tiga Varietas Jeruk Keprok dengan Perlakuan Degreening dan Suhu Penyimpanan *J. Hortik. Indones.* **5** 10
3. Albahry A 2013 Sortasi Jeruk Manis Menggunakan Citra Digital Dan Jaringan Syaraf Tiruan
4. Wiharja Y P and Harjoko A 2014 Pemrosesan Citra Digital untuk Klasifikasi Mutu Buah Pisang Menggunakan Jaringan Saraf Tiruan *IJEIS (Indonesian J. Electron. Instrum. Syst.* **4** 57–68
5. Saintika Y, Wijayanto A and WIguna C 2018 Perancangan Sistem Informasi Klasifikasi Wortel Berbasis Pengolahan Citra Digital *JRST (Jurnal Ris. Sains dan Teknol.* **2** 63
6. Fitria H and Nim N 2011 Pengukuran Cacat Tekstur Pada Kulit Jeruk Keprok dengan Klasifikasi Pixel 1–8

LIGHTING ENVIRONMENT OF PEDIATRIC HOME HEALTHCARE: THE NECESSARY ILLUMINANCE FOR TRACHEAL SUCTION DURING THE NIGHT

Michiko Nishitani[1]* and Hideki Sakai[1]

[1] *Graduate School of Human Life Science, Osaka City University, Japan.*

*Corresponding author: Michiko Nishitani, michiko.nishitani.ot@gmail.com

Keywords: Tracheal suction, Low illuminance, Color identification, Skin color

ABSTRACT

Caregivers of children using mechanical ventilation via tracheostomy at home have to possess the required knowledge and skills. Tracheal suctioning is important to maintain airway patency because it can remove secretions. When it is the family caregivers who provide skilled care to the child throughout the day, one of the family members has to wake up several times during the night to provide the child with the required care. A low level of illuminance is desirable to reduce the adverse effects of lighting on sleep during the night. In this study, we investigated the minimum level of illuminance under which safe tracheal suction could be performed. We arranged 11 subjects to conduct simulated operations at illuminance levels between 200 lx and 3 lx. The results revealed that even at an illumination level of 3 lx, no significant reduction in the visual acuity of the subjects occurred and that the subjects had no difficulty in identifying color differences that had Munsell values of ±1. However, the way how the subjects inserted the tube into the cannula hole differed significantly among the subjects. Three of the subjects could not perform an error-free tube insertion even at an illumination level of 50 lx. However, five of the subjects could perform the task easily even at an illuminance level of 3 lx. In the work environment guideline, high illuminance should be used as the illuminance level to be maintained to ensure that every caregiver can perform tube insertions safely. In pediatric home healthcare, the caregiver is specified (i.e., the mother or father of the child) and the lighting provided should be such that the caregiver is able to work easily. Our experiments revealed that tracheal suctioning could be performed at illumination levels as low as 3 lx.

INTRODUCTION

In recent years, the number of children who require medical care, such as tracheal suction and tube feeding, has increased. Even when they are at sleep, some children may require a suction every few hours to secure the respiratory tract and facilitate breathing. Although home-visit medical care and home-visit nursing services are available in Japan, a child is taken care of by the family, especially during nighttime; night care is a heavy burden on any family [1].

Because tracheal suction is an invasive medical practice, risk management is important for family caregivers handling tracheal suction. Safe and accurate operations require clean tools, whose cleanliness has to be verified through visual inspections. And it is necessary to check the child's facial expression and complexion during suction. Thus, lighting plays a significant role during nighttime. We investigated the lighting environment of a family providing home care; every time the caregiver woke up during nighttime to attend to the child, the ceiling lamp of the room was switched on by the caregiver, disturbing the other family members sleeping in the room. Although a high level of

illuminance ensures workability, a low level of illuminance would be desirable if the others sleeping in the room are not to be disturbed. Caring for a child with a chronic illness, which goes beyond normal parenting, involves frequent medical procedures, medication administration, and illness-specific stressors. The sleep instability that occurs in the parents of ventilator-assisted children is related to the multiple dimensions of health-related quality of life. In caregivers of children suffering from chronic illnesses, inconsistent sleep patterns could play a more important role than low average sleep durations, in producing poor health outcomes [2].

One of the authors (MN) of this paper, an occupational therapist, was involved in improving the lighting within a pediatric home healthcare environment. In this paper, we present our case report and the results of an experiment we conducted to determine the minimum level of illuminance required to perform tracheal suction in children at night.

CASE REPORT

We present here how we improved the lighting in a home healthcare environment in which a mother was taking care of her daughter suffering from spinal muscular atrophy. The child had undergone a tracheostomy and a gastrostomy and required suction and infusion during nighttime. Before we improved the lighting in the environment, the mother had to wake up and turned on the ceiling lamp every few hours to attend to her daughter when her condition became poor. The action of turning on the lights by the mother disturbed the other family members sleeping in the room. We improved the lighting of the room as shown in Figure 1.

First, a wooden shelf was built to partly cover the bed. Next, we installed at the top of the shelf a warm-colored LED lamp facing the wall and the ceiling to provide indirect lighting to the bed. Thus, the lighting illuminated only the areas where it was needed. Although this modification caused the illuminance of the light falling on the bed to decrease from 150 to 10 lx approximately, the mother indicated that even at reduced illuminance she could work as before and that the glare was also reduced.
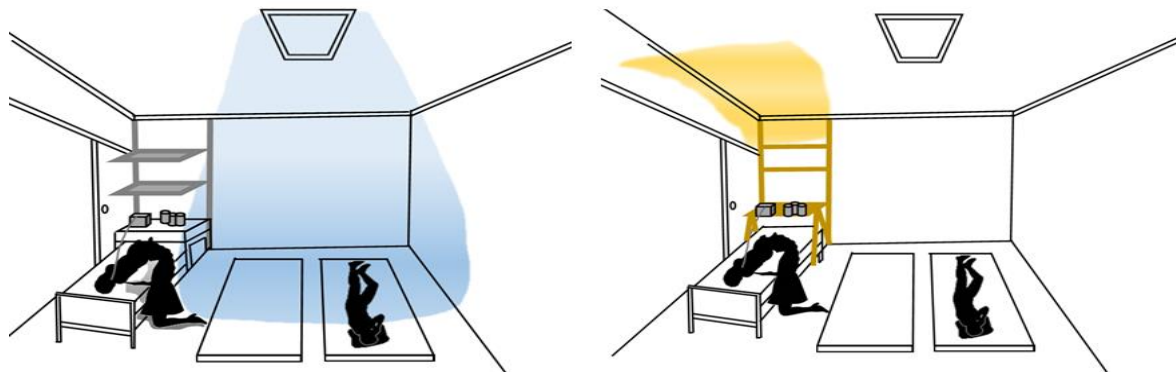
Before: ceiling lamp with 150–160 lx.   After: indirect lighting with 10–15 lx.
Figure 1. Home healthcare environment before and after lighting was improved

EXPERIMENTAL METHODS

In the previous section, we reported that healthcare could be performed without any stress even at an approximate illuminance level as low as 10 lx. We conducted an experiment to determine the minimum illuminance level required for healthcare [3].

The experiment was conducted in our laboratory by 11 healthy female college students (19–25

years in age). None of the subjects had any experience in suction operations. Tracheal suction requires disinfection of the fingers and tubes before and after performing suction to keep them clean. Caregivers inserted the tube into the tracheal cannula of the child, and performed the aspiration quickly and securely while monitoring the patient's facial expressions and complexion (Figure 2).
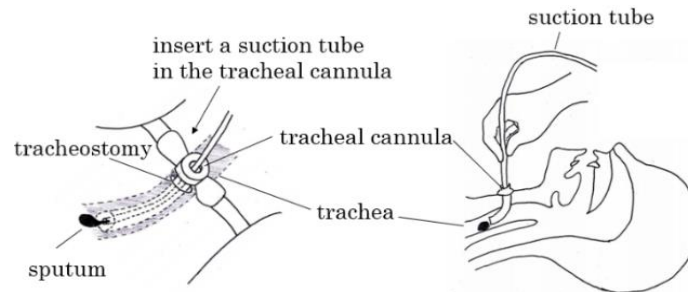

Figure 2. Tracheal suction

We prepared a booth that had walls painted in Munsell N5 gray (Figure 3). Three warm-colored LED light sources, commonly used as nightlights, were installed on the ceiling of the booth. The light sources were covered with a diffusion sheet to make uniform the illuminance of the light falling on the work surface. The illuminance in the booth was set at 200, 50, 12, 6, and 3 lx.
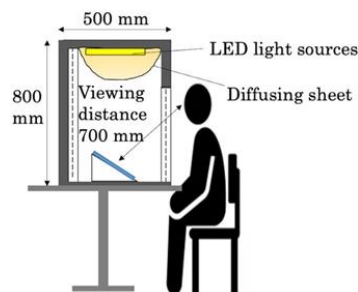

Figure 3. Setup of the experiment

Before conducting the experiment, we explained its purpose to the subjects and obtained their informed consent. The Frisby stereotests and Landolt C vision test were then performed by the subjects at an illuminance of 200 lx. Next, the subjects were asked to make color identification (Figure 4), insert the tube (Figure 5), and assess the level of difficulty experienced in inserting the tube. The illuminance within the booth was then reduced to 50, 12, 6, and 3 lx in steps. Three minutes were allowed for the subjects to get their eyes adapted to each level of illuminance. The Landolt C vision test was repeated for each level of illuminance.

The color identification experiment was designed as follows: During tracheal suction, hypoxemia can occur, causing the face and lips of the child to become whitish or dark. These abnormal color changes of the face and lips have to be noticeable to the caregiver to enable him/her to take any required action immediately. Therefore, to verify the identification of the abnormal color changes under each illuminance level, we presented four sets of three-color charts assuming that the face and lip colors were Munsell 5YR 7/4 and 7.5R 6/4, respectively, together with color charts with ±1 Munsell values (Figure 4). Thereafter, we asked the subjects to indicate the lighter or darker color among the three colors. For each subject, the order of the four sets of three-color charts and the position of the lighter or darker color chart within each set were randomized for each illuminance level.
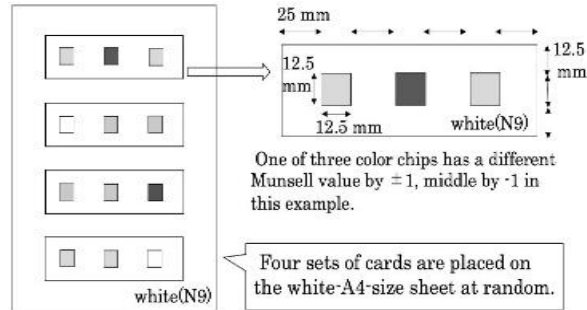
Figure 4. Color charts used for the color identification

The insertion operation experiment was designed as follows: The box used had three 6.5 mm holes near its upper edge and three 5.0 mm holes near its lower edge (Figure 5). A mechanism was in place within the box to make a buzzer sound when a tube was inserted into one of the holes. Each subject was given a suction tube that had a 2.7 mm outer diameter and was instructed to insert the tube through each of the three 6.5 mm upper holes until a buzzer sounded. Next, the subject was instructed to repeat the experiment using the 5.0 mm lower holes. The workability was evaluated on the basis of the number of times the tip of the tube touched the outside of the hole (counted as errors) and the time required for the work. The buzzer sounded three times in each experiment. Therefore, the working time was taken as the interval between the time the first buzzer sounded and the time that the third buzzer sounded. When an error was made, the subject was required to repeat the experiment and the time taken to complete an error-free experiment was measured.
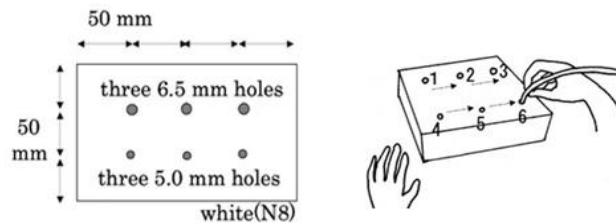

Figure 5. Box used for tube insertion

RESULTS

All of the 11 subjects could satisfactorily complete the Frisby stereotests. Their stereoscopic visions were unaffected. At an illuminance of 200 lx, all subjects had good visual acuity with a logMAR below 0. Their visual acuity decreased as the illuminance was decreased. However, the logMAR of the subject who had the worst visual acuity was less than 0.15 even at the minimum illuminance level of 3 lx.

In the color identification experiment, all subjects responded reliably even at the lowest illuminance of 3lx. Because this minimum illuminance level causes photopic vision, a color difference of approximately 1 Munsell can be judged through proper dark adaptation.

In the experiment of tube insertion, the tube had to be inserted into the 6.5 mm holes, which was easy, and in the other experiment, it had to be inserted into the 5.0 mm holes, which was difficult. In inserting the tube into 5.0 mm holes, most of the subjects made errors even when the illuminance level was brightest at 200 lx. Because inserting the tube into 5.0 mm holes was difficult, the effect of illuminance on tube insertion was not investigated. At 200 lx, all subjects could easily insert the

tube into the 6.5 mm holes without making errors. The effect of illuminance, therefore, is discussed for tube insertion into the 6.5 mm holes. At 200 lx, all subjects could insert the tube without making an error. However, at 50 lx, three of the subjects made errors. When the illuminance was reduced to 12 lx, two other subjects made errors, and when the illuminance was further reduced to 3 lx, another subject made an error. Thus, five out of the 11 subjects could work without making an error at all levels of illuminance up to 3 lx (Table 1). Even at a low illuminance of 3 lx, a 2.7 mm tube could be inserted into a 6.5 mm hole while observing the changes in the complexion and lip color of the child.

However, there were large differences (in the 200 to 3 lx range) in the minimum level of illuminance at which work could be performed by each subject without making errors. Therefore, in the work environment guideline in which the conditions under which everyone can work safely have to be indicated, the level of illuminance that is required to be maintained has to be stated as 200 lx. However, because home healthcare is provided by a family member, maintaining the lighting at a level at which that person can operate is sufficient. In the case reported here, the family member performed the work with ease at approximately 10 lx.

If the level of illumination during nighttime can be kept low, the other family members in the room are less likely to get disturbed during their sleep. High levels of illuminance can cause the caregiver to stay awake unnecessarily. At low levels of illuminance, the inhibition of subsequent sleep in the caregiver would be reduced and the quality of sleep of the caregiver improved.

The reason for the large differences in the minimum levels of illuminance at which tube insertion could be performed by different subjects is unclear because when the level of illuminance was reduced significantly, the visual acuity of the subjects reduced only slightly. The operating times of those who made errors varied with the level of illuminance as shown in Table 1. In addition, a tendency existed to evaluate the difficulty experienced in inserting the tube into a hole. We believe that even six subjects with errors would be able to perform tube insertion within a dark environment once they become familiar with the operations. We would like to conduct further studies on the factors causing the errors.

Table 1. Relative operating times (1.00 at 200 lx) and tube insertion errors

Subject No.	200 lx Relative time	Errors	50 lx Relative time	Errors	12 lx Relative time	Errors	6 lx Relative time	Errors	3 lx Relative time	Errors	Minimum illuminance
1	1.00		0.86		0.92		0.88		1.00		
2	1.00		0.93		0.95		1.11		1.07		
3	1.00		0.90		1.01		1.16		1.09		3 lx
4	1.00		0.91		1.01		0.95		1.12		
5	1.00		1.02		1.12		1.21		1.13		
6	1.00		0.74		0.77		0.82		0.82	○	6 lx
7	1.00		0.87		0.74	○	0.87		0.83		50 lx
8	1.00		0.99		0.91	○	1.12		1.37	○	
9	1.00		1.41	○	1.15		1.42		1.68		
10	1.00		1.17	○	1.39		1.46	○	1.58	○	200 lx
11	1.00		1.18	○	1.06	○	0.99		1.33	○	

CONCLUSIONS

Through this case report, we showed that at night, caregivers can work calmly even at an approximate illuminance as low as 10 lx when the glare also would be low.

Through the laboratory experiments, we showed that identifying the abnormal colors of the face and lip of a child is possible even at low color temperatures and low illuminance levels. Although large differences were noted in the tube insertion operations conducted by the subjects, some subjects could work even at a low illuminance of 3 lx. On the basis of these results, we plan to propose a lighting system suitable for a home care environment at night.

ACKNOWLEDGEMENT

REFERENCES

1. Keilty, K., Cohen, E., Ho, M., Spalding, K. & Stremler, R., (2015). Sleep disturbance in family caregivers of children who depend on medical technology. *A systematic review. Journal of Pediatric Rehabilitation Medicine: An Interdisciplinary Approach* 8, 113–130
2. Meltzer, L. J., Sanchez-Ortuno, M. J., Edinger, J. D., Avis, K. T., (2015). Sleep Patterns, Sleep Instability, and Health Related Quality of Life in Parents of Ventilator-Assisted Children. *Journal of Clinical Sleep Medicine 11(3)*, 251–258
3. Nishitani, M. & Sakai, H. (2022). Lighting environment of home medical care: the necessary illuminance for night-time tracheal suction of children requiring medical care. *Journal of Environmental Engineering 87 (Transactions of AIJ, Architectural Institute of Japan),* in press (in Japanese).

COLOR CALIBRATION APPLICATED AT THE POULTRY HOUSE VIDEO SURVEILLANCE

Tsung-Lin Lu[1]*, Ting Yu Wei[3], Pei-Yu Lai[2], Rui-Bin Chern[2], Tzung-Han Lin[3] and Yao-Chuan Tsai[2]

[1] *Graduate Institute of Applied Science and Technology, National Taiwan University of Science and Technology, Taiwan.*
[2] *Department of Bio-Industrial Mechatronics Engineering, National Chung Hsing University, Taiwan*
[3] *Graduate Institute of Colour and Illumination Technology, National Taiwan University of Science and Technology, Taiwan.*

*Corresponding author: Tsung-Lin Lu, sd023691@gmail.com

Keywords: Color calibration, Poultry surveillance, Poultry health

ABSTRACT

The digitalization of the livestock industry is developing during this decade. During the Covid-19 pandemic, remote management and monitor for poultry houses have become a new demand of the livestock industry. There are many types of researches that focus on using the computer vision system (CVS) to identify the situation of poultry and livestock. However, there are few kinds of research focusing on analyzing the color information of living poultry. In this research, we are dedicated on monitoring the situation of the poultry house by remote cameras. The illumination of poultry houses change frequently since they usually have an opening or semi-opening structure. Therefore, the color is too unstable to be controlled for identifying correct information including the health of the chicken. Fortunately, there are many studies of camera color calibration since 1990. A higher order polynomial equation, which is one of popular method, is a fast and efficient solution to calibrate the color of images. After applying a calibrated matrix on the video stream, it corrects video color to be meaningful for identifing the abnormal situations, such sick or dead, of chicken clearly. In our experiment, the color calibration reduced the root-mean-square deviation error (RMSE) of color samples from 91.86 to 10.44 and color difference ΔE from 26.72 to 7.21. This result will be helpful to monitor the native chicken and to identify the health of chicken in the poultry house. The color data of different chicken health conditions will be collected as a database to help veterinarians and poultry house staff to diagnose the illness.

INTRODUCTION

How to avoid the poultry disease pandemic is an important issue in the poultry industry. There have been much researches on the digitalization of the livestock industry in recent years [1-3]. After the pandemic of Covid-19, remote management and monitor of the poultry house have become a new demand of the livestock industry. There are many types of researches which focused on computer vision system (CVS) and long-period monitoring of humidity and temperature to identify the situation of poultry and livestock. However, there are few types of researches focusing on the color of living native poultry. Fortunately, the development of 5G mobile network makes it possible to monitor the situation of poultry houses with multiple high-resolution IP cameras in almost real-time. In this paper, we dedicated on monitoring the situation of a poultry house to identify the health of the chicken by remote cameras. However, the illumination of the poultry house frequently changed due to its semi-opening structure, so the color is too unstable to identify the situation of the chicken. Therefore, the main purpose of this research is the color calibration for surveillance images in a poultry house. The illumination which was changing of the semi-open poultry house was analyzed

to find the feasible time range for the chicken health checking. The color calibration algorithm was applied to the surveillance video. The color difference was calculated to identify the method's feasibility.

EXPERIMENT

There have been many studies of camera color calibration since the 1990s [4-8]. The polynomial transform method, which is one of the popular methods, is a fast, efficient solution to calibrate the color of images [4][8]. In this research, the polynomial transform method is applied to the surveillance video. To achieve a real-time calibration of surveillance video, the RGB to RGB polynomial transform was chosen. The polynomial functions were used to perform a mapping conversion between a color vector of camera c and a color vector of standard sRGB s as equation 1.

$$s = Ac \ (1)$$

Where A is the calibration matrix, for the linear transform, A is a 3×3 or a 3×10 matrix, and c is a 3×1 matrix. The internal values of matrix A are easily determined using methods of linear algebra as the Table 1.

Table 1:Definition of polynomial transforms used

A	Augmented matrix
3×3	$[R\ G\ B]$
3×10	$[R^2\ G^2\ B^2\ RG\ GB\ BR\ R\ G\ B\ 1]$

To relate the camera response and standard sRGB, the measured colors are installed in a working area of a surveillance camera. The color samples refer to the Macbeth ColorChecker, and the data show in Figure 1. In these 24 color samples, there are 17 colors from the Macbeth ColorChecker. CH1~CH4 colors are from the cockscomb color, and GD1 ~GD3 are those from the poultry house environment. The CIE Lab data of the color sample are measured by X-Rite RM200QC and converted into sRGB data to be the reference standard.

Red	Green	Blue	Magenta	Cyan	Yellow
R = 171	R = 102	R = 62	R = 174	R = 48	R = 220
G = 86	G = 153	G = 96	G = 104	G = 145	G = 187
B = 80	B = 82	B = 153	B = 143	B = 164	B = 54
White	**Neutral 8**	**Neutral 6.5**	**Neutral 5**	**Neutral 3.5**	**Black**
R = 233	R = 209	R = 182	R = 132	R = 129	R = 103
G = 238	G = 217	G = 192	G = 135	G = 132	G = 104
B = 245	B = 212	B = 182	B = 124	B = 123	B = 99
CH1	**CH2**	**CH3**	**CH4**	**GD1**	**GD2**
R = 221	R = 202	R = 194	R = 146	R = 228	R = 194
G = 154	G = 83	G = 156	G = 95	G = 225	G = 221
B = 153	B = 95	B = 152	B = 99	B = 205	B = 246
GD3	**Moderate Red**	**Blue Flower**	**Blue sky**	**Light skin**	**Dark skin**
R = 87	R = 179	R = 131	R = 114	R = 185	R = 125
G = 85	G = 105	G = 146	G = 137	G = 158	G = 101
B = 90	B = 102	B = 178	B = 132	B = 130	B = 86

Figure 1. Color sample and sRGB data

The color samples are installed in the poultry house for assisting for dynamic corrections, as Figure 2. The half of samples are placed at the center pillar, and the rest are placed on the surface of the feeding tube. The surveillance video was captured by the Axis-Q6128E 4K camera. The capturing condition is set as auto-focus, auto-exposure, and white balance of an outdoor scenario. The capturing time is from AM07:00 to PM5:00. The polynomial transform method was applied, and the camera color are captured the data from the 12:00 PM snapshot, the sRGB data of the color sample were used, and the two different order augmented matrixes were separately applied to calibrate the color.

Figure 2. The surveillance video snapshot in the poultry house at 12:00 PM

RESULT

The 3×3 and 3×10 matrixes were calculated and applied to the frame at 12:00 PM. The results of calibrated frames by different methods are shown in Figure 3. The result based a 3×3 matrix looks reddish, and that based on 3×10 matrix looks a bit warmer tones.

Figure 3. The Calibration result of 12:00 PM snapshot, 3×3 matrix(left), 3×10 matrix(right)

The data of calibration result is shown in Table 2. Before the calibration, the average RMSE is 91.89, and it is too high to identify the situation of chicken health. After the calibration, the average RMSE is reduced to 37.55 and 10.44 by 3×3 matrix and 3×10 matrix, respectively.

Table 2. The root-mean-square deviation error (RMSE) of calibration(before and after)

Color	12:00PM Camera responses	3×3 matrix	3×10 matrix
Average	91.89	37.55	10.44

By following the better RMSE result, the 3×10 calibration matrix has been applied all daytime to analyze the feasibility of our method to suppress the change of color due to daylight. The calibration result was calculated into the CIE Lab to analyze the color difference. The results for before and after calibration are shown in Figure 4. According to the result, the ∆E between the camera response and standard of all color samples is higher than 10.0, and the average ∆E is 26.71. It is too high to identify the health of the chicken. After applying the 3×10 calibration matrix, the average ∆E is reduced to 7.21. And from AM09:10 to PM1:40, the average ∆E of each time is lower than 8.0. As a result, it is expected precisely enough to identify the situation of chicken.
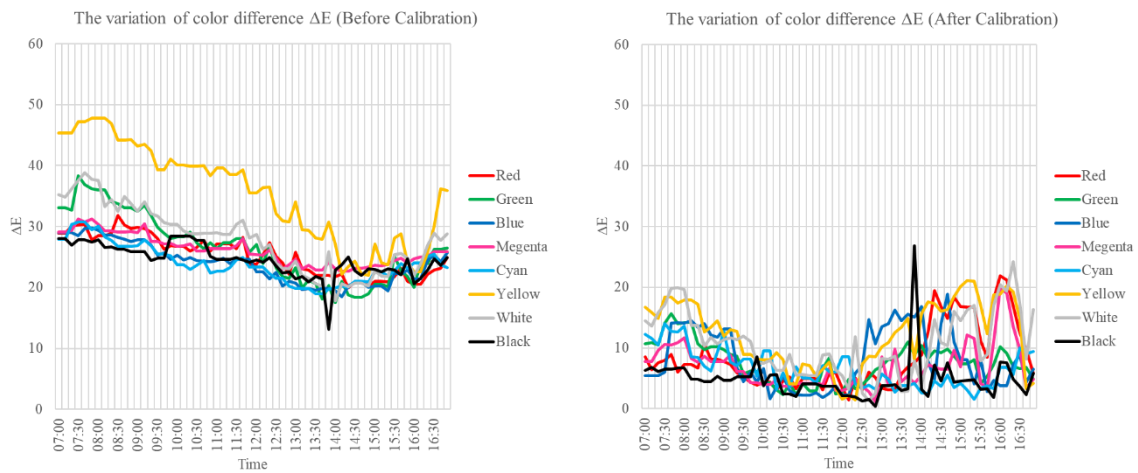
Figure 4. The variation of color difference ∆E, before calibration(left), after calibration(right)

CONCLUSION

In this research, the surveillance video of the poultry house was calibrated the color by polynomial transform method with 3×3 and 3×10 matrixes. The calibration results show great performance to reduce to color difference between the standard color data and camera response. Based on this result, the relationship between the color and health condition of chicken will be collected in the future to perform valuable digitalization data in the poultry industry.

ACKNOWLEDGEMENT

REFERENCES

1. Novas, R. V., &Usberti, F. L. (2017). Live Monitoring in Poultry Houses: A Broiler Detection Approach. *Proceedings - 30th Conference on Graphics, Patterns and Images, SIBGRAPI 2017*, 216–222. https://doi.org/10.1109/SIBGRAPI.2017.35

2. You, M., Liu, J., Zhang, J., Xv, M., &He, D. (2020). A novel chicken meat quality evaluation method based on color card localization and color correction. *IEEE Access*, *8*, 170093–170100. https://doi.org/10.1109/ACCESS.2020.2989439

3. Pereira, D. F., Lopes, F. A. A., Filho, L. R. A. G., Salgado, D. D. A., &Neto, M. M. (2020). Cluster index for estimating thermal poultry stress (gallus gallus domesticus). *Computers and Electronics in Agriculture*, *177*(April), 105704. https://doi.org/10.1016/j.compag.2020.105704

4. Cheung, V., Westland, S., Connah, D., &Ripamonti, C. (2004). A comparative study of the characterisation of colour cameras by means of neural networks and polynomial transforms. *Coloration Technology*, *120*(1), 19–25. https://doi.org/10.1111/j.1478-4408.2004.tb00201.x

5. Joshi, N. S. (2004). *Color Calibration for Arrays of Inexpensive Image Sensors Master's with Distinction in Research Report*. *March*.

6. Grana, C., Pellacani, G., Seidenari, S., &Cucchiara, R. (2004). Color calibration for a dermatological video camera system. *Proceedings - International Conference on Pattern Recognition*, *3*, 798–801. https://doi.org/10.1109/ICPR.2004.1334649

7. Funt, B., &Bastani, P. (2014). Irradiance-independent camera color calibration. *Color Research and Application*, *39*(6), 540–548. https://doi.org/10.1002/col.21849

8. Sunoj, S., Igathinathane, C., Saliendra, N., Hendrickson, J., &Archer, D. (2018). Color calibration of digital images for agriculture and other applications. *ISPRS Journal of Photogrammetry and Remote Sensing*, *146*(June), 221–234. https://doi.org/10.1016/j.isprsjprs.2018.09.015

ANALYSIS OF THAI SKIN COLOR ON CIEL*C*H*

Nutticha Pattarasoponkun[1]*, Chanprapha Phuangsuwan[2] and Mitsuo Ikeda[2]

[1]*Graduate School, Faculty of Mass Communication Technology, Rajamangala University of Technology Thanyaburi, Thailand.*
[2]*Color Research Center, Rajamangala University of Technology Thanyaburi, Thailand.*
.
*Corresponding author: Nutticha Pattarasoponkun, nootoon2538@gmail.com

Keywords: Thai skin color, Skin tone, Skin measurement, Facial skin color

ABSTRACT

The CIEL*c*h* color system is helpful to describe lightness (L*), chroma (c*), and angle of color or hue angle (h*). In this study, we wanted to analyze the results of the skin color of Thai people in the CIEL*c*h* color space system, using 171 Thai people aged 24-70 years old to measure all 5 points of the body, namely the left cheek and the right cheek, forehead, chin and inner arm by using the Konica Minolta CS-100A as a tool to measure the skin color of Thai people. The participants must not use any skincare or cosmetics before skin measuring. A white reference plate was measured in the same positions of a part that measured the real skin, and after that, the real skin was measured. The results showed that the inner arm area had the highest mean lightness, followed by the forehead, cheeks, and chin, which were 61.35, 57.92, 57.77, and 55.12, respectively. The distribution of chroma in the cheek tends to decrease as the skin lightness increases on the forehead and inner arms, although there is a slight tendency. For the average value of chroma, the cheek was the highest of chroma, followed by chin, forehead, and inner arm (23.87, 23.31, 22.93, and 22.03, respectively). However, when comparing the lightness with the Hue angle, there was no relationship in the cheek, forehead, chin, and inner arm. The inner arm was the highest for the average hue angle value, followed by forehead, cheek, and chin (57.88, 52.42, 52.16, and 51.32, respectively).

INTRODUCTION

Hemoglobin and melanin are substances in the body that are the constituents in the appearance of human skin color [1]. The amount of both substances varies for each individual. Including daily exposure to sunlight can also affect the amount of Hemoglobin and Melanin in different people, even if they are of the same ethnicity. Moreover, some studies have found that the redness of the skin on the face is greater than that of the trunk because there is better blood flow in the skin than the body [2]. It was found that the redness of the skin strongly depends on the location on the body [3]. Therefore, the location on the body might be a factor that can cause different skin tones.

CIEL*c*h* is a color system in the polar coordinate color space. Developed from the CIEL*a*b* color system, the lightness or L* is the same scale as CIELAB, ranging from 0-100, with 0 being black and 100 being white. The chroma or c* indicates the quality of a color's purity, intensity, or saturation. If the chroma value is low, the color will be dull. But if the higher the chroma value, the vividness of color. The hue angle or h*, 0 to 360 degrees, indicates red by 0 and 360 degrees, yellow by 90 degrees, green by 180 degrees, and blue by 270 degrees as indicated in Fig.1 [2]. The values L*, c*, and h* can be calculated from the equation 1, 2, and 3, respectively.

Normally, the skin color analysis is most often analyzed in the CIELAB color system because it can quantify the pigmentation of the skin, such as the redness or yellowness of the skin. But the

analysis using the CIEL*c*h* is not common in research in Thailand. Therefore, we wanted to analyze the results of the skin color of Thai people based on the CIEL*c*h* color system. In addition, also we investigated the different positions of the body that can affect the difference in lightness, chroma, and hue angle of the Thai skin.
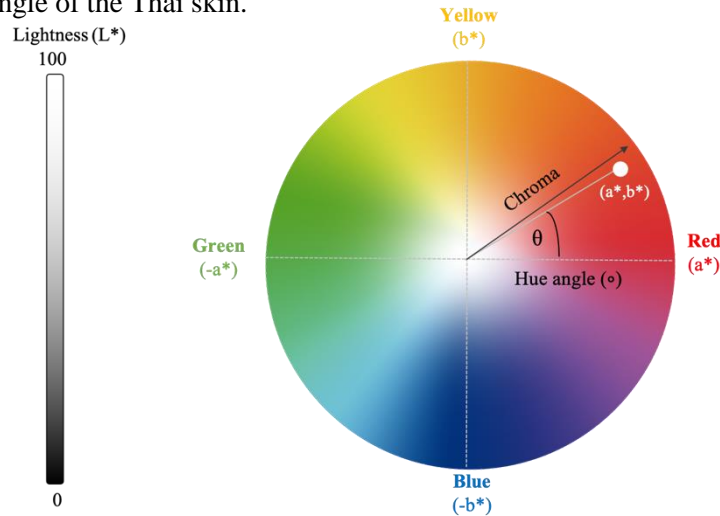

Figure 2. The CIEL*c*h* color system.

$$\text{Lightness, L*} = 116 \left(\frac{Y}{Y_0}\right)^{1/3} - 16 \tag{1}$$

$$\text{Chroma, c*} = \sqrt{(a*)^2 + (b*)^2} \tag{2}$$

$$\text{Hue angle (°), h*} = \text{atan}\left[\frac{b*}{a*}\right] \tag{3}$$

METHODOLOGY

171 Thai people had participated in this study including 81 males and 90 females. The age ranged 24 to 72 years old. Most of the participants were working outdoors and indoors. The four positions of the face were measured, left and right cheek, forehead, and chin which represent parts most exposed to the sunlight, and inner arm which represents part least exposed to the sunlight.

Konica Minolta CS-100A chromameter was used to measure the skin color of Thai people. This instrument was portable, lightweight, and gave the value close to the spectroradiometer CS-2000 that has been tested in a preliminary experiment for instrument testing. Moreover, the chromameter eliminated the problem of the pressure factor which affects skin color change. A disadvantage of this type of instrument was to require external light to measure the color. Therefore, it was necessary to measure the white reference plate as a reference.

(A)   **(B)**

Figure 2. (A) White reference plate measurement. (B) Real skin measurement.

Prior to the participants must not use any skincare or cosmetics or had to wash their face. Then, the personal informations were recorded such as age, gender, occupation, workplace characteristic, hometown province, and skincare and cosmetic use. The white reference plate was measured at the same position as the real skin. Five real skin positions were measured immediately after the white reference measurement as indicated in Fig. 2. One-way ANOVA was used with a significance level of 0.05 to check difference between two data.

RESULT AND DISCUSSION

The two sides of the cheek were averaged in one value to represent the cheek in each participant. The cheek and forehead were in the same range in lightness values of about 40 – 75 and had the average L^* were 57.77($\pm$7.99) and 57.92($\pm$7.42), respectively. The inner arm had a wider distribution of L^* than other three positions with a range of about 31-84 and the highest L^* of average value at 61.35 ($\pm$8.34). But the chin had the lowest in L^* with a range of about 38-70 with the average value of 55.12 ($\pm$6.95). Moreover, the distribution of chroma values of all positions was the same range about 15-33 as indicated in Fig.2. The average of chroma of cheek, forehead, chin, and inner arm was 23.87 ($\pm$2.66), 22.93 ($\pm$2.93), 23.31 ($\pm$2.94), and 22.03 ($\pm$2.93), respectively. The chin was a significantly different in L^* in cheek and forehead (P=0.008 and P=0.004, respectively). The L^* of the inner arm was significantly different from three parts of the face (P=0.000) as indicated in Fig.4. The inner arm also was significantly different from the position of face in saturation of skin or chroma as indicated in Fig.5 (inner arm vs. cheek; P=0.000, forehead; P=0.021 and chin; P=0.000, respectively). The cheek was significantly different from forehead when compared with other part of the face (P=0.013).

Figure 6. indicates hue angle, the inner arm showed the widest distribution in a range about 30° - 85°, while the parts of the face (cheek, forehead, and chin) were the same range about 30° - 65°. As a result of h^* of the inner arm, the highest in average was 57.88 ($\pm$5.01) and more towards yellow than the facial. The average h^* of cheek, forehead, and chin was 52.16 ($\pm$5.15), 52.42 ($\pm$5.16), and 51.32 ($\pm$6.94), respectively. The h^* of the inner arm was significantly different from cheek, forehead, and chin (P=0.000) as indicated in Fig.7.

The face is an area with more blood flow than the inner arm. As a result, the face has larger redness of the skin than the inner arms as well as the faces area being frequently exposed to sunlight

which affects the production of Melanin [3, 4, and 5]. Therefore, the skin color of the face was darker, higher in chroma, and a shade of red than the inner arm.
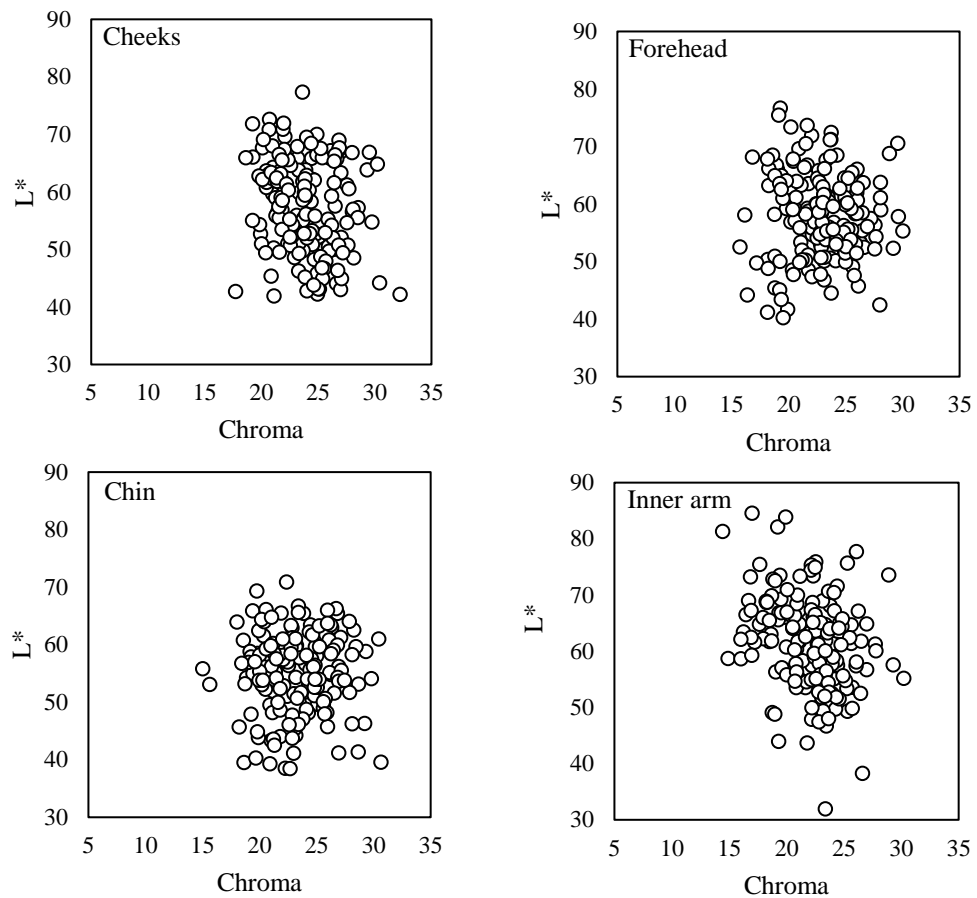

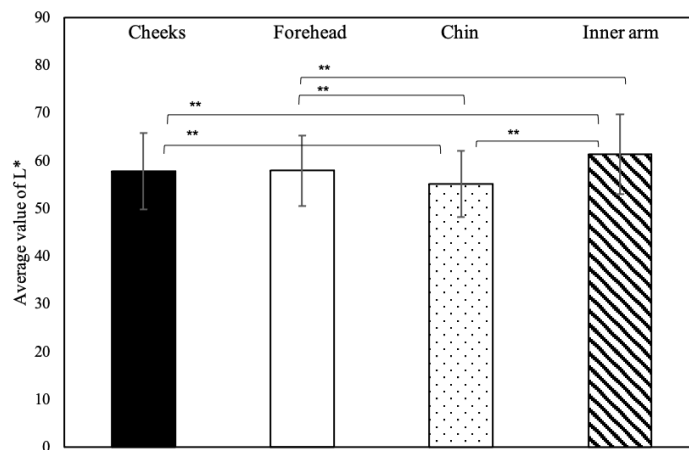**Figure 3. The distribution of Thai skin tone in each position of measurement between chroma and lightness**

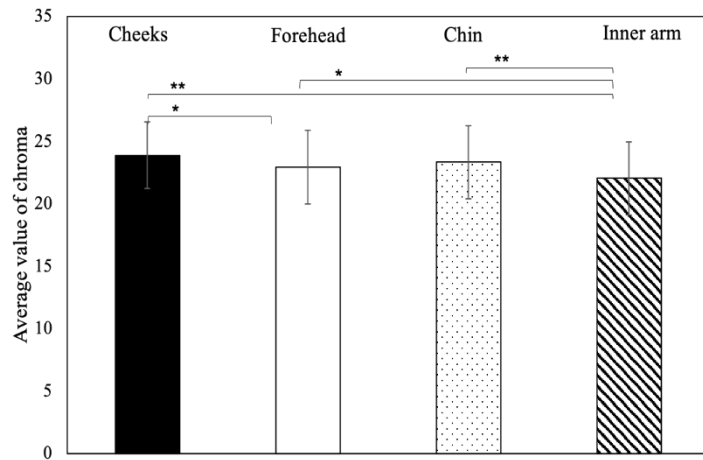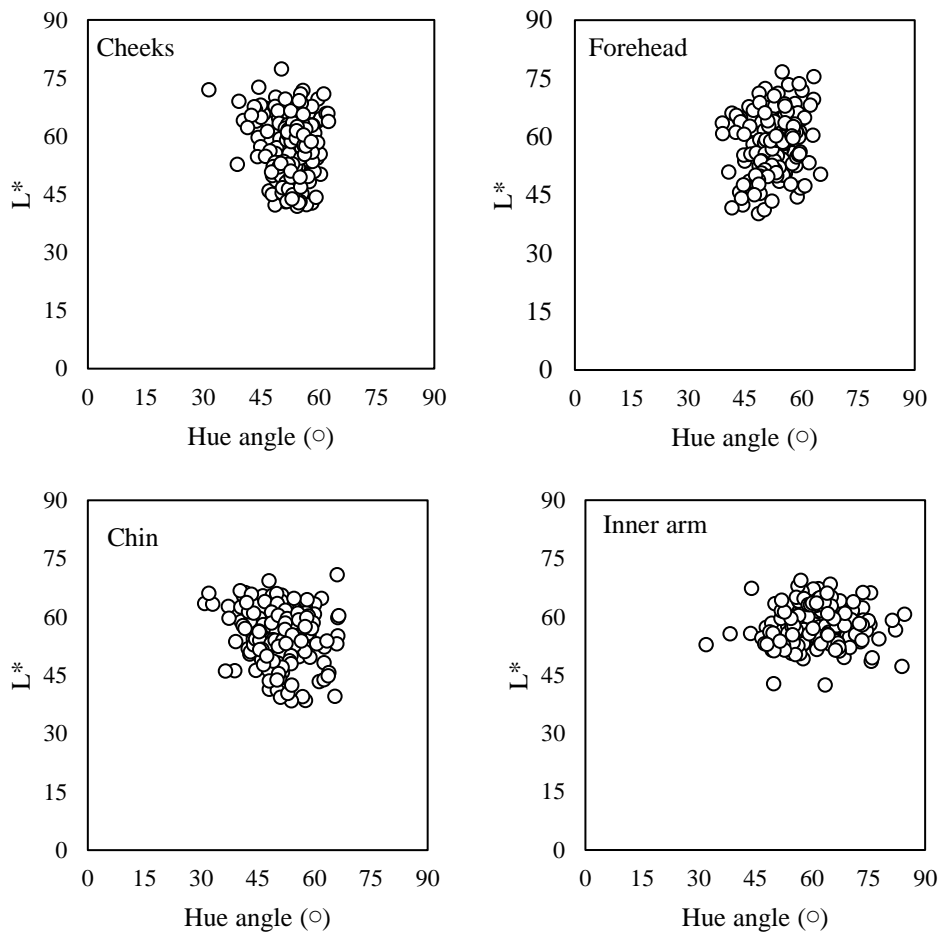**Figure 4. The average lightness of Thai skin tone in each position of body (* ; P<0.05 and**
**   **; P<0.00)**

**Figure 5. The average chroma of Thai skin tone in each position of body (* ; P<0.05 and
     ; P<0.00).

**Figure 6. The distribution of Thai skin tone in each position of measurement between chroma
and lightness**
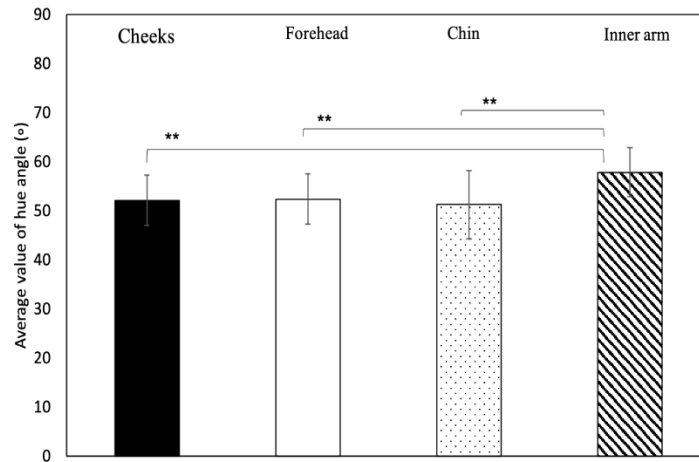
Figure 7. The average hue angle of Thai skin tone in each position of body (* ; P<0.05 and **; P<0.00).

CONCLUSION

The results suggested that the facial area which most exposed to the sunlight is affected to skin to become darker, more saturate and to tend to red color than the inner arm. The difference between body positions affected the lightness, chroma, and hue angle of Thai skin color.

REFERENCES

1. Takanori Igarashi, Ko Nishino and Shree K. Nayar. (2007). The Appearance of Human Skin: A Survey. Foundation and Trend in Computer Graphic and vision, 3(1), 1-95.
2. Weatherall IL and Coombs BD. (1992). Skin color measurements in terms of CIELAB color space values. J Invest Dermatol, 99, 468–473.
3. In Sik Yun, Won Jai Lee, Dong Kyun Rah, Yong Oock Kim and Be-young Yun Park. (2010). Skin color analysis using a spectrophotometer in Asians. *Skin Research and Technology*, 16, 311-315.
4. F. J. Ruiz, Nuria Agell, Cecilio Angulo and Monica Sanchez. (2012). A qualitative learning system for human sensory abilities in adjustment tasks. Conference: 26th International workshop on qualitative reasoning, California, United States of America.
5. Stucker M, Steinberg J, Memmel U et al. (2001). Differences in the two-dimensionally measured laser Doppler flow at different skin localisations. Skin Pharmacology and Applied Skin Physiology, 14, 44-51.

EFFECT OF LIGHTING ON LIPSTICK TEXTURE FOR ADVERTISING PHOTOGRAPHY

Jarunee Jarernros[1], Chanida Saksirikosol[1]* and Ploy Srisuro[1]

[1]*Department of Advertising and Public Relations Technology, Faculty of Mass Communication Technology, Rajamangala University of Technology Thanyaburi, Thailand.*

*Corresponding author: Chanida Saksirikosol, e-mail: chanida_s@rmutt.ac.th

ABSTRACT

The purpose of this study was to investigate the effect of lighting on lipstick texture in advertising photographs. The approach involves photographing four varieties of lipstick using soft and hard light: Lip Gloss, Tinted Balm, Matte Powder, and Liquid Lipstick. The researcher set the lipstick color to orange and red and set the picture size to close up (CU) and extreme close up (ECU). The photographs were given to thirty subjects, who were then asked to classify lipstick using a questionnaire. The finding showed that the influence of light has a little effect on different lipstick textures. The texture of lipstick may be seen more clearly in hard light than in soft light. The distinction between soft and hard light has no effect on lipstick classification. The accurate lipstick classification is influenced more by soft light than by hard light.

INTRODUCTION

Lipstick is a well-known and extensively used product. Customers may be perplexed when they view the image of the lipstick advertising since the lipstick has a range of textures and personalities. Because advertising pictures are crucial in influencing consumers' purchase decisions, photographers must consider the authenticity of the lipstick's texture when photographing the advertising.

When photography advertisements, lighting is important in order to correctly depict the texture of the lipstick. Photographers must use lighting that complements the textures. Depending on the light quality, the image will be influenced differently. Soft light, for example, will provide the sense of soft light with low contrast between dark and light, whereas hard light will give the impression of harsh light with strong contrast between dark and light. Soft and hard light, as well as differences in light and shadow, have an effect on the reflection of various object surfaces. Soft light has a less influence on object reflection than hard light. For example, if we want to photograph a luster item, we will see more reflections and less shine if we use soft light rather than hard light.

METHOD

The researchers used soft and hard light to photograph four different types of lipsticks in this study: Lip Gloss, Tinted Balm, Matte Powder, and Liquid. The researchers then used a questionnaire to analyze the photos in order to determine if the subjects could classify the lipstick. The following approaches were utilized by the researchers:

1. Set two types of light: Hard light with mono flash and standard reflector, soft light with mono flash, standard reflector and diffuser.

Figure 1. Example of the lighting for photography

2. Set four types of lipsticks: Matte Powder, Liquid Lipstick, Lip Gloss and Tinted Balm.

3. Set the color of lipstick from two popular colors which were red and orange.

4. Close-up (CU) and extreme close up (ECU) picture sizes were chosen from a survey of popular image sizes used in lipstick advertising.

5. The photos were presented to thirty subjects who are familiar with the sort of lipstick and have purchased it online. The subjects saw the pictures on a 10.9-inch Apple iPad Air screen in white light before answering the questionnaire using the methods below.

5.1 Place two example photos of the same lipstick type, color, and size, one shot with soft light and the other with hard light, side by side. The subjects selected the photograph that showed the texture of lipstick more clearly.

5.2 Bring the sample photos to the subjects and have them look at them one by one. The subjects were then asked to select a lipstick from four options: Matte Powder, Liquid Lipstick, Lip Gloss and Tinted Balm.
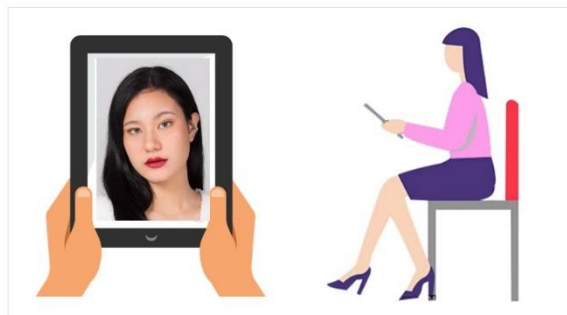

Figure 2. Scenario of the data collection method

Examples of photographs for lipstick advertising used in the study

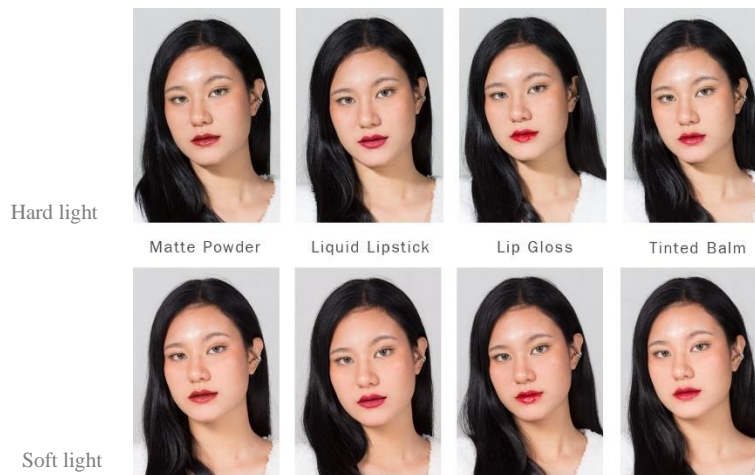**Figure 3. Example of the orange lipstick photo, Close Up (CU)**

Figure 4. Example of the red lipstick photo, Close Up (CU)

Figure 5. Example of the orange lipstick photo, Extreme Close Up (ECU)

Figure 6. Example of the red lipstick photo, Extreme Close Up (ECU)

RESULT

The result of the study of effect of lighting on lipstick texture for advertising photography was as the following.

1. Result of the study of clarity of showing the texture of lipstick was shown as Figure 7.
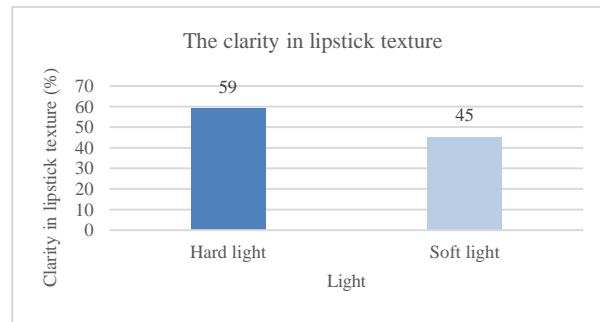
Figure 7. Shows results of clarity in lipstick texture

Hard light, according to the chart, may reveal 59 percent of the texture of the lipstick. Soft lighting may reveal 45 percent of the texture of a lipstick. As a result, hard light might reveal more lipstick texture than soft light. This might be because hard light accentuates the contrast between light and shadow, and the reflections of the subject texture are more prominent than soft light. It clarifies the texture of lipstick better than soft light.

2. Result of the study on the accuracy of lipstick classification
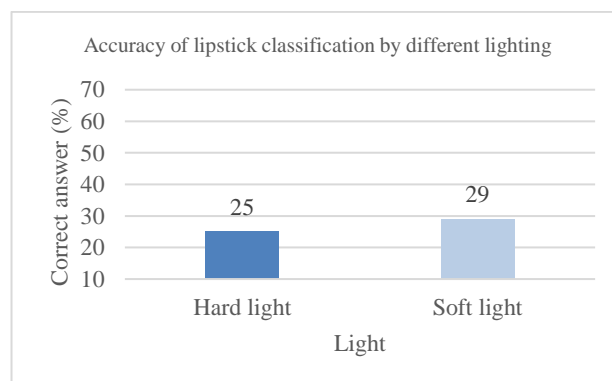2.1 The accuracy of the lipstick classification by the difference of lighting was shown as Figure 8.

Figure 8. Shows results of accuracy of lipstick classification by different lighting

According to the chart, soft light had a 29 percent effect on lipstick classification accuracy while hard light had a 25 percent effect. The difference between soft and hard light has no influence on lipstick classification accuracy. Soft light has a bigger effect on lipstick classification accuracy than hard light.

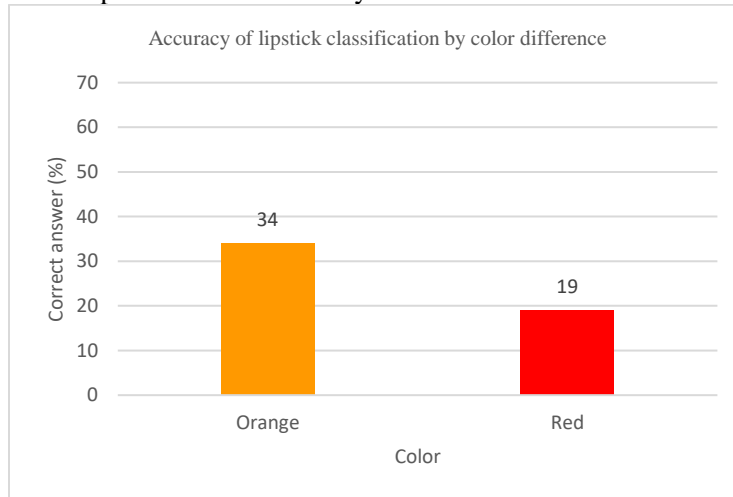2.2 The accuracy of the lipstick classification by the color difference was shown as Figure 9.

Figure 9. Shows results accuracy of lipstick classification by color difference

According to the chart, orange represented lipstick type accuracy of 34 percent, while red represented lipstick type accuracy of 19 percent. It is possible to conclude that orange indicates lipstick type accuracy more than red. This might be because red has a higher color intensity than orange, resulting in distinct reflections and a different perception of the lipstick texture.

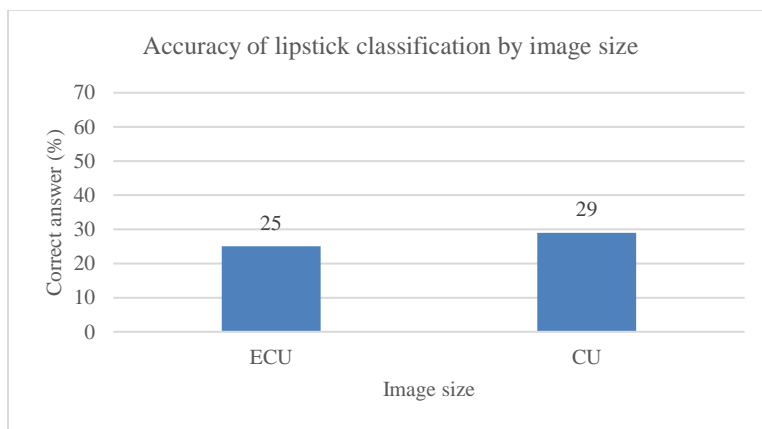2.3 The accuracy of the lipstick classification by the image size was shown as Figure 10.

Figure 10. Shows results of accuracy of lipstick classification by image size

According to the chart, a close-up (CU) image had a 29 percent accuracy in lipstick classification, while an Extreme Close Up (ECU) image had a 25 percent. Differences in picture size can have a

little impact on the accuracy of lipstick classification. The close-up can reveal considerably more about the accuracy of lipstick classification than the extreme close-up.

2.4 The accuracy of the lipstick classification by the texture of lipstick was shown as Figure 11.
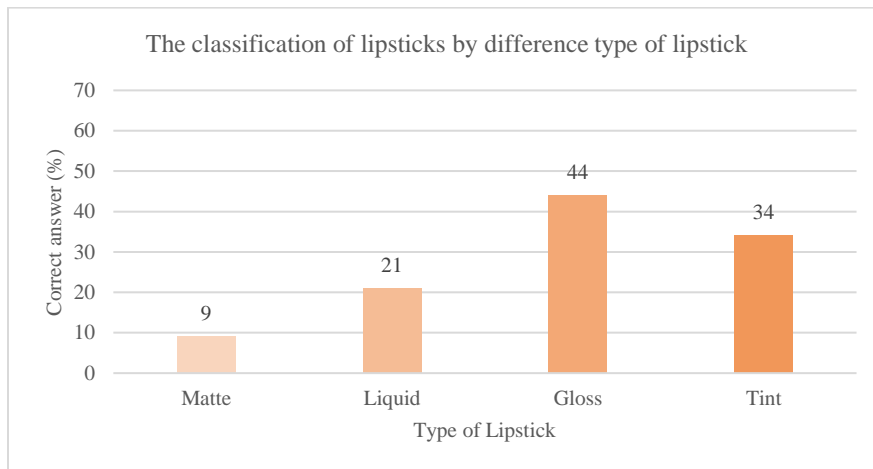

Figure 11. Shows results accuracy of lipstick by texture of lipstick

According to the chart, lip gloss was the most preferred lipstick texture, accounting for 44 percent, followed by tinted balm 34 percent, liquid lipstick 21 percent, and matted powder 9 percent. This might be due to the fact that lip gloss has a distinct glossy texture that distinguishes it from other types of lipsticks. This allows subjects to quickly classify the types of lipsticks. Matte powder lipsticks have the least texture, likely because they have a texture similar to liquid lipsticks, making it difficult for subjects to classify lipsticks

CONCLUSION

The findings of this study were separated into two categories: the clear texture of lipsticks and the accuracy of lipstick type. The research reveals that the lighting used in lipstick advertisement photography has minimal effect on the texture of lipstick when photos of the same size, color, and kind of lipstick are taken. However, with the varied lighting circumstances, soft light and hard light, there was a little difference between the two to highlight the clearer texture of the lipsticks. When the subjects saw the photos one by one and chose the type of lipsticks, they did it more properly with the soft light. There was, however, a minor variation between these two lightings. The explanation for the minor difference might be that the lips are generally matte. When a thin coating of lipstick is applied to the lips, the texture of the lipstick is not apparent. As a result, while photographing lipstick advertising, the difference in lighting should not be considered alone. However, additional factors must be considered, such as the direction of the light, the camera angle, or the consumer lipstick purchasing experience, among others.

ACKNOWLEDGEMENTS

REFERENCES

1. Earnest, A. (2019). The New Lighting for Product Photography: The Digital Photographer's Step-bye-Step Guide to Sculpting with Light. New York, NY: Amherst Media.
2. Freeman, M. (2006). The Complete Guide to Light & Lighting in Digital Photography. Utah, UT: Lark Book.
3. Jarearnros, J., Srisuro, P., Phuangsuwan, C. (2019). The Influence of Background Color of Silver Jewelry Advertising on Purchasing Decision. Proceeding of the 50th Annual Meeting of the Color Science Association of Japan Conference, pp.211-213.

DISPLAY WHITE POINT PERCEPTUALLY MATCHED WITH LIGHT BOOTH ILLUMINATION

Jiaxun Zhang[1], Haisong Xu[1]* and Hao Jiang[1]

[1]*State Key Laboratory of Modern Optical Instrumentation, College of Optical Science and Engineering, Zhejiang University, Hangzhou 310027, China.*

*Corresponding author: Haisong Xu, chsxu@zju.edu.cn

Keywords: Display white point, Display luminance, Color matching, Method of constant stimuli

ABSTRACT

This study focuses on the perceptual matching between the display white point and the neutral background of the light booth with a chromaticity of D65, which is a fundamental work for many color-relevant applications. Based on the psychophysical methods of adjustment and constant stimuli, a color matching experiment was carried out at three different display luminance levels by a panel of six observers. The white point accepted by most observers is referred to as an overall white point, which exhibits a slight increasing trend around 7300K with the display luminance. It also turns out that each observer has a distinct acceptable zone of white points, of which the size and the constant bias from the overall white point may be related to individual characteristics of the visual system.

INTRODUCTION

The white point is an important parameter in most display technology, acting as a chromatic reference for the displayed colors. Previous studies suggested that the white point should be configured appropriately to keep its neutral appearance, depending on the ambient lighting and the viewing condition [1,2]. Matching the display white point with the light booth illumination is a fundamental work for color reproduction applications [3] and psychophysical experiments [4], on which, however, few investigations have been reported so far.

In this study, a psychophysical experiment was carried out to investigate the color matching between the display white point and the D65 illumination of a light booth. The chromatic change of the white point with the display luminance and the inter-observer variation of the acceptable zones would also be discussed.

EXPERIMENT

The psychophysical experiment was conducted in a dark room, equipped with an X-rite SpectraLight QC light booth working in the D65 illumination mode. A gray board with a size of 300mm $\times$ 500mm (equivalent to a $20° \times 30°$ field of view) was installed in the light booth, at an angle of $45°$ to the bottom plane. At the center of the gray board was drawn a square black frame with a size of 70mm $\times$ 70mm (equivalent to a $4° \times 4°$ field of view) to help observers focus their eyes. The luminance inside the black frame was about 125cd/m^2. An EIZO CG241W professional desktop monitor was placed adjacent to the light booth, which displayed a large uniform color block with the same size of the gray board, as well as a similar black frame at the center of the screen. In the experiment, the monitor was set to three luminance levels, namely, 20cd/m^2, 36cd/m^2 and 50cd/m^2.
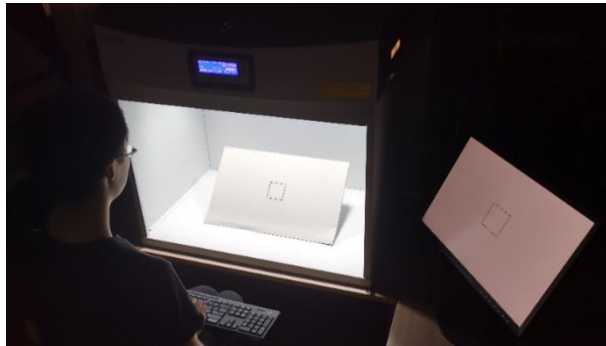
Figure 1. Experimental setup

Six observers with normal color vision, who had passed the Farnsworth-Munsell 100 Hue test (FM100 test), participated in the experiment. As illustrated in Figure 1, the observers were instructed to sit in front of the light booth and the monitor, allowing their gaze to shift back and forth to view the gray board or the screen along the normal. The viewing distance to the both media were about 1m.

Before the experiment, a 2-min dark adaptation and a 1-min background adaptation to the light booth illumination were performed. The experiment was separated into two sessions. The first session was based on the psychophysical method of adjustment, whereby the observers pressed arrow keys on a keyboard to adjust the chromaticity coordinates of the displayed color in CIE 1976 u'v' diagram, until it appeared as neutral as the gray board. This procedure was repeated 5 times with different starting points. The mean coordinates and the standard deviation value (represented by σ) of the adjustments were calculated to roughly estimate the range of accepted white points.

The second session was intended to obtain the acceptable zones of white points via the psychophysical method of constant stimuli. A series of test white points were calculated for each observer individually, with chromaticity coordinates being distributed around the mean coordinates of the adjustments at distances of 0.75σ, 1.5σ, 2.25σ and 3σ (see Figure 2). These test white points were displayed at a random order. The observers compared each of them with the gray board and made a judgement on whether it was perceived neutral by pressing the number keys (pressing "1" key for acceptance and pressing "0" key for rejection). Each test white point was assessed 4 times. The Probit analysis was adopted to calculate the T-50 points, which were then fitted into an ellipse, outlining the acceptable zone. The chromaticity inside the zone had a higher possibility to be accepted as a neutral white point than to be rejected. The entire experiment was repeated for each of the 3 luminance levels and the 6 observers.
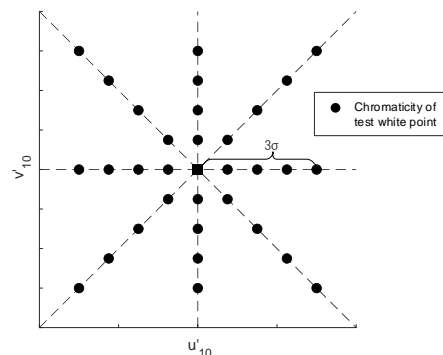

Figure 2. Example of chromatic distribution of the test white points

RESULTS AND DISCUSSION

Figure 3 plots the white point acceptable zones in CIE 1976 u'v' diagram, together with a daylight locus, corresponding to the six observers and the three display luminance levels, separately. For each luminance level, the center coordinates of the intersection of the most separate acceptable zones represent the chromaticity accepted by the most observers as an appropriate white point, dubbed overall white point. The correlated color temperatures (CCT) and the deviations to the daylight locus (Duv) of the overall white points are calculated and listed in Table 1.
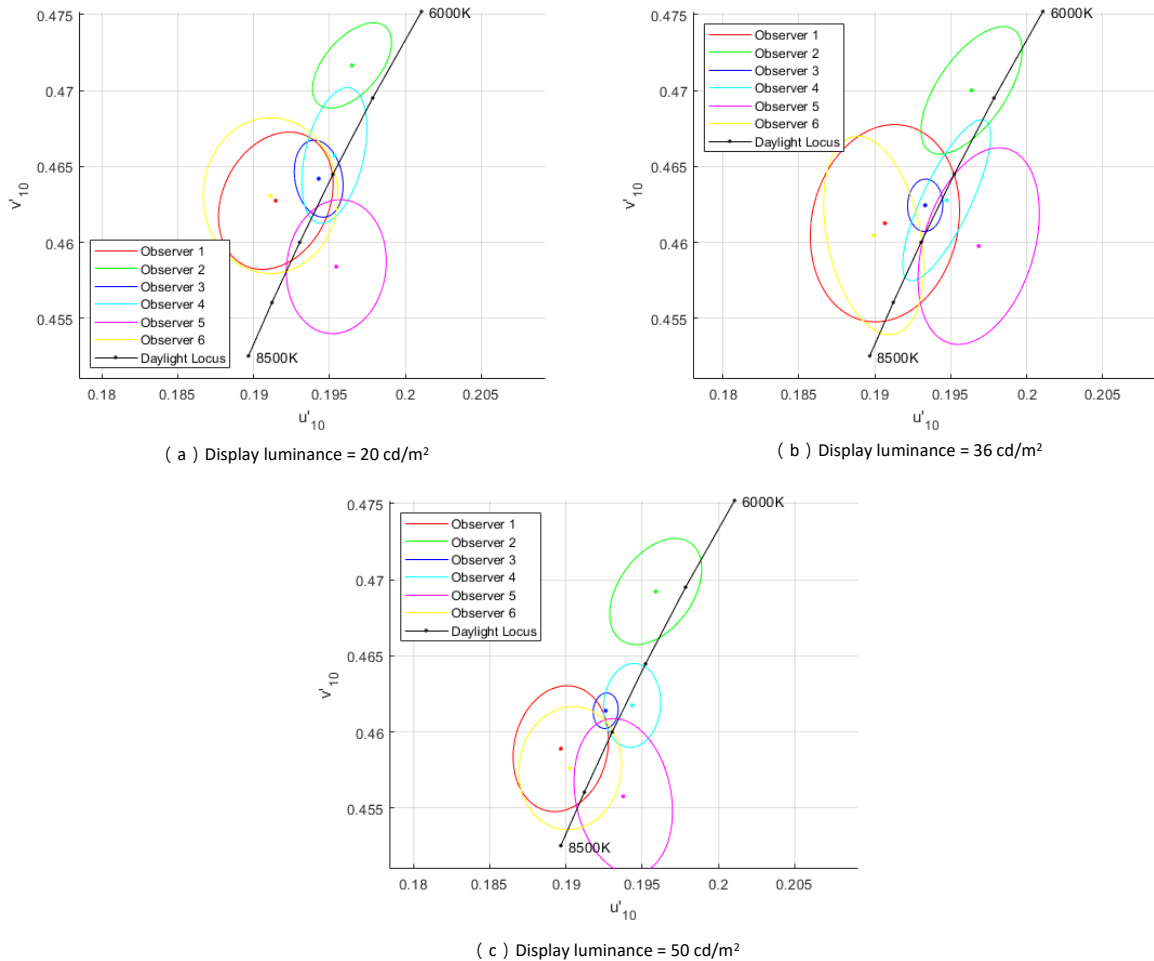

(a) Display luminance = 20 cd/m²   (b) Display luminance = 36 cd/m²

(c) Display luminance = 50 cd/m²

Figure 3. White point acceptable zones for six observers and three display luminance levels in CIE 1976 u'v' diagram

Table 1: CCT and Duv values of overall white points

Display luminance (cd/m²)	Overall white point CCT (K)	Overall white point Duv
20	7273	-0.0003
36	7318	-0.0001
50	7453	+0.0002

The results in this experiment show a good agreement with the previous studies. As listed in Table 1, the overall white points have higher CCTs than the D65 illumination and are located close to the daylight locus. Moreover, the white point CCT increases with the display luminance, gradually deviating from the D65 chromaticity of the light booth illumination. This trend is consistent to the findings of some previous studies which was derived from a pooling of observers' adjustments [4,5]. The dependency on the display luminance was considered as a consequence of chromatic adaptation [5]. From Figure 3, it can be seen that the major axes of the acceptable zones are mainly along the daylight locus, indicating that the observers are less sensitive to the change of CCT than the change of Duv value. Choi *et al.* have reported a similar result and suggested that the display white point may cover a large range in CCT [1].

Figure 3 also exhibits a significant inter-observer variation in the accepted display white points. Each observer has a distinct acceptable zone. For example, the white point that is highly possible to be accepted (close to the center of the acceptable zone) by Observer 6 may be rejected by Observer 4, while there is no any common white point accepted by both Observer 6 and Observer 2. Thereby, the overall white points are never accepted by all observers. This phenomenon reveals that the neutral perception varies across observers. According to a simulation performed by Oicherman *et al.*, the observer metamerism affects the achromatic color matching in cross-media color reproduction applications [6]. Therefore, in this experiment, the variation in white point selection may be related to the observer metamerism as well.

Additionally, each observer's acceptable zone seems to have a constant bias from the overall white point chromaticity, regardless of the display luminance. For example, Observer 4 tends to choose the white points with higher CCTs and negative Duv values, while Observer 2 tends to choose those with lower CCTs and positive Duv values. This constant bias may depend largely upon the individual characteristics of the visual system.

An ANOVA is adopted to the areas of the acceptable zones, which turns out that the acceptable zones are almost in the same size except those of Observer 3, who has significantly smaller zones than the other observers ($p = 0.002$). It is worth noting that Observer 3 was scored lowest in the FM100 test (2 points) among all observers (16 points in average), indicating that Observer 3 has an outstanding color discrimination ability. Therefore, Observer 3 is more sensitive to the chromatic change of the white point and only accept a small zone of chromaticities.

CONCLUSION

In this study, an experiment was carried out via the psychophysical methods of adjustment and constant stimuli to investigate the color matching between the display white point and the D65 illumination of a light booth. The most acceptable white point for all 6 observers exhibits a slightly increasing trend around 7300K with the display luminance. It also turns out that each observer has a distinct acceptable zone of white points, of which the size and the constant bias from the overall white point may be related to individual characteristics of the visual system.

REFERENCES

1. Choi, K. & Suk, H. (2016). Assessment of white for displays under dark- and chromatic-adapted conditions. *Optics Express, 24*(25), 28945–28957. https://doi.org/10.1364/OE.24.028945
2. Kwak, Y., Ha, H., Kim, H. & Seo, Y. (2019). Preferred display white prediction model based on mixed chromatic adaptation between "prototypical display white" and surround lighting color. *Optics Express, 27*(3), 2855–2866. https://doi.org/10.1364/OE.27.002855

3. Huang, M., He, R., Guo, C., Shi, C., Cui, G. & Melgosa, M. (2019). Influence of viewing conditions on cross-media color matching. *Optica Applicata, 49*(4). https://doi.org/10.37190/oa190408

4. Zhu, Y., Wei, M., & Luo, M. R. (2020). Investigation on effects of adapting chromaticities and luminance on color appearance on computer displays using memory colors. *Color Research & Application, 119*(5), 1–10. https://doi.org/10.1002/col.22500

5. Wei, M. & Chen, S. (2019). Effects of adapting luminance and CCT on appearance of white and degree of chromatic adaptation. *Optics Express, 27*(6), 9276–9286. https://doi.org/10.1364/OE.27.009276

6. Oicherman, B., Luo, M. R., Rigg, B. & Robertson, A. R. (2008). Effect of observer metamerism on colour matching of display and surface colours. *Color Research & Application, 33*(5), 346–359. https://doi.org/10.1002/col.20429

BRIGHTNESS PERCEPTION FOR COLORED LIGHT PRESENTED TO PERIPHERAL VISION

Kouya Yamammoto[1]* and Hiroshi Takahashi[1]

[1]*Department of Electrical & Electronic Engineering, Kanagawa Institute of Technology, Japan.*

* Corresponding author: Kouya Yamamoto, s1812045@cco.kanagawa-it.ac.jp

Keywords: Brightness sensitivity, Brightness-to-Luminance ratio, Helmholtz-Kohlrausch effect, Colored light, Peripheral vision

ABSTRACT

It is known that even if the luminance is the same, the feeling of brightness differs between white light and colored light, which looks bright when the color purity is high. This phenomenon, termed the Helmholtz–Kohlrausch effect, has been widely studied[1)2)3)4)]. However, these studies do not reveal the brightness sensitivity of colored light over the entire field of view. Therefore, the purpose of this study was to clarify brightness sensitivity to colored light in the peripheral visual field. Using a brightness matching method, subjects adjusted the brightness of a central light (test light) to the same level as a colored light presented in the peripheral visual field (reference light). The experiment was conducted in a dark room with a large display screen of background brightness 0.2 cd/m2. The reference light was presented in the right half visual field including the top and bottom at 90°, 45°, 0°, 315°, and 270°, with the horizontal right direction as 0° and eccentricity from 5° to 35° at 5° intervals. The experiment was repeated for each of the three primary colors of light: red, green, and blue. Brightness sensitivity to the colored light in the peripheral visual field was highest in the order of blue, red, and green for all directions except 90°; and the brightness sensitivity to blue and red light showed a decreasing trend as the degree of eccentricity increased. These results suggest that brightness sensitivity to green light is not easily affected by the degree of eccentricity.

INTRODUCTION

It is known that even for the same luminance, the feeling of brightness differs between white light and colored light, the latter of which looks bright when the color purity is high. This phenomenon, termed the Helmholtz–Kohlrausch effect, has been widely studied. However, these studies do not reveal the brightness sensitivity of colored light over the entire field of view. Therefore, the purpose of this study is to clarify the brightness sensitivity of peripheral vision to colored light.

EXPERIMENT

The experiment was conducted using a brightness-matching method in a darkened room. A reference light and a test light were presented on a display. The test light was presented at the center, and the reference light was presented at various angles from the center of the display. The background luminance was 0.2 cd/m^2. The experimental set up is shown schematically in Fig. 1. To control light modulation, a wireless ten-key pad was placed near the hand of the test subject, who was asked to place his chin on the provided chin rest provided to help maintain a constant viewpoint. The subject's viewpoint was aligned to the central part of the test light, and the luminance of the test light was adjusted so that it had brightness equal to the reference light. Figure 2 shows the distance from the test light to the reference light (the eccentricity) and the direction of test light presentation. The

reference light was presented in the right half visual field including the top and bottom at 90°, 45°, 0°, 315°, and 270°, with the horizontal right direction as 0° and eccentricity from 5° to 35° at 5° intervals. The experiment was repeated for each of the three primary colors of light: red (R), green (G), and blue (B).
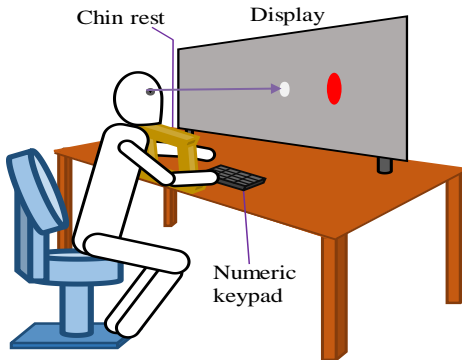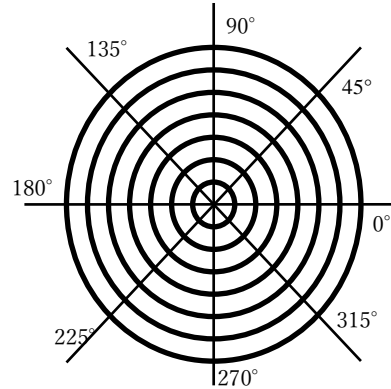

Figure 1. Experimental set up

Fig. 2. Eccentricity and direction of reference -light presentation

The experimental procedure was as follows:

(1) The subject adapted to the display brightness for 5 minutes.
(2) The subject was asked to fix their eyes on the test light at all times during the experiment.
(3) The reference light was presented, and the subject practiced dimming several times until they became familiar with how these levels of brightness felt.
(4) The subject was asked to dim the brightness of the test light equivalent to that of the reference light.
(5) The brightness of the test light was then reset to the initial value. The display direction and degree of eccentricity was changed randomly, and repeated four times.
(6) The color of the reference light was changed, and steps (4) and (5) were repeated, which comprised one set. Thus, the brightness of the test light was compared with that of the reference light and measured under the R, G, and B conditions.
(7) Steps 3 and 5 were performed as measures of the effects of practicing and ordering, respectively.

RESULTS AND DISCUSSION

Figures 3–5 show the relationship between the degree of eccentricity and luminance, for each color. For red and blue, the luminance of the test light decreased slightly with increasing degree of eccentricity. There was no change in luminance due to the degree of eccentricity for green, and luminance decreased slightly in all presentation directions for blue.

Figure 6 shows the relationship between eccentricity in the horizontal right direction and B/L, where B is the luminance of white light (test light) when adjusted to the same brightness as the reference light, and L is the brightness of the colored light (reference light). The B/L is ratio calculated as the index of the amount of brightness of the test light required to obtain the same brightness as the reference light. Figure 6 shows that B/L is highest for blue, and decreases in the order of red to green. The same was true for all presentation directions, except in the case of 90° and a high degree of eccentricity.

Figures 7–9 shows the relationship between the presentation direction for each color and B/L of the eccentricity direction. On Figures 7–9, B/L values for 135°, 180°, and 225° mirror those for 45°, 0°, and 315°. These figures show the brightness sensitivity decreases in the order of B, R, G, except when the presentation direction is 90 °. Focusing on the presentation direction of 90 °, it was found that the brightness sensitivity of R and G changed little with the degree of eccentricity, but that of B was affected by the degree of eccentricity.
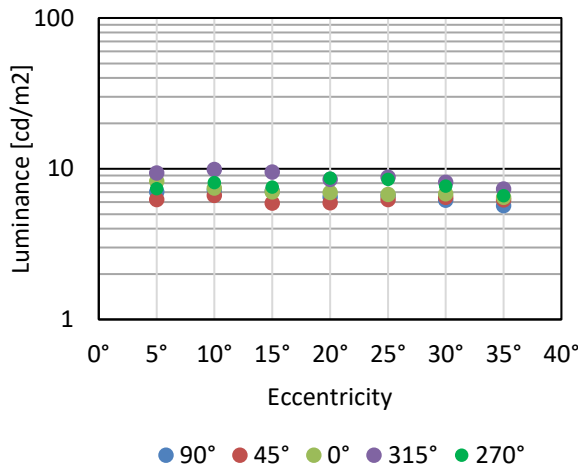

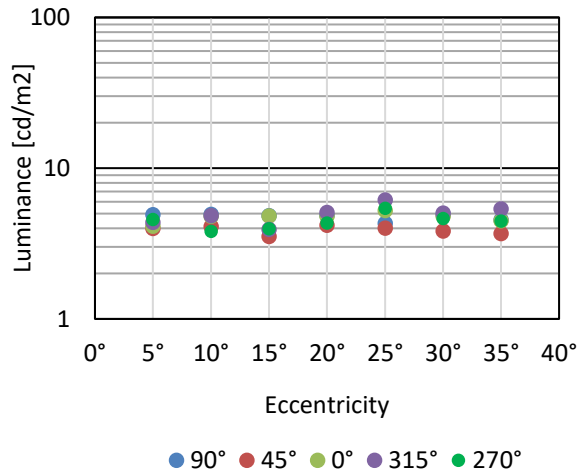**Figure 3. Relationship between eccentricity and luminance for red light**

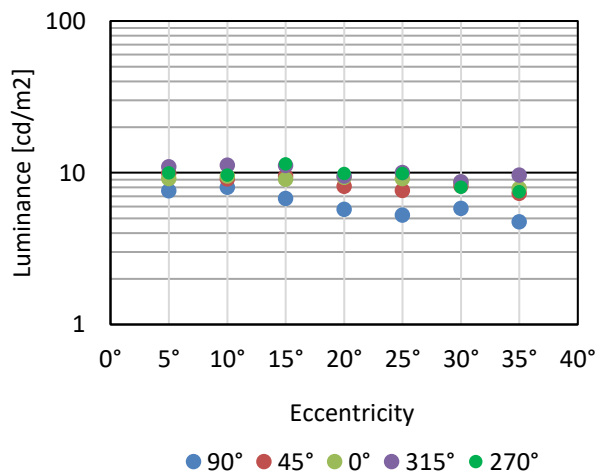**Figure 4. Relationship between eccentricity and luminance for green light**

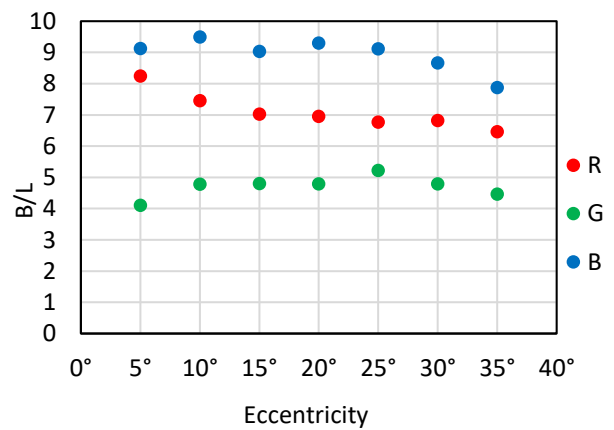**Figure 5. Relationship between eccentricity and luminance for blue light**

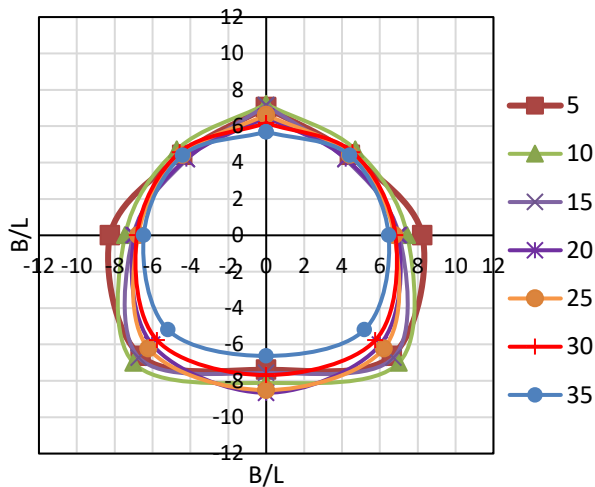**Figure 6. B/L in the horizontal right direction**

Figure. 7. Relationship between presentation direction and B / L for each degree of eccentricity of red light
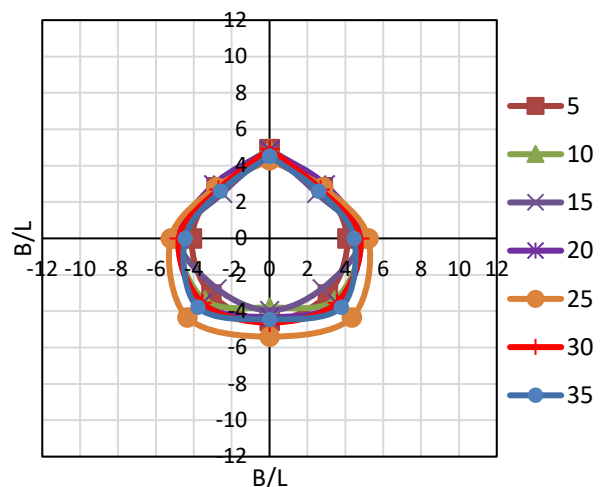

Figure 8. Relationship between presentation direction and B / L for each degree of eccentricity of green light
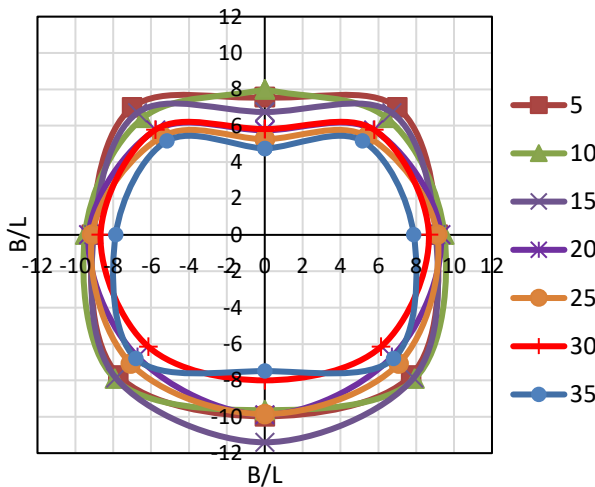
Figure 9. Relationship between presentation direction and B / L for each degree of eccentricity of blue light

CONCLUSION

This study investigated the perceived characteristics of brightness when colored light was presented in the peripheral visual field area.

The results are summarized as follows:

(1) Among the three colors, the brightness sensitivity of green light was least affected by the degree of eccentricity.

(2) Brightness sensitivity was highest for blue B/L, and decreased in the order of red to green.

REFERENCES

1. Shioda, H. & Saito, D. & Irikura, T. (2014). Influence of Retinal Eccentricity and Color Purity on Brightness-to-Luminance Ratio of Point Light Source. Biomedical Fuzzy Systems Association. Vol.16, No.1, pp.85-90.
2. Yaguchi, H. & Ikeda, M. (1980). Helmholtz-Kohlrausch Effect Investigated by the Brightness Additivity. J. Illum. Engng. Inst. Jpn. Vol.64, No.10, pp.566-570.
3. Nayatani, Y. & Tanaka, C. Tanaka, N. (1998). Prediction of the Helmholtzs-Kohlrausch Effect on Object and Luminous Colors-I. Estimation in case of the Variable-Achromatic-Color Method. Inst. Jpn. Vol.82, No.2, pp.131-136.
4. Nayatani, Y. & Tanaka, C. Tanaka, N. (1998). Prediction of the Helmholtz-Kohlrausch Effect on Object and Luminous Colors-II. Estimation in case of the Variable-Chromatic-Color Method. Inst. Jpn. Vol.82, No.2, pp.137-142.

GENDER DIFFERENCES IN COLOUR EMOTIONS
OF PLAIN FACE MASKS

Chien-Wei Chang[1], Chao-Lung Lee[2]*, Ray-Chin Wu[3], Ming-Hsiu Mia Chen[2] and Yun-Maw Cheng[2,4]

[1] The Department of Information Management, Tatung University, Taiwan
[2] The Graduate Institute of Design Science, Tatung University, Taiwan.
[3] The Department of Media Design, Tatung University, Taiwan.
[4] The Department of Computer Science and Engineering, Tatung University, Taiwan.

*Corresponding author: Chao-Lung Lee, longlee1221@gmail.com

Keywords: Colour emotion, Colour psychology, Face masks, Covid-19

ABSTRACT

Face masks have begun to play an important role in daily life during the COVID-19 outbreak. Many manufacturers produce various plain colour face masks to meet people's needs. However, different colour face masks may arouse various emotions among people of different genders. In Taiwan, it has been discussed whether pink face masks are feminine. We conducted a series of studies to explore colour emotions evoked by plain colour masks. This study investigated the colour emotions of different genders in plain colour face masks. We selected 11 plain colour masks which are commonly available on the market in Taiwan as our experimental stimuli. Observers were 97 people including 56 males and 41 females. The questionnaire included 10 pairs of bipolar colour emotion adjectives. Descriptive statistics and independent *t* test were used to compare the emotional reactions of different genders to 11 plain colour face masks. The results showed that many emotions for light red, light yellow, and bright yellow had statistically significant differences between genders, whereas there were no statistically significant gender differences for any of the emotions for strong red, light green, soft green, and light blue green. Also, compared with male observers, female observers expressed stronger emotions towards each colour mask stimulus. Finally, we found that females and males expressed opposite gender perspectives and colour emotions regarding yellow face masks. Male observers considered yellow face masks as masculine, whereas female observers thought they were feminine.

INTRODUCTION

Face masks have become an important accessory in our daily lives due to the outbreak of COVID-19. People started to consider wearing various colours to match their attire, and even to express their feelings. In Taiwan, a little boy who wore a pink face mask was taunted due to gender stereotypes. In Japan, most people supposed that a black face mask evokes negative emotions such as horror or severity. Some research has investigated gender differences in many facets of colours [1,2,3,4,5,6,12]. We analysed the results of the previous research [11] and aimed to explore the differences in the colour emotions of males and females evoked by plain face masks. In this paper, a few contributions regarding measuring the colour emotions of plain face masks for males and females are made. Gender differences in the colour emotions evoked by plain face masks are summarized.

METHODS AND RESULTS

This study applied the results of our previous study [11]. We accessed experimental responses from observers consisting of 56 males and 41 females, and investigated 10 pairs of bipolar colour emotion adjectives for 11 plain colour masks. These 10 pairs of bipolar colour emotion adjectives were 'clean/dirty', 'warm/cool', 'modern/classical', 'new/old', 'like/dislike', 'heavy/light', 'hard/soft', 'elegant/vulgar', 'fresh/stale', and 'masculine/feminine'. The 11 colours of plain face masks were black (BK), strong red (sR), light red (ltR), light yellow (ltY), bright yellow (bY), light green (ltG), soft green (sfG), light blue green (ltBG), light blue (ltB), light purple (ltP) and light red purple (ltRP). Descriptive statistics and independent sample t tests were used to analyse the differences in the colour emotions for different plain colour masks from the viewpoint of gender. Comparisons were demonstrated in the mean scale value of colour emotions for each plain face mask between genders, as shown in Figure 1. The mean values were plus when a plain face mask evoked the emotions of 'clean', 'warm', 'modern', 'new', 'like', 'heavy', 'hard', 'elegant', 'fresh', or 'masculine'. Conversely, minuses represented the emotions of 'dirty', 'cool', 'classical', 'old', 'dislike', 'light', 'soft', 'vulgar', 'stale', or 'feminine'.

The results of t-test showed that female observers gave higher colour emotion scores than male observers for each colour stimulus of most plain masks except warm/cool and fresh/stale. In addition, the colour emotions evoked by sfG were steadier than other colours. As shown in Figure 1, there was a tendency that colour emotions of the ltR mask were similar to the colour emotions of the ltP or ltRP masks. The colour emotions of the ltG mask were close to the colour emotions of the ltB mask. We also found that females and males expressed opposite gender perspectives and colour emotions regarding some colour face masks. Male observers considered that both yellow face masks were masculine ($M_{males-ltY} = 0.55$ and $M_{males-bY} = 0.14$), whereas female observers thought they were feminine ($M_{females-ltY} = -1.88$ and $M_{females-bY} = -1.71$). Males expressed the emotion of warm for ltB ($M_{males-ltB} = 0.18$) while females expressed the emotion of cool ($M_{females-ltB} = -0.49$) (M_* means the average scores).

We used t tests to test the statistical significance of the difference between genders in the same colour emotions for each colour face mask (under the level of significance $\alpha=0.05$). The males and females differed significantly in their expression of colour emotions (such as clean/dirty, like/dislike, heavy/light, hard/soft and masculine/feminine) for ltR, ltY and bY colour face masks ($p < 0.05$). The emotions of like/dislike, heavy/light and masculine/feminine for ltP and ltRP face masks showed significant differences between genders. There existed a significant difference in the emotion of masculine/feminine for ltB face mask between genders. The emotion of warm/cool on BK face masks showed a significant gender difference. Finally, all emotions for sR, ltG, sfG, and ltBG had no statistically significant gender differences.

CONCLUSION

This study examined colour emotion association with plain face masks by gender. We conclude that the present data bring additional findings to the previous experimental results on the investigation of plain face masks. Females and males expressed opposite gender perspectives in the emotion of "masculine/feminine" for yellow face masks. There were also statistically significant gender differences in ltR, ltY and bY masks for many emotions, whereas none of the emotions for sR, ltG, sfG and ltBG had any statistically significant gender differences. This paper only focuses on the colour of plain face masks and does not discuss texture, pattern, or shape. In the future, we will attempt to further analyse colour emotions for various properties of face masks.

Figure 1. Mean colour-emotion responses for each bipolar adjective on 11 plain face masks

REFERENCES

1. Al-Rasheed, A.S. (2015). An experimental study of gender and cultural differences in hue preference. *Frontiers in Psychology*, 6(30).
2. Bonnardel, V., Beniwal, S., Dubey, N., Pande, M. and Bimler, D. (2017). Gender difference in color preference across cultures: An archetypal pattern modulated by a female cultural stereotype. *Color Research and Application*, 43(2), 209–223.
3. Frassanito, P. & Pettorini, B. (2008). Pink and blue: the colour of gender. *Child's Nervous System*, 24(8), 881-882.
4. Fortmann-Roe, S. (2013). Effects of hue, saturation, and brightness on color preference in social networks: Gender-based color preference on the social networking site Twitter. *Color Research and Application*, 38(3), 196-202.
5. Hsu, M., Ou, L. and Guan, S. (2015). Colour preference for Taiwanese floral pattern fabrics. *Color Research and Application*, 41(1), 43–55.
6. Jonauskaite, D., Dael, N., Chèvre, L. & Althaus, B. (2019). Pink for Girls, Red for Boys, and Blue for Both Genders: Colour Preferences in Children and Adults. *Sex Roles*, 80, 630–642.
7. Jiang, Q., Chen, L. and Zhang, J. (2019). Perception and Preference Analysis of Fashion Colors: Solid Color Shirts. *Sustainability*, 11(8), 2405.
8. Kobayashi, S. (1981). The aim and method of the Color Image Scale. *Color Research and Application*, 6(2), 93–107.
9. Manav, B. (2007). Color-emotion associations and color preferences: A case study for residences. *Color Research and Application*, 32(2), 144–150.
10. Ou, L., Luo, M. R., Woodcock, A. and Wright. A. B. (2004). A study of color emotion and color preference, Part I: Color emotions for single colors. *Color Research and Application*, 29(3), 232–240.
11. Wu, R., Lee, C., Chen., M. M., Chang, C. and Cheng Y. (2021). A study on colour emotions of the mask. In: Proceedings of the International Colour Association (AIC) Conference 2021. Milan, Italy.
12. Zhang, Y., Liu, P., Han, B., Xiang, Y. and Li, L. (2019). Hue, chroma, and lightness preference in Chinese adults: Age and gender differences. *Color Research and Application*, 44(6), 967–980.

COLORS TO REPRESENT THAI ALTERNATIVE GENDERS

Jarunee Jarernros[1], Chanida Saksirikosol[1]*, Ploy Srisuro[1] and Kitirochna Rattanakasamsuk[2]

[1] *Department of Advertising and Public Relations Technology, Faculty of Mass Communication Technology, Rajamangala University of Technology Thanyaburi, Thailand.*
[2] *Color Research Center, Rajamangala University of Technology Thanyaburi, Thailand.*

*Corresponding author: Chanida Saksirikosol, e-mail: chanida_s@rmutt.ac.th

ABSTRACT

The rainbow color was commonly used to signify alternative genders, particularly in political or social movements. However, it is still debatable if the rainbow color actually represented the alternative genders. Previous research has shown that purple was more acceptable than the rainbow to be the representative color of the alternative gender. However, the previous result only identified Munsell hue of the representative color. Therefore, the objective of this study is to identify Munsell color which represents the color of the alternative genders. There were 62 alternative gender subjects and 60 non-alternative gender subjects. 198 Munsell color chips in the range of Munsell hue 10PB, 2.5P, 5P, 7.5P, 10P, 2.5RP were presented to the subjects. The subjects were asked to select the color chips which were the representative color of the alternative gender. The number of selections was no limit. The results showed that the most selected Value/Chroma was 4/12. The most selected color for the representative color was 7.5P 4/12 and 2.5P 4/12 respectively.

INTRODUCTION

Nowadays, the classification of gender identity is not limited to only "Male" and "Female". There is a group of people who identified themselves as "Lesbian (L)", "Gay (G)", "Bisexual (B)", "Transgender (T)", "Queer (Q)" and "Other (+)". The term "LGBTQ+" is generally used to represent these people. However, the term "LGBTQ+" is not popularly used in Thailand. People who have a variance of gender identity and variance of sexual orientation are normally called "Alternative Gender".

The color was used to represent this gender variance in many cases. In 1933-1945, the pink triangle was used as a badge to indicate the gay prisoner in a concentration camp during the Nazi regime [1]. In 1978, a gay activist, Gilbert Baker designed a rainbow color flag as a symbol of the LGBT rights movement. [2]. Until now, the rainbow color was perceived as the representative color of the alternative gender. However, this rainbow color was originally used in social and political movements. It is still questionable whether the rainbow color is suitable to represent the alternative gender in other circumstances. In the concept of minimalist design [3], fewer color is preferable. Therefore, a solid color that can refer to the alternative gender is more useful for a designer. For example, blue or black were used for male toilet sign and pink or red were used for female toilet sign. This standard color code has been already implemented in Japan and will be implemented in other countries. However, the rainbow color for alternative gender's toilet sign is still debatable because it is not harmonious to color design.

There was very little research that tried to investigate the representative color of the alternative gender based on our survey. Rattanakasamsuk et al. (2020) have conducted an experiment to identify

the representative color of the alternative genders [4]. A rainbow color, N1, N5, N9, and 40 Munsell color chips covered all Munsell Hue were presented to 120 Thai subjects. They were asked to select color chips that referred to the alternative gender. The result showed the rainbow color was a candidate for the representative color of alternative gender as expected. However, only one of 60 alternative gender subjects selected the rainbow color as the representative color of the alternative gender. Although the rainbow color flag has been used as the symbol of the alternative gender movement, Thai alternative gender subjects did not agree to use it as their representative color. Apart from the rainbow color, more than 50% of selected color chips were in the purple region. It is indicated that purple was more acceptable as the representative hue of the alternative gender by both alternative and non-alternative gender subjects. There were six Munsell hues (i.e., 10PB, 2.5P, 5P, 7.5P, 10P, 2.5RP) that were selected by more than 10% of the subjects.

In this research, we conducted an experiment to identified Munsell color of the representative color of the alternative gender. The stimuli were Munsell color chips in the region of purple covered from 10PB to 2.5RP. Sixty-two alternative gender subjects and sixty non-alternative gender subjects were asked to specify color chips which are represented the alternative gender.

METHODOLOGY

Stimuli

The stimuli were Munsell color chart of 10PB, 2.5P, 5P, 7.5P, 10P, 2.5RP as shown in Figure 1. The total number of the color chip was 198 color chips. Each color chip subtended two degrees of visual angle.
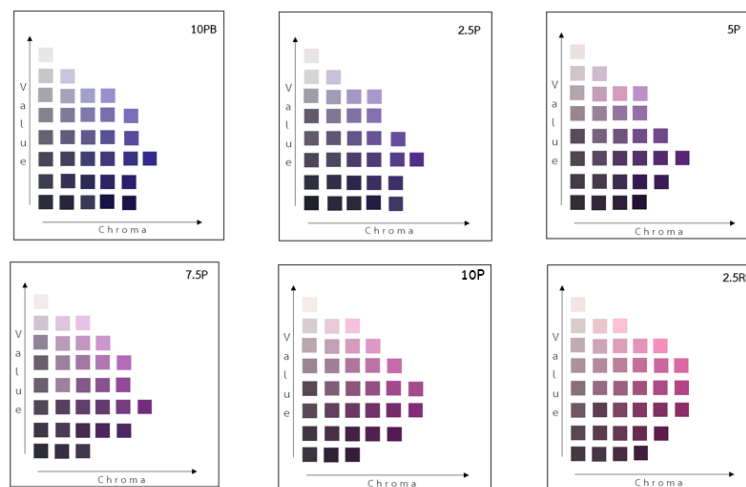

Figure 1. Schematic diagram of the stimuli.

(Note: color might not present the exact color appearance to subjects)

Subject

The subjects were 120 university students who volunteered to participate in this experiment. All subjects had a normal color vision. They were classified into two groups based on their gender identity. The first group, "Non-alternative Gender", was 30 male and 30 female subjects. The second group was 62 subjects who did not identify themselves as "Male" or "Female". They identified themselves as, "Alternative Gender". In the case of the alternative gender subjects, if they agreed, we collected their gender identities in detail. They could freely specify their gender identity such as

"Gay", "Lesbian", "Transgender", "Tomboy" or "Kratoey (Thai word means a man who wants to be a woman)". The subject's gender identity was shown in Table 1.

Table 1. Gender identity of the subjects

Gender Identity	Number
Non Alternative Gender	60
Male	30
Female	30
Alternative Gender	62
Lesbian	13
Gay	14
Bisexual	12
Transgender	8
Tomboy	11
Kratoey	4
Total	122

Experimental Procedure

The wall of the experimental room was covered by white wallpaper. There was a table covered with gray paper inside the experimental room. The room illuminance measured at the table was 1200 lux. The stimuli were presented by placing the Munsell color charts on the table. The Munsell chart was arranged to be 2 rows and 3 columns as shown in Figure 1. The position of each chart was random for each subject. Before starting the experiment, the subjects had to sit inside the experimental room for at least two minutes. After two minutes of adaptation, the stimuli were presented to the subjects. The subjects were asked to select the color chips which referred to the alternative gender. The subjects could select the color chips as many as they wanted.

RESULTS AND DISCUSSIONS

Figure 2 showed the results of the representative color of the alternative gender. Each panel represented the result of each hue. The abscissa represented the Munsell chroma and the ordinate represented the Munsell Value. Each circle represented the selected Munsell color of the representative color of the alternative gender. The size of the circle represented the number of the selected color. As described in the introduction part, purple was accepted as the representative hue of the alternative gender. In this result, most of the selected Munsell colors representative of the alternative gender were the high chroma color. Figure 3 showed the top five selected Munsell colors which were 7.5P4/12 followed by 2.5P 4/12, 7.5P 5/10, 7.5P 3/10, 5P 7/8 respectively. Note that the appearance of the Munsell colors in Figure 3 were simulated based on the Munsell Renotation Data [5,6]. Their color appearance might not be the exact color appearance of these Munsell colors chips. These five Munsell colors would be named "Purple" or "Violet" or "Lavender" in English. But in the Thai language, these five Munsell color chips would be named "Muang" which covered the appearance of "Purple", "Violet" and "Lavender". [7,8]

Figure 4 showed the selected Munsell color categorized by Value/Chroma. The size of the circle represented the number of the selected Munsell color. Regardless of Munsell hue, the highest selection Munsell Value/Chroma was 4/12 followed by 5/10, 3/10 and 4/10 respectively. These Munsell value/chroma covered more than 75% of the color which were selected to be the representative color of the alternative gender. We also asked the subjects for the reason for their

selection. Most of them answered that they had experienced the linkage between purple or violet or lavender and the alternative gender. In Thailand, before the word "LGBTQ+" was used, "Chao-See-Muang" which means "purple people" was popularly used to call the alternative gender. Therefore, the color chips in the range of high chroma (10-12) which clearly appeared "Muang" would be selected to be the representative color of the alternative gender.
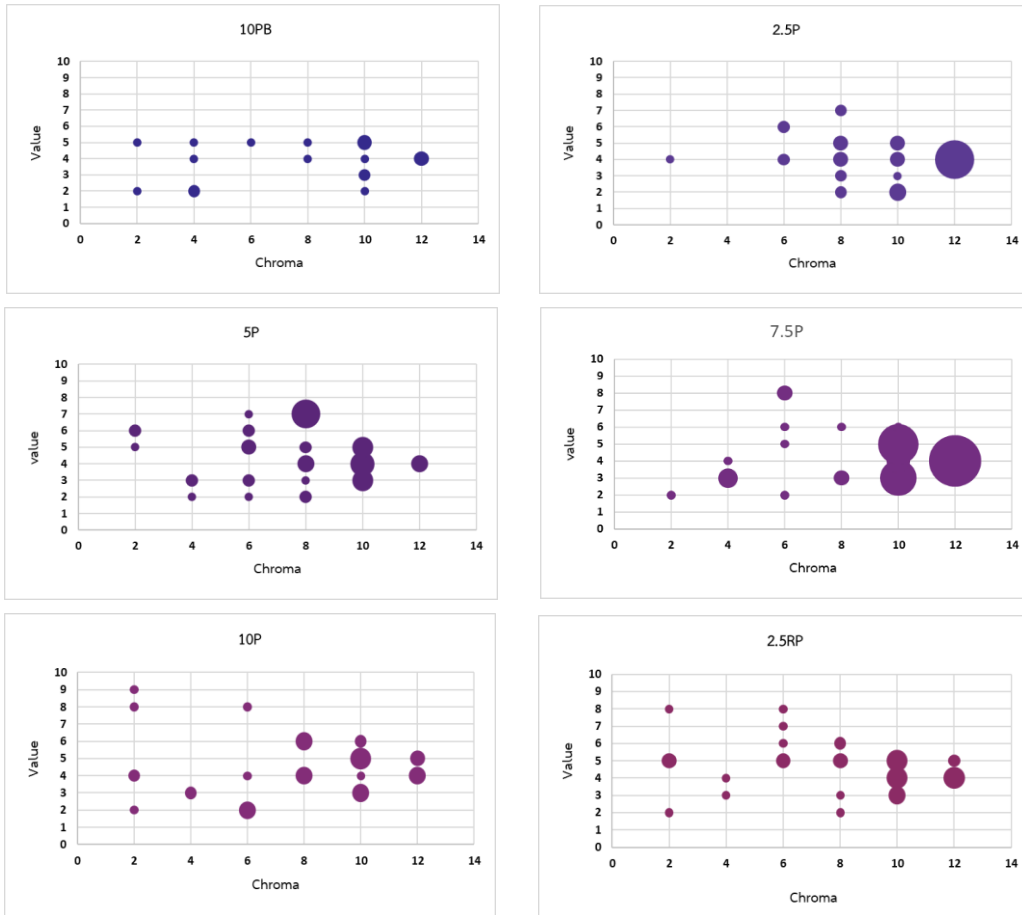

Figure 2. Selected Munsell color of the alternative gender. Size of circle represents number of selections.
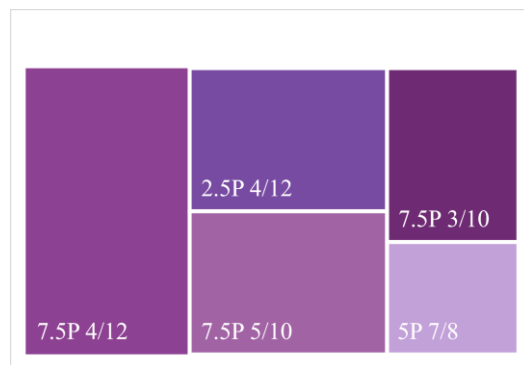

Figure 3. Top five representative color of the alternative gender by all subjects.
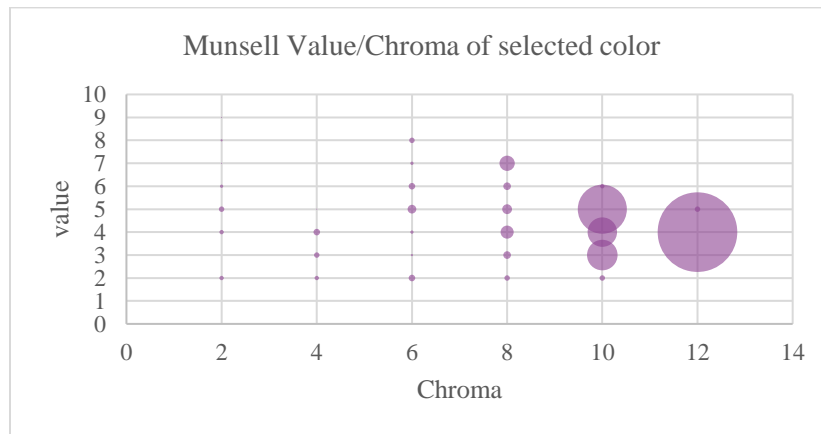(Note: color might not present the exact color appearance to subjects)

Figure 4. The selected color of the alternative gender categorized by chroma/value.

Comparison of the top five selected Munsell colors of the representative color of the alternative gender between the alternative gender subjects and the non-alternative gender subjects were shown in Figure 5. The area of each color represented the number of selections. 7.5P 4/12 was the largest number of the selected color by the alternative gender subjects followed by 7.5P 510, 7.5P3/10, 5P 7/8 and 7.5P 4/10, respectively. For the non-alternative gender subjects, 2.5P 4/12 was the largest number of the selected color followed by 7.5P 4/12, 7.5P 3/10, 7.5P 5/10 and 7.5P 4/10. Even though the number of 2.5P4/12 selection was largest for the non-alternative gender subject, the alternative gender subjects tended to be not interested in 2.5P 4/12. Its number of selections was very low.
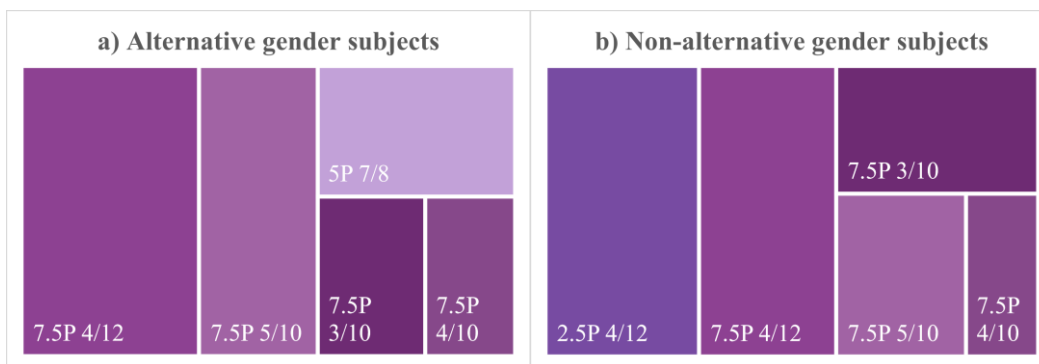

Figure 5. Top five representative color of the alternative gender by
a) alternative gender subjects and b) non-alternative gender subjects.

(Note: color might not present the exact color appearance to subjects)

From the subject's interview, several alternative gender subjects reported that 2.5P 4/12 were too bluish. When we asked some alternative gender subjects to do categorical color naming for 2.5P 4/12, some of them did not categorize 2.5P4/12 into "Purple" but categorized it into "Blue". An interesting result was also found for the alternative gender subjects. Regardless of their sex (physical characteristics at birth), 2.5P 4/12 was not selected by any of the alternative gender subjects who distinctly expressed the feminine characteristics (Transgender, Kratoey). We still questioned that these two aspects would associate with the discard of 2.5P 4/12 by the alternative gender subjects or

not. Previous research has shown that there was the existence of sex differences in color preference. [9, 10] Female preferred reddish or pinkish color to bluish color. In this research, the feminine characteristic alternative gender subjects might prefer reddish purple to bluish purple. However, there was a lack of evidence to support this assumption because the tendency to discard 2.5P 4/12 did not clearly exist in the case of female subjects.

CONCLUSION

In this research, Munsell color of the representative color of the alternative gender was identified. The results showed that the most selected Value/Chroma was 4/12. The most selected Munsell color was 7.5P 4/12 followed by 2.5P 4/12, 7.5P 5/10, 7.5P 3/10 respectively. There was a slight difference in the results obtained by the alternative and non-alternative gender subjects. 2.5P 4/12 was mostly selected by the non-alternative gender subjects but the alternative gender subjects rarely selected this color. Therefore, this research indicated that the representative color of the alternative gender was 7.5 P4/12. Other candidates for the representative color of the alternative gender (i.e., 7.5P 5/10 and 7.5P 3/10) also can be used to create a color palette for product design for the alternative gender.

ACKNOWLEDGEMENT

REFERENCES

1. Waxman, O. B. (2018). How Nazi Pink Triangles Symbol Was Reclaimed for LGBT Pride. Retrieved from https://time.com/5295476/gay-pride-pink-triangle-history/
2. Swanson, A. (2015, June 29). How the rainbow became the symbol of gay pride. Retrieved September 26, 2019, from https://www.washingtonpost.com/blogs/wonkblog/wp/2015/06/29/how-the-rainbow-became-the-symbol-of-gay-pride/
3. Obendorf, H. (2009). Minimalism, Simplicity and Rule of Design. In Minimalism: Designing simplicity., Springer.
4. Rattanakasamsuk, K., Nontawongsa, C., Srisuro, P. and Phuangsuwan, C. (2020) Does Rainbow Color Truly Represent Alternative Gender? Journal of the Color Science Association of Japan, 44 (3+), 27-28.
5. Newhall, S.M., Nickerson, D., & Judd, D.B. (1943). Final Report of the O.S.A. Subcommittee on the Spacing of the Munsell Colors. Journal of the Optical Society of America, 33, 385-418.
6. Munsell Color Science Lab. (n.d.). Munsell Renotation Data. Retrieved October 12, 2019, from https://www.rit.edu/cos/colorscience/rc_munsell_renotation.php.
7. Panitanang, N., Phuangsuwan, C., Kuriki, I., Tokunaga, R., and Ikeda, M. (2019). Thai Basic Color Terms and New Candidate Nomination. Proceedings of the 5th Asia Color Association Conference, 29 November - 2 December 2019, Nagoya, Japan, 164-169.
8. Panitanang, N., Phuangsuwan, C., and Ikeda, M. (2019). Thai Color Names in Different Regions of Thailand. Journal of the Color Science Association of Japan, 43(3+), 86-89.
9. Ellis, L., & Ficek, C. (2001). Color Preferences According to Gender and Sexual Orientation. Personality and Individual Differences, 31(8), 1375–1379. doi: 10.1016/s0191-8869(00)00231-2
10. Hurlbert, A. C., & Ling, Y. (2007). Biological Components of Sex Differences in Color Preference. Current Biology, 17(16). doi: 10.1016/j.cub.2007.06.022

A QUALITY FUNCTIONAL DEVELOPMENT(QFD) RESEARCH ON APPLIANCE OF COLOUR IMAGE SCALE TO SPATIAL COLOR COMBINATION OF DESIGN HOTEL(DH) INTERIOR DESIGN

Chen-Hsin Yang[1]*, Tseng-Ping Chiu[1], Shuo-Fang Liu[1], Jen-Hao Yu[2], Jen-Yu Huang[2]

[1]*Department of Industrial Design, College of Planning & Design, National Cheng Kung University, Taiwan*
[2] *Department of Mechanical Engineering, College of Engineering, National Cheng Kung University, Taiwan*

*Corresponding author: Chen-Hsin Yang, e-mail: p36094200@gs.ncku.edu.tw

ABSTRACT

Color is a significant interior element with the power to influence emotions and behaviors in a particular environment. (Cho, J. Y., & Suh, J., 2020). Therefore, various color strategies are applied to improve the user experience (O'Connor, 2019). To achieve this, in this content, we use quality management method: Quality Function Development (QFD) (Akao,1997) as the tool to analyze the appliance of Color Image Scale (Kobayashi, 1981), a Japan-origin color design strategy which has been used for more than 40 years in different industries, toward Taiwanese participants' visual preference among spatial color combinations design of Design Hotel (DH)'s bedroom.

INTRODUCTION

With the economic growth and the development of technology, people can enjoy convenience, but meanwhile, individuals are burden by the pressure, to withdraw from the environment, recreational travel is an option (Iso-Ahola,1983). Empirical studies indicate that temporary accommodation plays a vital role in realizing the main purposes of recreational traveling—rest and relaxation, and escape from routine (Iso-Ahola,1983). Therefore, the bedroom interior design of the temporary accommodation is worth discussing.

Among all categories of temporary accommodation in recreational traveling, Design Hotels (DH) is the suitable one. According to XOTELS, an international management company, DH is not luxury hotels, but the aesthetic of DH are typically high-styled, especially visual concepts.

Since the color of interior design is an essential visual factor. Therefore, in this paper, we conduct a two-stage research to investigate the preference tendency of Taiwanese environmental visual literacy among the appliance of color combinations that are referred from Image scale for 3-color combinations (1987 to present) on DH interior design. Specifically, the findings are based on the theory that the Color Image Scale will have differences under different time, space, and different industries. (1990, Kobayashi)

THEORETICAL BACKGROUND

Color Image Scale

Color Image Scale is proposed by Shigenobu Kobayashi in 1981, is a notable color theory in design. The purpose of this scale is to find out after viewing a specific color or a color combination, what perception can individuals can interpret literally. Kobayashi contended to find the standard for applying the color theory in Japanese Industries, he abstracted 130 colors and notates them based on

Munsell Color System and ISCC- NBS Method of Designating Colors, which is also the method for color selection in Japanese Industrial Standards (JIS).

The Color Image system based on the notations of Munsell Color System: hue, value, and chroma, transfer these three attributes into three axes: warm or cool, soft or hard, and clear or greyish, then transfer these axes into a Color Space. In order to find the words that connect these axes, the research adapts the Japanese language categorize system that was provided by Charles E. Osgood and Hiroshi Akuto and seek the relationship of these adjectives toward his axis. After choosing 20-25 pairs of adjectives, he started to do Semantic Differentiations (SD) questionnaires with color images showing the participants. In the process of the experiment, the finding shows that people are greatly dominated by hue and tone, especially when using color combinations in images. Therefore, the research converts the color space into a two-dimensional chart, while Hue (warm-cold) serve as the x-axis, and tone(hard-soft) serve as the y-axis (Figure 1), and to make it more diverse and specific for word-color connection, Kobayashi converted the color combination of 4 quadrants into 13 groups (Figure 2).
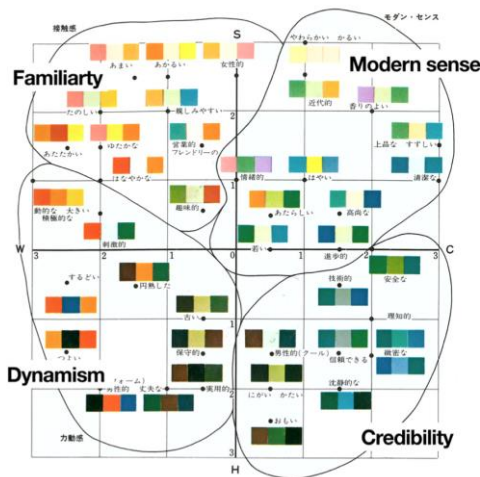

Figure 1. Image scale for 3-color combinations (1974) (Horiguchi & Iwamatsu, 2018)
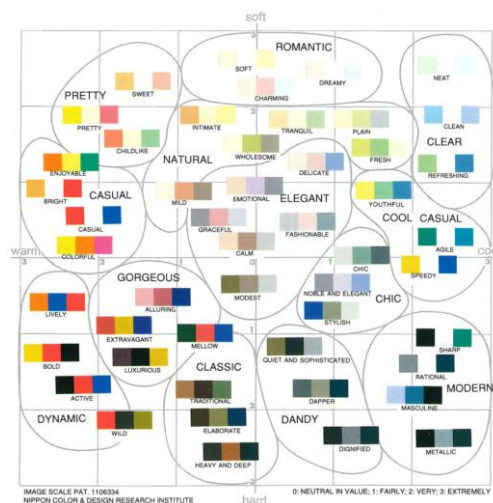
Figure 2. Image scale for 3-color combinations (1987 to present) (Horiguchi & Iwamatsu, 2018)

Also, Kobayashi mentioned, since the scale is psychological, not physical, judgment among people will have differences. Thus, it can be reconstructed based on preferences, industries, spatial and timing, and all sorts of factors. Therefore, with its credibility and flexibility, we use The Color Image Scale as the reference for the color combination in our DH bedroom design, and using QFD to quantified the Environmental Visual Literacy of Taiwanese.

Quality Function Development (QFD)

The concept was first presented by Yoji Akao in 1966 (Akao,1997). QFD is to conduct research processes and analyze research results after understanding customer needs, in order to achieve the quality management of the product functions required by the customer.

This method is a systematic and structured analysis method, from understanding the various needs of customers, finding solutions, and then systematically unfolding and analyzing the correlation of the matrix to establish the interrelationship between the various elements, so that the product can complete the complete quality management before entering the market.

More specifically, we can distinguish the concept into three main parts: Quality, Function, and Development.

Quality.

It is the factors that are extracted from that engineering characteristics that are needed to be discussed in the process of quality control. In this study, due to the credibility of Color Image Scale in industries, we use it as our quality.

Function.

It is the customer's requirements, also "customer's voice" in this system. In this study, "the customer's voice" stands for the statistic results of environmental visual literacy in the first stage of this study.

Development.

It is the result of showing what are the orders and factors should be done, in order to achieve the quality acquisitions. In this study, the development is to obtain the participants' environmental visual literacy toward the spatial color combinations in DH bedroom.

METHODOLOGY

First Stage

Color Image Scale is psychological, it can be reconstructed (Kobayashi, 1981) (a1) So, based on all the 13 groups of adjectives that are provided from Figure 1, we randomly compiled 30 images each from hundreds of actual design hotel images available on the web, in a total of 390(13*30) images and (a2) let six professionals (who have degrees in interior, industrial and graphic design) rate the most 6 corresponding images toward the color combinations provided by the 13 groups adjectives. Therefore, a total of 78(6*13) images are selected. (a3) We then create a questionnaire asking participants 2 specific questions: a 7-point scale measuring the degree of warm and cold (-3~3), hard and soft (-3~3), perceived from the set of photos, and ranking their preference of these 13-groups photos.

Second Stage

 (b1) Based on the result of the first stage, extract the 3-color combinations and adjectives from preference ranking from 1st~3rd; (b2) we then developed a 3D rendering platform of a standard DH bedroom using a computer-aided program (Blender) and applied the 12 sets of color combinations to it, while due to the placements of color, there are each set has 6 combinations, totally 72 pictures are rendered. (b3) Among these 72 phots, the same six professionals in (a3) are invited to rate the most preferable image in each set, a total of 12 images are selected. (b4) Based on these 12 images, we create a questionnaire asking participants most correspondent adjective toward the picture separately, and use QFD to analyze the result for investigating the purpose of this study: Taiwanese visual literacy among spatial color combinations of Design Hotel (DH) bedroom environment.

RESULTS AND DISCUSSION

First Stage

58 males and females, aging from 20-30, totally 116 participants participate in this stage.

Question 1.

Since we only after asking the participants their perception degree of warm and cold (WC), soft and hard(HS), from the photos. We analyze the result by descriptive statistics: find the Mode of the degree of WC, HS among the 13 groups, and point the position on a coordinate system. To correspond the original Color Image scale for 3-color combinations (1987 to present), we set WC degree as x-axis, while HS degree as y-axis, is listed below
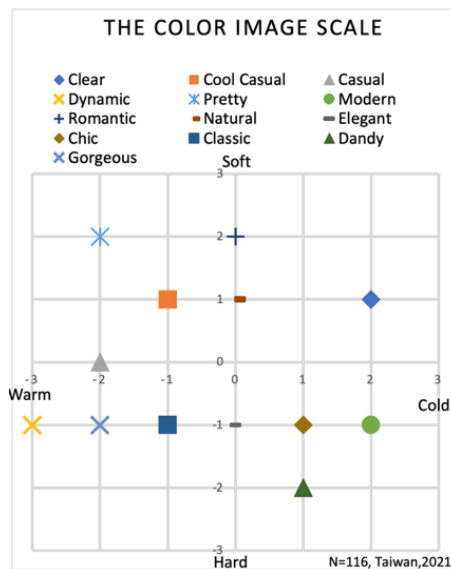

Figure 3. The Color Image Scale, n=116, Taiwan, 2021

From Figure 3 it indicates that there is a high correspondence of Environmental Visual Literacy between the participant and Figure 2, the differences are: (c1) in Cool Casual tends to be softer and warmer, which gives individuals the feeling of similarity, II Quadrant of Figure 1; (c2)as for Natural and Elegant, compare with the reference they are slightly harder, but also not that significant; (c3) lastly, in Classic, participants' perception slightly tend to be softer and warmer, but also not that significant.

Question 2.

After quantifying the ranking preference of the participants to these 13 groups of photos, as Figure 4, 1ST~3rd are: Natural, Clear, and Cool Casual. The total of these groups are higher than 200 points, and the ranking of Natural is even higher than 250 points.
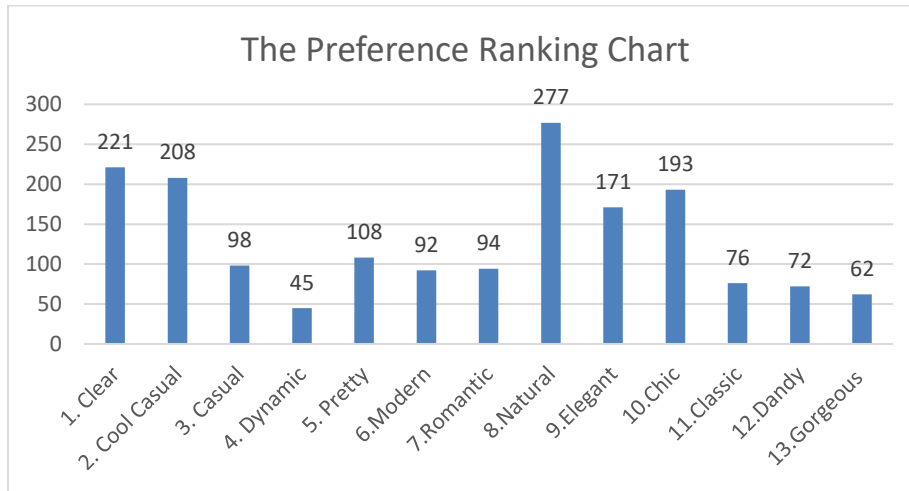
Figure 4. The Preference Ranking Chart, n=116, Taiwan, 2021, y-axis stands for the ranking preference quantification points

Second Stage

In order to increase the objectivity of the results, another 29 males and 34 females, aging from 20-30, totally 63 participants participate in this stage. Also, the 3 spatial areas for applying color combination appliances in this stage should be considered not only experimental but also reality. Therefore, we use ImageJ, an image area checking software developed by National Institutes of Health (NIH), to check the proportion (Figure 6) of the DH model image (Figure 5).

Figure 5. Basic DH model and the area to apply the 3-colors combination

	Area	Percentage (Selected Area/All)
All	2123082pixels	100%
Celling（Green）	469793 pixels	22.13%
Wall（Blue）	364546 pixels	17.17%
Furniture（Red）	206952 pixels	9.75%

Figure 6. Proportion of the color area appliance

After receiving all the results, to build the QFD Matrix, based on the group adjective, we count the ratio of each color combination to the adjective chosen by participants: The highest ratio gets 5 points(notation:◎), the second 3 points(notation: O), and the lowest 1point(notation:△), then fill in the central part of the matrix. Secondly, to decide the value of different "customer's voice", we take the Color Image Chart in Figure 2, and set the spot as the center of circle, and draw concentric circles, the closer the distance to the center of the circle, the higher the score, and use this to qualify the high and low value toward customer's need, and then multiply the points that are notated in the center of the matrix to get the absolute weighting, and divided the weighting to the total to get the result. All three groups of QFD matrixes are listed below:

Customer's Voice	Value of Customer's Voice	DH Model 3-Color Combination (1987)					
		Mild	Wholesome	Intimate	Tranquil	Fresh	Plain
Fresh	1	△	O	△	△	◎	△
Plain	1	O	O	△	O	△	O
Tranquil	3	O	O	△	◎	△	◎
Mild	1	◎	△	◎	◎	△	O
Intimate	3	O	△	◎	△	△	△
Wholesome	5	△	◎	O	O	◎	△
Importance	Absolute Weighting	32	44	40	42	38	30
	Percentage	14.16%	19.47%	17.70%	18.58%	16.81%	13.27%
Ranking		5	1	3	2	4	6

Figure 7. QFD Matrix of Natural

Customer's Voice	Value of Customer's Voice	DH Model 3-Color Combination (1987)		
		Clean	Neat	Refreshing
Neat	1	◎	◎	△
Clean	3	O	O	O
Refreshing	5	△	△	◎
Importance	Absolute Weighting	19	19	35
	Percentage	26.03%	26.03%	47.95%
Ranking		1	1	2

Figure 8. QFD Matrix of Clear

Customer's Voice	Value of Customer's Voice	DH Model 3-Color Combination(1987)		
		Youthful	Agile	Speedy
Agile	1	△	◎	O
Speedy	3	△	O	O
Youthful	5	◎	O	O
Importance	Absolute Weighting	29	29	27
	Percentage	34.12%	34.12%	31.76%
Ranking		1	1	2

Figure 9. QFD Matrix of Cool Casual

Figure 7 shows that in the group Natural, generally the adjective choice (Customer's Voice) of the participant toward the DH model 3-Color Combination (Kobayashi,1981) refers to the literature tend more familiar (softer and warmer), and the percentages of all the items are below 20%. Therefore, we assumed that the subjects can acknowledge the difference in spatial color, but there is no particularly big difference in the degree of preference for each color combination. Figure 8 shows that as for the group Clear, only the percentage of DH model 3-Color Combination-Refreshing is 47.95, which is much higher than 33.3%, as for the other 2, DH model 3-Color Combination-Clean and Neat only 26.03%. It indicates that the participants are more sensitive toward DH model 3-Color Combination-Refreshing than the other groups. Also, participants' perception (customer's choice) among DH model 3-Color Combination-Clean and Neat, Neat is relatively strong, they are all 5 points(notation:△). Finally, for the group Cool Casual, Figure 9 shows that percentages of all the items close or even higher than 33%, this means the correspondence between the DH model 3-Color Combination and Customer's Voice is significant and high, and easily to sense the difference in every color combination.

Consequently, from the first stage, despite different statistic analysing methods, the high correspondent of among our Taiwanese participants in 2021 and Figure 2, which is done in Japan, 1987. From the second stage, it indicates that the participants' color distinguish ability and perception in this study, tends to be sensitive in warm and soft colours.

CONCLUSION AND FUTURE STUDY

To sum up, empirical study contends that historical, geographical and other extrinsic factors can affect the neurophysiological factors of a group of people at a certain time, and complex neurophysiological factors are involved in visual perceptions (Gordon, 2004). While relation between Japan and Taiwan, the tropical island, has been tied by a shared history, common values, economic ties, strategic alignment, and social networks between their political and business elite (Peng-Er, 2004). In this study also indicates The Colour Image Scale among the Taiwanese participants in this study compare with the literature which was done in Japan, 1987, has a high correspondence. In addition, the QFD matrixes of this study also show the participants have high distinguishable ability and preference among soft and warm colors for DH interior design.

In this study, since this is an on-line based study, we can't assure the difference of colour on different devices, also bio-signals are not able to examine.

Therefore, in the future study, we will use examine eye tracking machine to understand the bio-signals from the participants' pupil, which represents the changing of their mood (Cho, J. Y., & Suh, J., 2020), correlates to the respond of the questionnaire.

REFERENCES

1. Akao, Y. (1997). QFD: Past, present, and future. In International Symposium on QFD (Vol. 97, No. 2, pp. 1-12).
2. Cho, J. Y., & Suh, J. (2020). Spatial Color Efficacy in Perceived Luxury and Preference to Stay: An Eye-Tracking Study of Retail Interior Environment. *Frontiers in psychology*, *11*, 296.
3. Gordon, I. E. (2004). *Theories of visual perception*. Psychology press.
4. Horiguchi, S., & Iwamatsu, K. (2018). From Munsell color system to a new color psychology system. *Color Research & Application*, *43*(6), 827-839.
5. Iso-Ahola, S. E. (1983). Towards a social psychology of recreational travel. *Leisure studies*, *2*(1), 45-56.
6. Kobayashi, S. (1981). The aim and method of the color image scale. *Color research & application*, *6*(2), 93-107.
7. Kobayashi, S. (1992). *Color Image Scale* (1st ed.). Kodansha USA.
8. O'Connor, Z. (2019). Effective environmental visual literacy: Pedestrian crossing design and the key roles of colour and contrast. Plenary lecture, *AIC2019: Midterm meeting of the International Association of Colour*, Buenos Aires, 14-17 October.
9. Peng-Er, L. (2004). Japan-Taiwan relations: Between affinity and reality. *Asian Affairs: An American Review*, *30*(4), 249-267.

DETECTION OF GREENERY AREA IN IMAGE
BY USING MASK R-CNN FOR MEASUREMENT
OF GREEN VISIBILITY RATIO SURVEY

Motonori Doi[1]*, Ren Kawagiwa[1], Akira Kimachi[1] and Shogo Nishi[1]

[1]Graduate School of Engineering, Osaka electro-communication university, Japan.

*Corresponding author: Motonori Doi, doi@oecu.jp

ABSTRACT

Green visibility ratio (GVR) is one of the important indices for urban environment assessment. The GVR is defined as the ratio of the greenery area in an image. Some artificial green objects often exist in the urban scene. The discrimination of the vegetation green from other green objects is required for automatic GVR measurement. We proposed a GVR measurement method based on color and texture analysis in AIC2015. The implemented system detected the green leaves. However, the guideline for the GVR survey published by Osaka prefecture in Japan defined the greenery area as vegetation green areas including brown trunks and branches of trees. The detection of trunks and branches was difficult for the previous method. This paper proposes the GVR detecting system by using the Mask R-CNN. The Mask R-CNN is a segmentation method by using deep learning techniques. Our method detects the tree areas and grass areas from images of outdoor scenes by the Mask R-CNN and calculates the GVR from the detected area. We trained the Mask R-CNN with our original dataset including trees with branches and trunks. In the fundamental stage of our research, we found that errors often occurred in the area of overlapped roadside trees. Therefore, the dataset including many images of overlapped roadside trees are used for our system. We conducted experiments with images taken according to the guideline. The results show good detection of trees in comparison with the training without overlapped trees. In a case of an image including roadside trees, the proposed method detected only tree area, but the output of the system trained without overlapped trees included undesirable areas. In this case, the GVR by manual detection and the proposed system were 19.9% and 18.5%, respectively. The experimental results show good feasibility of the proposed method.

INTRODUCTION

Green visibility ratio (GVR) is one of the important indices for urban environment assessment. The GVR is defined as the ratio of greenery area in an image. The GVR is often used by Japanese local governments. The green area is usually detected manually in their survey. There is a method for automatic GVR measurement proposed by Takizawa [1], which measures the GVR using color information. However, some artificial green objects, such as ad boards and walls of buildings, often exist in urban scenes. Therefore, the discrimination of the vegetation green from other green objects is required for automatic GVR measurement. We proposed a GVR measurement method based on color and texture analysis in AIC2015 [2]. The method detected the green leaves by using green color information and fine texture information. However, the guideline for the GVR survey published by Osaka prefectural government in Japan defined the greenery area as vegetation green areas including brown trunks and branches of trees. The detection of trunks and branches was difficult for the previous method.

This paper proposes the GVR detecting system by using the Mask R-CNN. The Mask R-CNN [3] is a segmentation method by using deep learning techniques. Our method detects tree areas and grass areas from images of outdoor scenes based on the Mask R-CNN and estimates the GVR from detected area.

GVR ESTIMATION BY USING MASK R-CNN

MASK R-CNN

The Mask R-CNN detects objects in an image while simultaneously generating a segmentation mask for each object. Mask R-CNN is a region-based convolutional network (R-CNN) that outputs masks representing the pixel areas of target objects. The network is trained by images and annotation data for objects in these images. The annotation data include the name of objects and the vertices of polygon regions of these objects.

The Mask R-CNN showed good performance in image segmentation tests for the COCO dataset [4]. The code of Mask R-CNN with network trained by the COCO dataset are provided. The COCO dataset have 80 object categories, including *potted plant* category. Trees and grasses are not included in the categories of the COCO dataset. It was difficult to detect roadside trees and grasses as potted plant by the Mask R-CNN trained with the original COCO dataset.

Original training data for detection of roadside trees

We trained the Mask R-CNN by using our original dataset including trees and grasses. The training was done for the pre-trained network by the COCO dataset. In the fundamental stage of our research, we trained the Mask R-CNN with dataset with tree and grass images taken from Flickr [5]. However, detection errors often occurred in the area of overlapped trees. In urban scenes, there are many overlapped trees at roadside. We analyzed errors and found that trees in the training dataset were not overlapped.

Therefore, we considered the training data and generated new dataset. The new dataset including many images of overlapped roadside trees with branches and trunks in urban scenes are used for the training of our system.

GVR estimation

Our system detects masks for trees and grasses. The occupancy of green target in an image could be obtained as the percentage of mask area in the whole image. Since detected masks often overlap, we merged the masks. Then, the occupancy of mask in the image is calculated as the GVR in the scene. The detected mask has scores that shows likelihood of the target objects. It is possible to select mask by thresholding with scores.

EXPERIMENTS

We conducted experiments with images taken according to the guideline by Osaka prefectural government. For evaluations, we constructed a system to visualize detected masks and manual detection areas in a scene. Manual detection of trees and grasses for trainings and verifications are done by using the VGG image annotator [6]. Figure 1 shows an example of the result. Red area shows the detected mask by the proposed method and green area shows the manual detection area of trees and grasses.

We compared the output of our system with the output by the system trained with dataset that don't include overlapped trees. Example images of tree areas detected manually in each dataset are shown in Figure 2. The detection results by these two systems are shown in Figure 3. The results show good detection of trees by our proposed system in comparison with the system trained without overlapped trees. The proposed method detected only tree area, but the output of the system trained

without overlapped trees included undesirable areas. In this case, the GVR by manual detection, the proposed system and the compared system were 19.9%, 18.5% and 22.4% respectively. The experimental results show good feasibility of the proposed method.

CONCLUSIONS

This paper proposed the GVR estimation method based on the Mask R-CNN that is a segmentation method by using deep learning technology. In the fundamental stage of our research, the problem caused in the detection of overlapped trees, such as roadside trees. We considered the training data of Mask R-CNN for detection of roadside trees. We collected images of scene with the roadside trees and constructed a new dataset including many images of overlapped roadside trees with branches and trunks. Then, we trained Mask R-CNN with the new dataset. We compared the output of our system with the output by the system trained without overlapped trees. The results show that the proposed method detected only tree area, but the output of the system trained without overlapped trees included undesirable areas. The experimental results show good feasibility of the proposed method. As future works, we have plan to evaluate our system quantitatively.
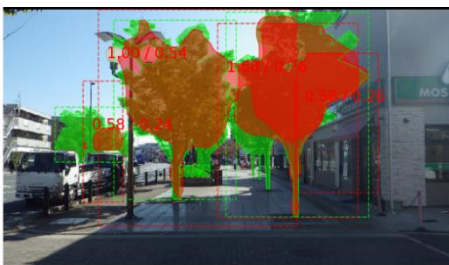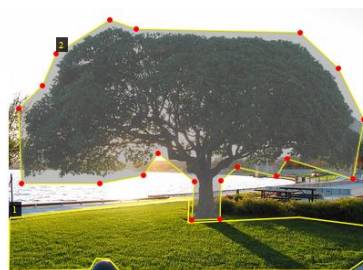

Figure 1. Example of visualization of result

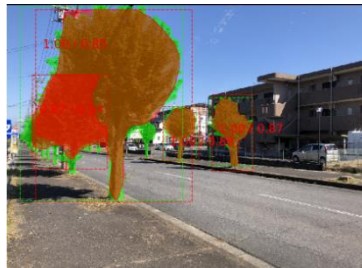(a) Dataset with overlapped trees   (b) Dataset without overlapped trees

Figure 2. Example images of tree areas detected manually in datasets with overlapped trees and without overlapped trees

(a) Input image

(b) Output by system trained with overlapped trees

(c) Output by system trained without overlapped trees

Figure 3. Example of detection results

REFERENCES

1. Takizawa, S., Mori, T. & Sagawa, K. (2013). Development of an instrument for the urban-green measure. *the 44th Annual Meeting of Color Science Association of Japan*, 314-315. (in Japanese)
2. Doi, M. Kimachi, A and Nishi, S. (2015). Real-time Green Visibility Ratio Measurement. *Proceedings of Midterm Meeting of the International Color Association (AIC2015)*, 609-614.
3. He, K., Gkioxari, G., Dollar P., & Girshick, R. (2017) Mask R-CNN, *IEEE International Conference on Computer Vision (ICCV2017)*, 2980-2988.
4. Lin, T.Y., et al. (2014). Microsoft COCO: Common Objects in Context. *Lecture Notes in Computer Science*, 740-755.
5. Flickr, https://www.flickr.com/
6. VGG image annotator, https://www.robots.ox.ac.uk/~vgg/software/via/